ZooKeys 1087: 1–18 (2022)
doi: 10.3897/zookeys.1087.71280
https://zookeys.pensoft.net

RESEARCH ARTICLE

A peer-reviewed open-access journal
ZooKeys
Launched to accelerate biodiversity research

Redescription of the giant Southeast Asian millipede *Spirobolus macrurus* Pocock, 1893 and its assignment to the new genus *Macrurobolus* gen. nov. (Diplopoda, Spirobolida, Pachybolidae)

Piyatida Pimvichai[1], Henrik Enghoff[2], Thierry Backeljau[3,4]

1 *Department of Biology, Faculty of Science, Mahasarakham University, Mahasarakham 44150, Thailand* **2** *Natural History Museum of Denmark, University of Copenhagen, Universitetsparken 15, DK-2100 Copenhagen Ø, Denmark* **3** *Royal Belgian Institute of Natural Sciences, Vautierstraat 29, B-1000 Brussels, Belgium* **4** *Evolutionary Ecology Group, University of Antwerp, Universiteitsplein 1, B-2610 Antwerp, Belgium*

Corresponding author: Piyatida Pimvichai (piyatida.p@msu.ac.th)

Academic editor: Pavel Stoev | Received 8 July 2021 | Accepted 24 August 2021 | Published 22 February 2022

http://zoobank.org/37A2596C-A036-4DFF-8037-5E649FC93FDC

Citation: Pimvichai P, Enghoff H, Backeljau T (2022) Redescription of the giant Southeast Asian millipede *Spirobolus macrurus* Pocock, 1893 and its assignment to the new genus *Macrurobolus* gen. nov. (Diplopoda, Spirobolida, Pachybolidae). ZooKeys 1087: 1–18. https://doi.org/10.3897/zookeys.1087.71280

Abstract

A new genus of the millipede family Pachybolidae from Southeast Asia is described: *Macrurobolus* **gen. nov.**, with *Spirobolus macrurus* Pocock, 1893 as type species. This latter species is DNA barcoded (COI) and redescribed based on male morphological characters, which hitherto were unknown. The new genus differs from other pachybolid genera by having (1) the preanal ring process long and protruding beyond the anal valves and (2) the anterior gonopod telopodite distally abruptly narrowed, forming an extremely long, slender, elevated process curved caudad. Given that *Macrurobolus* **gen. nov.** is a monotypic genus, it is aphyletic and thus requires further taxonomic revision.

Keywords

Aphyly, Myanmar, taxonomy, Thailand

Introduction

Spirobolus macrurus Pocock, 1893 is, with its length of up to 110 mm and diameter of up to 10 mm, the largest pachybolid millipede in SE Asia, but despite its large size, the species is still poorly known. Its original description was based on a single female specimen from Kawkareet, Tenasserim, Myanmar, and did not include the genital parts. Yet, Pocock (1893) separated *S. macrurus* from other *Spirobolus* species by its much longer and thinner preanal ring process. Much later, Hoffman (1962: 773) transferred the species to the genus *Tonkinbolus* Verhoeff, 1938 and remarked "said to be closely related to *moulmeinensis*, differing only in the longer and more slender epiproct". However, based on gonopod characters and strongly supported by DNA sequence data, Pimvichai et al. (2018) assigned *Tonkinbolus scaber* Verhoeff, 1938 (type species of *Tonkinbolus*) to the genus *Litostrophus* Chamberlin, 1921. Thus, *Tonkinbolus* became a subjective junior synonym of *Litostrophus*. At the same time, Pimvichai et al. (2018) moved all other *Tonkinbolus* species, including *T. macrurus*, to the genus *Atopochetus* Attems, 1953 because they share the unique anterior gonopod telopodite of this genus. Yet, since *T. macrurus* was until then only characterised on the basis of a single female specimen, its transfer to *Atopochetus* was qualified as "incertae sedis" (Pimvichai et al. 2018).

In the present paper we redescribe and barcode *Spirobolus macrurus* based on an old male specimen discovered in the collections of the Natural History Museum of Denmark, Copenhagen, and new live material, including an adult male specimen, collected during recent fieldwork in Thailand. As a result we also create the new genus *Macrurobolous* gen. nov. to accommodate *Spirobolus macrurus*, so that this species will be referred to as *Macrurobolus macrurus* comb. nov.

Material and methods

Live specimens were hand collected and preserved in 70% ethanol for morphological study or placed in a freezer at –20 °C for DNA analysis. Specimens were also examined from the following collections:

CUMZ Museum of Zoology, Chulalongkorn University, Bangkok, Thailand;
NHMD Natural History Museum of Denmark, University of Copenhagen, Denmark.

This research was conducted under the approval of the Animal Care and Use regulations (numbers U1-07304-2560 and IACUC-MSU-037/2019) of the Thai government.

Morphology

Gonopods were photographed with a digital camera manipulated via the program Helicon Remote (v. 3.1.1.w). The Zerene Stacker Pro software was used for image-

stacking. Drawings were made using a stereomicroscope. Samples for scanning electron microscopy (SEM) were air-dried directly from alcohol and sputter-coated for 250 s with gold. SEM micrographs were taken with an environmental scanning electron microscope (ESEM)-FEI Quanta 200. Voucher specimens were deposited in the collections of CUMZ and NHMD.

DNA extraction, amplification, and sequencing

Total genomic DNA was extracted from legs of a male specimen of *Macrurobolus macrurus*, comb. nov. from Wat Tham Inthanin, Mae Sot District, Tak Province, Thailand (CUMZ-D00147) using the NucleoSpin Tissue kit (Macherey-Nagel, Düren, Germany) following the manufacturer's instructions. PCR amplifications and sequencing of the standard mitochondrial COI DNA barcoding fragment (Hebert et al. 2003) were done as described by Pimvichai et al. (2020). The COI fragment was amplified with the primers LCO-1490 and HCO-2198 (Folmer et al. 1994). The new COI nucleotide sequence has been deposited in GenBank under accession number MZ905519. Sample data and voucher codes are provided in Table 1.

Alignment and phylogenetic analysis

The COI data included 48 specimens, representing 17 genera and 40 nominal species of ingroup taxa (Table 1). Three species of the order Spirostreptida, viz. *Anurostreptus barthelemyae* Demange, 1961 (Harpagophoridae), *Chonecambala crassicauda* Mauriès & Enghoff, 1990 (Pericambalidae), and *Thyropygus allevatus* (Karsch, 1881) (Harpagophoridae) were used as outgroup.

CodonCode Aligner (v. 4.0.4, CodonCode Corporation) was used to assemble the forward and reverse sequences and to check for errors and ambiguities. Sequences were checked with the Basic Local Alignment Search Tool (BLAST) provided by NCBI and compared with reference sequences in GenBank. Next, sequences were aligned using MUSCLE (v. 3.6, see http://www.drive5.com/muscle; Edgar 2004). The COI alignments consisted of 660 bp. The sequences were checked for ambiguous nucleotide sites, saturation and phylogenetic signal using DAMBE (v. 5.2.65. see http://www.dambe.bio.uottawa.ca/DAMBE/dambe.aspx; Xia 2018). MEGA (v. X, see http://www.megasoftware.net; Kumar et al. 2018) was used to (1) check for stop codons, (2) translate COI protein-coding sequences into amino acids, and (3) calculate uncorrected pairwise *p*-distances among sequences.

Phylogenetic trees were constructed using maximum likelihood (ML), Bayesian inference (BI), and neighbor-joining (NJ). The shape parameter of the gamma distribution, based on 16 rate categories, was estimated using maximum-likelihood analysis. ML trees were inferred with RAxML (v. 8.2.12, see http://www.phylo.org/index.php/tools/raxmlhpc2_tgb.html; Stamatakis 2014) through the CIPRES Science Gateway (Miller et al. 2010) using a GTR+G substitution model and 1000 bootstrap replicates to assess branch support. BI trees were constructed with MrBayes (v. 3.2.7a, see http://

www.phylo.org/index.php/tools/mrbayes_xsede.html; Huelsenbeck and Ronquist 2001). Substitution models were inferred using PartitionFinder 2 on XSEDE (v. 2.1.1, see http://www.phylo.org//index.php/tools/partitionfinder2_xsede.html; Lanfear et al. 2017) through the CIPRES Science Gateway (Miller et al. 2010). BI trees were run for 2 million generations (heating parameter was 0.05), sampling every 1000 generations. Convergences were confirmed by verifying that the standard deviations of split frequencies were below 0.01. Then the first 1000 trees were discarded as burn-in, so that the final consensus tree was built from the last 3002 trees. Support for nodes was assessed by posterior probabilities. NJ trees were constructed with MEGA v. X using the Kimura 2-parameter model and 1000 bootstrap replicates.

For ML and NJ trees we consider branches with bootstrap values (BV) of ≥ 70% to be well supported (Hillis and Bull 1993) and < 70% as poorly supported. For BI trees, we consider branches with posterior probabilities (PP) of ≥ 0.95 to be well supported (San Mauro and Agorreta 2010) and below as poorly supported.

Table 1. Specimens from which the COI gene fragment was sequenced. CUMZ, Museum of Zoology, Chulalongkorn University, Bangkok, Thailand; NHMD, Natural History Museum of Denmark; NHMW, Naturhistorisches Museum, Vienna, Austria; NHM, The Natural History Museum, London, United Kingdom. Names of countries are in capitals. Abbreviations after species names refer to the isolate of each sequence. GenBank accession numbers are indicated for each species.

	Voucher code	Locality	COI
Genus *Apeuthes*			
A. maculatus Amc	NHMW-Inv. No.2395	South Annam, Vietnam	MF187404
A. maculatus Am26	NHMD-621697	Nha Trang, Bao Dai Villas Hotel, in garden, Vietnam	MZ567159
A. fimbriatus BMP	CUMZ-D00144	Bach Ma Peak, Da Nang, Vietnam	MZ567160
A. longeligulatus TPP	CUMZ-D00140	Tham Phet Po Thong, Klong Hard, Sa Kaeo, Thailand	MZ567161
A. pollex SMR	CUMZ-D00141	Sra Morakot, Klongthom, Krabi, Thailand	MZ567162
A. pollex SML	CUMZ-D00142	Koh 8, Similan islands, Phang-Nga, Thailand	MZ567163
A. pollex WTS	CUMZ-D00143	Tham Sue Temple, Muang, Krabi, Thailand	MZ567164
?*A. spininavis* ABB	CUMZ-D00145	Air Banun, Perak, Malaysia	MZ567165
Genus *Atopochetus*			
A. anaticeps SVL	CUMZ-D00091	Srivilai temple, Chalermprakiet, Saraburi, Thailand	MF187405
A. dollfusii DOL	NHM	Cochinchina, Vietnam	MF187412
A. helix SPT	CUMZ-D00094	Suan Pa Thong Pha Phum, Kanchanaburi, Thailand	MF187416
A. moulmeinensis TAK	CUMZ-D00095	km 87, Tha Song Yang, Tak, Thailand	MF187417
A. setiferus HPT	CUMZ-D00097	Hub Pa Tard, Lan-Sak, Uthaithani, Thailand	MF187419
A. spinimargo Ton27	NHMD-00047013	Koh Yo, Songkhla, Thailand	MF187423
A. truncatus SML	CUMZ-D00101	Koh 8, Similan islands, Phang-Nga, Thailand	MF187424
A. uncinatus KMR	CUMZ-D00102	Khao Mar Rong, Bangsapan, Prachuapkhirikhan, Thailand	MF187425
A. weseneri Tos29	NHMD-00047003	Supar Royal Beach Hotel, Khanom, Nakhonsrithammarat, Thailand	MF187431
Genus *Aulacobolus*			
A. uncopygus Auc	NHMW-Inv. No.2375	Nilgiris, South India, India	MF187433
Genus *Benoitolus*			
B. birgitae BBG	NHMD 621687	Chiang Dao, Chiang-Mai, Thailand	MT328992
Genus *Coxobolellus*			
C. albiceps Stpw	CUMZ-D00121	Tham Pha Tub, Muang District, Nan Province, Thailand (green individual)	MT328994
C. compactogonus SKR	CUMZ-D00134	Sakaerat Environmental Research Station, Wang Nam Khiao District, Nakhon Ratchasima Province, Thailand	MT328998

	Voucher code	Locality	COI
C. fuscus HKK	CUMZ-D00133	Kroeng Krawia waterfall, Sangkhla Buri District, Kanchanaburi Province, Thailand	MT328999
C. nodosus SPW	CUMZ-D00126	Chao Por Phawo Shrine, Mae Sot District, Tak Province, Thailand	MT329000
C. serratus KKL	CUMZ-D00132	Khao Kalok, Pran Buri District, Prachuap Khiri Khan Province, Thailand	MT329001
C. simplex TNP	CUMZ-D00136	Tham Pha Pha Ngam, Mae Prik District, Lampang Province, Thailand	MT329002
C. tenebris TPL	CUMZ-D00120	Wat Tham Phrom Lok Khao Yai, Sai Yok District, Kanchanaburi Province, Thailand	MT329004
C. tigris TYE	CUMZ-D00131	Tham Yai I, Pathio District, Chumphon Province, Thailand	MT329006
C. transversalis Stpg	CUMZ-D00125	Tham Pha Tub, Muang District, Nan Province, Thailand	MT329007
C. valvatus BRC	CUMZ-D00128	Tham Borichinda, Chom Thong District, Chiang-Mai Province, Thailand	MT329008
Genus *Leptogoniulus*			
L. sorornus BTN	CUMZ-D00109	Botanical Garden, Penang, Malaysia	MF187434
Genus *Litostrophus*			
L. chamaeleon PPT	CUMZ-D00111	Phu Pha terb, Mukdahan, Thailand	MF187436
L. saraburensis PKS	CUMZ-D00113	Phukhae Botanical Garden, Saraburi, Thailand	MF187438
L. segregatus Ls19	NHMD 621686	Koh Kut, Trad, Thailand	MF187440
Genus *Macrurobolus* gen. nov.			
M. macrurus comb. nov.	CUMZ- D00147	Wat Tham Inthanin, Mae Sot District, Tak Province, Thailand	MZ905519
Genus *Madabolus*			
M. maximus Mm4	NHMD-00047007	de Toliara Province, Parc National de Bermaraha, South Bank of Manambolo River, Near Tombeau Vazimba, Madagascar	MF187441
Genus *Narceus*			
N. annularis			NC_003343.1
Genus *Parabolus*			
P. dimorphus Pd34	NHMD-00047004	Dar es Salaam, Tanzania	MF187442
Genus *Paraspirobolus*			
P. lucifugus			AB608779.1
Genus *Pelmatojulus*			
P. tigrinus Pt2	NHMD-00047008	Southern part of the Comoé N.P., 30 km north of Kakpin, Côte d'Ivoire	MF187443
P. togoensis Pto6	NHMD-00047006	Biakpa, Ghana	MF187444
Genus *Pseudospirobolellus*			
P. avernus GPG	CUMZ-D00117	Gua Pulai, Gua Musang, Kelantan, Malaysia	MT329011
Pseudospirobolellus sp. KCS	CUMZ-D00118	Koh Chuang, Sattahip, Chonburi, Thailand	MT329012
Genus *Rhinocricus*			
R. parcus Rp49	NHMD-00047009	Puerto Rico, Usa	MF187449
Genus Trachelomegalus			
Trachelomgalus sp. Tr54	NHMD-00047012	Borneo Sabah, Malaysia	MF187445
Genus *Trigoniulus*			
T. corallinus Tco15	NHMD-00047010	Vientiane, Laos	MF187446
Outgroup			
Genus *Anurostreptus*			
A. barthelemyae Tlb	CUMZ-D00003	Thale-Ban N.P., Khuan-Don, Satun, Thailand	KC519469
Genus *Chonecambala*			
C. crassicauda Ttp	CUMZ-D00001	Ton-Tong waterfall, Pua, Nan, Thailand	KC519467
Genus *Thyropygus*			
T. allevatus Bb	CUMZ-D00013	BangBan, Ayutthaya, Thailand	KC519479

Results

The uncorrected *p*-distance between the sequences ranged from 0.03 to 0.25 (Tables 2, 3). The mean interspecific sequence divergence within *Atopochetus* was 0.13 (range: 0.08–0.16). The mean sequence divergence between *Atopochetus* and *M. macrurus* comb. nov. was 0.15 (range: 0.14–0.17). The mean interspecific sequence divergence within *Litostrophus* was 0.10 (range: 0.09–0.11). The mean sequence divergence between *Litostrophus* and *M. macrurus* comb. nov. was 0.13 (range: 0.11–0.14).

PartitionFinder indicated that the best substitution model for BI analysis was GTR+ G. The ML, BI, and NJ trees were congruent with respect to some of the well-supported branches (by visual inspection of the branching pattern). Yet, in several instances BI provided good support for branches that were not well-supported by both ML and NJ (e.g., the *Litostrophus* + *Benoitolus* clade or the *Coxobolellus* + *Pseudospirobolellus* clade).

In the phylogenetic trees (Fig. 1) the clade of Pachybolidae + *Benoitolus* is poorly supported by ML (BV = 63) and NJ (BV = 27), but well supported by BI (PP = 0.97), while Trigoniulinae is well supported by the three methods (BV = 96 and 92; PP = 1.00). Although the monophyly of Pachybolidae is clearly challenged by the inclusion of *Benoitolus*, which involves a long branch, removing *Benoitolus* from the analysis yields a Pachybolidae clade with the same pattern of support as the Pachybolidae + *Benoitolus* clade (Suppl. material 1).

Irrespective of the in- or exclusion of *Benoitolus*, *Macrurobolus macrurus* comb. nov. is nested within a clade comprising *Litostrophus* and *Atopochetus*. Yet, this clade is poorly supported by ML, well supported (but just so) by NJ, and convincingly well supported by BI. The position of *M. macrurus* comb. nov. within this clade, however, is poorly supported by the three methods.

Taxonomy

Class DIPLOPODA de Blainville in Gervais, 1844
Order SPIROBOLIDA Bollman, 1893
Suborder TRIGONIULIDEA Attems, 1909
Family PACHYBOLIDAE Cook, 1897

Genus *Macrurobolus* gen. nov.
http://zoobank.org/A428FDFE-D777-4B7B-8D29-F603088A0AC2
Figures 1–5

Diagnosis. A genus of Pachybolidae characterised by the following combination of characters: preanal ring with long process protruding beyond anal valves; the anterior gonopod telopodite distally abruptly narrowed, forming an extremely long, slender, elevated process curved caudad.

Etymology. The generic name is a combination of the name of the type species and "-bolus", the ending of many pachybolid genus names.

Type species. *Macrurobolus macrurus* (Pocock, 1893) comb. nov.
Spirobolus macrurus Pocock 1893: 396.
Tonkinbolus macrurus: Hoffman 1962: 773.
Atopochetus macrurus: Pimvichai et al. 2018: 174.

***Macrurobolus macrurus* (Pocock, 1893), comb. nov.** The original description was based exclusively on a female from "Kawkareet" (Tenasserim), Myanmar (see Distribution section for information on this locality). Pocock (1893) described the female external morphology and mentioned that this species differed from *Spirobolus caudulanus* [= *Atopochetus caudulanus* (Karsch, 1881)] and *Spirobolus moulmeinensis* [= *Atopochetus moulmeinensis* (Pocock, 1893)] by having a "much longer and thinner tail".

Material studied. Thailand, 1 ♂, 3 ♀♀; Tak Province, Mae Sot District, Wat Tham Inthanin; 16°45'59"N, 98°40'21"E; 660 m a.s.l.; 27 July 2016; P. Pimvichai, T. Backeljau and P. Prasankok leg. (CUMZ). • Myanmar, 1 ♂; Meetan; Fea; "ex typ."; NHMD 621698.

Description of Thai specimens. Adult male with 51 podous rings, no apodous rings. Length ca 11 cm, diameter ca 9.0 mm. Adult females with 48–51 podous rings, no apodous rings. Length ca 10–11 cm, diameter ca 10.0–10.4 mm.

Head capsule smooth, area below antennal sockets with wrinkles (Fig. 2A). Occipital furrow extending down between, but not beyond eyes; clypeal furrow reaching level of antennal sockets. Area below antennal sockets and eyes impressed, forming part of antennal furrow. Incisura lateralis open. 2+2 labral teeth, a row of labral setae, 1+1 supralabral setae (mentioned as "the labral region furnished with 4 punctures" by Pocock 1893: 401). Diameter of eyes ca half of interocular space; 9 vertical rows of ommatidia, 8 horizontal rows, 53–55 ommatidia per eye. Antennae short, not reaching beyond collum when stretched back, accommodated in a shallow furrow composed of a horizontal segment in the head capsule and a vertical segment in the mandibular cardo and stipes. Antennomere lengths 2 > 3 = 5 > 4 > 6 > 1 > 7; antennomere 1 glabrous, 2 and 3 with some ventral setae, 4, 5 and 6 densely setose; 4 apical sensilla. Mandibles: stipes (Mst) broad at base, apically gradually narrowed. Gnathochilarium (Fig. 2B): each stipes (Gst) with 3 apical setae; each lamella lingualis with 2 setae, one behind the other. Basal part of mentum (Me) transversely wrinkled; basal part of stipites longitudinally wrinkled.

Collum smooth, with a marginal furrow along lateral part of anterior margin; lateral lobes narrowly rounded, extending as far ventrad as the ventral margin of body ring 2.

Body rings 2–5 ventrally concave, hence with distinct ventrolateral "corners". Body rings very smooth, parallel-sided in dorsal view. Prozona smooth. 'Tergo-pleural' suture visible on pro- and mesozona; mesozona ventrally with fine oblique striae, dorsally punctate; metazona ventrally with fine longitudinal striae, otherwise smooth. "Pleural" parts of rings with fine oblique striae. Sterna transversely striate. Ozopores from ring 6, situated in mesozona, ca 1/2 pore diameter in front of metazona (mentioned as "the repugnatorial pores situated in front of the transverse sulcus" by Pocock 1893: 401).

Telson smooth; preanal ring with slightly concave dorsal profile, with thick and long process protruding beyond anal valves (Fig. 2C). Anal valves (Av) impressed submarginally (Fig. 2D); margins hence distinctly protruding, liplike. Subanal scale (Sub) broadly triangular.

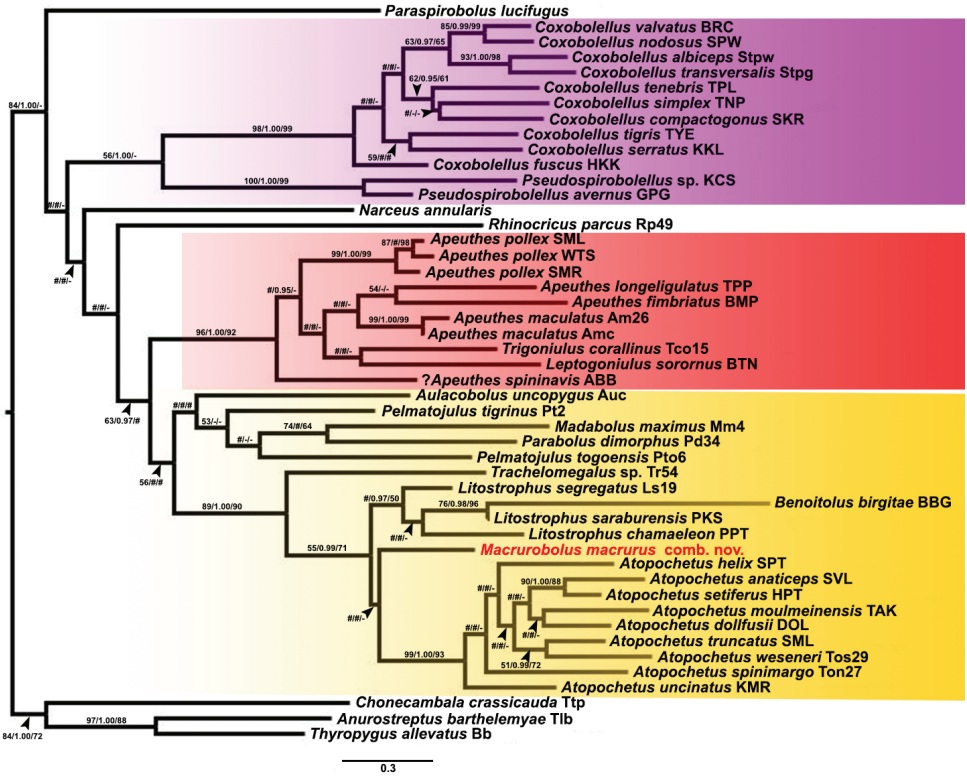

Figure 1. Phylogenetic relationships of pachybolid and several other spirobolidan millipede species based on maximum likelihood analysis (ML) of a 660 bp COI gene fragment. Numbers at nodes indicate branch support based on bootstrapping (ML) / posterior probabilities (BI) / bootstrapping (NJ). Scale bar: 0.3 substitutions/site. # indicates branches with < 50% ML and NJ bootstrap support or < 0.95 posterior probability, - indicates non-supported branches. The coloured areas mark the Pseudospirobolellidae (minus *Benoitolus*) (purple), Trigoniulinae (red), and non-trigoniuline Pachybolidae (plus *Benoitolus*) (yellow).

Legs (Fig. 2E): length of midbody legs 72–77% of body diameter in males, 54–56% of body diameter in females. Prefemur basally constricted, tarsus longer than other podomeres. First and second legs with 2 or 3 prefemoral, 2 or 3 femoral, 2 or 3 postfemoral, and 2–4 tibial setae, and 4 or 5 ventral and 1 dorsal apical setae on tarsi, numbers of setae reaching constancy from pair 3: each leg podomere from coxa to tibia with 1 seta; tarsi with 2 ventral apical and 1 dorsal apical seta, the apical ventral seta larger than the more basal one. Claw very slender, more than half as long as tarsus.

Colour. Living animal reddish brown except for grey pro- and mesozona (Fig. 4).

Male sexual characters. Tarsus from third to before the last 4 body rings with large ventral soft pad occupying entire ventral surface. Body ring 7 entirely fused ventrally, no trace of a suture. Tip of anterior gonopods visible when the animal is stretched out (not when it is rolled up).

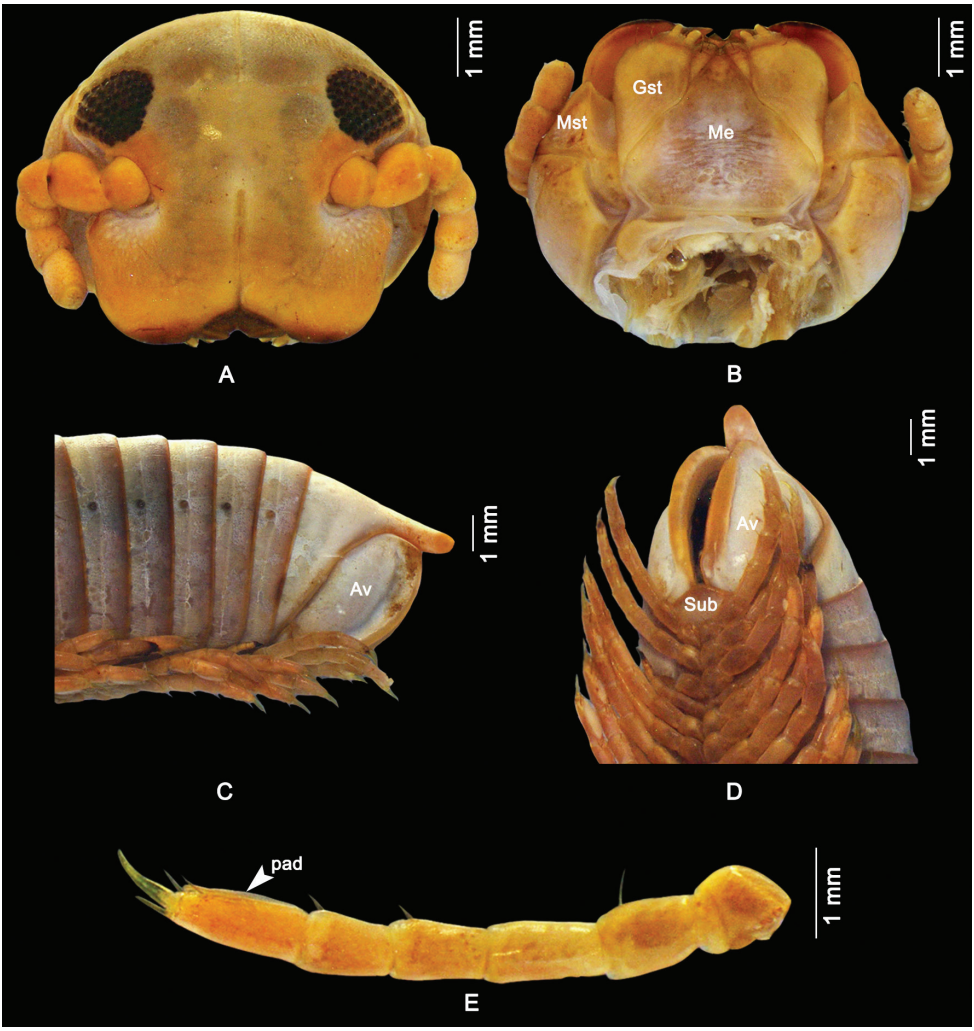

Figure 2. External morphology of a male *Macrurobolus macrurus* comb. nov. from Wat Tham Inthanin, Thailand, CUMZ-D00147-1 **A** head, frontal view **B** gnathochilarium, ventral view **C** posterior end, lateral view **D** posterior end, latero-ventral view **E** midbody leg, latero-ventral view. Av = anal valves; Gst = gnathochilarial stipes; Me = mentum; Mst = mandibular stipes; Sub = subanal scale.

Anterior gonopods (Fig. 3A, B, D, E) with triangular mesal sternal process, not reaching so far as the tip of coxae, apical margin bilobed, with basal longitudinal triangular ridge in posterior view. Coxa oval, apically gradually narrowed, rounded, projecting slightly beyond sternal process. Telopodite apically far overreaching coxa, distally abruptly narrowed, forming an extremely long, slender, elevated process curved caudad.

Posterior gonopods (Fig. 3C, F, H–I) strongly curved mesad, laterally with a massive ridge; with efferent canal (Enghoff 2011) running along mesal margin terminating in slender, pointed meso-distad process, covered with fine hairlike spinules

Table 2. Estimates of COI sequence divergences (uncorrected *p*-distances) within and among Pachybolidae species and related taxa (rounded to two decimals).

1	***Macrurobolus macrurus* comb. nov.**	1	2	3	4	5	6	7	8	9	10	11	12	13	14	15	16	17	18	19	20	21	22	23	24	25	26	27
2	*Apeuthes longeligulatus* TPP	0.18																										
3	*?Apeuthes spininavis* ABB	0.18	0.14																									
4	*Apeuthes fimbriatus* BMP1	0.21	0.15	0.16																								
5	*Apeuthes pollex* SML	0.18	0.14	0.15	0.15																							
6	*Apeuthes pollex* SMR	0.18	0.14	0.14	0.15	0.06																						
7	*Apeuthes pollex* WTS	0.18	0.15	0.15	0.15	0.04	0.07																					
8	*Apeuthes maculatus* Amc	0.17	0.11	0.12	0.14	0.11	0.11	0.11																				
9	*Apeuthes maculatus* Am26	0.18	0.13	0.14	0.15	0.13	0.13	0.13	0.03																			
10	*Atopochetus anaticeps* SVL	0.16	0.20	0.19	0.23	0.18	0.18	0.19	0.19	0.20																		
11	*Atopochetus dollfusii* DOL	0.14	0.19	0.20	0.22	0.19	0.19	0.20	0.20	0.21	0.11																	
12	*Atopochetus helix* SPT	0.15	0.23	0.19	0.22	0.20	0.21	0.20	0.21	0.22	0.14	0.13																
13	*Atopochetus moulmeinensis* TAK	0.17	0.22	0.22	0.23	0.22	0.23	0.23	0.22	0.23	0.14	0.12	0.15															
14	*Atopochetus setiferus* HPT	0.14	0.20	0.20	0.22	0.18	0.18	0.19	0.19	0.20	0.08	0.09	0.14	0.13														
15	*Atopochetus spinimargo* Ton27	0.17	0.22	0.22	0.22	0.21	0.20	0.20	0.22	0.22	0.15	0.14	0.14	0.16	0.14													
16	*Atopochetus truncatus* SML	0.15	0.20	0.20	0.22	0.20	0.19	0.21	0.19	0.21	0.13	0.10	0.12	0.14	0.12	0.14												
17	*Atopochetus uncinatus* KMR	0.16	0.21	0.20	0.21	0.19	0.20	0.20	0.20	0.22	0.13	0.14	0.14	0.15	0.13	0.15	0.13											
18	*Atopochetus weseneri* Tos29	0.16	0.21	0.20	0.21	0.21	0.20	0.22	0.20	0.21	0.14	0.12	0.14	0.13	0.12	0.16	0.10	0.13										
19	*Aulacobolus uncopygus* Auc	0.17	0.17	0.18	0.20	0.16	0.17	0.17	0.17	0.18	0.18	0.18	0.20	0.21	0.19	0.22	0.19	0.20	0.22									
20	*Coxobolellus albiceps* Stpw	0.21	0.18	0.21	0.20	0.18	0.17	0.18	0.18	0.19	0.20	0.22	0.22	0.24	0.22	0.23	0.21	0.21	0.22	0.18								
21	*Coxobolellus compactogonus* SKR	0.23	0.18	0.19	0.21	0.19	0.18	0.19	0.19	0.21	0.21	0.21	0.22	0.24	0.21	0.23	0.21	0.21	0.22	0.19	0.14							
22	*Coxobolellus fuscus* HKK	0.22	0.19	0.20	0.20	0.17	0.18	0.18	0.20	0.21	0.20	0.22	0.22	0.24	0.20	0.23	0.23	0.20	0.23	0.19	0.12	0.13						
23	*Coxobolellus nodosus* SPW	0.21	0.18	0.20	0.22	0.18	0.19	0.19	0.20	0.20	0.21	0.20	0.21	0.24	0.21	0.23	0.22	0.22	0.23	0.18	0.11	0.13	0.11					
24	*Coxobolellus serratus* KKL	0.21	0.18	0.20	0.20	0.18	0.18	0.18	0.18	0.20	0.20	0.21	0.22	0.23	0.20	0.23	0.21	0.22	0.22	0.19	0.13	0.14	0.12	0.13				
25	*Coxobolellus simplex* TNP	0.20	0.18	0.18	0.20	0.18	0.18	0.18	0.19	0.20	0.21	0.22	0.21	0.23	0.22	0.23	0.23	0.23	0.22	0.20	0.13	0.12	0.12	0.12	0.11			
26	*Coxobolellus tenebris* TPL	0.22	0.19	0.18	0.21	0.18	0.18	0.18	0.18	0.20	0.21	0.22	0.23	0.25	0.22	0.24	0.23	0.23	0.23	0.19	0.13	0.10	0.12	0.12	0.14	0.11		
27	*Coxobolellus tigris* TYE	0.23	0.19	0.21	0.22	0.20	0.20	0.20	0.20	0.20	0.19	0.22	0.22	0.25	0.21	0.24	0.22	0.22	0.22	0.21	0.13	0.14	0.12	0.13	0.12	0.13	0.15	
28	*Coxobolellus transversalis* Stpg	0.21	0.18	0.20	0.21	0.18	0.18	0.19	0.18	0.19	0.20	0.20	0.20	0.23	0.21	0.21	0.20	0.22	0.22	0.18	0.08	0.15	0.12	0.11	0.12	0.12	0.14	0.13
29	*Coxobolellus valvatus* BRC	0.21	0.17	0.19	0.20	0.16	0.16	0.17	0.17	0.18	0.20	0.21	0.20	0.24	0.20	0.23	0.22	0.22	0.22	0.17	0.10	0.13	0.11	0.07	0.13	0.12	0.12	0.13
30	*Paraspirobolus lucifugus*	0.25	0.25	0.22	0.23	0.22	0.22	0.22	0.22	0.23	0.23	0.23	0.23	0.23	0.23	0.23	0.23	0.23	0.24	0.24	0.24	0.23	0.23	0.24	0.25	0.25	0.24	0.24
31	*Leptogoniulus sorornus* BTN	0.18	0.16	0.14	0.16	0.14	0.14	0.15	0.13	0.14	0.18	0.18	0.19	0.21	0.19	0.20	0.19	0.22	0.22	0.17	0.21	0.20	0.20	0.19	0.19	0.18	0.20	0.20
32	*Litostrophus chamaeleon* PPT	0.14	0.20	0.19	0.20	0.18	0.18	0.20	0.18	0.19	0.17	0.16	0.15	0.18	0.16	0.18	0.15	0.17	0.17	0.19	0.20	0.21	0.20	0.20	0.20	0.21	0.21	0.20
33	*Litostrophus saraburensis* PKS	0.11	0.18	0.18	0.20	0.18	0.17	0.18	0.16	0.17	0.16	0.15	0.15	0.17	0.15	0.16	0.14	0.16	0.18	0.18	0.18	0.20	0.19	0.19	0.20	0.20	0.20	0.20
34	*Litostrophus segregatus* Ls19	0.13	0.19	0.19	0.20	0.18	0.18	0.19	0.18	0.20	0.13	0.13	0.15	0.16	0.13	0.15	0.14	0.14	0.17	0.18	0.21	0.21	0.21	0.21	0.20	0.22	0.21	0.21
35	*Madabolus maximus* Mm4	0.19	0.20	0.18	0.20	0.19	0.19	0.20	0.20	0.21	0.21	0.20	0.19	0.22	0.22	0.21	0.20	0.20	0.22	0.18	0.20	0.23	0.22	0.21	0.22	0.22	0.24	0.22
36	*Narceus annularis*	0.20	0.21	0.20	0.20	0.21	0.21	0.21	0.21	0.22	0.23	0.20	0.21	0.22	0.21	0.20	0.20	0.21	0.21	0.20	0.22	0.23	0.21	0.23	0.22	0.22	0.23	0.22
37	*Parabolus dimorphus* Pd34	0.20	0.21	0.21	0.22	0.19	0.19	0.19	0.20	0.21	0.18	0.20	0.19	0.22	0.18	0.20	0.21	0.19	0.21	0.19	0.18	0.22	0.19	0.18	0.20	0.20	0.20	0.17
38	*Pelmatojulus tigrinus* Pt2	0.18	0.18	0.18	0.19	0.18	0.17	0.19	0.17	0.18	0.22	0.22	0.20	0.23	0.22	0.23	0.22	0.22	0.22	0.16	0.20	0.20	0.20	0.21	0.22	0.22	0.22	0.20
39	*Pelmatojulus togoensis* Pto6	0.21	0.19	0.20	0.18	0.18	0.17	0.17	0.18	0.20	0.21	0.22	0.22	0.22	0.20	0.20	0.21	0.20	0.21	0.17	0.19	0.20	0.20	0.19	0.19	0.21	0.20	0.20
40	*Pseudospirobolellus avernus* GPG	0.21	0.21	0.19	0.23	0.19	0.20	0.20	0.20	0.22	0.21	0.22	0.22	0.23	0.21	0.23	0.22	0.23	0.23	0.20	0.20	0.21	0.20	0.21	0.20	0.21	0.21	0.20
41	*Pseudospirobolellus* sp. KCS	0.23	0.22	0.22	0.22	0.22	0.22	0.21	0.23	0.23	0.23	0.23	0.21	0.23	0.23	0.22	0.22	0.23	0.23	0.22	0.22	0.22	0.21	0.21	0.22	0.22	0.23	0.22
42	*Rhinocricus parcus* Rp49	0.24	0.24	0.23	0.23	0.23	0.23	0.22	0.23	0.24	0.24	0.21	0.22	0.22	0.24	0.21	0.23	0.22	0.23	0.22	0.25	0.25	0.25	0.25	0.25	0.25	0.25	0.24
43	*Trachelomegalus* sp. Tr54	0.19	0.20	0.19	0.20	0.19	0.19	0.20	0.20	0.22	0.19	0.18	0.17	0.20	0.19	0.18	0.18	0.18	0.18	0.20	0.21	0.22	0.24	0.23	0.22	0.22	0.23	0.24
44	*Trigoniulus corallinus* Tco15	0.18	0.15	0.14	0.13	0.13	0.13	0.14	0.12	0.12	0.18	0.19	0.20	0.23	0.19	0.20	0.20	0.21	0.21	0.17	0.18	0.18	0.17	0.18	0.19	0.17	0.18	0.17
45	*Anurostreptus barthelemyae* Tlb	0.23	0.21	0.21	0.22	0.20	0.20	0.19	0.21	0.22	0.22	0.22	0.23	0.24	0.23	0.22	0.24	0.23	0.24	0.20	0.19	0.21	0.19	0.19	0.20	0.19	0.20	0.19
46	*Chonecambala crassicauda*	0.24	0.23	0.22	0.21	0.22	0.22	0.21	0.21	0.23	0.24	0.24	0.24	0.23	0.24	0.23	0.24	0.22	0.24	0.22	0.23	0.23	0.22	0.23	0.22	0.22	0.23	0.22
47	*Thyropygus allevatus* Bb	0.21	0.21	0.21	0.21	0.20	0.21	0.20	0.21	0.22	0.21	0.21	0.22	0.23	0.23	0.23	0.22	0.21	0.24	0.20	0.20	0.19	0.20	0.20	0.19	0.19	0.20	0.19

Table 2. Continued.

1	***Macrurobolus macrurus* comb. nov.**	28	29	30	31	32	33	34	35	36	37	38	39	40	41	42	43	44	45	46
2	*Apeuthes longeligulatus* TPP																			
3	*?Apeuthes spininavis* ABB																			
4	*Apeuthes fimbriatus* BMP1																			
5	*Apeuthes pollex* SML																			
6	*Apeuthes pollex* SMR																			
7	*Apeuthes pollex* WTS																			
8	*Apeuthes maculatus* Amc																			
9	*Apeuthes maculatus* Am26																			
10	*Atopochetus anaticeps* SVL																			
11	*Atopochetus dollfusii* DOL																			
12	*Atopochetus helix* SPT																			
13	*Atopochetus moulmeinensis* TAK																			
14	*Atopochetus setiferus* HPT																			
15	*Atopochetus spinimargo* Ton27																			
16	*Atopochetus truncatus* SML																			
17	*Atopochetus uncinatus* KMR																			
18	*Atopochetus weseneri* Tos29																			
19	*Aulacobolus uncopygus* Auc																			
20	*Coxobolellus albiceps* Stpw																			
21	*Coxobolellus compactogonus* SKR																			
22	*Coxobolellus fuscus* HKK																			
23	*Coxobolellus nodosus* SPW																			
24	*Coxobolellus serratus* KKL																			
25	*Coxobolellus simplex* TNP																			
26	*Coxobolellus tenebris* TPL																			
27	*Coxobolellus tigris* TYE																			
28	*Coxobolellus transversalis* Stpg																			
29	*Coxobolellus valvatus* BRC	0.11																		
30	*Paraspirobolus lucifugus*	0.24	0.23																	
31	*Leptogoniulus sorornus* BTN	0.19	0.19	0.24																
32	*Litostrophus chamaeleon* PPT	0.21	0.20	0.24	0.18															
33	*Litostrophus sarahurensis* PKS	0.18	0.19	0.24	0.18	0.11														
34	*Litostrophus segregatus* Ls19	0.20	0.20	0.25	0.18	0.11	0.09													
35	*Madabolus maximus* Mm4	0.21	0.20	0.24	0.20	0.19	0.18	0.20												
36	*Narceus annularis*	0.22	0.22	0.21	0.21	0.20	0.20	0.21	0.20											
37	*Parabolus dimorphus* Pd34	0.19	0.18	0.25	0.21	0.19	0.18	0.20	0.17	0.20										
38	*Pelmatojulus tigrinus* Pt2	0.21	0.19	0.24	0.19	0.20	0.20	0.20	0.18	0.19	0.19									
39	*Pelmatojulus togoensis* Pto6	0.20	0.18	0.25	0.18	0.18	0.18	0.19	0.19	0.20	0.18	0.17								
40	*Pseudospirobolellus avernus* GPG	0.20	0.21	0.22	0.19	0.23	0.21	0.21	0.21	0.22	0.23	0.20	0.21							
41	*Pseudospirobolellus* sp. KCS	0.22	0.22	0.22	0.21	0.23	0.22	0.22	0.24	0.22	0.21	0.22	0.22	0.14						
42	*Rhinocricus parcus* Rp49	0.25	0.24	0.22	0.22	0.22	0.23	0.23	0.22	0.20	0.23	0.21	0.22	0.22	0.21					
43	*Trachelomegalus* sp. Tr54	0.22	0.23	0.24	0.21	0.18	0.17	0.15	0.21	0.21	0.21	0.19	0.21	0.22	0.20	0.22				
44	*Trigoniulus corallinus* Tco15	0.17	0.16	0.23	0.14	0.18	0.16	0.17	0.18	0.20	0.19	0.18	0.17	0.23	0.22	0.23	0.20			
45	*Anurostreptus barthelemyae* Tlb	0.19	0.18	0.23	0.22	0.21	0.20	0.22	0.22	0.21	0.21	0.21	0.20	0.22	0.21	0.23	0.23	0.19		
46	*Chonecambala crassicauda*	0.22	0.21	0.23	0.21	0.23	0.22	0.24	0.24	0.23	0.21	0.22	0.24	0.23	0.23	0.23	0.22	0.22	0.19	
47	*Thyropygus allevatus* Bb	0.20	0.19	0.22	0.20	0.21	0.20	0.22	0.21	0.20	0.21	0.23	0.21	0.22	0.22	0.21	0.24	0.20	0.15	0.20

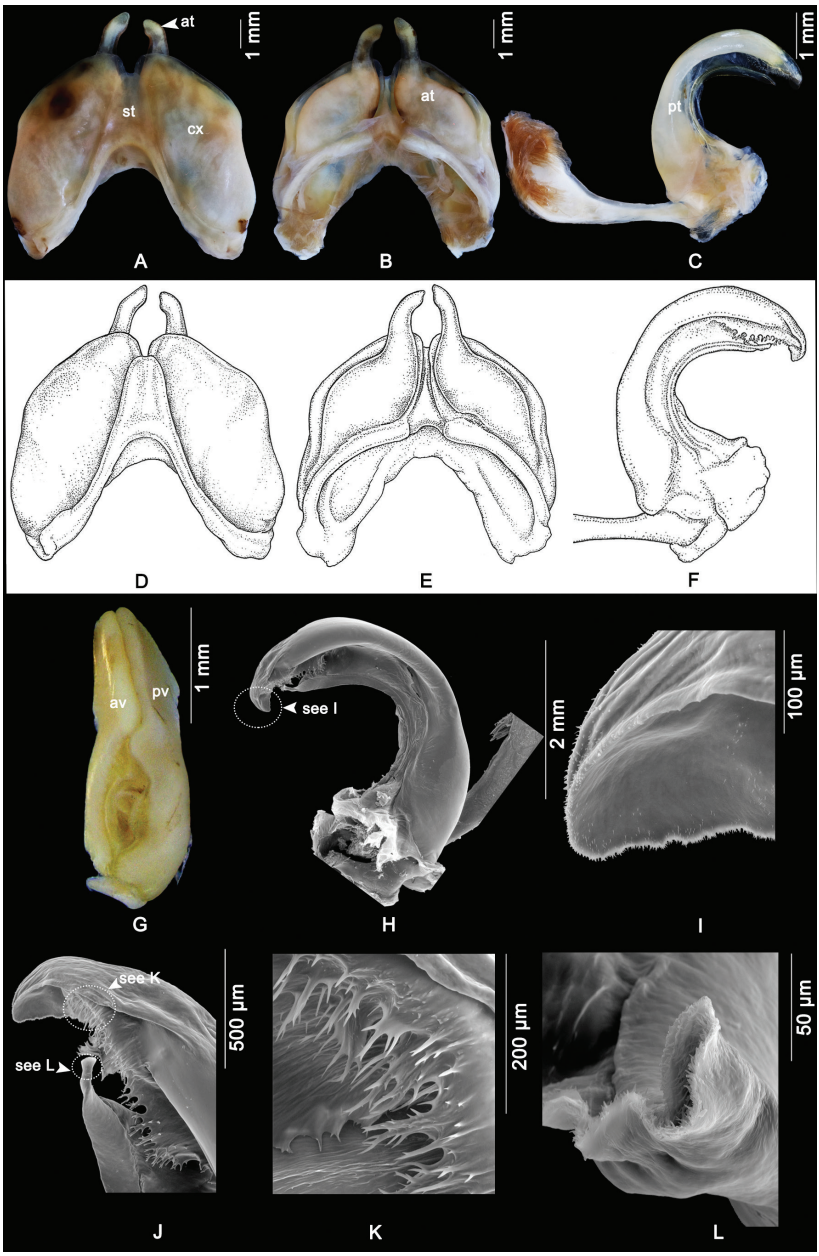

Figure 3. Male (A–F, H–L) and female (G) genital parts of *Macrurobolus macrurus* comb. nov. (specimens from Wat Tham Inthanin, Thailand, CUMZ-D00147-1) **A** anterior gonopod, anterior view **B** anterior gonopod, posterior view **C** right posterior gonopod, posterior-mesal view **D** anterior gonopod, anterior view **E** anterior gonopod, posterior view **F** right posterior gonopod, posterior-mesal view **G** left female vulva, posterior mesal view **H–L** SEM **H** left posterior gonopod, posterior-mesal view **I** tip of posterior gonopod, mesal view **J** apical part of posterior gonopod, mesal view **K** spiny lamellae near tip of posterior gonopod, mesal view **L** meso-distad process of posterior gonopod, posterior-mesal view. at = anterior gonopod telopodite; av = anterior valve; cx = coxa; pt = posterior gonopod telopodite; pv = posterior valve; st = sternum.

Figure 4. Live female *Macrurobolus macrurus* comb. nov. from Wat Tham Inthanin, Thailand (CUMZ-D00147-3).

(Fig. 3L); tip of posterior gonopod concave, apically ending in a rounded lobe (Fig. 3I, showed serrated margin, dorsally covered with short spines); with spiny lamellae mesally near tip.

Female vulvae (Fig. 3G). Valves prominent, of equal size; basally with open space between free margins.

DNA barcode. The GenBank accession number of the COI barcode of the Thai specimen is MZ905519 (voucher code CUMZ-D00147).

Ecology. Found under leaf litter.

Notes on the male from Meetan, Myanmar. This specimen is labelled as "ex typ" in the NHMD collection and was, like the female type specimen, collected by Fea. It agrees with the Thai male in all characters, including all details of gonopod shape, with the following exceptions: Colour after > 100 years in alcohol is faded, but there is still a clear contrast between greyish pro- and mesozone and reddish-brown metazona. Size: length ca 8 cm, diameter 6.7 mm, 50 podous rings, no apodous rings in front of telson. Head capsule smooth. 11 vertical rows of ommatidia, of which 3 are very incomplete, 7 horizontal rows, 47 ommatidia per eye. Antennomeres 2–4 with some ventral setae, 5 and 6 densely setose. Gnathochilarium not dissected.

Distribution. Tak Province, Thailand; Kawkareet (Tenasserim) and Meetan, Myanmar (Fig. 5). The names Kawkareet and Meetan do not appear on maps available to us. However, Brandis (2002: 1312) mentioned "Meetan (= Mitan Chaung (= river) 15°59'00"N 98°24'00"E at the south-west slope of the Dawna mountain", whereas Randall and Page (2012: 344) located Meetan at "16.555556°N, 98.24°E (coordinates estimated)". Annandale (1911: 118) stated that Kawkareet refers to Kawkareik and remarked in a footnote that "This locality [i.e. Kawkareik] is often referred to in zoological literature as Kawkareet or Kawkarit, or even Kokarit". Finally, Likhitrakarn et al. (2017) located Kawkareet (= Kawkareik) at 16°33'20"N, 98°14'24"E and Meetan (= Mi Tan) at 16°00'12"N, 98°23'25"E.

Figure 5. Distribution of *Macrurobolus macrurus* comb. nov.

Discussion

The male specimen of *Spirobolus macrurus* from Meetan in NHMD, although labelled "ex typ.", should not a priori be regarded as a type (ICZN Art. 72.4.7.) because Pocock (1893: 396) explicitly mentioned that the species description was based on "A single ♀ from Kawkareet (Tenasserim)". However, its non-sexual characters agree with Pocock's (1893) description. Hence, we do not hesitate to refer it to *Macrurobolus macrurus* comb. nov.

The new male specimen from Thailand and the old specimen from Myanmar share the long preanal ring process with the female type specimen, which is a remarkable character for a pachybolid, since most pachybolid genera (except *Aulacobolus* Pocock, 1903 and *Trachelomegalus* Silvestri, 1896) have a short preanal ring process. So, in this respect, *Macrurobolus* gen. nov. is clearly differentiated from most other pachybolid genera, including *Atopochetus* and *Litostrophus*, the two genera with which *Macrurobolus* gen. nov. appears the be most closely related in our phylogenetic tree (Fig. 1). Similarly, the anterior gonopod telopodites of *Macrurobolus* (telopodite distally abruptly

Table 3. Estimates of COI mean sequence divergences within (on diagonal) and among (below diagonal) pachybolid and pseudospirobolellid genera (range in parentheses) (data based on Pimvichai et al. 2018, 2020, 2022).

	1	2	3	4	5
1. *Apeuthes*	14 (11–16)				
2. *Atopochetus*	21 (18–23)	13 (8–16)			
3. *Coxobolellus*	19 (16–22)	22 (19–25)	12 (7–15)		
4. *Litostrophus*	19 (16–20)	16 (13–18)	20 (18–22)	11 (9–11)	
5. *Pseudospirobolellus*	21 (19–23)	22 (21–23)	21 (20–23)	22 (21–23)	14
6. *Macrurobolus macrurus* comb. nov.	18 (18–21)	15 (14–17)	21 (20–23)	13 (11–14)	22 (21–23)

narrowed, forming an extremely long, slender, elevated process curved caudad) clearly differ from those of *Litostrophus* (telopodite simple, without process, narrowly rounded) or *Atopochetus* (telopodite with a triangular process directed laterad originating on posterior surface at ~1/2 or 2/3–4/5 of its height). Hence, given that *Macrurobolus* shares neither the defining morphological synapomorphies of *Atopochetus*, nor those of *Litostrophus*, we think that the creation as a separate monotypic genus is warranted.

The interpretation of *Macrurobolus* as a separate genus is somehow in line with the COI tree (Fig. 1), which places the new genus in a clade comprising *Atopochetus* and *Litostrophus*, but which supports neither joining *M. macrurus* comb. nov. with *Atopochetus* (which itself forms a consistently well-supported clade), nor joining it with *Litostrophus* (which itself forms also a well-supported clade) (Fig. 1). Moreover, the mean interspecific COI sequence divergence between *M. macrurus* and other pachybolid and pseudospirobolellid species is 18% (range: 11–23%) (Tables 2, 3), a value that rather points to an intergeneric divergence (Table 3).

In conclusion, this study suggests that Pimvichai et al. (2018) appropriately labelled the transfer of *Tonkinbolus macrurus* to the genus *Atopochetus* as "incertae sedis". Indeed, the species can be accommodated in neither *Atopochetus* nor *Litostrophus*, i.e., the two genera with which it appears to be most closely associated. Hence, it would be ill-advised to maintain *Macrurobolus macrurus* comb. nov. in the genus *Atopochetus*, for this would undermine both the definition and the support of the monophyly of this taxon. Therefore, the creation of the monotypic genus *Macrurobolus* gen. nov. seems the best solution to provide a generic name for *Spirobolus macrurus* Pocock, 1893. Still, the monotypy of *Macrurobolus* gen. nov. renders it aphyletic *sensu* Ebach and Williams (2010), and hence in need of further study (Williams and Ebach 2020: 134).

Acknowledgements

This research was funded by the Thailand Science Research and Innovation (TSRI) together with Mahasarakham University as a TRF Research Career Development Grant (2019–2022; RSA6280051) (to P. Pimvichai). Additional funding came from the Roy-

al Belgian Institute of Natural Sciences (RBINS). We thank, Pongpun Prasankok for assistance in collecting material. We are indebted to Julien Cillis (RBINS) for help with SEM photographs, to Yves Barette (RBINS) for help with gonopod photographs and to Thita Krutchuen for the excellent drawings. Last but not least, we thank Thomas Wesener (Bonn) and Sergei Golovatch (Moscow) for their helpful reviews of this paper.

References

Annandale N (1911) The Fauna of Britih India, including Ceylon and Burma. Freshwater Sponges, Hydroids & Polyzoa. Taylor and Francis, London.

Brandis D (2002) On the taxonomic status and biogeography of the Isolapotamidae Bott, 1970 (Decapoda, Brachyura). Journal of Natural History 36: 1291–1339. https://doi.org/10.1080/00222930110051743

Ebach MC, Williams DM (2010) Aphyly: a systematic designation for a taxonomic problem. Evolutionary Biology 37: 123–127. https://doi.org/10.1007/s11692-010-9084-5

Edgar RC (2004) MUSCLE: multiple sequence alignment with high accuracy and high throughput. Nucleic Acids Research 32: 1792–1797. https://doi.org/10.1093/nar/gkh340

Enghoff H (2011) East African giant millipedes of the tribe Pachybolini (Diplopoda, Spirobolida, Pachybolidae). Zootaxa 2753: 1–41. https://doi.org/10.11646/zootaxa.2753.1.1

Folmer O, Black M, Hoeh W, Lutz R, Vrijenhoek R (1994) DNA primers for amplification of mitochondrial cytochrome c oxidase subunit I from diverse metazoan invertebrates. Molecular Marine Biology and Biotechnology 3: 294–299.

Hebert PDN, Cywinska A, Ball SL, DeWaard JR (2003) Biological identifications through DNA barcodes. Proceedings of the Royal Society London Series B 270: 313–321. https://doi.org/10.1098/rspb.2002.2218

Hillis D, Bull J (1993) An empirical test of bootstrapping as a method for assessing confidence in phylogenetic analysis. Systematic Biology 42: 182–192. https://doi.org/10.1093/sysbio/42.2.182

Hoffman RL (1962) Studies on spiroboloid millipeds IV. Systematic and nomenclatorial notes on the family Pachybolidae. Revue Suisse de Zoologie 69 : 759–783. https://doi.org/10.5962/bhl.part.75592

Huelsenbeck JP, Ronquist F (2001) MRBAYES: Bayesian inference of phylogeny. Bioinformatics 17: 754–755. https://doi.org/10.1093/bioinformatics/17.8.754

Kumar S, Stecher G, Li M, Knyaz C, Tamura K (2018) MEGA X: Molecular Evolutionary Genetics Analysis across computing platforms. Molecular Biology and Evolution 35: 1547–1549. https://doi.org/10.1093/molbev/msy096

Lanfear R, Frandsen PB, Wright AM, Senfeld T, Calcott B (2017) PartitionFinder 2: new methods for selecting partitioned models of evolution for molecular and morphological phylogenetic analyses. Molecular Biology and Evolution 34: 772–773. https://doi.org/10.1093/molbev/msw260

Likhitrakarn N, Jirapatrasilp P, Golovatch S, Panha S (2017) A checklist of the millipedes (Diplopoda) of Myanmar, with an updated list of Leonardo Fea's collecting localities. Zootaxa 4350: 001–0046. https://doi.org/10.11646/zootaxa.4350.1.1

Miller MA, Pfeiffer W, Schwartz T (2010) Creating the CIPRES Science Gateway for inference of large phylogenetic trees. In: IEEE 'Proceedings of the Gateway Computing Environments Workshop (GCE)', 14 November 2010, New Orleans, LA, USA. INSPEC Accession Number: 11705685, 1–8. https://doi.org/10.1109/GCE.2010.5676129

Pimvichai P, Enghoff H, Panha S, Backeljau T (2018) Morphological and mitochondrial DNA data reshuffle the taxonomy of the genera *Atopochetus* Attems, *Litostrophus* Chamberlin and *Tonkinbolus* Verhoeff (Diplopoda: Spirobolida: Pachybolidae), with descriptions of nine new species. Invertebrate Systematics 32: 159–195. https://doi.org/10.1071/IS17052

Pimvichai P, Enghoff H, Panha S, Backeljau T (2020) Integrative taxonomy of the new millipede genus *Coxobolellus*, gen. nov. (Diplopoda: Spirobolida: Pseudospirobolellidae), with descriptions of ten new species. Invertebrate Systematics 34(6): 591–617. https://doi.org/10.1071/IS20031

Pimvichai P, Panha S, Backeljau T (2022) Combining mitochondrial DNA and morphological data to delineate four new millipede species and provisional assignment to the genus *Apeuthes* Hoffman & Keeton (Diplopoda: Spirobolida: Pachybolidae: Trigoniulinae). Invertebrate Systematics 36(2): 91–112. https://doi.org/10.1071/IS21038

Pocock RI (1893) Viaggio di Leonardo Fea in Birmania e regioni vicine LV. On the Myriopoda of Burma. Pt 3. Report upon the Julidae, Chordeumidae and Polyzonidae collected by Sig. L. Fea and Mr. E.W. Oates. Annali del Museo civico di Storia naturale di Genova 33: 386–406.

Randall ZS, Page LM (2012) Resurrection of the genus *Homalopteroides* (Teleostei: Balitoridae) with a redescription of *H. modestus* (Vinciguerra 1890). Zootaxa 3586: 329–346. https://doi.org/10.11646/zootaxa.3586.1.31

San Mauro D, Agorreta A (2010) Molecular systematics: a synthesis of the common methods and the state of knowledge. Cellular & Molecular Biology Letters 15: 311–341. https://doi.org/10.2478/s11658-010-0010-8

Stamatakis A (2014) RAxML version 8: a tool for phylogenetic analysis and post-analysis of large phylogenies. Bioinformatics 30: 1312–1313. https://doi.org/10.1093/bioinformatics/btu033

Williams DM, Ebach MC (2020) Cladistics – a Guide to Biological Classification (3rd edn.). Systematics Association Special Volume 88, Cambridge University Press, UK.

Xia X (2018) DAMBE7: new and improved tools for data analysis in molecular biology and evolution. Molecular Biology and Evolution 35: 1550–1552. https://doi.org/10.1093 /molbev/msy073

Supplementary material 1

Redescription of the giant SE Asian millipede *Spirobolus macrurus* Pocock, 1893 and its assignment to the new genus *Macrurobolus* gen. nov. (Diplopoda, Spirobolida, Pachybolidae)

Authors: Piyatida Pimvichai, Henrik Enghoff, Thierry Backeljau

Data type: Jpg file.

Explanation note: Phylogenetic relationships of pachybolid and several other spiroboloidan millipede species (excluding *Benoitolus birgitae*) based on maximum likelihood analysis (ML) of a 660 bp COI gene fragment.

Link: https://doi.org/10.3897/zookeys.1087.71280.suppl1

Supplementary material 2

Table S2

Authors: Piyatida Pimvichai, Henrik Enghoff, Thierry Backeljau

Data type: Xlsx file.

Explanation note: Estimates of COI sequence divergences (uncorrected *p*-distances) within and among Pachybolidae species and related taxa.

Link: https://doi.org/10.3897/zookeys.1087.71280.suppl2

ZooKeys 1087: 19–104 (2022)
doi: 10.3897/zookeys.1087.64382
https://zookeys.pensoft.net

RESEARCH ARTICLE

A peer-reviewed open-access journal
ZooKeys
Launched to accelerate biodiversity research

Revision of Neotropical Scythrididae moths and descriptions of 22 new species from Argentina, Chile, and Peru (Lepidoptera, Gelechioidea)

Kari Nupponen[1†], Pasi Sihvonen[2]

1 *Merenneidontie 19 D, FI-02320 Espoo, Finland* **2** *Finnish Museum of Natural History, P.O. Box 17, Pohjoinen Rautatiekatu 13, 00014 University of Helsinki, Finland*

Corresponding author: Pasi Sihvonen (pasi.sihvonen@helsinki.fi)

Academic editor: E. J. van Nieukerken | Received 13 February 2021 | Accepted 31 January 2022 | Published 22 February 2022

http://zoobank.org/94F2384E-640E-4A58-B8B4-D9D06675D2C2

Citation: Nupponen K, Sihvonen P (2022) Revision of Neotropical Scythrididae moths and descriptions of 22 new species from Argentina, Chile, and Peru (Lepidoptera, Gelechioidea). ZooKeys 1087: 19–104. https://doi.org/10.3897/zookeys.1087.64382

Abstract

The taxonomy of South American Scythrididae (Lepidoptera: Gelechioidea) is revised, based on external morphology, genitalia, male abdominal segment VIII, and DNA barcodes using genetic distances, BINs, and a tentative molecular phylogeny. Data include both historical and fresh specimens from Argentina, Brazil, Colombia, Chile, Ecuador, Paraguay, and Peru. Thirty-four species are recognised as valid, and the fauna classified in three genera. Type specimens and morphology of all species are described and figured in detail. DNA barcode sequences of the COI gene were successful for 22 species, the average genetic divergence between species being 5.1%. A key to Neotropical Scythrididae species is provided, based on the male genitalia and abdominal segment VIII, which show most and easily accessible interspecific differences.

Our study revealed that the Scythridae fauna of South America is more or less completely unknown. As a result, 22 new species are described, increasing the number of South American Scythrididae species from 13 to 34. All new species are authored by Kari Nupponen (incertae sedis means the genus combination is uncertain and needs further research, country of the type locality is given in parentheses): *Rhamphura subdimota* **sp. nov.** (Argentina), *R. pozohondaensis* **sp. nov.** (Argentina), *R. spiniuncus* **sp. nov.** (Argentina), *R. angulisociella* **sp. nov.** incertae sedis (Argentina), *R. curvisociella* **sp. nov.** incertae sedis (Argentina), *R. tetrafasciella* **sp. nov.** incertae sedis (Argentina), *Landryia ankylosauroides* **sp. nov.** incertae sedis (Argentina), *L. chilensis* **sp. nov.** incertae sedis (Chile), *Scythris directiphallella* **sp. nov.** (Argentina),

† Mr Kari Nupponen fell seriously ill during the preparation of the manuscript and died as a result of the rapidly progressing illness. Pasi wishes to dedicate the present work to Kari (15.1.1962–2.12.2021), to honour his extensive knowledge on Lepidoptera, particularly on Scythrididae.

S. furciphallella **sp. nov.** (Argentina), *S. manchaoensis* **sp. nov.** (Argentina), *S. salinasgrandensis* **sp. nov.** (Argentina), *S. angustivalvella* **sp. nov.** (Argentina), *S. caimancitoensis* **sp. nov.** (Argentina), *S. lequetepequensis* **sp. nov.** (Peru), *S. sanfriscoensis* **sp. nov.** (Argentina), *S. tigrensis* **sp. nov.** (Argentina), *S. bicoloristrigella* **sp. nov.** incertae sedis (Argentina), *S. saldaitisi* **sp. nov.** incertae sedis (Argentina), *S. wikstromi* **sp. nov.** incertae sedis (Argentina), *S. andensis* **sp. nov.** incertae sedis (Argentina), *S. mendozaensis* **sp. nov.** incertae sedis (Argentina).

The following new combinations are proposed: *Scythris depressa* Meyrick, 1931 and *Scythris dimota* Meyrick, 1931 are transferred from *Scythris* Hübner, 1825 to *Rhamphura* Landry, 1991, **comb. nov.** Three species classified in *Scythris* earlier are now classified as *Scythris* (incertae sedis): *Scythris dividua* Meyrick, 1916, *S. medullata* Meyrick, 1916 and *S. notorrhoa* Meyrick, 1921. The taxon *Syntetrernis neocompsa* Meyrick, 1933, recently classified in Scythrididae: *Scythris*, is excluded from Scythrididae and it is now classified in Cosmopterigidae incertae sedis.

Keywords

Biodiversity, COI phylogeny, DNA barcode, morphology, new species

Introduction

The family Scythrididae has a world-wide distribution, excluding the Antarctic. Scythridids occur also on several isolated islands, such as Hawaii (Walsingham 1907), the Galapagos Islands (Bucheli 2005), and the Maldives (Nupponen and Saldaitis 2013). More than 850 species of Scythrididae are described, but the true diversity of the family is much higher: in various museum collections there are known to be several hundred taxa awaiting description (Landry 1991). Many large areas still remain more or less unexplored, e.g., China, Mongolia, South and South-East Asia, Australia, central parts of Africa, and the majority of South and Central America. The scythridid fauna of the Neotropical realm is poorly known. To date, only thirteen species of *Scythris* Hübner, 1825 have been described from continental South America, all by Edward Meyrick in his monumental works on exotic Microlepidoptera (Meyrick 1912–1916, 1916–1923, 1923–1930, 1930–1936, 1936–1937; Meyrick 1931), from Argentina (1 sp.), Brazil (2 spp.), Colombia (2 spp.), Ecuador (1 sp.), Paraguay (3 spp.), and Peru (6 spp.).

There are few characters discovered in Scythrididae that would unambiguously define the family (Landry 1991; Bengtsson 2014; Heikkilä et al. 2014). In several cases the external appearance of the moth gives the impression of a scythridid: they are more pronouncedly teardrop-shaped, with more pointed wing apices, have an abdomen that extends at least 2/3 of the forewing length, and have narrow head scales compared to Blastobasidae, Cosmopterigidae, and Momphidae (Landry 1991). Scythrididae and Stathmopodidae are considered sister taxa, which is supported by molecular and morphological data, particularly the similarly expanded ductus seminalis (Heikkilä et al. 2014: fig. 6). In the present work, we have followed Landry (1991) and included taxa in Scythrididae if the following diagnostic features were present: base of haustellum scaled; head scales appressed and very narrow; labial palps with article 3 shorter than article 2; R4 and R5 of forewing stalked, R4 extended to costa, R5 to termen;

tarsomeres 1–4 with two subapical spurs; phallus ankylosed by juxta or manica; signum absent. All these characters are homoplastic within Gelechioidea if treated alone, but the combination seems unique for Scythrididae. Further, in the male, abdominal segment VIII tergum and sternum are typically modified. A narrow or very narrow ductus bursae in the female genitalia was considered a further diagnostic character of Scythrididae (Landry 1991), but later it was shown that this character is not ubiquitously present in Scythrididae (Kaila 2004). Heikkilä et al. (2014) found a unique synapomorphy in the larva: spiracle on A7 is smaller than other spiracles, and the shape of stipular setae of the larval spinneret being long and thin seems uniform in Scythrididae, and only occasionally observed in single species of other families. We did not include immature stages in our study due to lack of material.

The male genitalia of Scythrididae are notorious for their extraordinary morphological diversification, making interpretations of homology difficult (Landry 1991). Asymmetry is widespread, and among the Lepidoptera, the only known case of antisymmetry has been reported from a Spanish *Scythris* species (Nupponen 2009).

The genus-level classification of Scythrididae is in its infancy. It is estimated that undescribed taxa outnumber described ones by a factor of ten (Landry 1991). This, combined with the lack of a global view and extreme structural heterogeneity, has largely resulted in unsatisfactory dumping of more and more species into an undefined concept of *Scythris*. The generic name has been used in very broad sense and instead of describing new genera, the species group concept has been widely applied (e.g., Jäckh 1977; Bengtsson 2014). Landry (1991) provided a phylogenetic framework for the Nearctic Scythrididae, including descriptions of three new genera. He used informal supraspecific lineages and concluded that his (1991: 206) "initial proposal represents a working hypothesis to be tested by studying more taxa and characters".

The present paper is based on examination of all of Meyrick's described *Scythris* material from continental South America, housed in the Natural History Museum London, examination of Nearctic Scythrididae as presented in Landry (1991), and new materials of Scythrididae collected during 2017 and 2019 in the course of three Finnish–Estonian expeditions to Argentina, Chile, and Peru. The aim of the trips was to document the richness of the scythridid fauna at the foothills of the Andes before habitat loss causes fragmented distributional areas of many species, or possibly even extinctions.

Materials and methods

Material

The Finnish–Estonian expeditions to Argentina and Chile took place from 25 January–7 February 2017, and to Peru from 26 January–5 February 2019, and the Finnish expedition to Argentina during 13–25 September 2019. 30 collecting sites were sampled in areas of central Chile, NW Argentina, and the Andean and coastal regions of central Peru. A total of 145 scythridid specimens were collected during these expeditions.

The material was collected by light trapping at night. Four to five light traps were used every night, with various UV-tubes and LED-lamps, as well as 160 W incandescent lamps. Considerably effort was done to collect material during the day by sweeping vegetation by net.

All Meyrick's *Scythris* type specimens from South America in The Natural History Museum London (**NHMUK**) were examined and photographed, including the adults and the genitalia mounted on permanent slides. Data of type specimens are detailed under each species below. Because Meyrick's *Scythris* type specimens have been dissected by J. F. G. Clarke (details are available in Clarke (1965)), we did not do any further dissecting on this material. Adult photographs were arranged by NHMUK staff under the Digital Collections Programme. Landry's revision (1991) on Nearctic Scythrididae formed the basis of our study with regard to species-level and genus-level taxonomy.

Species delimitation and genus combinations

When making taxonomic decisions, we used all available information, including external features such as wing pattern, structural morphology, and new and existing knowledge on genetic variation in DNA barcodes of Scythrididae and the BIN system as implemented on BOLD (Ratnasingham and Hebert 2007, 2013). Sexes were associated based on wing patterns and DNA barcodes. To understand how the names were applied to the taxa described earlier, all *Scythris* species described by Meyrick during 1916–1933 that are stored in the NHMUK were examined.

Assigning species to Scythrididae genera was done as follows. The majority of the new taxa described in this article were DNA barcoded, and those barcodes were analysed in phylogenetic context using the maximum likelihood approach (see 'DNA barcoding, genetic analyses, and phylogeny'). Our new DNA barcodes were analysed together with all public Scythrididae DNA barcodes available on the Barcode of Life Data System (BOLD v4 http://boldsystems.org/) from North and South America (data extracted in September 2021, n = 725, barcodes > 500 bp were included, search term "Scythrididae"). This tentative phylogeny gave a rough estimate on the systematic position of each species (see Suppl. material 2). We then compared our material against the morphological diagnoses and descriptions of relevant genera as in Landry (1991), and other literature as detailed under each species, to combine taxa in genera. We did not describe new genera, because the phylogenetic framework for Scythrididae is in its infancy (Landry 1991). If the genus combination was doubtful, we either classified those in incertae sedis, or in *Scythris*, following Meyrick (1916, 1921, 1928, 1931, 1933), who classified all South American species in *Scythris*. We highlighted the cases where further research is needed.

Dissection and photography

The genitalia preparations were made following standard techniques (Robinson 1976). Genitalia were separated from the abdomen, and mostly mounted in ventral aspect,

some also in lateral aspect to show structural details not clearly visible in ventral aspect. The abdomen was cut laterally and spread out.

Photographs of adult specimens were taken with a Canon EOS 7D Mark II, MP-E 65 mm EF 100 mm macro lens. Focus stacking was done with Cognisys StackShot and Zerene Stacker, and final image editing with Adobe Photoshop 2021. Images of Meyrick's adult type specimens in the NHMUK were provided under the museum's Digital Collection Programme. The genitalia in the research collection of Kari and Timo Nupponen (coll. **NUPP**) were photographed with a Leica DM1000 microscope and integrated Leica DF295 digital camera. The genitalia in coll. NHMUK were photographed in Sackler Imaging Suite using a Zeiss Axioskop. Most genitalia dissections in both coll. NHMUK and coll. NUPP were photographed in 2–6 images in different focal planes and combined into single images using image-stacking software as implemented in Photoshop 2021. Images were edited in Photoshop 2021 and plates were compiled in CorelDraw 2018. Genitalia figures are not in scale.

DNA barcoding, genetic analyses, and phylogeny

Tissue samples (dried legs) of 87 specimens were sent to the Canadian Centre for DNA barcoding (**CCDB**, Biodiversity Institute of Ontario, University of Guelph). DNA extraction, PCR amplification and sequencing of the barcode region of the mitochondrial cytochrome oxidase I (COI) gene (658 base pair region near the 5' terminus of the COI gene) were carried out following standard high-throughput protocols (deWaard et al. 2008). The taxonomic and collection data, voucher image, COI sequences, and other metadata including sex are provided on the BOLD database https://v4.boldsystems.org through the public dataset DS-SCYNEO "Scythrididae of South America", https://dx.doi.org/10.5883/DS-SCYNEO. These data were compared with public DNA barcodes of all other Scythrididae material available on BOLD in September 2021. Suppl. material 1 contains GenBank accession numbers (MW564588–MW564622). Analytical tools on BOLD under taxon ID tree (Kimura 2-parameter model), barcode gap analysis and BIN were utilised for genetic analyses (Ratnasingham and Hebert 2007, 2013). Genetic distances between species are reported as minimum pairwise distances, while intraspecific variation is reported as maximum pairwise distances. Genetic distances of the barcodes developed for this article were visualised using the taxon ID tree tool on BOLD and finalised in CorelDraw 2021 (Fig. 81).

For phylogenetic analysis, COI sequences were aligned with MUSCLE implemented in MEGA6 (Tamura et al. 2013). Maximum likelihood (ML) analysis was carried out in the IQ-TREE web server (http://iqtree.cibiv.univie.ac.at; Trifinopoulos et al. 2016). The best substitution model was selected automatically by ModelFinder (Kalyaanamoorthy et al. 2017) as implemented in IQ-TREE. The best-fit model was identified as 'GTR+F+I+G4' for COI. To construct the phylogenetic tree, ML analysis with ultrafast bootstrap approximation model UFBoot (1,000 replicates) was applied (Minh et al. 2013). The tree was generated using FigTree v.1.4.2 (Rambaut 2015) and modified using Corel Draw 2021.

Designation of types and terminology

When possible, holotypes of new species were chosen among dissected specimens with full-length barcodes. The material is deposited in the research collection of Kari and Timo Nupponen (coll. NUPP, Espoo, Finland), to be deposited in MZH. The coordinates are presented in degrees and decimal minutes.

The terminology used here mainly follows Klots (1970), Landry (1991), Kristensen (2003), and is applied as in Bengtsson (2014) and Nupponen (2018). When homologies were difficult to interpret, we used descriptive terms instead. Under descriptions the prefix "sub" means that the structure in question resembles, or is close to, the mentioned shape. For instance, subtriangular means that shape is close to triangular. The term 'dirty white' is used to describe the colour on the ventral side of the abdomen in many species. This colour is white mixed with various tones of grey, and is reminiscent of snow blanket at late spring at forests in southern Finland. Meyrick calls that colour as 'cloudy white', but the variation of cloud colour is wider than forest snow.

Abbreviations

JFGC	John Frederick Gates Clarke.
MZH	Finnish Museum of Natural History, University of Helsinki, Finland.
NHMUK	The Natural History Museum, London, UK.
NUPP	research collection of Kari and Timo Nupponen, Espoo, Finland.
ZMUC	Zoological Museum, Natural History Museum of Denmark, Copenhagen, Denmark.

Results

Altogether 145 specimens representing 25 species were recorded during the expeditions; 22 species/130 specimens in Argentina, 1 species/1 specimen in Chile, and 3 species/14 specimens in Peru. DNA barcodes were obtained for 35 specimens representing 22 species (Fig. 81, Suppl. material 2). Examination of our material against the earlier described fauna revealed that 22 of our species are undescribed. As a result, the described Neotropical Scythrididae fauna increases from 13 (Meyrick 1916, 1921, 1928, 1931, 1933; Landry 1991) to 34 species in continental South America, which is an increase of 162%. The expeditions rediscovered three species described by Meyrick, confirmed by morphology: *Scythris depressa* (classified here as *Rhamphura depressa*, Meyrick recorded it from Paraguay, we report it from Argentina), *S. medullata* (classified here as *Scythris* (incertae sedis) *medulla*, Meyrick reported it from Peru, Colombia and Ecuador, we report it from Peru and Argentina) and *S. tibicina* (Meyrick reported it from Peru, we report it from Peru).

The examined Neotropical specimens are externally similar to their congeners elsewhere in the world. Forewings of many species have different shades of brown, beige and sand, with rather diffuse pale blotches or an elongate longitudinal streak along

the fold. Hindwings are lanceolate with a sharp apex, and with long fringes. The male genitalia and abdominal segment VIII are extremely diverse, often asymmetrical, and homologies are often difficult to establish. In many species the phallus is reduced in size, often to the degree that it is difficult to identify.

In the explored South American areas, all observed Scythrididae species are nocturnal. Considerable effort was made to find moths during the day, but none were encountered, even when vegetation was swept with a net. Out of three different light models used, the UV light tubes proved to attract Scythrididae most effectively. Based on our experience, the night-active species on the lower slopes of the Andes are virtually impossible to detect without light traps because shrubs and many herbaceous plants are thorny and prickly.

Our COI maximum likelihood phylogeny is limited in terms of molecular data, but the tree is well-resolved and the support for the nodes is reasonable, judged by the UFBoot support values shown in Suppl. material 2. In our analysis, taxa named as *Arotrura* on BOLD forms the most basal Scythrididae lineage, agreeing with the cladistic hypothesis of Landry (1991: fig. 450). This is sister to *Rhamphura* and all other Scythrididae lineages, and *Landryia* is among the most apical lineages in both our COI maximum likelihood tree and in the cladistic analysis of Landry (1991). *Scythris* was recovered as a large monophyletic genus, but with several genetically distant lineages. Our Neotropical taxa are scattered throughout the tree with other American Scythrididae, but often the South American taxa cluster together within bigger clades. For instance, this is the case in *Rhamphura*.

Those South American taxa, which did not fit any of the genera diagnosed by Landry (1991), are now highlighted with their tentative phylogenetic position based on their barcodes (Suppl. material 2), waiting for further research. The average genetic distance between DNA barcoded species was 5.1% (min. 2.5%, max. 7.4%) according to the barcode gap analysis as implemented on BOLD.

Key to Neotropical Scythrididae based on characters of the male genitalia and abdominal segment VIII

1 Valvae asymmetrical **2**
– Valvae symmetrical **12**
2 Valvae narrow, long (Figs 56–59) **3**
– Valvae wide, short or medium length (e.g., Figs 43, 51, 55, 60) **6**
3 Gnathos sclerotised, straight, ventral margin tooth-like extensions (Fig. 59) . ..... ***Scythris andensis***
– Gnathos sclerotised, upcurved, ventral margin smooth (Figs 56–58) **4**
4 Sternum VIII posterior extensions wide, bare (Fig. 58) .... ***Scythris wikstromi***
– Sternum VIII posterior extensions narrow, setose (Figs. 56, 57) **5**
5 Sternum VIII posterior extensions without extended base (Fig. 56) .... ***Scythris bicoloristrigella***
– Sternum VIII posterior extensions with extended base (Fig. 57) .... ***Scythris saldaitisi***

6 Sternum VIII with anterior apodemes, apex widened (Figs 42, 43) **7**
– Sternum VIII without anterior apodemes (e.g., Figs 57, 60) **8**
7 Posterior margin of sternum VIII V-shaped, left arm setose (Fig. 42) ..... ***Landryia ankylosauroides***
– Posterior margin of sternum VIII U-shaped, both arms bare (Fig. 43) ..... ***Landryia chilensis***
8 Valvae entirely setose, weakly sclerotised (Fig. 55) ..... ***Scythris tigrensis***
– Valvae partly setose, strongly sclerotised (Figs 51, 60–62) **9**
9 Valvae apex pointed, bare (Fig. 51) ..... ***Scythris inanima***
– Valvae apex rounded, with long setae (Figs 60–62) **10**
10 Basal portion of sternum VIII bare (Fig. 62) ..... ***Scythris notorrhoa***
– Basal portion of sternum VIII with sclerotisations, either arched (Fig. 60) or V-shaped (Fig. 61) **11**
11 Sternum VIII posteriorly with two bifurcate process (Fig. 60) ..... ***Scythris dividua***
– Sternum VIII posteriorly with one bifurcate process (Fig. 61) ..... ***Scythris medullata***
12 Valvae pointing upwards, sternum VIII with triangular process at middle (Fig. 54) ..... ***Scythris sanfranciscoensis***
– Valvae pointing laterally or downwards, sternum VIII without triangular process (Figs 35–41, 44–50, 52, 53) **13**
13 Valvae with sub-oval bristled extension (Fig. 53) ..... ***Scythris tibicina***
– Valvae without sub-oval bristled extension (Figs 35–41, 44–50, 52) **14**
14 Posterior margin of sternum VIII pointed (Fig. 50) ..... ***Scythris fluvialis***
– Posterior margin of sternum VIII not pointed (Figs 35–41, 44–49, 52) **15**
15 Posterior margin of tergum VIII folded, covered by minute spines (Fig. 52) ..... ***Scythris lequetepequensis***
– Posterior margin of tergum VIII not folded, not covered by minute spines (Figs 35–41, 44–49) **16**
16 Sternum and tergum VIII simple (Fig. 40) ..... ***Rhamphura angulisociella***
– Sternum and tergum modified (Figs 35–39, 41, 44–49) **17**
17 Sternum VIII with anteriorly directed apodemes (Figs 35–39) **18**
– Sternum VIII without anteriorly directed apodemes (Figs 41, 44–49) **22**
18 Tergum VIII 3-pronged (Fig. 37) ..... ***Rhamphura subdimota***
– Sternum VIII not 3-pronged (Figs 35, 36, 38, 39) **19**
19 Valvea with dorsal setose lobes (Fig. 38) ..... ***Rhamphura immunis***
– Valvae without dorsal lobes (Figs 35, 36, 39) **20**
20 Uncus triangular (Fig. 36) ..... ***Rhamphura dimota***
– Uncus bifurcate (Figs 35, 39) **21**
21 Valvae long, constant width, apex round (Fig. 35) ..... ***Rhamphura depressa***
– Valvae long, tapering, apex pointed (Fig. 39) ..... ***Rhamphura spiniuncus***
22 Socii long, curved (Fig. 41) ..... ***Rhamphura curvisociella***
– Socii absent (Figs 44–49) **23**

23 Valvae very long, blade-like, sternum VIII anteriorly deeply indented (Fig. 49).....***Scythris caimancitoensis***

– Valvae not very long, not blade-like, sternum VIII anteriroly weakly concave (Figs 44–48). **24**

24 Valvae narrow, inner margin evenly curved, apex thorn-like (Fig. 44) ....***Scythris directiphallella***

– Valvae wide or narrow, inner margin with extension, apex round (Figs 45–48).....**25**

25 Uncus large, bilobed, valvae subapically with small triangular tooth (Fig. 48) .....***Scythris zeugmatica***

– Uncus small, bilobed, valvae subapically with large horn or lobe (Figs 45–47).....**26**

26 Valvae subapically with large dorsally directed lobe (Fig. 45)..... ..... ***Scythris furciphallella***

– Valvae subapically with ventrally directed horn (Figs 46, 47) **27**

27 Valvae apex with distinctly enlarged lobe, posterior appendices of sternum VIII converging (Fig. 46).....***Scythris manchaoensis***

– Valvae apex with weakly enlarged lobe, posterior appendices of sternum VIII diverging (Fig. 47) .....***Scythris angustivalvella***

Males of the following species are unknown: *Scythris ejiciens* Meyrick, *Scythris mendozaensis* sp. nov., *Scythris plocogastra* Meyrick, *Rhamphura pozohondaensis* sp. nov., *Scythris salinasgrandensis* sp. nov., *Rhamphura tetrafasciella* sp. nov.

A key to the female genitalia is not given, as the female of only 11 of 35 recognised species is known.

Taxonomy

The phylogenetic relationships of South American Scythrididae are currently inadequately resolved, making the genus classification difficult. Our approach to combine the DNA barcode phylogeny with morphology, mostly utilising the genitalia, abdominal segments VII and VIII and wing patterns and compared against the diagnoses in Landry (1991), gives an indicative first step in an iterative approach to solve the relationships of studied taxa. More genetic data are needed, and global taxon sampling on Scythrididae, to build a robust support for the evolutionary relationships.

We present the genera in the order roughly following our COI maximum likelihood phylogeny (Suppl. material 2) and the phylogenetic hypothesis of Landry (1991): *Rhamphura*, *Rhamphura* incertae sedis, *Landryia* incertae sedis, *Scythris*, *Scythris* incertae sedis. Within each genus we first present species groups (if any), arranged alphabetically by species, and then isolated species are presented alphabetically by species. We exclude one species from Scythrididae, and this is treated at the end.

Checklist of South American Scythrididae

***Rhamphura* Landry, 1991**

The *depressa* species group
Rhamphura depressa (Meyrick, 1931), comb. nov.
Rhamphura dimota (Meyrick, 1931), comb. nov.
Rhamphura subdimota Nupponen, sp. nov.

Not assigned to a species group
Rhamphura immunis (Meyrick, 1916)
Rhamphura pozohondaensis Nupponen, sp. nov.
Rhamphura spiniuncus Nupponen, sp. nov.
Rhamphura angulisociella Nupponen, sp. nov., genus combination incertae sedis
Rhamphura curvisociella Nupponen, sp. nov., genus combination incertae sedis
Rhamphura tetrafasciella Nupponen, sp. nov., genus combination incertae sedis

***Landryia* Kemal & Koçak, 2006**

The *ankylosauroides* species group
Landryia ankylosauroides Nupponen, sp. nov., genus combination incertae sedis
Landryia chilensis Nupponen, sp. nov., genus combination incertae sedis

***Scythris* Hübner, 1825**

The *directiphallella* species group
Scythris angustivalvella Nupponen sp. nov.
Scythris directiphallella Nupponen, sp. nov.
Scythris furciphallella Nupponen, sp. nov.
Scythris manchaoensis Nupponen, sp. nov.
Scythris salinasgrandensis Nupponen, sp. nov.
Scythris zeugmatica Meyrick, 1931

Not assigned to a species group
Scythris caimancitoensis Nupponen, sp. nov.
Scythris ejiciens Meyrick, 1928
Scythris fluvialis Meyrick, 1916
Scythris inanima Meyrick, 1916
Scythris lequetepequensis Nupponen, sp. nov.
Scythris plocogastra Meyrick, 1931
Scythris tibicina Meyrick, 1916
Scythris sanfranciscoensis Nupponen, sp. nov.
Scythris tigrensis Nupponen, sp. nov.

The *bicoloristrigella* species group
Scythris bicoloristrigella Nupponen, sp. nov., genus combination incertae sedis
Scythris saldaitisi Nupponen, sp. nov., genus combination incertae sedis
Scythris wikstromi Nupponen, sp. nov., genus combination incertae sedis

The *andensis* species group
Scythris andensis Nupponen, sp. nov., genus combination incertae sedis
Scythris mendozaensis Nupponen, sp. nov., genus combination incertae sedis

The *dividua* species group
Scythris dividua (Meyrick, 1916), genus combination incertae sedis
Scythris medullata (Meyrick, 1916), genus combination incertae sedis
Scythris notorrhoa (Meyrick, 1921), genus combination incertae sedis

Taxonomic treatments

Rhamphura Landry, 1991

The *depressa* species group

Valvae narrow and straight, distal 1/3 somewhat broadened dorsally. Male sternum VIII rectangular basally, lateral reinforcement extended anteriorly forming prongs. Phallus short and thick. Tegumen laterally with parallel and heavily sclerotised processes (absent in *depressa*). Anteriorly to tegumen attached a large formation, consisting of two parallel, basally fused sclerotised pouches (absent in *depressa*). Species included: *depressa*, *dimota*, *subdimota*.

Rhamphura depressa (Meyrick, 1931), comb. nov.
Figs 1, 35

Scythris depressa Meyrick, 1931. Zoological Journal of the Linnean Society 37: 282.

Material examined. *Holotype*. Paraguay • ♂; Chaco region, Makthlawaiya; GSC [G. S. Carter]; 11.26.; [genitalia slide] JFGC No. 8061; NHMUK ID 010922355; NHMUK slide ID 010316669; coll. NHMUK.

Other material. Argentina • 2 ♂; prov. Santiago del Estero, Pozo Honda village S, by salt lake; 27°17.2'S, 64°28.0'W, 260 m a.s.l.; 19 Sep. 2017; K. Nupponen & R. Haverinen leg.; [BOLD sample ID] KN01044; [genitalia slide] K. Nupponen prep. no. 2/9 Dec. 2019; coll. NUPP (MZH).

Diagnosis. Externally hardly separable from *R. dimota* and *R. subdimota*. Reliable determination can be achieved by genitalia examination (DNA barcode not available for *R. dimota* yet). Gnathos is labiate, short and sclerotised in *R. depressa*; gnathos base is

triangular hood, distal arm is short and bent in *R. dimota*; absent in *R. subdimota*. Lateral processes of tegumen absent in *R. depressa*; triangular, granulate and heavily sclerotised in *R. dimota*; sub-oval, granulate, with longitudinal cleavage and heavily sclerotised in *R. subdimota*. Male tergum VIII trapezoid in *R. depressa*; rectangular with long diverging anterior apodemes in *R. dimota* ((note: structures shown are not in comparable position, potentially deformed during dissection); pentagonal and medioposteriorly extended in *R. dimota*).

Description. The original description is quoted: "Wingspan 11 mm ♂. Head and thorax dark purplish-grey, sternum white. Palpi dark grey, basal joint and basal half of second white. Abdomen blackish, anal tuft grey segmental margins on ventral surface pale ochreous-grey. Forewings dark purplish-grey; a few whitish scales on fold towards middle: cilia grey. Hind wings 0.6, 4 and 5 separate; dark grey; cilia grey."

***Male genitalia*.** Uncus large, bifurcate; united by transverse sclerotisation. Gnathos labiate, short and sclerotised. Anteriorly to tegumen attached a large formation, consisting of two parallel, curved, medially fused pouches. Phallus short and thick, vase-shaped. Valvae symmetrical, long and slender, of constant width, tip rounded and setose. Sternum VIII rectangular basally, posterior reinforcement extended laterally; lateral apodemes sclerotised and extended anteriorly forming prongs with spoon-shaped apices. Tergum VIII trapezoid plate, posterior margin with numerous minute setae.

Distribution. Argentina, Paraguay.

Habitat. In Argentina the species was collected in a dry bushy area near a salt lake shore (Fig. 78).

Genetic data. BIN: BOLD:ADY6755 (n = 2 from Argentina). Maximum intraspecific variation 0%. Nearest neighbour: North American *Rhamphura* sp. (Scythrididae, BIN: BOLD:AAA9059, 2.89%).

Remarks. New to Argentina. Female unknown. Based on COI maximum likelihood phylogeny, the South American taxa *subdimota*, *depressa*, *pozohondaensis*, *spiniuncus*, *angulisociella*, *tetrafasciella* and *curvisociella* group together, associating next to the North American taxa classified in *Rhamphura* on BOLD (Suppl. material 2). Structurally these taxa are heterogeneous and the external characters, male and/or female genitalia show varying degrees of similarities to North American *Rhamphura*, as diagnosed and illustrated in Landry (1991). With regard to *depressa*, it has male sternum VIII with long, anteriorly directed, free apodemes, which is diagnostic in *Rhamphura*. For these reasons, we reclassified *Scythris depressa* Meyrick, 1931 as *Rhamphura depressa* (Meyrick, 1931), new combination.

Rhamphura dimota (Meyrick, 1931), comb. nov.

Figs 2, 36

Scythris dimota Meyrick, 1931. Zoological Journal of the Linnean Society 37: 282.

Material examined. ***Lectotype*.** Paraguay • ♂; Chaco region, Makthlawaiya; •; GSC [G. S. Carter]; 5.27.; [genitalia slide] JFGC No. 8062; NHMUK ID 010922356; NHMUK slide ID 010316670; coll. NHMUK.

Paralectotype. Paraguay • 1 ♂; same data as for lectotype; coll. NHMUK.

Diagnosis. Externally hardly separable from *R. dimota* and *R. subdimota*. Reliable determination can be achieved by genitalia examination (DNA barcode not available for *R. dimota* yet). Gnathos is labiate, short and sclerotised in *R. depressa*; gnathos base is triangular hood, distal arm is short and bent in *R. dimota*; absent in *R. subdimota*. Lateral processes of tegumen absent in *R. depressa*; triangular, granulate and heavily sclerotised in *R. dimota*; sub-oval, granulate, with longitudinal cleavage and heavily sclerotised in *R. subdimota*. Male tergum VIII trapezoid in *R. depressa*; rectangular with long diverging anterior apodemes in *R. dimota* ((note: structures shown are not in comparable position, potentially deformed during dissection); pentagonal and medioposteriorly extended in *R. dimota*).

Description. The original description is quoted: "Wingspan 12 mm ♂, ♀. Head and thorax bronzy-fuscous, some white scales on posterior edge of thorax. Palpi dark fuscous, basal joint and base of second ochreous-white. Abdomen dark fuscous, ♂ beneath ochreous-white except last two segments. Forewings dark purplish-fuscous; a white streak along fold from base to near middle of wing, ♂ thicker and irregular, and its apex connected with dorsum by irregular white suffusion; some cloudy white suffusion about end of fold and tornus: cilia rather dark grey. Hindwings 0.66, 4 and 5 separate; dark fuscous; cilia rather dark grey."

Male genitalia. Uncus triangular. Gnathos base small triangular hood; distal arm short, bent, tip pointed. Tegumen hood-shaped, laterally broadly thickened, with two parallel triangular and heavily sclerotised processes. Between tegumen and valvae large formation, consisting of two parallel elongated, basally fused sclerotised pouches. Phallus short and thick, weakly sclerotised (illustrated in Clarke (1965: 472, fig. 4a)). Valvae ~ 1.5 × as long as tegumen and uncus together; narrow and straight, distal 1/3 somewhat broadened dorsally, apex slightly elongated and setose. Vinculum arched, short. Sternum VIII rectangular basally, posterior reinforcement extended laterally, lateral apodemes sclerotised and extended anteriorly forming prongs with spoon-shaped apices. Tergum VIII rectangular, ~ 2 × as wide as long, with long, diverging anterior apodemes.

Distribution. Paraguay.

Remarks. Female unknown. The original description states that one male and one female were available, but Clarke (1965) reported that both are males. The asymmetry in the male valvae (Fig. 36) is an artefact of preparation due to a partly folded left valva on the slide mount. *R. dimota* is morphologically similar to *R. depressa*, particularly the bronzy-fuscous wings, long and narrow valvae and free apodemes on sternum VIII. For these reasons, we reclassify *Scythris dimota* Meyrick, 1931 as *Rhamphura dimota* (Meyrick, 1931) new combination.

Rhamphura subdimota Nupponen, sp. nov.

http://zoobank.org/18C0487C-633F-455C-83B9-CDDBC05A9004

Figs 3, 37

Type material. ***Holotype.*** Argentina • ♂; prov. Santiago del Estero, Pozo Honda village S, by salt lake; 27°17.2'S, 64°28.0'W; 260 m a.s.l.; 19 Sep. 2017; K. Nupponen &

R. Haverinen leg.; [BOLD sample ID] KN01046; [genitalia slide] K. Nupponen prep. no. 5/12 Dec. 2019; coll. NUPP (MZH).

Diagnosis. Externally hardly separable from *R. depressa* and *R. dimota*. Reliable determination can be achieved by genitalia examination (DNA barcode not available for *R. dimota* yet). Gnathos is labiate, short and sclerotised in *R. depressa*; gnathos base is triangular hood, distal arm is short and bent in *R. dimota*; absent in *R. subdimota*. Lateral processes of tegumen is absent in *R. depressa*; triangular, granulate and heavily sclerotised in *R. dimota*; sub-oval, granulate, with longitudinal cleavage and heavily sclerotised in *R. subdimota*. Tergum VIII is trapezoid in *R. depressa*; rectangular with long diverging anterior apodemes in *R. dimota* ((note: structures shown are not in comparable position, potentially deformed during dissection); pentagonal and medioposteriorly extended in *R. dimota*).

Description. Wingspan 10 mm. Head dark brown, laterally mixed with white. Neck tuft and haustellum white. Collar and tegula dark brown with scattered cream scales. Thorax dark brown. Scape dorsally dark brown, ventrally dirty white; pecten dirty white and a little longer than diameter of scape. Flagellum dark brown, 0.65 × length of forewing, ciliate, sensillae ~ 1/2 as long as diameter of flagellum. Labial palp white, except lower surface of palpomeres II and III dark brown. Legs: lower surfaces white, otherwise fuscous with scattered dirty white, except upper surface of forelegs dark brown. Abdomen dorsally fuscous, ventrally dirty white. Forewing dark brown; fold indistinctly cream from base to cell end; small blackish spot under fold at 0.25, 0.45, 0.6, and above tornus. Hindwing dark fuscous.

***Male genitalia*.** Uncus triangular, projected. Gnathos absent (not detected). Tegumen hood-shaped, anterior margin medially deeply concave with heavily sclerotised minute spine at left margin of incurvation; laterally two parallel sub-oval and heavily sclerotised processes with longitudinal cleavage, surface spinuliform. Anteriorly to tegumen attached a large formation, consists of two parallel round, basally fused sclerotised pouches; at base two small and heavily sclerotised triangular extensions. Phallus short, apex somewhat extended, tip pointed. Valvae symmetrical; 1.4 × longer than tegumen and uncus together; basal 0.65 of constant width, distal 1/3 dorsally slightly broadened, apex slightly lobate. Saccus arched, short. Sternum VIII rectangular basally, posterior reinforcement extended laterally; anterior apodemes with spoon-shaped apices. Tergum VIII pentagonal basally, anterior margin widely concave; medioposteriorly long and tapered extension.

Etymology. A participle in nominative singular. The species name alludes to a close relationship with *S. dimota*, based on morphology of the male genitalia.

Distribution. NW Argentina.

Habitat. The collecting site is a dry shrubby area near a salt lake shore (Fig. 77).

Genetic data. BIN: BOLD:ADZ0695 (n = 1 from Argentina). Nearest neighbour: An unidentified *Rhamphura* sp. (Scythrididae) from North America (BIN: BOLD:AAA9059, 2.57%).

Remarks. Female unknown. Based on COI maximum likelihood phylogeny, the South American taxa *subdimota*, *depressa*, *pozohondaensis*, *spiniuncus*, *angulisociella*,

tetrafasciella, and *curvisociella* group together, associating next to the North American taxa classified in *Rhamphura* on BOLD (Suppl. material 2). Structurally these taxa are heterogeneous and the external characters, male and/or female genitalia show varying degrhees of similarities to the North American *Rhamphura*, as diagnosed and illustrated in Landry (1991). With regard to *subdimota*, it has male sternum VIII with long, anteriorly directed, free apodemes and tergum VIII Y-shaped, both diagnostic in *Rhamphura*. We therefore classified this taxon as *Rhamphura subdimota*.

***Rhamphura immunis* (Meyrick, 1916)**
Figs 4, 38

Scythris immunis Meyrick, 1916. Exotic Microlepidoptera, vol. 2 (part 1): 13.

Material examined. ***Lectotype.*** Peru • ♂; Oroya; [11°31'S, 75°53'W]; 12200 feet a.s.l.; 5–14.; Parish leg.; [genitalia slide] JFGC No. 8056; NHMUK ID 010922360; NHMUK slide ID 010316668; coll. NHMUK.

Paralectotype. Peru • 1 ♂; same data as for lectotype; coll. NHMUK.

Diagnosis. A small (wingspan 9 mm), dark species externally similar to several other dark species, e.g., *S. inanima*, *S. depressa*, and less contrasting specimens of *S. medullata*. Genitalia dissection is required for confident determination. *Scythris immunis* is readily separated from the other described species by details in the male genitalia: long bifurcate teguminal processes with lateral setose extensions; tegumen with pair of beak-like processes dorsally; row of pegs ventrally; valvae with dorsal, setose lobes; sternum VIII with long, anteriorly directed free apodemes.

Description. The original description is quoted: "Wingspan 9 mm ♂, ♀. Head, palpi and thorax dark grey sprinkled with whitish. Antennal ciliations of ♂ 0.75. Abdomen stout in both sexes, bronzy-grey, beneath suffused and mixed with whitish. Forewings lanceolate; dark grey; two blackish longitudinal streaks from base, upper median, reaching to about 0.75, lower running to tornus, some slight whitish irroration on or between these; a similar less distinct streak above dorsum from base to middle: cilia grey. Hindwings with 4 and 5 separate; in ♂ pale grey, thinly scaled, in ♀ grey; cilia greyish, towards base ochreous-tinged."

Male genitalia. Tegumen with beak-like processes on posterior margin, row of pegs on ventral margin, apex bifurcate and setose. Phallus straight, short and thick, basal 1/2 tapered. Valva narrow, long, with dorsal setose lobes, freely articulated to vinculum. Sternum VIII rectangular, with long, anteriorly directed free apodemes. Tergum VIII medioposteriorly concave, with group of stout setae on both lateral sides.

Distribution. Peru.

Remarks. Female unknown. *Scythris immunis* was combined to *Rhamphura* by Landry (1991). We agree with the classification, because *immunis* has the diagnostic male tegumen with a pair of large beak-like processes extended from the posterior margin and with ventral rows of clusters or pegs. Further, male sternum VIII is sclerotised,

with long, anteriorly directed, free apodemes. Meyrick (1916) described the species based on three specimens, stated to include both males and females. Clarke (1965) indicated that all three syntypes are actually males.

***Rhamphura pozohondaensis* Nupponen, sp. nov.**
http://zoobank.org/F40CAB6D-DA8A-4C3F-A0C6-7ADB6861F6F1
Figs 5, 63

Type material. ***Holotype*.** Argentina • ♀; prov. Santiago del Estero, Pozo Honda village S, by salt lake; 27°17.2'S, 64°28.0'W; 260 m a.s.l.; 19 Sep. 2017; K. Nupponen & R. Haverinen leg.; [BOLD sample ID] KN01047; [genitalia slide] K. Nupponen prep. no. 1/14 Dec. 2019; coll. NUPP (MZH).

Diagnosis. Externally easily separated from other species treated herein by the blackish brown forewings with a distinct whitish dirty pale beige streak in fold, and blackish hindwings. In the female genitalia of *S. pozohondaensis*, sterigma resembles that of *S. ankylosauroides*, but differs by parallel triangular posterior flaps (trapezoid flap in *S. ankylosauroides*) and presence of cleavage at anterior tip.

Description. Wingspan 11 mm. Head and thorax blackish brown, Few dirty white scales exist around eye. Collar, neck tuft and tegula dark fuscous, paler than head. Haustellum white. Scape dorsally dark brown, ventrally pale fuscous; pecten dirty cream and ca. as long as diameter of scape. Flagellum dark brown, 0.55 × length of forewing. Labial palp white, except lower surfaces of palpomere III and distal 1/2 of palpomere II dark brown. Legs dirty white, upper surfaces of foreleg and midleg mixed with fuscous. Abdomen dorsally fuscous, ventrally white. Forewing blackish brown, distinct whitish dirty pale beige streak in fold from base to 0.75; scattered dirty pale beige scales at apical 1/3. Hindwing blackish brown.

Female genitalia. Sterigma triangular, posterolateral corners laterally elongate; posteriorly two large parallel flaps; anterior tip with narrow cleavage. Ostium small, situated at anterior tip of sterigma. Sternum VII quadrangular; posterior margin shallowly concave. Apophyses anteriores 0.55 × length of apophyses posteriores.

Etymology. Latinised adjective in the nominative singular. The species is named after the type locality, the village of Pozo Honda.

Distribution. NW Argentina.

Habitat. The habitat at the collecting site is a dry shrubby area near a salt lake shore (Fig. 77).

Genetic data. BIN: BOLD:ADY8268 (*n* = 1 from Argentina). Nearest neighbour: *Rhamphura depressa* (BIN: BOLD:ADY6755, 3.3%).

Remarks. Male unknown. Based on COI maximum likelihood phylogeny, the South American taxa *subdimota*, *depressa*, *pozohondaensis*, *spiniuncus*, *angulisociella*, *tetrafasciella*, and *curvisociella* group together, associating next to the North American taxa classified in *Rhamphura* on BOLD (Suppl. material 2). Structurally these taxa are heterogeneous and the external characters, male and/or female genitalia show varying

degrees of similarities to the North American *Rhamphura*, as diagnosed and illustrated in Landry (1991). With regard to *pozohondaensis*, it has female sterigma as triangular cone, projected anteriorly, which is diagnostic in *Rhamphura*. We therefore classified this taxon as *Rhamphura pozohondaensis*.

***Rhamphura spiniuncus* Nupponen, sp. nov.**
http://zoobank.org/06D285D0-42C0-4124-A983-8F2D7646B877
Figs 6, 39

Type material. ***Holotype*.** Argentina • ♂; prov. San Juan, Andes Mts., salt lake by Cordillera del Tigre; 30°52.8'S, 68°52.4'W, 1620 m a.s.l.; 26 Jan. 2017; K. Nupponen & R. Haverinen leg.; [BOLD sample ID] KN01045; [genitalia slide] K. Nupponen prep. no. 4/12 Dec. 2019; coll. NUPP (MZH).

Diagnosis. Wings mottled beige and brown forewing and an indistinct pale beige streak in fold. Genitalia examination is needed for a reliable identification. In the male genitalia, the bifurcate, robust uncus with heavily sclerotised ventral spines and falcate shape of the valvae are unmistakable.

Description. Wingspan 10 mm. Head brown, few white scales around eye. Haustellum pale fuscous. Neck tuft white. Collar, tegula and thorax pale brown. Scape dorsally brown, ventrally pale fuscous; pecten dirty cream and longer than diameter of scape. Flagellum dark brown, 0.55 × length of forewing, ciliate, sensillae ~ 0.65 × as long as diameter of flagellum. Labial palp white, except palpomeres II and III brown at lower surface and terminally. Legs white, shallowly mixed with fuscous. Abdomen whitish fuscous, ventrally paler. Forewing brown of various tones, fold and terminal 1/3 mixed with dirty pale beige scales; indistinct dark brown dash in fold at 0.5; small blackish spot in cell end. Hindwing fuscous. Fringes darker than wings.

***Male genitalia*.** Uncus robust, 0.6 × as long as valva, bifurcate; at base of furcation ~ 15 heavily sclerotised minute spines. Phallus heavily melanised, short. Valva long and narrow, subbasally a little broadened, then evenly tapered, distal quarter bent downwards, tip pointed. Saccus short, semi-circular. Juxta narrow, 0.8 × length of phallus. Sternum VIII basally a rectangular plate; reinforcement continues posterolaterally at backwards directed extensions; long anterolateral apodemes with spatular tips. Tergum VIII trapezoid, 1.4 × wider than high.

Etymology. A noun in apposition. The species name refers to the spinose uncus of the male genitalia.

Distribution. NW Argentina.

Habitat. The collecting site is a xerothermic habitat with sparse halophytic shrubs near a dry salt lake at medium altitude of the Andes (Fig. 78).

Genetic data. BIN: BOLD:ADY6426 (*n* = 1 from Argentina). Nearest neighbour: An unidentified *Rhamphura* sp. (Scythrididae) from North America (BIN: BOLD:AAA9059, 3.05%).

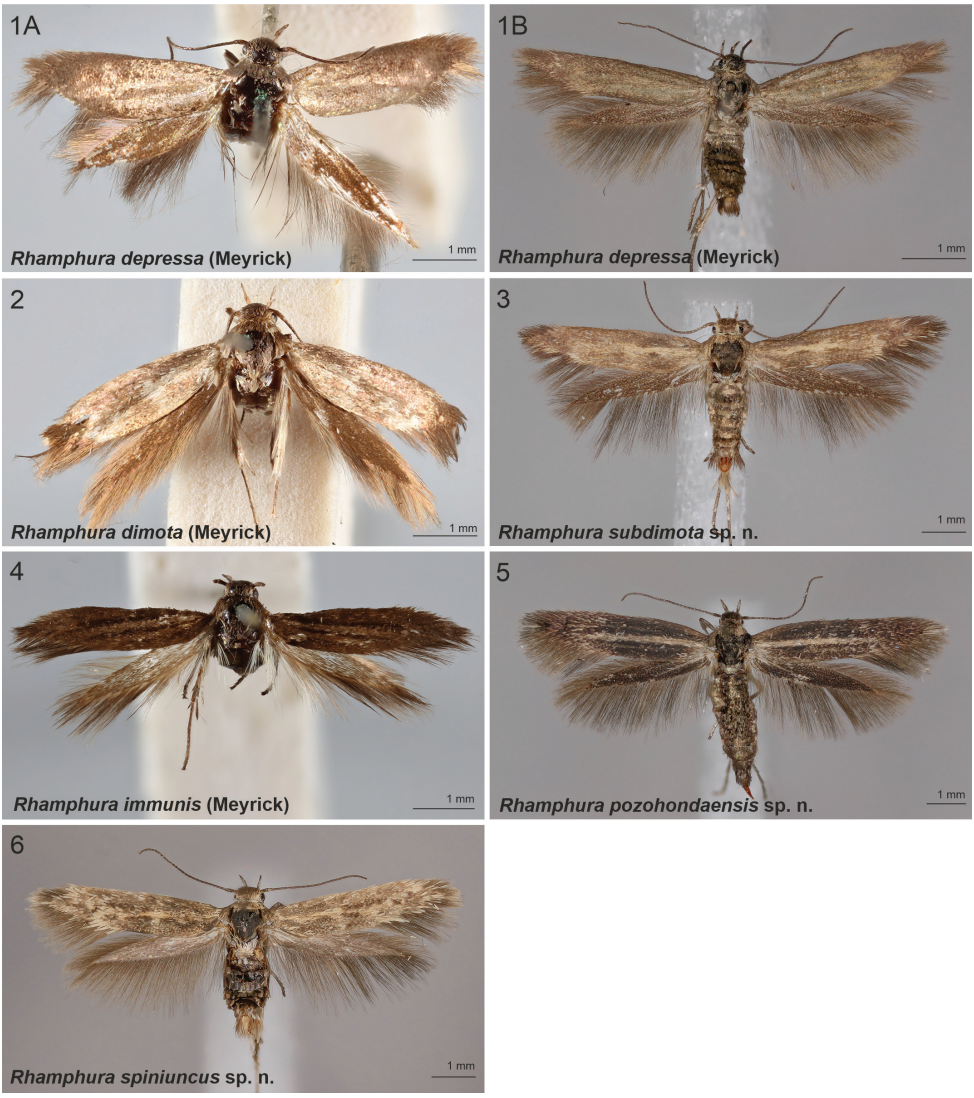

Figures 1–6. Scythrididae adults, genus *Rhamphura* **1A** *R. depressa* (Meyrick, 1931), male, holotype **1B** *R. depressa* (Meyrick, 1931), male, holotype **2** *R. dimota* (Meyrick, 1931), male, lectotype **3** *R. subdimota* Nupponen, sp. nov., male, holotype **4** *R. immunis* (Meyrick, 1916), male, lectotype **5** *R. pozohondaensis* Nupponen, sp. nov., female, holotype **6** *R. spiniuncus* Nupponen, sp. nov., male holotype.

Remarks. Female unknown. Based on the COI maximum likelihood phylogeny, the South American taxa *subdimota*, *depressa*, *pozohondaensis*, *spiniuncus*, *angulisociella*, *tetrafasciella*, and *curvisociella* group together, associating next to the North American taxa classified in *Rhamphura* on BOLD (Suppl. material 2). Structurally these taxa are heterogeneous and the external characters, male and/or female genitalia show varying degrees of similarities to the North American *Rhamphura*, as diagnosed and illustrated

in Landry (1991). With regard to *spiniuncus*, it has a bifurcate uncus with ventral spines, male sternum VIII with long, anteriorly directed, free apodemes, which are diagnostic for *Rhamphura*. We therefore classified this taxon as *Rhamphura spiniuncus*.

Rhamphura angulisociella **Nupponen, sp. nov., genus combination incertae sedis**
http://zoobank.org/10DE3851-DA34-45F8-861B-D7EFF3D4390A
Figs 7, 40

Type material. ***Holotype.*** Argentina • ♂; prov. Jujuy, Rio San Francisco, by Caimancito village; 23°43.8'S, 64°36.3'W; 400 m a.s.l.; 18 Sep. 2017; K. Nupponen & R. Haverinen leg.; [BOLD sample ID] KN01038; [genitalia slide] K. Nupponen prep. no. 1/10 Dec. 2019; coll. NUPP (MZH).

Diagnosis. Externally may be separated from other described taxa by pale brown forewings with characteristic black patches at basal 1/2 of dorsum. In the male genitalia of *R. angulisociella*, anteriorly to tegumen is attached a large formation, which resembles that of *R. depressa*, but *R. angulisociella* has long and angled socii and narrower valvae.

Description. Wingspan 13.5 mm. Head, collar, neck tuft, tegula and thorax pale brown; few white scales around eye and at posterior margin of thorax. Haustellum white with a little pale brown at middle. Scape dorsally dark brown, ventrally dirty cream; pecten dirty cream and longer than diameter of scape. Flagellum dark brown, 0.65 × length of forewing, ciliate, sensillae ~ 1/2 as long as diameter of flagellum. Labial palps white, except lower surface of palpomeres II and III dark brown. Legs with lower surfaces white, otherwise fuscous with scattered dirty white. Abdomen dorsally fuscous, ventrally white, anal tuft pale brown. Forewing pale brown, basal 1/2 between fold and dorsum paler than costal area; irregular black patches at dorsum at 0.2 and 0.5, dorsal and apical areas mixed with sparsely scattered white scales. Hindwing fuscous, darker than forewing.

Male genitalia. Uncus small, semi-circular plate. Socii long and setose shanks, basal 0.75 straight, then bent 80°; anterolaterally bulged with very long setae. Tegumen arched, anterior margin concave, with tuft of long setae posterio-laterally. Note: the following structures are bent 180° (unrolled) ventrally during dissection, which explains why the valvae appear as a dorsal structure in Fig. 40. Anteriorly to tegumen attached a large formation, consists of two parallel sub-ovals, basally fused and posteriorly heavily sclerotised pouches. Phallus short, slightly tapered, tip bent and pointed. Valva longer than uncus and tegumen together, very slender, apical area setose. Sternum VIII rectangular, 1.5 × as wide as high. Tergum VIII trapezoid, anterior margin sclerotised.

Etymology. Diminutive noun in apposition. The species name refers to angular socii in the male genitalia.

Distribution. NW Argentina.

Habitat. The collecting site is a dry river bed surrounded by forests and plantations. Plants of the family Amaranthaceae were frequent at the riverside (Fig. 79).

Genetic data. BIN: BOLD:ADY9489 (*n* = 1 from Argentina). Nearest neighbour: a North American *Rhamphura* sp. (Scythrididae, BIN: BOLD:AAA9059, 4.82%).

Remarks. Female unknown. Based on COI maximum likelihood phylogeny, the South American taxa *subdimota*, *depressa*, *pozohondaensis*, *spiniuncus*, *angulisociella*, *tetrafasciella*, and *curvisociella* group together, associating next to the North American taxa classified in *Rhamphura* on BOLD (Suppl. material 2). Structurally these taxa are heterogeneous and the external characters, male and/or female genitalia show varying degrees of similarities to the North American *Rhamphura*, as diagnosed and illustrated in Landry (1991). With regard to *angulisociella*, the structural differences are notable and we therefore took a conservative view and classified this taxon in *Rhamphura* (incertae sedis), highlighting the need for further research.

Rhamphura curvisociella Nupponen, sp. nov., genus combination incertae sedis

http://zoobank.org/92CA4B67-3C76-4FF7-A771-820303B9CE0B

Figs 8, 41

Type material. ***Holotype.*** Argentina • ♂; prov. Santiago del Estero, Pozo Honda village S, by salt lake; 27°17.2'S, 64°28.0'W; 260 m a.s.l.; 19 Sep. 2017; K. Nupponen & R. Haverinen leg.; [BOLD sample ID] KN01041; [genitalia slide] K. Nupponen prep. no. 1/12 Dec. 2019; coll. NUPP (MZH).

Diagnosis. Beige forewings with dark brown costa do not allow unambiguous identification. In the male genitalia of *R. curvisociella*, a large, ventrally curved and distally split phallus is diagnostic, in addition to long curved socii, and triangular extensions near apex of the valvae. In *R. angulisociella* the socii are angled, and valvae are without triangular extensions near the apex.

Description. Wingspan 12.5 mm. Head beige mixed with pale brown, frons paler. Collar, neck tuft, haustellum, tegula and thorax pale beige, neck tuft slightly paler than head. Scape dorsally dark brown, ventrally beige; pecten beige, as long as diameter of scape. Flagellum mixed with beige and dark brown, 0.7 × length of forewing, ciliate, sensillae ~ 1/2 as long as diameter of flagellum. Labial palp white, except lower surface of palpomere II from 0.5 to 0.8 and middle of palpomere III dark brown. Legs: femur and lower surfaces white, otherwise different shades of beige scattered with pale fuscous. Abdomen dorsally fuscous, ventrally dirty white. Forewing beige; costal belt densely covered by dark brown from base to 0.7, dorsal and apical areas with sparsely scattered dark brown scales; at cell end a small black spot. Hindwing dark fuscous, darker than forewing.

Male genitalia. Uncus heart-shaped setose plate. Gnathos rectangular elongate plate. Socii long recurved processes. Tegumen with deep incision anteromedially. Phallus large, basally heavily sclerotised, slightly bent, apical quarter split and tapered. Valva longer than uncus and tegumen combined, narrow, apical quarter slightly broadened and setose; dorsally with subapical triangular extension. Sternum VIII rectangular, 2 × as wide as high, anterior margin concave, anterolateral margin elongated and somewhat

sclerotised. Tergum VIII rectangular, anterior margin concave and reinforced; posterior margin with two parallel setose lobes with wrinkled surface.

Etymology. Diminutive noun in apposition. The species name refers to the curved socii in the male genitalia.

Distribution. NW Argentina.

Habitat. The collecting site is a dry, shrubby area near a salt lake shore (Fig. 77).

Genetic data. BIN: BOLD:ADY6339 (*n* = 1 from Argentina). Nearest neighbour: Unidentified *Scythris* from Argentina (Scythrididae, BIN: BOLD:ACW4357, 4.98%).

Remarks. Female unknown. The ventral and dorsal aspects were difficult to interpret in the male genitalia because only a single male is known, and the structures are distorted under the cover glass. Based on COI maximum likelihood phylogeny, the South American taxa *subdimota*, *depressa*, *pozohondaensis*, *spiniuncus*, *angulisociella*, *tetrafasciella*, and *curvisociella* group together, associating next to the North American taxa classified in *Rhamphura* on BOLD (Suppl. material 2). Structurally these taxa are heterogeneous and the external characters, male and/or female genitalia show varying degrees of similarities to the North American *Rhamphura*, as diagnosed and illustrated in Landry (1991). With regard to *curvisociella*, the structural differences are notable and we therefore took a conservative view and classified this taxon in *Rhamphura* (incertae sedis), highlighting the need for further research.

Rhamphura tetrafasciella Nupponen, sp. nov., genus combination incertae sedis

http://zoobank.org/5E53FDE0-EF2C-4DCC-8656-F22115260D1D
Figs 9, 64

Type material. ***Holotype.*** Argentina • ♀; prov. La Rioja, valley east of Sierra de Sanogasta; 29°51.7'S, 67°09.9'W; 670 m a.s.l.; 22 Sep. 2017; K. Nupponen & R. Haverinen leg.; [BOLD sample ID] KN01040; [genitalia slide] K. Nupponen prep. no. 3/13 Dec. 2019; coll. NUPP (MZH).

Diagnosis. Externally distinctive species, readily recognised by four transverse dark brown fasciae on forewing. The female genitalia are characterised by the funnel-shaped sterigma attached anteriorly to an arched plate.

Description. Wingspan 10 mm. Head dark brown, forehead mixed with white. White scales around eye. Neck tuft white. Collar, haustellum, tegula and thorax dark brown with scattered white. Scape dark brown, ventrally mixed with white; pecten as long as diameter of scape. Flagellum dark brown, 0.6 × length of forewing. Labial palp white, palpomere III mixed with dark brown. Legs: femur and tarsi white, each tarsus two dark brown patches at upper surface; tibiae mixed with fuscous. Abdomen anterior 1/2 of each segment dorsally dark brown, otherwise white. Forewing dirty white, cut by four irregular transverse dark brown fasciae belts subbasally, at 0.45, 0.7, and subapically. Hindwing pale fuscous.

Female genitalia. Sterigma funnel-shaped, distally tapered, posterior 1/2 more sclerotised; anteriorly attached to arched sclerotisation. Ostium small, situated at tip

of sterigma. Sternum VII trapezoid, 1.3 × wider than high. Apophyses anteriores 0.7 × length of apophyses posteriores.

Etymology. Diminutive noun in apposition. The species name refers to the forewing patterning of the moth.

Distribution. NW Argentina.

Habitat. The collecting site is a xerothermic saline valley at foothills of the Andes, with rather sparse vegetation.

Genetic data. BIN: BOLD:ADZ0119 (*n* = 1 from Argentina). Nearest neighbour: *Scythris* sp. (BIN: BOLD:ADZ0118, 5.65%).

Remarks. Male unknown. Based on COI maximum likelihood phylogeny, the South American taxa *subdimota*, *depressa*, *pozohondaensis*, *spiniuncus*, *angulisociella*, *tetrafasciella*, and *curvisociella* group together, associating next to the North American taxa classified in *Rhamphura* on BOLD (Suppl. material 2). Structurally these taxa are heterogeneous and the external characters, male and/or female genitalia show varying degrees of similarities to the North American *Rhamphura*, as diagnosed and illustrated in Landry (1991). With regard to *tetrafasciella*, the structural differences are notable and we therefore took a conservative view and classified this taxon in *Rhamphura* (incertae sedis), highlighting the need for further research.

Landryia Kemal & Koçak, 2006

Nomenclatural note. *Landryia* Kemal & Koçak, 2006 is a replacement name for *Asymmetrura* Landry, 1991 (Kemal and Koçak 2006).

The *ankylosauroides* species group

Distal arm of gnathos very long, sigmoid, and at tip round extension covered by minute thorns. Valvae asymmetrical with heavily sclerotised extensions. Male sternum VIII large plate with anterior apodemes. Male tergum VIII posteriorly with long and heavily sclerotised spines. Species included: *ankylosauroides*, *chilensis*.

Landryia ankylosauroides Nupponen, sp. nov., genus combination incertae sedis

http://zoobank.org/5173B006-37BB-467F-A1CF-187F5B523FC2
Figs 10, 42, 65

Type material. ***Holotype.*** Argentina • ♂; prov. Santiago del Estero, Pozo Honda village S, by salt lake; 27°17.2'S, 64°28.0'W; 260 m a.s.l.; 20 Sep. 2017; K. Nupponen & R. Haverinen leg.; [BOLD sample ID] KN01059; [genitalia slide] K. Nupponen prep. No. 4/13 Jan. 2019; coll. NUPP (MZH).

Paratypes. Argentina • 20 ♂, 9 ♀; same data as for holotype; [BOLD sample ID] KN01060; [genitalia slide] K. Nupponen prep. No. 2/13 Jan. 2019 ♂; coll.

NUPP; • 21 ♂, 12 ♀; same data as for holotype except collecting date; 19 Sep. 2017; [BOLD sample IDs] KN01061, KN01062; [genitalia slide] K. Nupponen prep. No. 1/15 Dec. 2019 ♀; coll. NUPP; • 1 ♀; prov. La Rioja, valley east of Sierra de Sanogasta; 29°51.7'S, 67°09.9'W; 670 m a.s.l.; 22 Sep. 2017; K. Nupponen & R. Haverinen leg.; coll. NUPP.

Diagnosis. A pale streak in forewing is diagnostic. In the male genitalia of *L. ankylosauroides*, the S-shaped distal arm of gnathos is distinctive, and similar structure is found only in *L. chilensis*. The two taxa are readily separated by several details in the male genitalia: in *L. ankylosauroides* the left valva is much shorter than the right one (in *L. chilensis* valvae ca. equal length) and the right valva is without large distal lobe (in *L. chilensis* a large distal lobe is present), tergum VIII has narrow lateral arms with melanised spikes (in *L. chilensis* spikes are absent and posterior margin is deeply concave). In the female genitalia of *L. ankylosauroides*, sterigma is an inverted cone, which resembles that of *R. pozohondaensis*, but differs by trapezoid posterior flap (parallel triangular flaps in *R. pozohondaensis*) and absence of cleavage at anterior tip.

Description. Wingspan 10.5–12 mm. Head, collar, tegula and thorax pale fuscous; few white scales around eye, and small blotch of same colour at medioposterior margin of thorax. Neck tuft and haustellum white. Scape dorsally dark brown, ventrally dirty white, pecten longer than diameter of scape. Flagellum dark brown, 0.65 × length of forewing, in male ciliate, sensillae ~ 0.75 × as long as diameter of flagellum. Labial palps: palpomere I white; lower surface of posterior 1/2 of palpomere II and palpomere III dark brown, otherwise white. Legs cream, upper surfaces more or less mixed with different tones of brown. Abdomen dorsally fuscous, ventrally dirty white. Forewing grey, costal area slightly darker than dorsal one; more or less distinct white streak in forewing from base to termen, in dorsal margin edged by interrupted dark brown line; few white scales at apical area. Hindwing pale grey.

Male genitalia. Uncus heavily sclerotised, subtriangular, basal part heart-shaped. Gnathos base small belt; distal arm long, strongly sigmoid (S-shaped), tip club-shaped covered by minute spines. Tegumen rectangular. Phallus 0.7 × length of right valva, straight, shaped as elongated bottle. Valvae asymmetrical, fused at basal 1/2, dorsal margins setose; left valva short, oval; right valva 1.4 × longer than left, of constant width, subapically with small extension, apex bent, heavily sclerotised, tip shallowly indented. Saccus as long as right valva, triangular. Sternum VIII large hexagonal plate, medioposteriorly deeply U-shaped; posterior margin with two asymmetrical and diverging extensions, longer one with numerous long and thin setae; latero-anterior corners with parallel long and narrow extensions, tips spatulate. Tergum VIII trapezoid basally, anterior margin concave; medioposteriorly with digitate extension; mediolaterally at both sides long and upwards directed extensions, distal 1/2 with ~ ten long and heavily sclerotised spiniform setae.

Female genitalia. Sterigma triangular. Ostium small, situated at anterior tip of sterigma. Sternum VII trapezoid; lateroposteriorly small triangular flaps at both sides, anterior corners extended. Sternum VIII with two, suboval, sclerotised plates. Apophyses anteriores 0.35 × length of apophyses posteriores.

Etymology. Latinised adjective in the nominative singular. The species name alludes to the shape of the gnathos arm, reminiscent of the tail of Ankylosauridae (Reptilia: Dinosauria).

Distribution. NW Argentina.

Habitat. The habitat at the type locality of Pozo Honda is a dry shrubby area near a salt lake shore (Fig. 78); the other collecting site is an open valley with halophytic vegetation.

Genetic data. BIN: BOLD:ADZ2684 (*n* = 3 from Argentina). Genetically rather homogenous, maximum variation 0.32%. Nearest neighbour: North American *Landryia matutella* (Clemens, 1860) (Scythrididae, BIN: BOLD:AAE6120, 1.25%).

Remarks. Based on our COI maximum likelihood phylogeny, the South American taxa *ankylosauroides* and *chilensis* group inside a large clade, whose taxa are classified in *Landryia* on BOLD (Suppl. material 2). However, *ankylosauroides* and *chilensis* do not have the diagnostic morphological characters of *Landryia*, such as a greatly enlarged bulbus ejaculatorius (unless accidentally removed during dissection) in the male genitalia and the pincer-like projections on the caudal margin of female sternum VII (Landry 1991). Also, male sternum VIII of *ankylosauroides* and *chilensis* are distinct with their spiniform setae and long apodemes, but such are not present in North American *Landryia* (Landry 1991). Further, North American *L. matutella*, which is genetically the nearest neighbour to taxon *ankylosauroides*, is morphologically different. We therefore classified these two taxa in *Landryia* (incertae sedis), highlighting the need for further research.

Landryia chilensis Nupponen, sp. nov., genus combination incertae sedis

http://zoobank.org/F4FCD502-354B-4B1B-812B-DF54C443D4EC
Figs 11, 43

Type material. ***Holotype.*** Chile • ♂; Coquimbo district, near Comparbala village; 30°52.4'S, 71°10.9'W; 660 m a.s.l.; 1 Feb. 2017; K. Nupponen & R. Haverinen leg.; [BOLD sample ID] KN01096; [genitalia slide] K. Nupponen prep. no. 3/18 Dec. 2019; coll. NUPP (MZH).

Diagnosis. Wings without any distinct pattern, and may be confused with several patternless, similarly sized species, e,g., *S. tigrensis*. In the male genitalia of *L. chilensis*, the shape of distal arm of the gnathos is distinctive; a similarly shaped narrow and curved gnathos is found only in *L. ankylosauroides.* The two taxa are readily separated by several details in the male genitalia: in *L. chilensis*, the valvae are subequal in length (in *L. ankylosauroides* the left valva is much shorter), the right valva has large sclerotised lobe (absent in *L. ankylosauroides*), and shape of both tergum VIII and sternum VIII are unique.

Description. Wingspan 14.5 mm. Head, collar, haustellum, tegula and thorax fuscous mixed with dirty white. Few white scales exist around eye. Neck tuft white. Scape fuscous mixed with dirty white, pecten pale cream and longer than diameter of

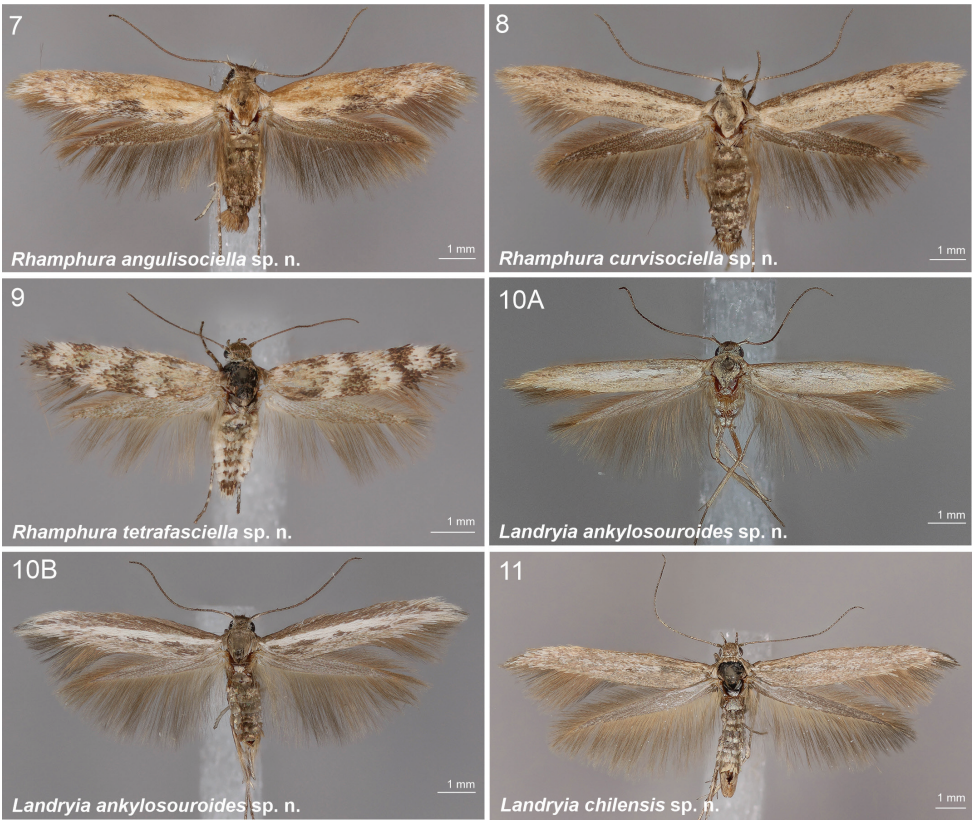

Figures 7–11. Scythrididae adults, genera *Rhamphura* and *Landryia* **7** *R. angulisociella* Nupponen, sp. nov., genus combination incertae sedis, male, holotype **8** *R. curvisociella* Nupponen, sp. nov., genus combination incertae sedis, male, holotype **9** *R. tetrafasciella* Nupponen, sp. nov., genus combination incertae sedis, female, holotype **10A** *L. ankylosauroides* Nupponen sp. nov., genus combination incertae sedis, male, holotype **10B** *L. ankylosauroides* Nupponen, sp. nov., genus combination incertae sedis, male, paratype **11** *L. chilensis* Nupponen, sp. nov., genus combination incertae sedis, male, holotype.

scape. Flagellum dark brown, 0.65 × length of forewing, ciliate, sensillae 1/2 as long as diameter of flagellum. Labial palps with palpomere I and base of palpomere II white, otherwise fuscous more or less mixed with white. Legs fuscous, lower surface suffused with dirty white. Abdomen dorsally lead grey, each segment posteriorly edged by greyish white; ventrally dirty white. Forewing narrow, grey; scattered with dirty white scales densely in fold and at apical area, and sparsely in costal area. Hindwing fuscous.

Male genitalia. Uncus small, heavily sclerotised rectangular plate. Gnathos base uneven plate; distal arm 1.65 longer than valva, sigmoid and somewhat unevenly thick, apex club-shaped, covered with microtrichia. Tegumen hood-shaped. Phallus short, drop-shaped, laterally with narrow extensions. Valvae asymmetrical, short and straight, dorsally with subbasal triangular lobes, subapically with small transverse flaps, distally setose; right valva basally with complex heavily sclerotised lobe. Saccus rectangular,

broad. Sternum VIII hexagonal basally, medioposteriorly with large U-shaped depression, posterior shanks somewhat asymmetrical; mediolaterally extended as small flaps at both sides, attached to two long and narrow medio-anterior apodemes. Tergum VIII narrow, tongue-shaped, lateral and posterior margins folded and furnished with ~ twelve long heavily sclerotised spiniform setae; anteriorly with two long and narrow diverging apodemes.

Etymology. Latinised adjective in the nominative singular. The species name refers to the country in which the taxon was discovered.

Distribution. Central Chile.

Habitat. The habitat is a shrubby riverside spot with sparse vegetation in the Andes foothills.

Genetic data. BIN: BOLD:ADZ5419 (n = 1 from Chile). Nearest neighbour: *Landryia* JFL138 from USA: California (BIN: BOLD:AAE6120, 6.18%).

Remarks. Female unknown. Based on COI maximum likelihood phylogeny, the South American taxa *ankylosauroides* and *chilensis* group inside a large clade, whose taxa are classified in *Landryia* on BOLD (Suppl. material 2). However, *ankylosauroides* and *chilensis* do not have the diagnostic morphological characters of *Landryia*, such as greatly enlarged bulbus ejaculatorius (unless accidentally removed during dissection) in the male genitalia and the pincer-like projections on caudal margin of female sternum VII (Landry 1991). Also, male sternum VIII of *ankylosauroides* and *chilensis* are distinct with their spiniform setae and long apodemes, but such are not present in North American *Landryia* (Landry 1991). We therefore classified these two taxa in *Landryia* (incertae sedis), highlighting the need for further research.

Scythris Hübner, 1825

The *directiphallella* species group

Distal arm of gnathos and phallus long and slim. Ventral margin of valva often with large extension. Male sternum VIII pentagonal with distinct and sharp posterior shanks. Species included: *directiphallella*, *furciphallella*, *manchaoensis*, *salinasgrandensis*, *angustivalvella*, *zeugmatica*.

Male genitalia of *directiphallella* species group resemble the African *Haploscythris*, particularly the bilobed uncus, divided valva in several species and V-shaped anterior margin of vinculum (compare against illustrations in Bengtsson 2014). More data are needed to confirm or reject potential *Haploscythris* association.

Scythris directiphallella Nupponen, sp. nov.

http://zoobank.org/24086F7E-BD7F-400B-B3D0-8D165AAEB9B6
Figs 12, 44

Type material. ***Holotype.*** Argentina • ♂; prov. Santiago del Estero, Pozo Honda village S, by salt lake; 27°17.2'S, 64°28.0'W; 260 m a.s.l.; 19 Sep. 2017; K. Nupponen &

R. Haverinen leg.; [BOLD sample ID] KN01052; [genitalia slide] K. Nupponen prep. no. 3/28 Dec. 2019; coll. NUPP (MZH).

Paratype. Argentina • 1 ♂; same data as for holotype; coll. NUPP.

Diagnosis. Wings grey, impossible to separate externally from *S. furciphallella*. The male genitalia of *S. directiphallella* are by having narrow valvae with a ventral thorn-like process apically, a straight phallus and pincer-like extensions on posterior margin of male sternite VIII.

Description. Wingspan 9–10.5 mm. Head, collar, neck tuft, haustellum, tegula and thorax grey. Scape grey, ventrally mixed with dirty white; pecten grey and as long as diameter of scape. Flagellum fuscous, 0.7 × length of forewing, ciliate, sensillae ~ 1/2 as long as diameter of flagellum. Labial palp: palpomere I dirty white, palpomeres II and III fuscous mixed with dirty white. Legs fuscous, more or less suffused with dirty white. Abdomen dorsally pale grey, ventrally a little paler, anal tuft cream. Forewing grey, over the wing sparsely scattered dark fuscous scales. Hindwing pale fuscous.

Male genitalia. Gnathos (homology interpretation of gnathos and uncus based on Landry (1991)) base broad, weakly sclerotised belt; distally long, slender and bent downwards, tip pointed. Uncus bilobed plate, posterior shanks subapically with small nipple-like extensions. Tegumen elongated hood, dorsally widely open. Phallus 0.75 × length of valva, straight, tip pointed. Valva long and narrow; apex setose and slightly incurved; apically with robust ventral thorn-like process. Saccus short, triangular. Juxta narrow, 0.8 × length of phallus. Sternum VIII pentagonal; posteriorly bifurcate, shanks short, bent inwards with tips pointed. Tergum VIII trapezoid, anterior margin widely concave and weakly sclerotised, posterior margin convex.

Etymology. Diminutive noun in apposition. The species name refers to the straight phallus of the male, which is a diagnostic character of the species.

Distribution. NW Argentina.

Habitat. The collecting site is a dry, shrubby area near a salt lake shore (Fig. 77).

Genetic data. BIN: BOLD:ADY7318 (n = 2 from Argentina). Nearest neighbour: *Scythris salinasgrandensis* Nupponen, sp. nov. (BIN: BOLD:ADY7738, 4.49%).

Remarks. Female unknown. Based on COI maximum likelihood phylogeny, the South American taxa *salinasgrandensis*, *furciphallella*, *manchaoensis*, *angustivalvella*, and *directiphallella* group together, associating within a clade, whose taxa are classified in apparently non-monophyletic *Scythris* on BOLD (Suppl. material 2). We classify these taxa in *Scythris*.

Scythris furciphallella Nupponen, sp. nov.

http://zoobank.org/D8D83C42-B864-4ECD-85A8-90E0F26587CA

Figs 13, 45, 66

Type material. ***Holotype.*** Argentina • ♂; prov. Cordoba, Salinas Grandes SE shore; 29°50.5'S, 64°40.2'W; 185 m a.s.l.; 24 Sep. 2017; K. Nupponen & R. Haverinen leg.; [BOLD sample ID] KN01053; [genitalia slide] K. Nupponen prep. no. 2/16 Dec. 2019; coll. NUPP (MZH).

***Paratypes*.** Argentina • 6 ♂, 2 ♀; same data as for holotype; [genitalia slides] K. Nupponen prep. no. 3/16-XII-2019 ♀, 3/13-I-2019 ♂; coll. NUPP; • 1 ♂; prov. La Rioja, Andes Mts., Sierra de Famatina, Famatina village 15 km NNW; 28°46.4'S, 67°35.0'W; 2085 m a.s.l.; 27 Jan. 2017; K. Nupponen & R. Haverinen leg.; [BOLD sample ID] KN01050; [genitalia slide] K. Nupponen prep. no. 1/17 Dec. 2019; coll. NUPP.

Diagnosis. A grey species, externally indistinguishable from *S. directiphallella*. In the male genitalia, a posteriorly bifurcate phallus and large backwards directed ventral lobes of the valvae are diagnostic.

Description. Wingspan 9.5–10.5 mm. Head, collar, neck tuft, haustellum, tegula and thorax grey. Scape grey, ventrally mixed with cream; pecten grey and longer than diameter of scape. Flagellum fuscous, 0.7 × length of forewing, ciliate, sensillae ~ 0.8 × as long as diameter of flagellum. Labial palp: palpomere I dirty white, palpomeres II and III fuscous mixed with dirty white. Legs fuscous, more or less suffused with dirty white. Abdomen fuscous, ventrally paler, anal tuft ventrally cream. Forewing grey, wing irrorated with black scales; in some specimens' very indistinct whitish streak in fold at basal 1/3. Hindwing pale fuscous.

***Male genitalia*.** Gnathos basally semi-circular; distally long, slender and bent downwards. Uncus rectangular plate, medioposteriorly with small indentation. Tegumen hood-shaped. Phallus 0.65 × length of valva, bent, apex bifurcate, slender branch twice longer than the other. Valva long and narrow, distally spatular; ventral margins subapically with huge, anteriorly-directed, slightly asymmetrical lobes. Saccus short, labiate. Juxta narrow, 0.5 × length of phallus. Sternum VIII pentagonal, paired posterior projections diverging, straight, tips pointed; anterior margin slightly concave. Tergum VIII trapezoid, elongated, posteriorly round and setose, anteriorly incurved.

***Female genitalia*.** Sterigma long and straight, rather stout, at 0.65 a little broadened, terminal 1/3 sclerotised, tip blunt. Ostium round, margins sclerotised, situated at 0.65 of sterigma. Sternum VII rectangular, 1.35 × wider than high, posterior margin medially incurved, anterior margin concave and sclerotised. Apophyses anteriores 0.55 × length of apophyses posteriores.

Etymology. Diminutive noun in apposition. The species name refers to a bifurcate phallus of the male.

Distribution. NW Argentina.

Habitat. The collecting site is a shore of a large salt lake, in the edge between dry bushy area and low saline vegetation (Fig. 75).

Genetic data. BIN: BOLD:ADY9699 (n = 2 from Argentina). The two barcode sequences are 0.96% distant. Nearest neighbour: *Scythris salinasgrandensis* Nupponen, sp. nov. (BIN: BOLD:ADY7738, 4.49%).

Remarks. Based on COI maximum likelihood phylogeny, South American taxa *salinasgrandensis*, *furciphallella*, *manchaoensis*, *angustivalvella* and *directiphallella* group together, associating within a clade, whose taxa are classified in apparently non-monophyletic *Scythris* on BOLD (Suppl. material 2). We classify these taxa in *Scythris*.

***Scythris manchaoensis* Nupponen, sp. nov.**
http://zoobank.org/F426C532-CE83-4009-9BE0-2946412EB563
Figs 14, 46

Type material. ***Holotype*.** Argentina • ♂; prov. Catamarca, Sierra de Manchao; 28°43.6'S, 66°21.1'W; 1190 m a.s.l.; 23 Sep. 2017; K. Nupponen & R. Haverinen leg.; [BOLD sample ID] KN01032; [genitalia slide] K. Nupponen prep. no. 1/11 Dec. 2019; coll. NUPP (MZH).

Diagnosis. A fuscous species, externally similar to *S. salinasgrandensis*, but distinguished by the fringes being the same colour as the forewing surface (distinctly darker in *S. salinasgrandensis*) and a small spot at cell end (lacking in *S. salinasgrandensis*). The male genitalia of *S. manchaoensis* resemble those of *S. angustivalvella*, but differ in the distally broader valva and the sigmoid phallus, short and converging appendices on posterior margin of sternum VIII (narrower valva, arched phallus, long and diverging appendices in *S. angustivalvella*).

Description. Wingspan 15.5 mm. Head, collar, neck tuft, haustellum, tegula and thorax fuscous, same colour as forewing. Scape fuscous; pecten paler and longer than diameter of scape. Flagellum fuscous, 0.65 × length of forewing, in male ciliate, sensillae as long as diameter of flagellum. Labial palp: palpomere I pale fuscous white; palpomere II: inner surface dirty white fuscous, otherwise fuscous with faintly scattered dirty white; palpomere III pale fuscous with distal 1/2 suffused faintly darker. Legs fuscous, mixed with dirty white, more so in hind legs. Abdomen dorsally pale fuscous, ventrally dirty whitish fuscous. Forewing fuscous with sparsely scattered blackish scales, indistinct dark spot at cell end. Hindwing fuscous, slightly paler than forewing.

***Male genitalia*.** Uncus bilobed plate, tips of posterior lobes bent ventrad and pointed. Gnathos base hood-like, rather weakly sclerotised; distal arm long and slender, bent 90° at basal 1/2, tip bent downwards and pointed. Phallus slender, shallowly sigmoid, 0.8 × length of gnathos arm, tip pointed. Valva straight and broad at basal 0.6; distal 0.4 narrow and bent, tip widened, spatular and setose; ventrally at middle long, robust, incurved, horn-like process. Saccus short, triangular. Juxta narrow, elongate, 1.15 × length of phallus. Sternum VIII pentagonal, posteriorly bifurcate, shanks short and converging; anterior corners widened, anterior margin incurved and somewhat sclerotised. Tergum VIII triangular, posteriorly elongate with blunt tip, anterior margin wide, concave.

Etymology. Latinised adjective in the nominative singular. The species is named after the type locality, in the Manchao range of the Andes.

Distribution. NW Argentina.

Habitat. The collecting site is a dry and xerothermic rocky slope with low vegetation and sparse shrubs (Fig. 76).

Genetic data. BIN: BOLD:ADY8793 (*n* = 1 from Argentina). Nearest neighbour: *Scythris angustivalvella* Nupponen, sp. nov. (BIN: BOLD:ADY8789, 2.75%). *Scythris salinasgrandensis*, whose male is unknown, is externally similar, and its barcode differs by 5.62%.

Remarks. Female unknown. Based on COI maximum likelihood phylogeny, South American taxa *salinasgrandensis*, *furciphallella*, *manchaoensis*, *angustivalvella*, and *directiphallella* group together, associating within a clade, whose taxa are classified in apparently non-monophyletic *Scythris* on BOLD (Suppl. material 2). We classify these taxa in *Scythris*. The male genitalia of *angustivalvella* and *manchaoensis* are similar to *S. zhakovi* Bidzilya & Budashkin, 2017 from Ukraine (Bidzilya et al. 2017).

Scythris salinasgrandensis **Nupponen, sp. nov.**
http://zoobank.org/92E7893B-FB97-4B21-8577-5626BB509745
Figs 15, 67

Type material. ***Holotype.*** Argentina • ♀; prov. Cordoba, Salinas Grandes SE shore; 29°50.5'S, 64°40.2'W; 185 m a.s.l.; 24 Sep. 2017; K. Nupponen & R. Haverinen leg.; [BOLD sample ID] KN01033; [genitalia slide] K. Nupponen prep. no. 3/11 Dec. 2019; coll. NUPP (MZH).

Paratypes. Argentina • 10 ♀; same data as for holotype; [BOLD sample ID] KN01034; coll. NUPP; • 1 ♀; same data as for holotype except collecting date; 13 Sep. 2017; coll. NUPP.

Diagnosis. Wings pale grey, finely peppered with brown fuscous species, externally easily mixed with *S. manchaoensis*, but separated by fringes being distinctly darker than forewing (same colour as forewing in *S. manchaoensis*) and absence of small spot at cell end (present in *S. manchaoensis*). In the female genitalia, a large and distinctly defined oval sterigma is diagnostic.

Description. Wingspan 15–18 mm. Head, collar, neck tuft, haustellum, tegula and thorax fuscous, same colour as forewing, head and haustellum mixed with dirty white. Scape fuscous except ventral surface and pecten whitish grey, pectin longer than diameter of scape. Flagellum fuscous, 0.6 × length of forewing. Labial palp: palpomere I pale dirty white; palpomeres II and III: upper surface dirty white, otherwise fuscous mixed with a few dirty white scales. Legs fuscous, mixed with dirty white. Abdomen dorsally pale fuscous, ventrally dirty white. Forewing pale grey, finely peppered with brown, fringes darker than wing. Hindwing slightly paler than forewing.

Female genitalia. Sterigma oval ring with sclerotised margin, anteriorly with quadrangular sclerotised extension. Ostium situated anteriorly in ring. Sternum VII quadrangular; posterior margin medially incurved, anterior margin sclerotised. Apophyses anteriores 0.5 × length of apophyses posteriores.

Etymology. Latinised adjective in the nominative singular. The species is named after the type locality, the Salinas Grandes salt lake.

Distribution. NW Argentina.

Habitat. The collecting site is the shore of a large salt lake, in the zone between a dry shrubby area and low halophytic vegetation.

Genetic data. BIN: BOLD:ADY7738 (*n* = 2 from Argentina). Nearest neighbour: *Scythris furciphallella* Nupponen, sp. nov. (BIN: BOLD:ADY9699, 4.49%). *Scythris manchaoensis* is externally similar, and its barcode differs by 5.62%.

Remarks. Male unknown. Based on COI maximum likelihood phylogeny, South American taxa *salinasgrandensis*, *furciphallella*, *manchaoensis*, *angustivalvella* and *directiphallella* group together, associating within a clade, whose taxa are classified in apparently non-monophyletic *Scythris* on BOLD (Suppl. material 2). We classify these taxa in *Scythris*.

***Scythris angustivalvella* Nupponen, sp. nov.**
http://zoobank.org/A3BEA5B6-87AB-4846-B264-F06E0A51F110
Figs 16, 47

Type material. ***Holotype*.** Argentina • ♂; prov. Santiago del Estero, Pozo Honda village S, by salt lake; 27°17.2'S, 64°28.0'W; 260 m a.s.l.; 19 Sep. 2017; K. Nupponen & R. Haverinen leg.; [BOLD sample ID] KN01051; [genitalia slide] K. Nupponen prep. no. 4/16 Dec. 2019; coll. NUPP (MZH).

Diagnosis. Both fore- and hindwings are fuscous. The male genitalia of *S. angustivalvella* resemble those of *S. manchaoensis*, but differ by the distally narrower valva and arched phallus (sigmoid in *S. manchaoensis*), as well as in details of sternum VIII (posteromedial prongs long and diverging in *angustivalvella*, short with apices converging in *manchaoensis*) and details of tergum VIII (posterior margin indented in *angustivalvella*, with medial extension rounded in *manchaoensis*).

Description. Wingspan 11 mm. Head, collar, neck tuft, haustellum, tegula and thorax fuscous, with scattered dirty white scales. Scape dorsally fuscous, ventrally dirty white, pecten dirty white and longer than diameter of scape. Flagellum brown, 0.7 × length of forewing, ciliate, sensillae as long as diameter of flagellum. Labial palp: palpomere I white; palpomeres II and III: lower surface dark brown, otherwise dirty white. Legs dirty white, tibiae and tarsi mixed with brown. Abdomen dorsally fuscous, ventrally dirty white. Forewing fuscous; narrow indistinct whitish streak in fold from base to midwing; small dark brown spot at cell end. Hindwing fuscous.

***Male genitalia*.** Uncus a bifurcate plate, tips of posterior lobes blunt. Gnathos base a broad belt; distal arm long, slightly upcurved, basal 1/2 tapered, posterior 1/2 slender, tip pointed. Tegumen broader than high, margins reinforced. Phallus 0.65 × length of valva, slim and arched, tip pointed. Valva long and narrow; basal 1/2 tapered, distal 1/2 slender and incurved, apex spatular; a robust, downcurved horn-like projection ventrally at 0.5. Saccus short, triangular. Juxta narrow, 0.55 × length of phallus. Sternum VIII pentagonal, posteromedial prongs divergent, straight, tips pointed; anterior margin slightly concave. Tergum VIII trapezoid, anterior margin widely incurved, posterior margin slightly indented.

Etymology. Diminutive noun in apposition. The species name refers to the narrow valvae in the male genitalia.

Distribution. NW Argentina.

Habitat. The collecting site is a dry shrubby area near a salt lake shore (Fig. 77).

Genetic data. BIN: BOLD:ADY8789 (n = 1 from Argentina). Nearest neighbour: *Scythris manchaoensis* Nupponen, sp. nov. (BIN: BOLD:ADY8793, 2.57%).

Remarks. Female unknown. Based on COI maximum likelihood phylogeny, South American taxa *salinasgrandensis*, *furciphallella*, *manchaoensis*, *angustivalvella*, and *directiphallella* group together, associating within a clade, whose taxa are classified in apparently non-monophyletic *Scythris* on BOLD (Suppl. material 2). We classify these taxa in *Scythris*. The male genitalia of *angustivalvella* and *manchaoensis* are similar to *S. zhakovi* Bidzilya & Budashkin, 2017 from Ukraine (Bidzilya et al. 2017).

Scythris zeugmatica Meyrick, 1931

Figs 17, 48

Scythris zeugmatica Meyrick, 1931. Exotic Microlepidoptera 4 (part 6): 179.

Material examined. ***Holotype*** (fixed by monotypy, Art. 73.1.2 (ICZN 2000). Brazil • ♂; Santarem; 8.19.; Parish leg.; [genitalia slide] JFGC No. 8050; NHMUK ID 010922366; NHMUK slide ID 010316662; coll. NHMUK.

Diagnosis. A small species (10 mm), externally resembles to some extent *S. zeugmatica* with similar whitish streak on forewing. *Scythris zeugmatica* is readily separated from the other described species by characters in the male genitalia, particularly by bilobed uncus, a peculiar vertical sclerotisation with lateral expansion (homology unclear), and broad, symmetrical valvae with a small subapical ventral tooth.

Description. The original description is quoted: "Wingspan ♂ 10 mm. Head whitish. Palpi whitish, terminal joint suffused grey. Thorax bronzy-grey. Abdomen dark grey, beneath whitish-ochreous. Forewings elongate-lanceolate; rather dark purple-grey; a rather broad suffused yellow-whitish streak along fold throughout, crossed at its middle by a fasciate bar reaching dorsum but not reaching costa, beyond this attenuated and indistinct, but expanded into an oval spot on tornus, a somewhat inwards-oblique spot on costa towards apex rather beyond this: cilia grey. Hindwings 0.75, grey; cilia grey."

Male genitalia. Uncus bilobed, basally fused by narrow transverse sclerotisation. Gnathos base U-shaped. Tegumen hood-shaped, anterior margin medially deeply cleft. Ventrad of tegumen are situated two sclerotised, vertical structures (homologies are unclear): other rather straight with sharp apexes (Fig. 48 on left), other slightly longer, at middle triangularly extended (Fig. 48 on right). Valva broad and straight, dorsal margin at basal quarter somewhat folded; ventrally slightly broadened beyond middle, subapically with small triangular tooth. Saccus short, triangular, at base with small digitate process. Sternum VIII trapezoid, anterolaterally with small lobes, posteriorly with pair of stout parallel horn-like projections. Tergum VIII subrectangular, laterally concave, anterior margin sclerotised.

Distribution. Brazil.

Remarks. Female unknown. DNA barcode is not available yet for *S. zeugmatica*. We place *S. zeugmatica* in the *directiphallella* species group based on morphology. It has a similar long and slim gnathos, long and slim phallus, and male sternum VIII has sharp posterior shanks.

***Scythris caimancitoensis* Nupponen, sp. nov.**
http://zoobank.org/BC28429D-6162-4356-865E-6C5DA7B1F9E9
Figs 18, 49

Type material. ***Holotype*.** Argentina • ♂; prov. Jujuy, Rio San Francisco, by Caimancito village; 23°43.8'S, 64°36.3'W, 400 m a.s.l.; 18 Sep. 2017; K. Nupponen & R. Haverinen leg.; [BOLD sample ID] KN01037; [genitalia slide] K. Nupponen prep. no. 3/9 Dec. 2019; coll. NUPP (MZH).

Diagnosis. Externally somewhat resembling *S. tibicina*, but distinguished by the more contrasty pattern and cream colour of the forewings. In the male genitalia, the strikingly long and blade-like valvae (which sticks out from the abdomen, see Fig. 18) and an elongate sternum VIII are diagnostic.

Description. Wingspan 13.5 mm. Head brown, laterally paler. Collar and neck tuft mixed with various shades of brown and dirty white, tegula pale brown. Haustellum dirty white. Thorax dark brown. Scape dorsally dark brown, ventrally dirty cream; pecten dirty cream and longer than diameter of scape. Flagellum dark brown, 0.7 × length of forewing, ciliate, sensillae ~ 1/2 as long as diameter of flagellum. Labial palps white, except lower surface of palpomeres II and III dark brown. Legs dirty white, except tibia and tarsus of foreleg brown, and upper surface of hindleg tarsus with pale brown hair. Abdomen dorsally dark fuscous, ventrally white. Forewing dark brown, blackish at basal 1/2 of wing at costal and widely at dorsal areas; fold broadly cream, connected to dash of same colour at cell end, the latter extended to subapical area. Hindwing dark fuscous.

***Male genitalia*.** Uncus small and labiate. Gnathos reduced to small transverse flap. Tegumen hood-shaped. Phallus short, basally indented, distal 1/2 tapered, tip extended, bent and pointed. Valva very long, straight and of constant width, apically tapered and bent inwards, tip pointed; costal and dorsal margins sclerotised and setose. Saccus U-shaped, ca. as long as tegumen. Sternum VIII subrectangular, strongly elongated and narrow, deeply indented both postero- and anteromedially; anterior margin with two parallel triangular lobes; at anterior 1/3 of plate two longitudinal setose ridges. Tergum VIII small, rectangular, posterior margin widely concave, anterior corners extended.

Etymology. Latinised adjective in the nominative singular. The species is named after the type locality, the village of Caimancito.

Distribution. NW Argentina.

Habitat. The collecting site is a dry river bed surrounded by forests and plantations. Plants of the family Amaranthaceae were common along the river banks (Fig. 79).

Genetic data. Not obtained (specimen submitted to barcode analysis but the sample failed).

Remarks. Female unknown. The male genitalia do not show affinities to other described American Scythrididae. The very large male genitalia is diagnostic for *Arotrura* Walsingham 1888, but *caimancitoensis* does not have the other diagnostic characters of that genus (Landry 1991). We classify *caimancitoensis* in *Scythris*, but the genus combination needs more research.

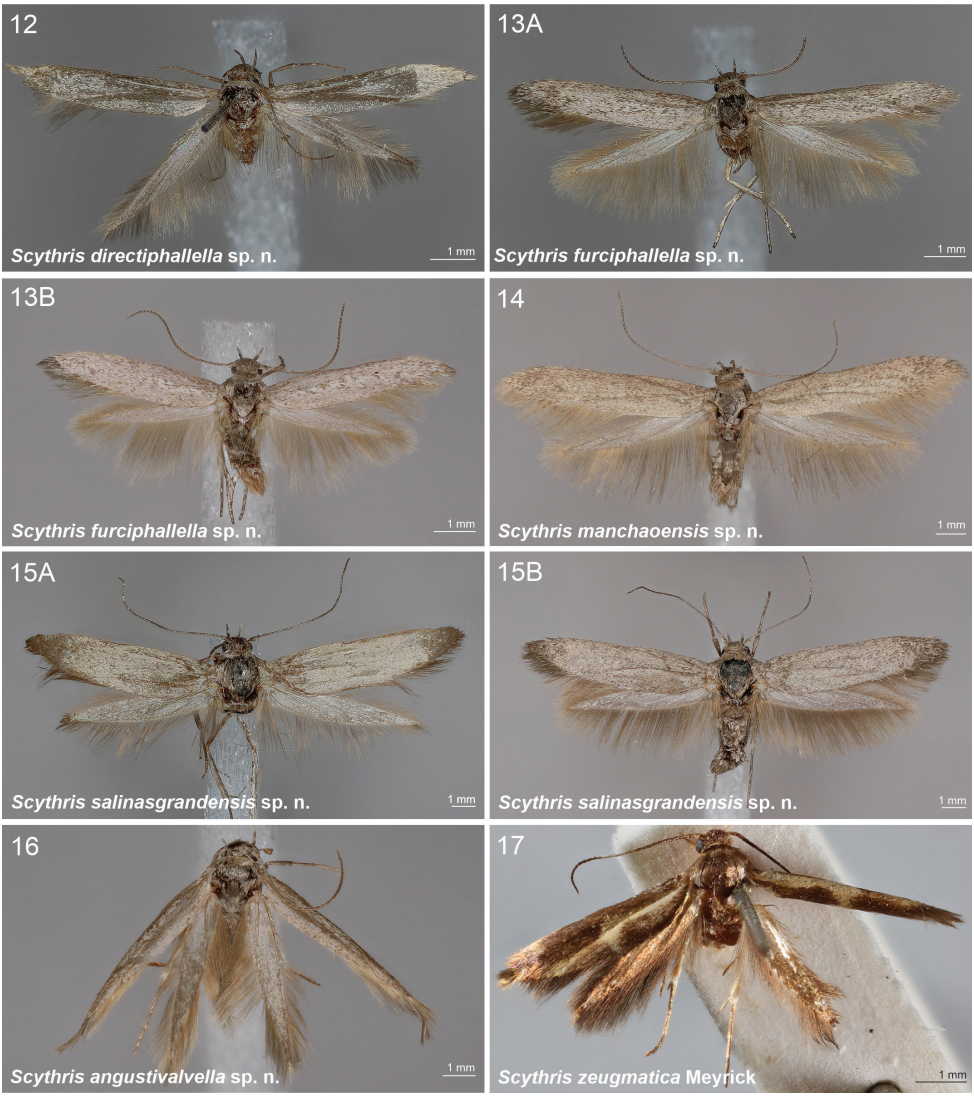

Figures 12–17. Scythrididae adults, genus *Scythris*. **12** *S. directiphallella* Nupponen, sp. nov., male, holotype **13A** *S. furciphallella* Nupponen sp. nov., male, holotype **13B** *S. furciphallella* Nupponen sp. nov., male, paratype **14** *S. manchaoensis* Nupponen, sp. nov., male holotype **15A** *S. salinasgrandensis* Nupponen sp. nov., female, holotype **15B** *S. salinasgrandensis* Nupponen sp. nov., female, paratype **16** *S. angustivalvella* Nupponen sp. nov., male, holotype **17** *S. zeugmatica* Meyrick, 1916, male, holotype.

Scythris ejiciens Meyrick, 1928

Fig. 19

Scythris ejiciens Meyrick, 1928. Exotic Microlepidoptera, vol. 3 (part 13): 412.

Material examined. ***Holotype*** (fixed by monotypy, Art. 73.1.2 (ICZN 2000)). Peru • ♀; Cocapata; 12.000 feet a.s.l.; NHMUK ID 010922358; coll. NHMUK.

Diagnosis. The abdomen of the type is missing. A small species (wingspan 9 mm). Externally *S. ejiciens* may be separated from the other described Neotropical *Scythris* by a distinct whitish-ochreous streak along the fold from base to the end of cell, followed by whitish-ochreous spot.

Description. The original description is quoted: "Wingspan 9 mm ♀. Head, thorax rather dark purplish-fuscous. Palpi grey. Forewings rather dark purplish-fuscous; a whitish-ochreous streak along fold from base to beyond middle of wing; a roundish whitish-ochreous spot in disc at 0.75: cilia fuscous. Hindwings dark grey; cilia fuscous."

Distribution. Peru.

Remarks. Male unknown. The type specimen of *S. ejiciens* lacks the abdomen and does not have a genital preparation label. Clarke (1965) reported "The abdomen is missing."

Scythris fluvialis Meyrick, 1916

Figs 20, 50

Scythris fluvialis Meyrick, 1916. Exotic Microlepidoptera, vol. 2 (part 1): 15.

Material examined. ***Lectotype.*** Colombia • ♂; Cali; 500 feet a.s.l.; 5–14.; Parish leg.; [genitalia slide] JFGC No. 8052; NHMUK ID 010922359; NHMUK slide ID 010316664; coll. NHMUK.

Paralectotype. Colombia • ♀; same data as for lectotype; coll. NHMUK.

Diagnosis. *Scythris fluvialis* and North American *S. trivinctella* (Zeller, 1873) and *S. ypsilon* Braun, 1920, in addition to five undescribed species, form a compact group, sharing twisted apex of the distal arm of the gnathos, terminating into a small, warped plate (Landry 1991). Posterior margin of male abdominal tergum VIII is elongated in *S. fluvialis*, bifurcate in *S. trivinctella* and distinctly concave with lateral setae in *S. ypsilon*. See Landry (1991) for further details.

Description. The original description is quoted: "Wingspan 12–13 mm ♂, ♀. Head, palpi, and thorax dark bronzy-fuscous. Antennal ciliations of ♂ 0.5. Abdomen bronzy-fuscous, beneath in ♂ suffused with pale ochreous, in ♀ white except anal segment. Forewings lanceolate; dark violet-fuscous, towards costa and dorsum suffused with grey; a thick suffused ochreous-whitish streak from base of dorsum, curved upwards to above middle and returning to fold before middle of wing, where it joins an ochreous tinged patch extending along dorsum to tornus; a thick ochreous-whitish streak from 0.2 of costa to fold parallel to termen, with a , with a projection on posterior edge in middle, tending to connect with a whitish mark on termen above tornus; some ochreous tinge towards termen above this; in ♂ specimen an ochreous-whitish mark at apex: cilia rather dark violet-fuscous. Hindwings with 4 and 5 separate; dark fuscous; cilia dark grey."

Male genitalia. Uncus trapezoid plate. Gnathos base broad belt, dorsally a semicircular extension covered by minute thorns; distal arm long, sigmoid, tip pointed with small flap. Tegumen hood-shaped. Phallus 1/2 length of valva, basal 2/3 straight and of

constant width, distal 1/3 bent ventrally and tapered. Valva long and narrow, distal 1/2 weakly broadened dorsally, tip round and setose. Saccus 0.6 ×as long as valva, broad. Sternum VIII pentagonal plate basally, laterally broadened, apex elongated. Tergum VIII pentagonal plate, posterior extension long and digitate, anterior margin concave, U-shaped.

***Female genitalia*.** Not dissected.

Distribution. Colombia.

Remarks. We leave *fluvialis* in *Scythris*, more precisely next to *S. trivinctella* and *S. ypsilon*, following the diagnostic characters provided by Landry (1991).

Scythris inanima Meyrick, 1916

Figs 21, 51

Scythris inanima Meyrick, 1916. Exotic Microlepidoptera, vol. 2 (part 1): 13.

Material examined. ***Holotype*.** Peru • ♂; Huancayo; 10650 feet a.s.l.; i.7.14.; Parish leg.; [genitalia slide] JFGC No. 8051; NHMUK ID 010922361; NHMUK slide ID 010316663M coll. NHMUK.

Diagnosis. Forewings bronzy-grey without distinctive external features. Genitalia dissection is required for recognition. *Scythris inanima* is readily separated from the other described species by details of the male genitalia: wide, inwards curved, pointed and asymmetrical valvae, a tubular phallus bent at 90° angle in basal 1/3, and "anchor-shaped" abdominal segment VIII with two curved projections are unique among the examined materials.

Description. The original description is quoted: "Wingspan 10 mm ♂. Head, palpi, thorax, and abdomen light bronzy-grey. Antennal ciliations 1. Forewings lanceolate; bronzy-grey, somewhat darker-springled in disc: cilia greyish."

***Male genitalia*.** Uncus trapezoid sclerotised plate. Gnathos base broad belt; distal arm short, robust, directed upwards and heavily sclerotised. Tegumen hood-shaped. Phallus slim, a little longer than valva, basal 1/3 bent at 90° angle, distally straight. Valvae asymmetrical, left broader and shorter; basal 2/3 broad, distal 1/3 tapered and bent inwards, tip more or less pointed. Saccus arched, short. Sternum VIII pentagonal, anterior margin broadly reinforced, mediolaterally somewhat extended. Tergum VIII consists of two laterally arched sclerotised belts; medioposterior portion triangular with backwards directed lateral extensions.

Distribution. Peru.

Remarks. Female unknown.

Scythris lequetepequensis Nupponen, sp. nov.

http://zoobank.org/3062C052-50C6-441C-B222-0B19036C60EF

Figs 22, 52

Type material. ***Holotype*.** Peru • ♂; prov. La Libertad, Lequetepeque River, near El Huabal village; 7°16.9'S, 79°18.2'W; 200 m a.s.l.; 1 Feb. 2019; K. Nupponen &

R. Haverinen leg.; [BOLD sample ID] KN01074; [genitalia slide] K. Nupponen prep. no. 2/8 Dec. 2019; coll. NUPP (MZH).

Paratype. Peru • ♂; prov. Cajamarca, Lequetepeque River, near Chilete village; 7°12.9'S, 78°45.3'W; 980 m a.s.l.; 4 Feb. 2019; K. Nupponen & R. Haverinen leg.; coll. NUPP.

Diagnosis. Rather reliably determined externally by pale brown forewings with indefinite paler areas at midwing, a dark brown subapical spot and fringe under tornus being darker than those at apical area. In the male genitalia of *S. lequetepequensis*, the gnathos with massive base and dorsally expanded pouch, and a transverse and sclerotised arched sclerite at tergum VIII are diagnostic.

Description. Wingspan 13 mm. Head, collar, neck tuft, tegula and thorax pale brown. Few whitish brown scales around eye; thorax posteriorly edged by white scales. Haustellum white. Scape dorsally pale brown, ventrally paler, pecten longer than diameter of scape. Flagellum dark brown, 0.75 × length of forewing, ciliate, sensillae ~ 1/2 as long as diameter of flagellum. Labial palp: palpomere I white; palpomeres II and III with lower surface brown, otherwise whitish brown. Legs pale cream, upper surfaces of tibiae and tarsi mixed with pale brown in mid- and hindlegs, and darker brown in foreleg. Abdomen dorsally fuscous, ventrally white. Forewing pale brown, middle part of wing indefinite paler than costal and dorsal areas; at cell end whitish cream blotch, subapically small dark brown spot; fringe under tornus darker than those at apical area. Hindwing dark fuscous, darker than forewing.

Male genitalia. Uncus bifurcate plate, posterior lobes broad, rounded. Gnathos as long as phallus; base massive with dorsally expanded pouch; distal arm tapered, tip with T-shaped hook. Tegumen round hood. Phallus 0.7 × length of valva, medially bent, distal 1/2 tapered, tip pointed. Valva straight, distal 1/2 dorsally somewhat widened and setose, apex round. Saccus labiate, ~ 1/3 as long as valva. Sternum VIII trapezoid, medioposteriorly shallowly indented; anterior margin concave and reinforced. Tergum VIII tongue-shaped, lateral and posterior margins folded, anterior margin medially with V-shaped indentation; subposteriorly with transverse and arched ridge covered by minute spines.

Etymology. Latinised adjective in the nominative singular. The species is named after the type locality, valley of the River Lequetepeque.

Distribution. Peru.

Habitat. The collecting locality is a moist riverside meadow (Fig. 80).

Genetic data. Not obtained (specimen submitted to barcode analysis but the sample failed).

Remarks. Female unknown. We classify taxon *lequetepequensis* in genus *Scythris*, based on the somewhat similar male genitalia between *S. lequetepequensis* and North American (Landry 1991) and African (Bengtsson 2014) species such as *S. mixaula* Meyrick, 1916 from South-West USA and *S. cretiflua* Meyrick, 1913 from South Africa. These include for instance massive gnathos, horizontally narrow point of articulation between tegumen and valva, and symmetrical and apically setose valva.

***Scythris plocogastra* Meyrick, 1931**
Figs 23, 68

Scythris plocogastra Meyrick, 1931. Zoological Journal of the Linnean Society 37: 282.

Material examined. ***Holotype*.** Paraguay • ♀; Chaco: Makthlawaiya; • GSC [G. S. Carter]; 5.27.; [genitalia slide] JFGC No. 8063; NHMUK ID 010922365; NHMUK slide ID 010316672; coll. NHMUK.

Diagnosis. Wings rather uniform purplish-grey, speckled weakly with white, without distinguishing external features. Genitalia examination is necessary for confident determination. In the female genitalia, the candleflame-shaped sterigma is characteristic.

Description. The original description is quoted: "Wingspan ♀ 12 mm. Head and thorax purplish-grey, irregularly mixed white. Palpi dark grey sprinkled white, base white. Abdomen blackish, thickly strewn with white hair-scales, anal segment whitish, ventral surface wholly suffused white, apex ochreous-yellow. Forewings purplish-grey speckled dark fuscous and sprinkled whitish: cilia pale grey; cilia grey."

***Female genitalia*.** Sterigma distinct, candleflame-shaped plate; posterior apex melanised; anterior margin weakly concave. Sternum VII rectangular, 1.4 × as high as wide; posterior margin with medial incision. Apophyses anteriores 0.7 × length of apophyses posteriores.

Distribution. Paraguay.

Remarks. Male unknown.

***Scythris tibicina* Meyrick, 1916**
Figs 24, 53, 69

Scythris tibicina Meyrick, 1916. Exotic Microlepidoptera, vol. 2 (part 1): 12.

Material examined. ***Lectotype*.** Peru • ♂; Chosica; 2800 feet a.s.l.; 7.14.; Parish leg.; [genitalia slide] JFGC No. 8053; NHMUK ID 010922365; NHMUK slide ID 010316665; coll. NHMUK.

***Paralectotype*.** Peru • 11 exx.; same data as for lectotype; coll. NHMUK.

Other material. Peru • 1 ♂; prov. Ancash, near Huanchay village; 10°30.4'S, 77°25.5'W; 1520 m a.s.l.; 5 Feb. 2019; K. Nupponen & R. Haverinen leg.; [BOLD sample ID] KN01075; [genitalia slide] K. Nupponen prep. no. 5/11 Dec. 2019; coll. NUPP. • 2 ♂, 2 ♀; prov. Ancash, Fortaleza River, Raquia village 13 km SW; 10°13.1'S, 77°33.6'W; 1180 m a.s.l.; 31 Jan. 2019; K. Nupponen & R. Haverinen leg. [BOLD sample IDs] KN01076, KN01077; [genitalia slides] K. Nupponen prep. no. 1/18-XII-2019 ♀, 4/17-XII-2019 ♂; coll. NUPP.

Diagnosis. Forewings with whitish streak on brownish background. Genitalia dissection is required for confident determination. The male genitalia are unmistakable,

particularly the narrow, ventrally curved, hook-shaped gnathos; and phallus that bends at 90° angle; and densely bristled valvae. In the female genitalia, a crater-shaped margin of sterigma, adjoined by needle-like sclerotisation, are diagnostic.

Description. The original description is quoted: "Wingspan 12–13 mm ♂, ♀. Head ochreous-grey more or less mixed with white. Palpi grey, suffused with white internally and at apex of second joint. Antennal ciliations of ♂ 1. Thorax ochreous-grey partially mixed with whitish. Abdomen light grey, anal tuft pale ochreous, ventral surface whitish. Forewings lanceolate; light grey: a double finely separated or united median whitish streak, from base, upper portion extending to about middle, lower to 0.33, both more or less enlarged into suffused spots posteriorly; an irregular elongate undefined spot of whitish suffusion in disc at 0.66; each of these whitish markings followed by a few indistinct dark fuscous scales, representing the stigmata: cilia grey, base mixed with whitish. Hindwings with 4 and 5 separate; grey; cilia grey."

***Male genitalia*.** Uncus posterolaterally extended trapezoid plate, margin concave medially. Gnathos asymmetrical, basally channel-like, apex spoon-shaped. Distal arm of gnathos thin, curved ventrally, hook-shaped. Tegumen hood-shaped. Phallus 0.6 × length of valva; basal 2/3 straight, then bent at 90° angle, distal 1/3 slender and straight, tip pointed. Valva long and narrow, bent at 0.4 length, distal portion straight and setose; ventrally at middle sub-oval bristled extension. Vinculum arched, short. Sternum VIII large trapezoid plate, medioposteriorly with small V-shaped indentation, laterally at 0.3 with anteriorly directed lobes. Tergum VIII small trapezoid plate.

***Female genitalia*.** Sterigma crater-shaped, twice as wide as high, adjoined by needle-like sclerotisation. Ostium situated at bottom of crater. Sternum VII semi-circular, medioposteriorly with small concave notch. Apophyses anteriores 0.25 × length of apophyses posteriores.

Distribution. Peru.

Habitat. Adults were collected in moist riverside meadows.

Genetic data. BIN: BOLD:ADZ4797 (n = 3 from Peru). Genetically homogenous, variation 0%. Nearest neighbour: Unidentified Scythrididae from Argentina (BIN: BOLD:ACY3332, 6.54%), see Suppl. material 2.

Remarks. Based on COI maximum likelihood phylogeny, taxa *tibicina* and *sanfranciscoensis* group together, associating with other Central and South American taxa, classified in apparently non-monophyletic *Scythris* on BOLD (Suppl. material 2). With regard to *tibicina*, the male genitalia are similar to *S. mixaula* Meyrick, 1916 from California, Texas and Montana, sharing for instance narrow and setose valva, spear-shaped uncus (termed distal arm of gnathos in Landry (1991)) and mediodorsally convex vinculum. We have interpreted the mediodorsal structure as uncus (gnathos in Landry (1991) and the sclerotised structure on its ventral side as gnathos. We justify this interpretation by the origin of the narrow and ventrally curved process, which originates from the cup-shaped apex of gnathos. See Fig. 53, which shows the origin of the structure in lateral view. We classify *tibicina* and *sanfranciscoensis* in *Scythris*.

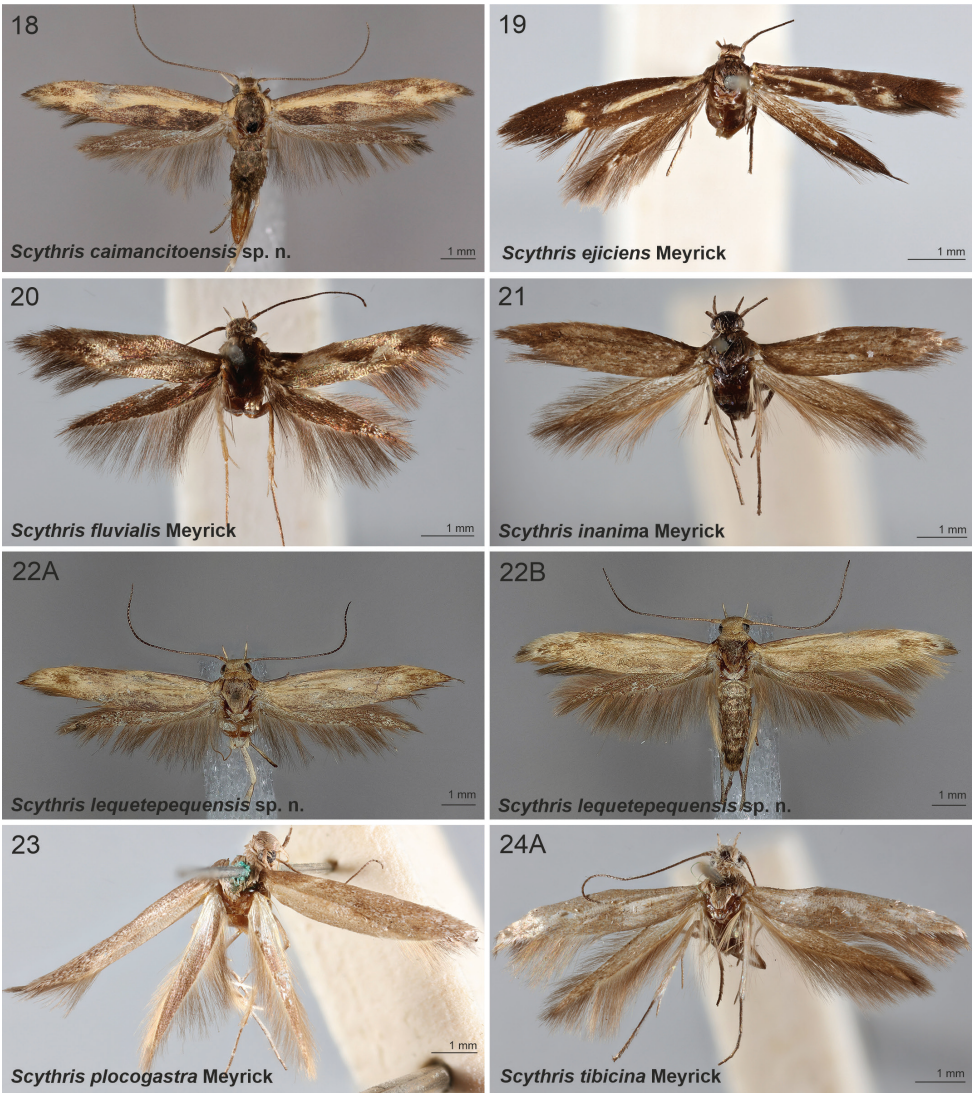

Figures 18–24A. Scythrididae adults, genus *Scythris* **18** *S. caimancitoensis* Nupponen, sp. nov., male, holotype **19** *S. ejiciens* Meyrick, 1928, male, holotype **20** *S. fluvialis* Meyrick, 1916, male, lectotype **21** *S. inanima* Meyrick, 1916, male, holotype **22A** *S. lequetepequensis* Nupponen sp. nov., male, holotype **22B** *S. lequetepequensis* Nupponen sp. nov., male, paratype **23** *S. plocogastra* Meyrick, 1931, female, holotype **24A** *S. tibicina* Meyrick, 1916, male, lectotype.

Scythris sanfranciscoensis Nupponen, sp. nov.

http://zoobank.org/BDCD7172-CA15-49CD-9A47-D8C2D3FB9527
Figs 25, 54, 70

Type material. ***Holotype.*** Argentina • ♂; prov. Jujuy, Rio San Francisco, by Caimancito village; 23°43.8'S, 64°36.3'W; 400 m a.s.l.; 18 Sep. 2017; K. Nupponen &

Figures 24B–29. Scythrididae adults, genus *Scythris* **24B** *S. tibicina* Meyrick, 1916, male **25A** *S. sanfranciscoensis* Nupponen sp. nov., male, holotype **25B** *S. sanfriscoensis* Nupponen sp. nov., male, paratype **26** *S. tigrensis* Nupponen, sp. nov., male, holotype **27A** *S. bicoloristrigella* Nupponen sp. nov., genus combination incertae sedis, male, holotype **27B** *S. bicoloristrigella* Nupponen sp. nov., genus combination incertae sedis, male, paratype **28** *S. saldaitisi* Nupponen sp. nov., genus combination incertae sedis, male, holotype **29** *S. wikstromi* Nupponen, sp. nov., genus combination incertae sedis, male, holotype.

R. Haverinen leg.; [BOLD sample ID] KN01036; [genitalia slide] K. Nupponen prep. no. 2/10 Dec. 2019; coll. NUPP (MZH).

Paratypes. Argentina • 3 ♂, 2 ♀; same data as for holotype; [BOLD sample ID] KN01035; [genitalia slide] K. Nupponen prep. no. 3/14 Dec. 2019 ♀; coll. NUPP.

Diagnosis. Large species (wingspan 20.5–22 mm), greyish brown species, forewing with 3–5 black spots apically near cilia. The weakly resembling "batman" appearance of the male genitalia is distinctive, as well as sternum VIII with a triangular process at middle, attached to transverse plate and enormous round, anterolateral projections. In the female genitalia, a large subtriangular sterigma is characteristic.

Description. Wingspan 20.5–22 mm. Head, collar, neck tuft, haustellum, tegula and thorax unicoloured greyish brown. Scape dorsally beige, ventrally cream; pecten cream and longer than diameter of scape. Flagellum dark brown, 0.65 × length of forewing, in male ciliate, sensillae ~ 1/2 as long as diameter of flagellum. Labial palp: palpomere I white, palpomeres II and III fuscous with a few whitish scales. Legs: foreleg femur dirty white, tibia and tarsus dark brown; midleg and hindleg dirty white except tarsus pale fuscous. Abdomen pale brown, ventrally mixed with white. Forewing greyish brown with sparsely scattered blackish scales; middle part of wing widely but irregularly whitish cream, more whitish at apical area; at 0.7 and 0.85 blackish blotches at middle of wing; apically 3–5 black spots at row near cilia line. Hindwing pale fuscous, fringe slightly darker.

Male genitalia. Uncus quadrangular plate with deep U-shaped medioposterior indentation; sublaterally with small setose flaps. Gnathos not detected. Phallus robust, longer than valva, distal portion tapered. Anterior part of valva wide with round margin, posterior part pointing upwards, incurved, with acute apex. Sternum VIII with large round anterolateral projections, anterior margin widely concave; posterior margin folded forming large transverse bent plate with projected posterolateral corners, and heavily sclerotised triangular process in middle of plate. Tergum VIII trapezoid, posterior portion quadrangular, anterolateral corners broad with small marginal fold.

Female genitalia. Sterigma large subtriangular plate, posterior portion hood-like and heavily sclerotised, tip blunt. Ostium situated in squared sclerotisation at medioposterior margin of sterigma. Sternum VII rectangular. Apophyses anteriores 0.3 × length of apophyses posteriores.

Etymology. Latinised adjective in the nominative singular. The species is named after the type locality, the River San Francisco.

Distribution. NW Argentina.

Habitat. The collecting site is a dry river bed surrounded by forests and plantations. Plants of the family Amaranthaceae were common at riverside (Fig. 79).

Genetic data. BIN: BOLD:ADZ5418 (*n* = 2 from Argentina). Nearest neighbour: *Scythris tibicina* Meyrick, 1916 (BIN: BOLD:ADZ4797, 6.68%).

Remarks. Based on COI maximum likelihood phylogeny, taxa *tibicina* and *sanfranciscoensis* group together, associating with other Central and South American taxa, classified in apparently non-monophyletic *Scythris* on BOLD (Suppl. material 2). We classify *tibicina* and *sanfranciscoensis* in *Scythris*.

***Scythris tigrensis* Nupponen, sp. nov.**
http://zoobank.org/A186B8F5-710B-4CD6-8838-5C1C27C6E9FB
Figs 26, 55

Type material. ***Holotype.*** Argentina • ♂; prov. Mendoza, Andes Mts., Cordillera del Tigre, Mendoza River valley near Uspallata village; 32°35.9'S, 69°22.9'W; 1900 m a.s.l.; 25 Jan. 2017; K. Nupponen & R. Haverinen leg.; [BOLD sample ID] KN01042; [genitalia slide] K. Nupponen prep. no. 1/8 Dec. 2019; coll. NUPP (MZH).

Paratype. Argentina • 1 ♂; same data as for holotype; coll. NUPP.

Diagnosis. Wings elongated without any distinct pattern, and genitalia examination is indispensable for reliable determination. In the male genitalia of *S. tigrensis*, a narrow distal arm of the gnathos, broad valvae and a conspicuous bifurcate formation attached anteriorly to tegumen are distinctive.

Description. Wingspan 14 mm. Head, haustellum, tegula and thorax beige mixed with cream. Neck tuft white, collar pale beige. Scape dark brown, ventrally with few paler scales; pecten brown and longer than diameter of scape. Flagellum dark brown, 0.65 × length of forewing. Labial palp: palpomere I and base of palpomere II white, otherwise brown more or less mixed with white. Legs: femur and tibia pale beige mixed with fuscous, tarsi fuscous. Abdomen grey, dorsally each segment paler grey scales at posterior margin. Forewing pale beige; indistinct blackish spot in fold at 0.4, and small fuscous spot at cell end; greyish white scales densely scattered in apical area. Hindwing pale fuscous.

Male genitalia. Uncus narrow, digitate, slightly bent downwards. Gnathos base rectangular hood; distal arm narrow, downcurved. Phallus as long as width of valva, bent at middle. Valvae broad and straight, slightly asymmetrical: left one basally with round flap and distally more tapered. Anteriorly to tegumen large bifurcate structure of uncertain homology is attached; left furca (when viewed ventrally) funnel-shaped, longer than valva; right furca 1/2 × shorter, cylindrical, tip pointed, apex with very long and thick seta. Sternum VIII rectangular, 1.7 × higher than wide; posteriorly sclerotised with two narrow and curved projections. Tergum VIII asymmetrical, semi-trapezoid plate.

Etymology. Latinised adjective in the nominative singular. The species is named after the type locality, the mountain range of the Tigre in the Andes.

Distribution. NW Argentina.

Habitat. The collecting site is a dry and xerothermic valley of the River Mendoza at medium altitude of the Andes, surrounded by rocky slopes with sparse and low vegetation.

Genetic data. BIN: BOLD:ADZ5721 (*n* = 1 from Argentina). Nearest neighbour: North American *Neoscythris* sp. (BIN: BOLD:ABA1135, 6.57%).

Remarks. Female unknown. Based on the COI maximum likelihood phylogeny, taxon *tigrensis* belongs to an isolated lineage, being sister to a large lineage containing taxa classified in *Scythris* or in Scythrididae on BOLD (Suppl. material 2). Its morphology does not resemble any other species covered in the study, and even though the barcode gap analysis suggests *Neoscythris* as the nearest neighbour, it does not have the

diagnostic characters of that genus (Landry 1991). For practical reasons, we classify *tigrensis* in *Scythris*, but more research is needed.

In our COI maximum likelihood analysis, there are five species, which are structurally heterogenous from each other, and which are distributed in different lineages in the middle-part of the tree (Suppl. material 2, marked with red vertical bar). These are difficult to combine with any North American Scythrididae genus as diagnosed in Landry (1991). We classify these five species, and morphologically similar species without DNA barcodes, to *Scythris* (incertae sedis), highlighting the need for further research. Potentially these taxa should be classified in several genera. These taxa are *S. bicoloristrigella* species group (*bicoloristrigella*, *saldaitisi*, *wikstromi*), *S. andensis* species group (*andensis*, *mendozaensis*) and *S. dividua* species group (*dividua*, *medullata*, *notorrhoa*).

The *bicoloristrigella* species group

Distal arm of gnathos upcurved, robust and heavily sclerotised. Valvae asymmetrical. Male sternum VIII elongated, lateromedially with pair of obliquely backwards directed extensions. Species included: *bicoloristrigella*, *saldaitisi*, *wikstromi*.

Scythris bicoloristrigella Nupponen, sp. nov., genus combination incertae sedis

http://zoobank.org/DE27AA3E-8F19-4576-AFF5-AE6C56175C14
Figs 27, 56

Type material. ***Holotype.*** Argentina • ♂; prov. Mendoza, Andes Mts., Cordillera del Tigre, Mendoza River valley near Uspallata village; 32°35.9'S, 69°22.9'W; 1900 m a.s.l.; 25 Jan. 2017; K. Nupponen & R. Haverinen leg.; [BOLD sample ID] KN01056; [genitalia slide] K. Nupponen prep. no. 1/9 Dec. 2019; coll. NUPP (MZH).

Paratype. Argentina • 1 ♂; prov. San Juan, Andes Mts., salt lake by Cordillera del Tigre; 30°52.8'S, 68°52.4'W; 1620 m a.s.l.; 26 Jan. 2017; K. Nupponen & R. Haverinen leg.; coll. NUPP.

Diagnosis. Externally similar to *L. ankylosauroides*, sharing broad white streak in fold of forewing (dorsally and basally white, costally and terminally cream). Examination of the male genitalia is required to safely identify between *S. bicoloristrigella*, *S. saldaitisi* and *S. wikstromi*. In the male genitalia of *S. saldaitisi*, shape of asymmetrical valvae (left one very short) and anterior margin of sternum VIII straight are distinctive (valvae ca. equal length with incurved apexes and anterior margin of sternum VIII concave in *S. wikstromi*, valvae ca. equal length, right valva setose and anterior margin of sternum VIII concave in *S. bicoloristrigella*).

Description. Wingspan 15–16.5 mm. Head, collar, haustellum, tegula and thorax pale beige with scattered cream scales; posterior 1/2 of thorax with longitudinal cream line. Neck tuft white. Scape dorsally fuscous, ventrally pale beige, pecten longer than diameter of scape. Flagellum dark brown, 0.75 × length of forewing, ciliate, sensillae ~ 1.1 × as long as diameter of flagellum. Labial palps: palpomere I white; lower surface of posterior 1/2 of palpomere II and palpomere III dark brown, otherwise greyish white.

Legs beige, tibiae darker. Abdomen dorsally beige, ventrally dirty white. Forewing pale fuscous; in fold broad streak from base to cell end: dorsally white from base to 0.6, edged by dark brown line dorsally, costally, and terminally cream; dark brown spots in midwing at 0.5, 0.65 and 0.7; in apical area few dark brown scales. Hindwing pale fuscous.

Male genitalia. Uncus heavily sclerotised hood distally, medioposteriorly indented. Gnathos massive, upturned 90° at basal 1/3, distal portion robust and heavily sclerotised, distally tapered, tip pointed. Tegumen elongated hood, dorsally widely open. Phallus ca. as long as uncus, rather broad, beyond middle bent and chute-shaped. Valvae asymmetrical, left valva 1.3 × as long as right; left valva with semi-circular indentation ventrally at 0.3, distal 0.7 tapered, setose, apically bent, tip pointed; right valva with large triangular lobe ventrally at base, distal 1/2 with numerous thin spiniform setae, dorsally folded, subapically tapered, apex with few minute spines and dense setae. Sternum VIII rectangular, elongated, 3 × longer than wide; posteromedially with very deep U-shaped depression, posterior shanks long, setose; lateromedially margin sclerotised, forming tapered extensions; anterior margin with two short, parallel apodemes. Tergum VIII hexagonal, anterior margin widely concave.

Etymology. Diminuitive noun in apposition. The species name alludes to the bicolored streak in the fold of the forewing.

Distribution. NW Argentina.

Habitat. The habitat is a dry and xerothermic valley of the River Mendoza at medium altitude of the Andes, surrounded by rocky slopes with sparse and low vegetation. The paratype was collected at a xerothermic locality in the middle of a dry lake with sparse halophytic shrubs (Fig. 79).

Genetic data. BIN: BOLD:ADY8267 (*n* = 1 from Argentina). Nearest species: *Scythris saldaitisi* Nupponen, sp. nov. (BIN: BOLD:ADZ5132, 5.3%).

Remarks. Female unknown. Based on COI maximum likelihood phylogeny and morphology, South American taxa *bicoloristrigella*, *saldaitisi*, and *wikstromi* group together, associating next to the North American taxa classified in *Scythris*, *Rhamphura*, or *Neoscythris* on BOLD (Suppl. material 2). We are unable to classify these with certainty to any Scythrididae genus as diagnosed and illustrated in Landry (1991) and Bengtsson (2014). We therefore took a conservative view and classified these taxa in *Scythris* (incertae sedis), highlighting the need for further research.

Scythris saldaitisi Nupponen, sp. nov., genus combination incertae sedis

http://zoobank.org/AC91FD2A-C150-4280-B406-CF2057BB5E97
Figs 28, 57

Type material. ***Holotype.*** Argentina • ♂; prov. Catamarca, Sierra de Manchao; 28°47.9'S, 66°23.2'W; 970 m a.s.l.; 21 Sep. 2017; K. Nupponen & R. Haverinen leg.; [BOLD sample ID] KN01049; [genitalia slide] K. Nupponen prep. no. 4/11 Dec. 2019; coll. NUPP (MZH).

Diagnosis. Identification requires examination of the genitalia. In the male genitalia of *S. saldaitisi*, shape of asymmetrical valvae (left one very short) and an-

terior margin of sternum VIII straight are distinctive (valvae ca. equal length with incurved apexes and anterior margin of sternum VIII concave in *S. wikstromi*, valvae ca. equal length, right valva setose and anterior margin of sternum VIII concave in *S. bicoloristrigella*).

Description. Wingspan 13 mm. Head, collar, neck tuft, haustellum, tegula and thorax dark brown. Few dirty white scales exist around eye and laterally at thorax. Scape dorsally dark brown, ventrally pale beige, pecten longer than diameter of scape. Flagellum dark brown, 0.7 × length of forewing, ciliate, sensillae ~ 1/2 as long as diameter of flagellum. Labial palp: palpomere I dirty white, palpomeres II and III dark brown mixed with a few dirty white scales. Legs: lower surfaces dirty white, otherwise foreleg and midleg dark brown and hindleg fuscous. Abdomen dorsally fuscous, ventrally dirty white. Forewing with costal and apical areas dark brown, dorsal area at basal 1/2 slightly paler; black blotches in fold at 0.2, 0.35, 0.55, and at cell end, between two basal ones pale beige dash; scattered with white scales, more pronounced at apical area. Hindwing fuscous, slightly paler than forewing.

Male genitalia. Uncus elongated hood, posterior 1/2 heavily sclerotised. Gnathos base broad; distal arm upcurved, robust, heavily sclerotised and of constant width, tip blunt. Tegumen oval hood, dorsally widely open. Phallus 1/2 as long as left valva, rather slim, slightly bent. Valvae asymmetrical; left valva short, almost straight; right valva twice longer and wider, basal 0.7 straight, apical quarter somewhat twisted and curved ventrad, tip heavily sclerotised with hook-shaped process. Saccus labiate, ~ 1/2 length of left valva. Juxta narrow, 1.4 × length of phallus. Sternum VIII rectangular, elongated, 3.5 × longer than wide; posteromedially with two pronged projections with pointed tips; laterobasally with a pair of tapered extensions, directed obliquely anteriorly. Tergum VIII trapezoid, anterior margin concave and sclerotised.

Etymology. Noun in the genitive case. The species is dedicated to Aidas Saldaitis, a Lithuanian lepidopterist, to acknowledge his contributions to Scythrididae systematics.

Distribution. NW Argentina.

Habitat. Habitat is a dry and xerothermic rocky slope with low vegetation and rather densely occuring bushes.

Genetic data. BIN: BOLD:ADZ5132 (n = 1 from Argentina). Nearest neighbour: *S. bicoloristrigella* (BIN: BOLD:ADY8267, 5.3%).

Remarks. Female unknown. Based on COI maximum likelihood phylogeny and morphology, South American taxa *bicoloristrigella*, *saldaitisi*, and *wikstromi* group together, associating next to the North American taxa classified in *Scythris*, *Rhamphura*, or *Neoscythris* on BOLD (Suppl. material 2). We are unable to classify these with certainty to any Scythrididae genus as diagnosed and illustrated in Landry (1991) and Bengtsson (2014). We therefore took a conservative view and classified these taxa in *Scythris* (incertae sedis), highlighting the need for further research.

***Scythris wikstromi* Nupponen, sp. nov., genus combination incertae sedis**
http://zoobank.org/A3D5F3E0-DC48-4A99-B453-A20C1D2A51CB
Figs 29, 58

Type material. ***Holotype*.** Argentina • ♂; prov. Cordoba, Salinas Grandes SE shore; 29°50.5'S, 64°40.2'W; 185 m a.s.l.; 24 Sep. 2017; K. Nupponen & R. Haverinen leg.; [BOLD sample ID] KN01067; [genitalia slide] K. Nupponen prep. no. 2/12 Dec. 2019; coll. NUPP (MZH).

Diagnosis. Safely determined only by dissecting the genitalia. In the male genitalia of *S. wikstromi*, the valvae are asymmetrical and sickle-shaped (right arm short and setose in *S. bicoloristrigella*, left arm short in *S. saldaitisi*), and sternum VIII posteriorly with wide indentation and wide projections (narrower indentation and long projections in *S. bicoloristrigella* and *S. saldaitisi*).

Description. Wingspan 11.5 mm. Head, collar, neck tuft, haustellum, tegula and thorax brown with scattered cream scales. Scape dorsally brown, ventrally somewhat paler, pecten longer than diameter of scape. Flagellum dark brown, 0.7 × length of forewing, ciliate, sensillae ~ 0.65 × as long as diameter of flagellum. Labial palp: palpomere I pale cream, palpomeres II and III beige of various tones. Legs: foreleg dark brown, midleg and hindleg pale brown; lower surface pale beige. Abdomen dorsally fuscous, ventrally whitish grey. Forewing brown; black blotches in dorsum at 0.1, midwing at 0.35, and small ones above tornus and at cell end; white blotch in midwing at 0.25. Hindwing fuscous.

***Male genitalia*.** Uncus elongate hood, posterior 1/2 heavily sclerotised with small semi-circular flap at middle. Gnathos base broad bel, attached to tegumen by membrane; distal arm upcurved, robust, heavily sclerotised and of constant width, tip blunt. Tegumen oval hood, dorsally widely open. Phallus ca. as long as uncus, rather slim, medially little constricted. Valvae asymmetrical, long and slender, basally fused by hood-like formation; basal 1/2 of both valvae rather broad, dorsally with small triangular lobes at 0.4; distal 1/2 tapered and incurved (sickle-shaped), tips heavily sclerotised and pointed, right valva 1.2 × longer. Juxta narrow, 1.1 × length of phallus. Sternum VIII hexagonal basally, medioposteriorly wide and deep U-shaped indentation; medio-anteriorly with sclerotised semicircle. Tergum VIII trapezoid, anterior margin concave and sclerotised.

Etymology. Noun in the genitive case. The diacritic mark "ö" is deleted, following ICZN (2000) paragraph 32.5.2.1.The species is dedicated to Bo Wikström, a Finnish lepidopterist.

Distribution. NW Argentina.

Habitat. The collecting site is the shore of a large salt lake, in the zone between a dry shrubby area and low halophytic vegetation.

Genetic data. Not obtained (specimen submitted to barcode analysis but the sample failed).

Remarks. Female unknown. Based on COI maximum likelihood phylogeny and morphology, South American taxa *bicoloristrigella*, *saldaitisi*, and *wikstromi* group

together, associating next to the North American taxa classified in *Scythris*, *Rhamphura*, or *Neoscythris* on BOLD (Suppl. material 2). We are unable to classify these with certainty to any Scythrididae genus, as diagnosed and illustrated in Landry (1991) and Bengtsson (2014). We therefore took a conservative view and classified these taxa in *Scythris* (incertae sedis), highlighting the need for further research.

The *andensis* species group

Sterigma rocket-shaped (pentagonal) in the female genitalia. Gnathos of *S. andensis* with large, tooth-like extensions on ventral margin. Male of *S. mendozaensis* is unknown. Species included: *andensis*, *mendozaensis*.

Scythris andensis Nupponen, sp. nov., genus combination incertae sedis

http://zoobank.org/7515D97A-17AB-43C9-9603-4DD29DCAD6C5
Figs 30, 59, 71

Type material. ***Holotype.*** Argentina • ♂; prov. La Rioja, Andes Mts., Sierra de Famatina, Famatina village 15 km NNW; 28°46.4'S, 67°35.0'W; 2085 m a.s.l.; 27 Jan. 2017; K. Nupponen & R. Haverinen leg.; BOLD sample ID KN01064; [genitalia slide] K. Nupponen prep. no. 2/15 Dec. 2019; coll. NUPP (MZH).

Paratypes. Argentina • 14 ♂, 2 ♀; same data as for holotype; [BOLD sample IDs] KN01063, KN01065, KN01066; [genitalia slide] K. Nupponen prep. no. 1/13 Jan. 2019 ♂; coll. NUPP; • 1 ♀; prov. San Juan, Andes Mts., salt lake by Cordillera del Tigre; 30°52.8'S, 68°52.4'W; 1620 m a.s.l.; 26 Jan. 2017; K. Nupponen & R. Haverinen leg.; [genitalia slide] K. Nupponen prep. no. 4/14 Dec. 2019; coll. NUPP.

Diagnosis. Externally resembling *S. saldaitisi* and *S. wikstromi*, sharing with those whitish blotches on forewings, and reliable determination can be achieved by genitalia examination. In the male genitalia of *S. andensis*, gnathos with tooth-like extensions on ventral margin, valvae are slim and asymmetrical, phallus is very short, and sclerites on segment VIII are asymmetrical and elongated. In the female genitalia the sclerotised, rocket-shaped sterigma is characteristic.

Description. Wingspan 12.5–13 mm. Head, collar, tegula and thorax pale fuscous; thorax laterally and collar with few white scales. Neck tuft white. Haustellum base cream. Scape dorsally dark brown, ventrally white with pecten of same colour. Flagellum dark brown, 0.7 × length of forewing, in male ciliate, sensillae ~ 1/2 as long as diameter of flagellum. Labial palp pale brown, palpomere I and upper surface mixed with white. Legs white, upper surfaces more or less mixed with different tones of brown. Abdomen dorsally fuscous, ventrally dirty white in male and white in female. Forewing pale fuscous, more or less densely scattered by white scales; large white blotches at midwing subbasally, at 0.35 between fold and dorsum, and above tornus; large dark brown blotches between fold and dorsum at 0.2 and 0.45, and spot of same colour at cell end. Hindwing pale fuscous.

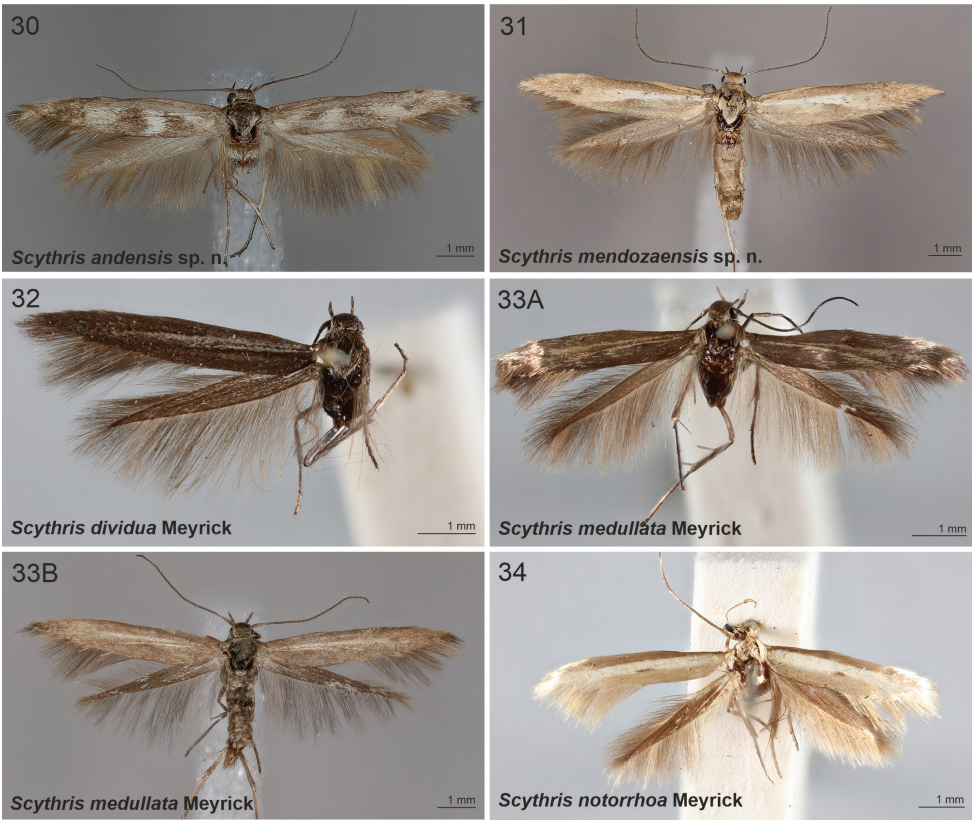

Figures 30–34. Scythrididae adults, genus *Scythris* **30** *S. andensis* Nupponen sp. nov., genus combination incertae sedis, male, holotype **31** *S. mendozaensis* Nupponen sp. nov., genus combination incertae sedis, female, holotype **32** *S. dividua* Meyrick, 1916, genus combination incertae sedis, male, lectotype **33A** *S. medullata* Meyrick, genus combination incertae sedis, 1916, male, lectotype **33B** *S. medullata* Meyrick, 1916, genus combination incertae sedis, male **34** *S. notorrhoa* Meyrick, 1921, genus combination incertae sedis, male, lectotype.

Male genitalia. Uncus as long as gnathos and tegumen together, basally subquadrangular, distally narrow and shallowly upcurved, tip pointed. Gnathos long and robust, tip bifurcate, at base large asymmetrical extension; ventral edges with heavily sclerotised tooth-like extensions, four on right side and five on left side; dorsal surface subapically long and slender with weakly sclerotised extension, with two small basal thorns (potentially anal tube). Tegumen hood-shaped. Phallus thick, straight and very short. Valvae long and narrow, asymmetrical; left valva tapered distally, right distally spatulate. Saccus short, labiate. Sternum VIII large, elongated, triangular basally but asymmetrical, posteriorly digitate. Tergum VIII narrower and little longer than sternum VIII, otherwise similar. Segment VIII is somewhat twisted *in situ*.

Female genitalia. Sterigma rocket-shaped, thick and robust. Ostium small, situated at tip of sterigma. Sternum VII rectangular, 1.4 × wider than high. Apophyses anteriores 1/2 length of apophyses posteriores.

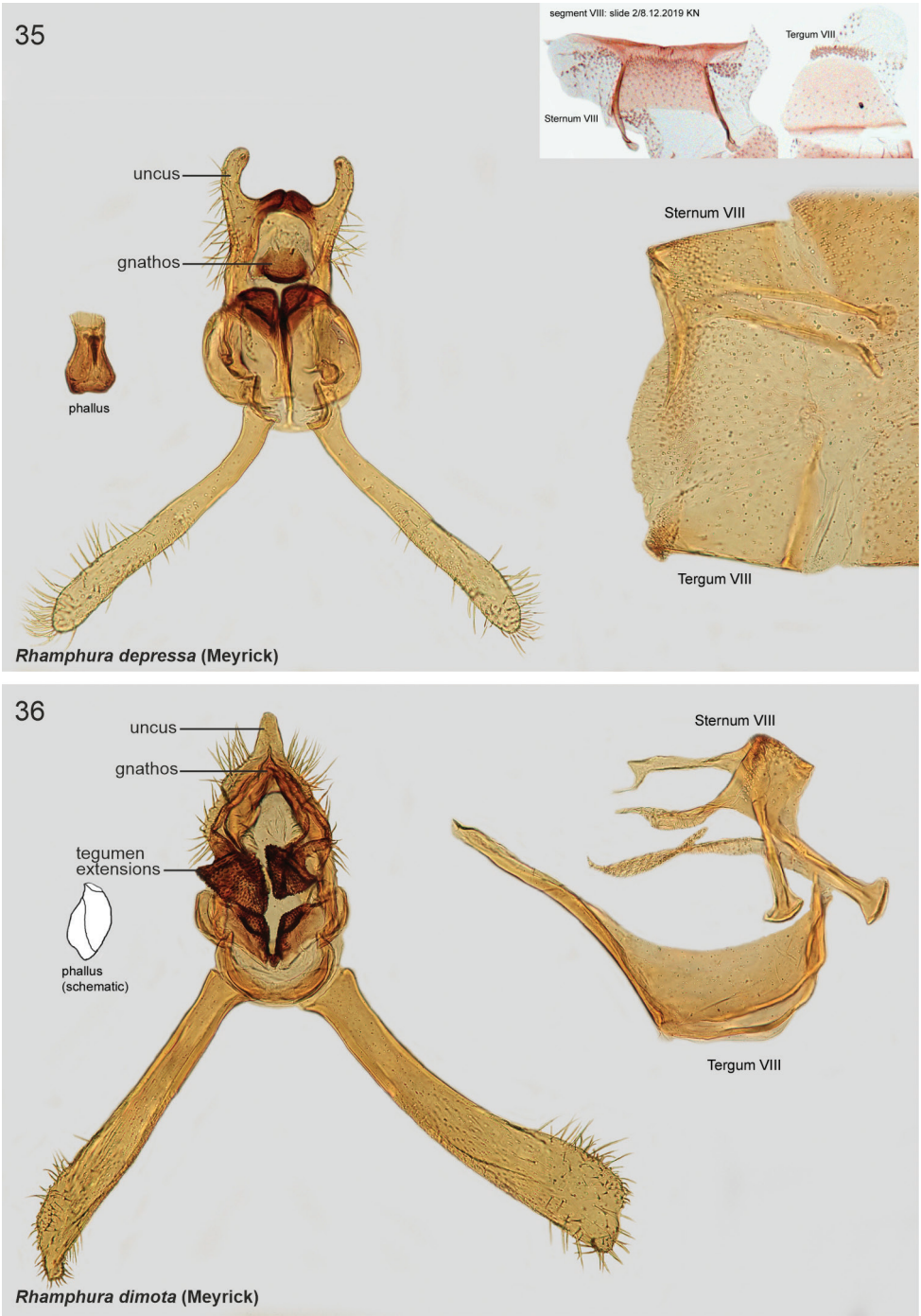

Figures 35–36. Male genitalia of *Rhamphura* **35** *R. depressa* (Meyrick, 1931), holotype, slide JFGC No. 8061 **36** *R. dimota* (Meyrick, 1931), lectotype, slide JFGC No. 8062.

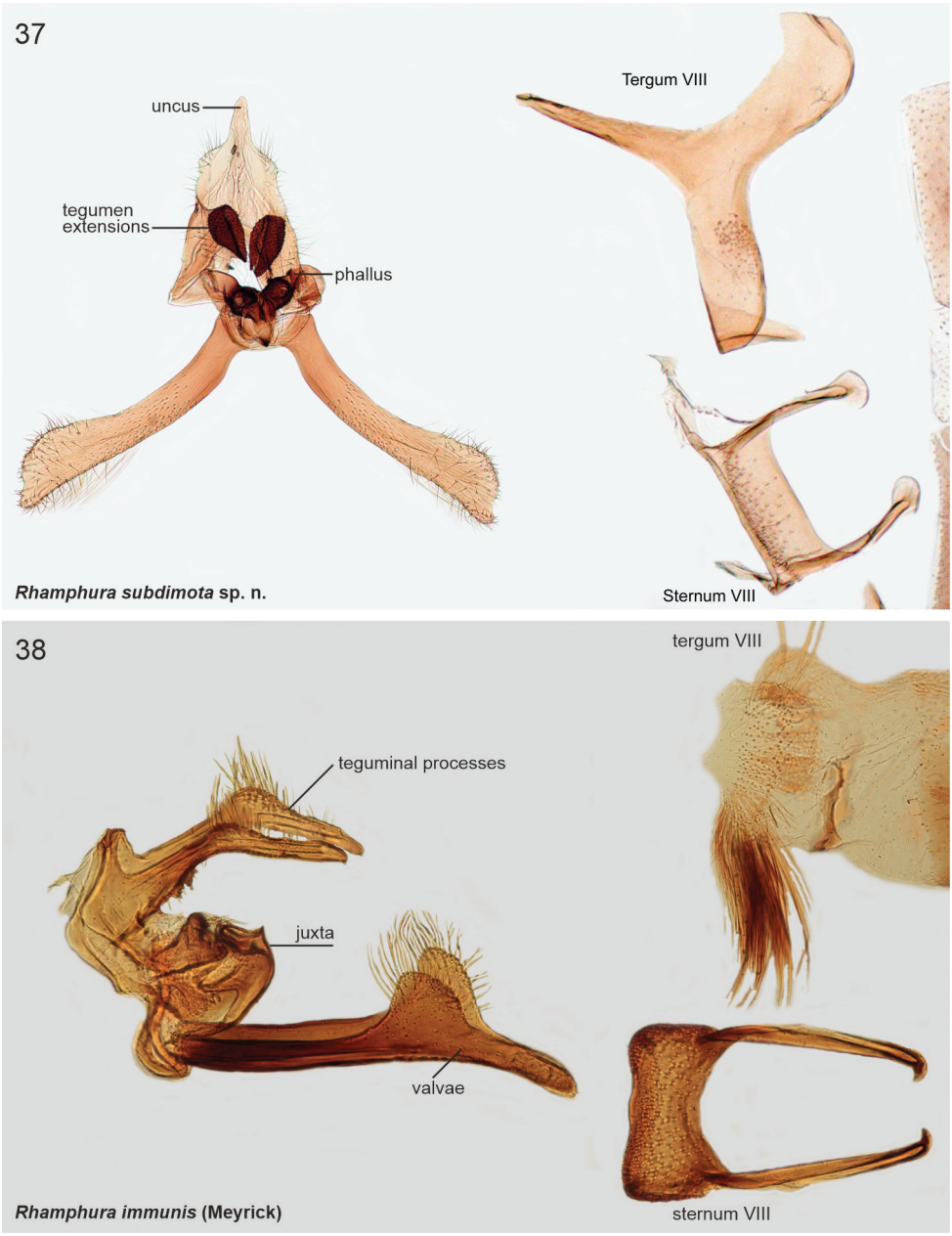

Figures 37–38. Male genitalia of *Rhamphura* **37** *R. subdimota* Nupponen sp. nov., holotype, slide 5/12 Dec. 2019 KN **38** *R. immunis* (Meyrick, 1916), lectotype, slide JFGC No. 8056, genitalia shown in lateral view.

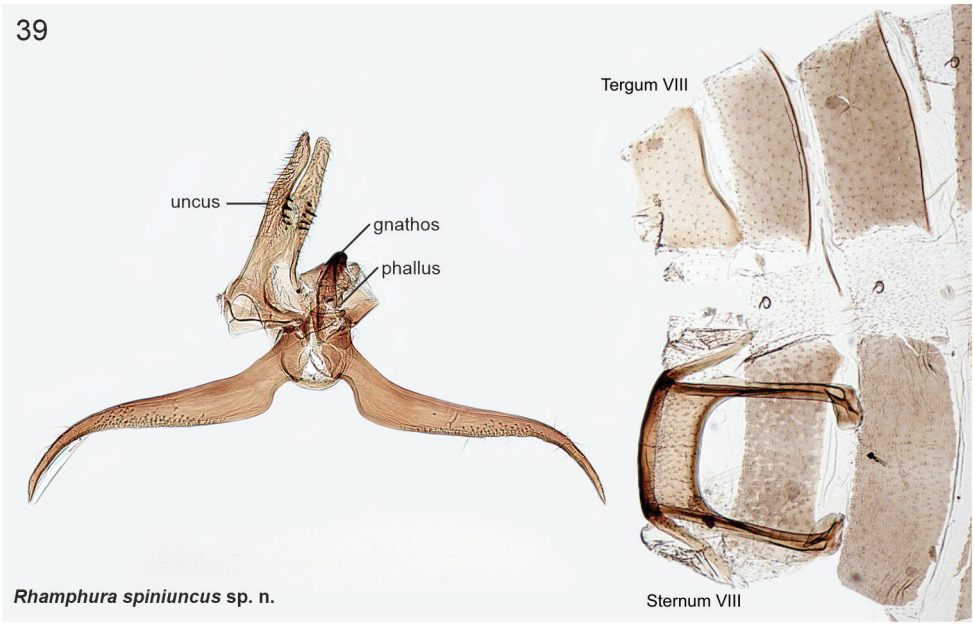

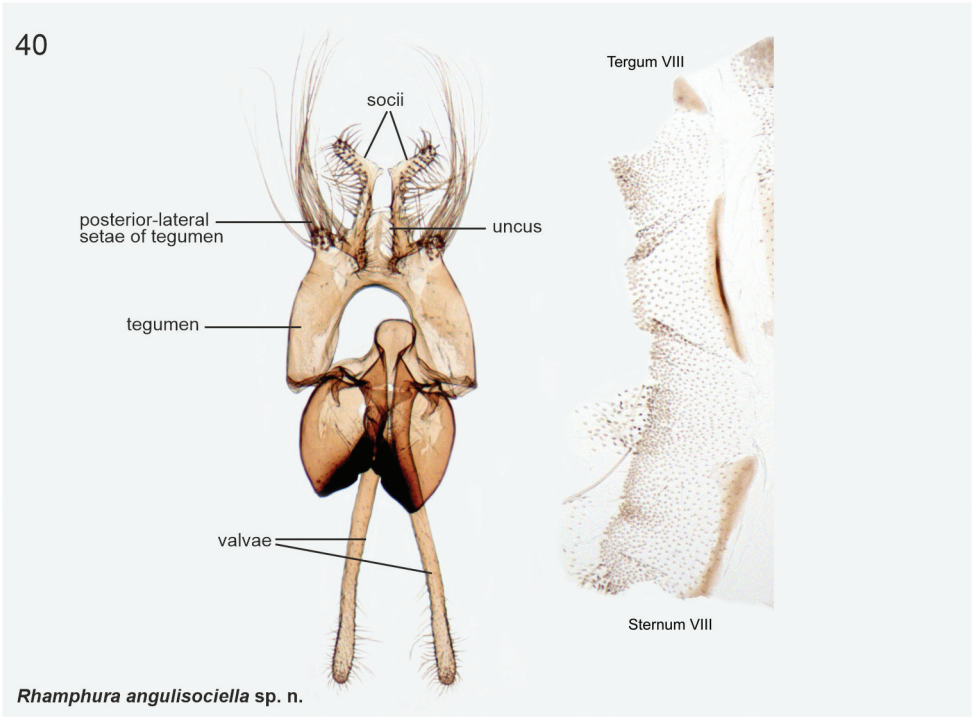

Figures 39–40. Male genitalia of *Rhamphura* **39** *R. spiniuncus* Nupponen sp. nov., holotype, slide 4/12 Dec. 2019 KN) **40** *R. angulisociella* Nupponen sp. nov., genus combination incertae sedis, holotype, slide 1/10 Dec. 2019 KN.

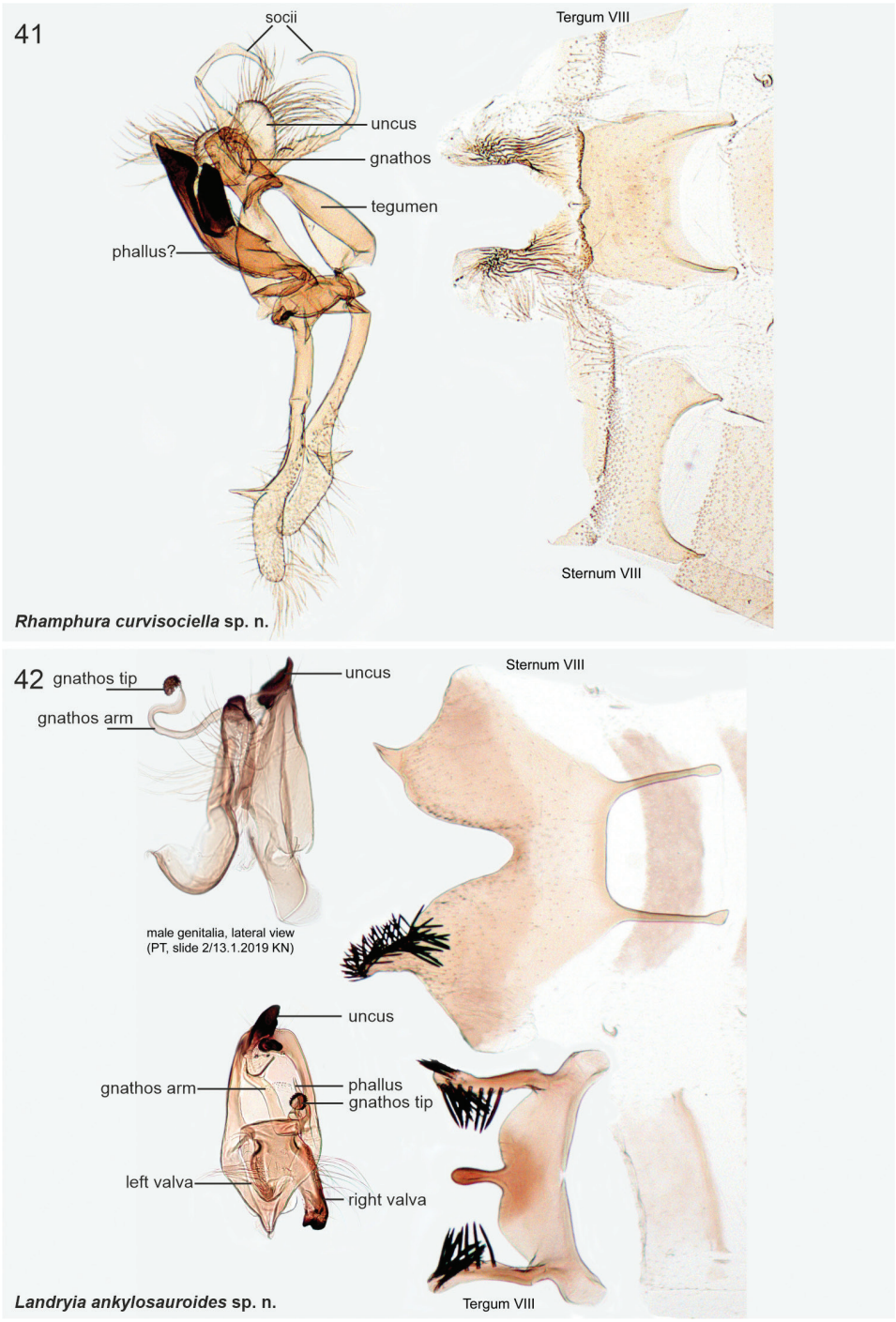

Figures 41–42. Male genitalia of *Rhamphura* and *Landryia* **41** *R. curvisociella* Nupponen sp. nov., genus combination incertae sedis, holotype, slide 1/12 Dec. 2019 KN **42** *L. ankylosauroides* Nupponen, sp. nov., genus combination incertae sedis, holotype, above (lateral view): slide 4/13 Dec.2019 KN, below (ventral view): slide 2/13 Dec. 2019 KN (paratype).

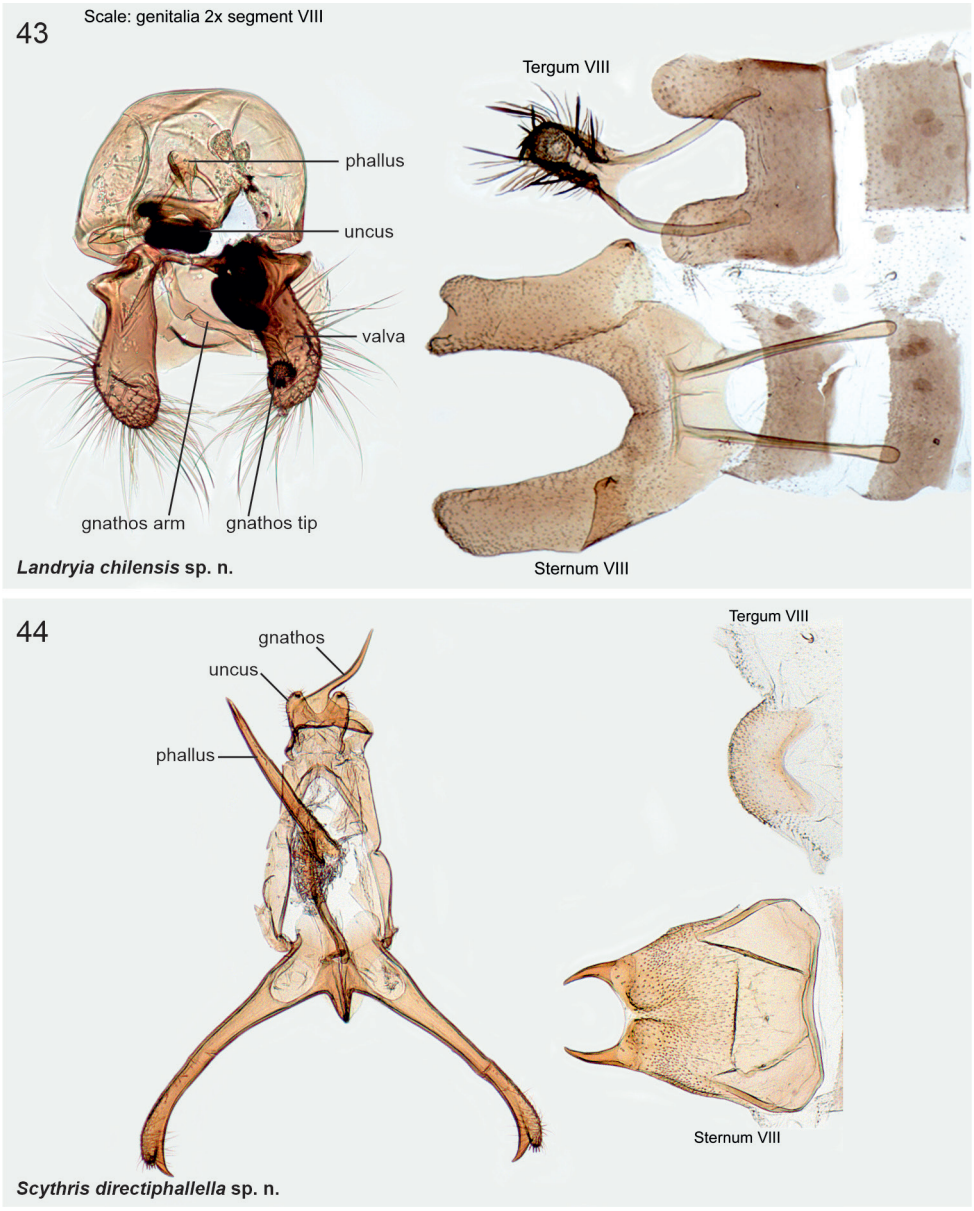

Figures 43–44. Male genitalia of *Landryia* and *Scythris* **43** *L. chilensis* Nupponen sp. nov., genus combination incertae sedis, holotype, slide 3/18 Dec. 2019 KN **44** *S. directiphallella* Nupponen sp. nov., holotype; slide 3/28 Dec.2019 KN.

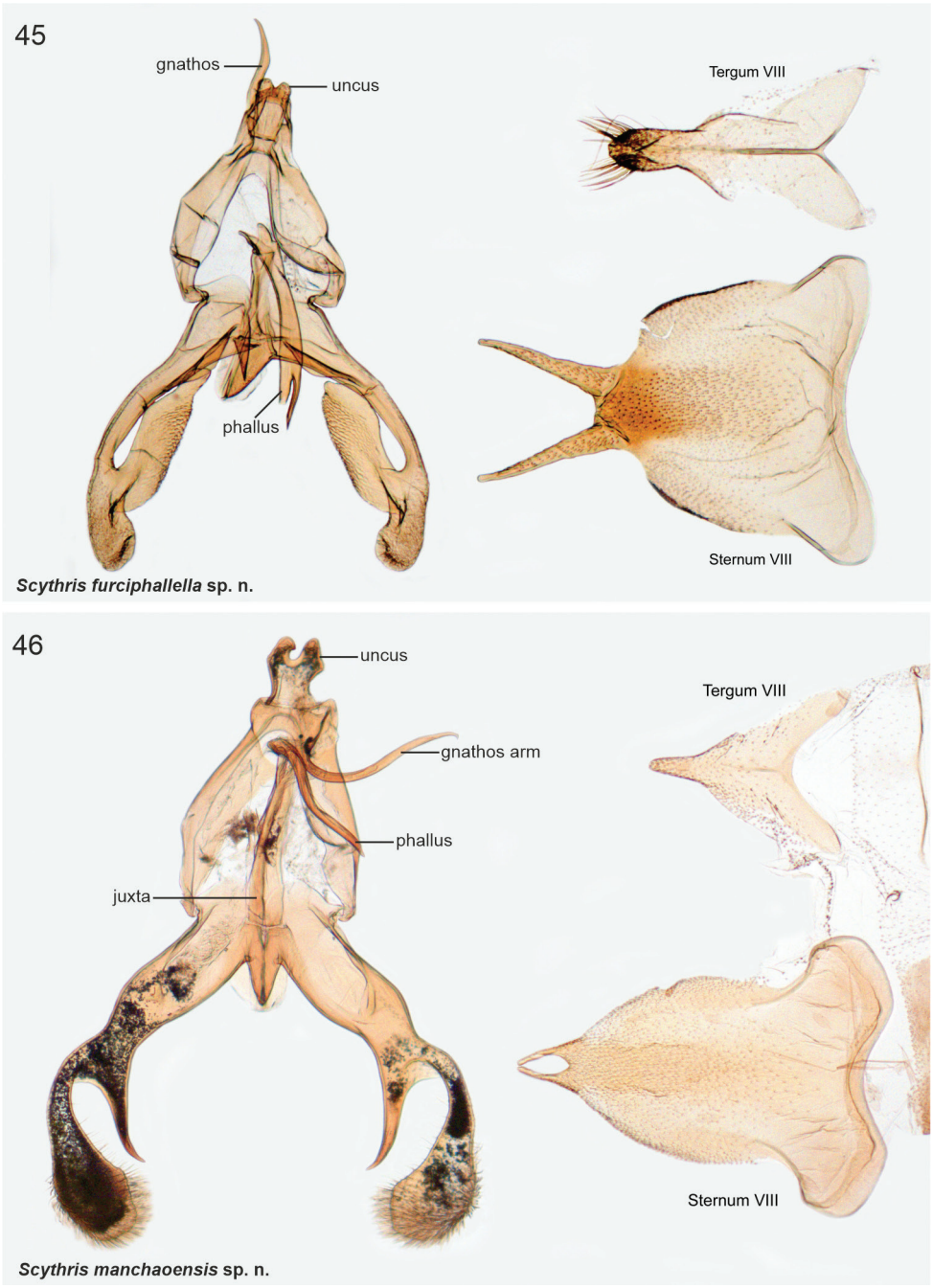

Figures 45–46. Male genitalia of *Scythris* **45** *S. furciphallella* Nupponen sp. nov., holotype, slide 2/16 Dec. 2019 KN **46** *S. manchaoensis* Nupponen sp. nov., holotype, slide 1/11 Dec. 2019 KN.

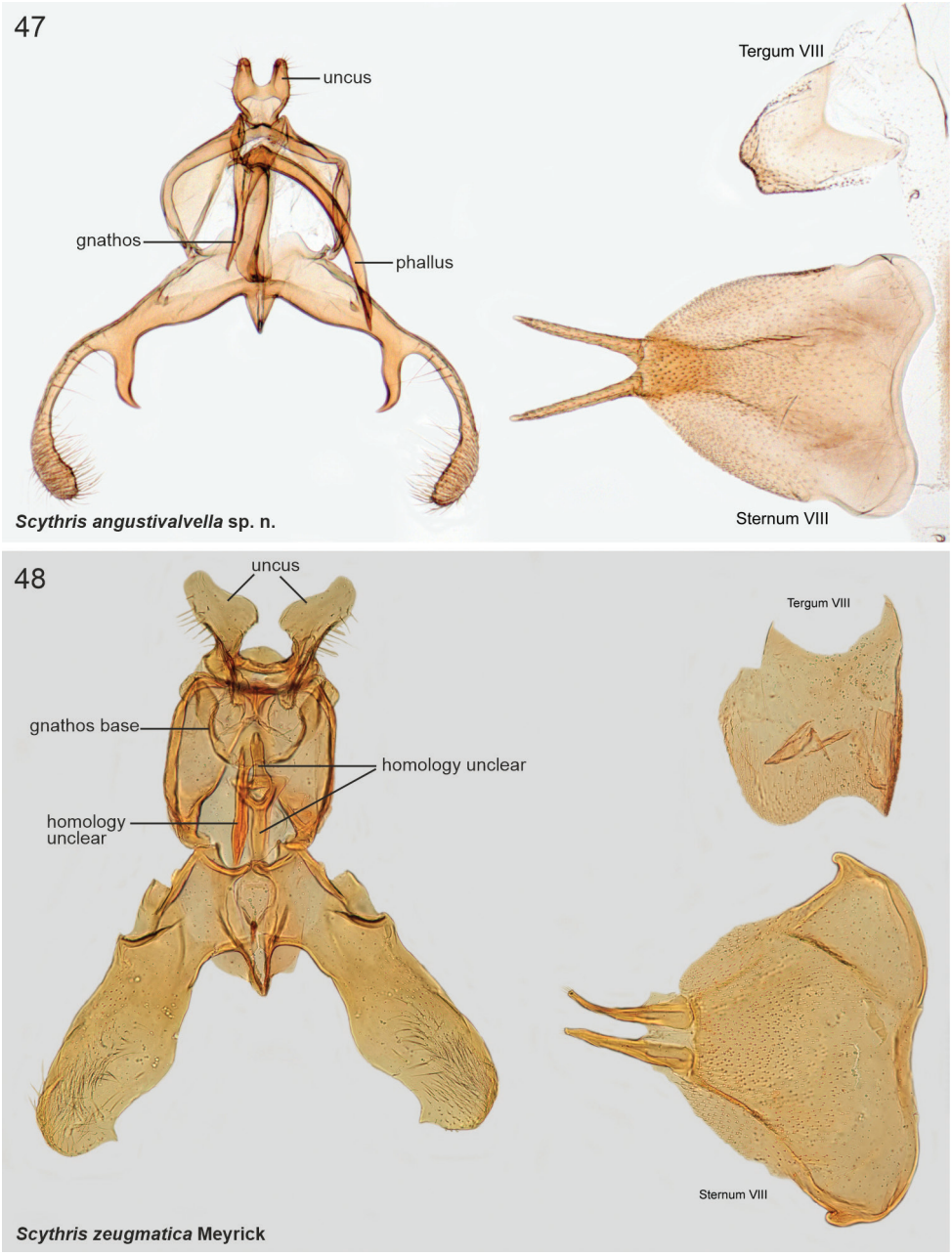

Figures 47–48. Male genitalia of *Scythris* **47** *S. angustivalvella* Nupponen sp. nov., holotype, slide 4/16 Dec. 2019 KN **48** *S. zeugmatica* Meyrick, 1931, holotype, slide JFGC No. 8050.

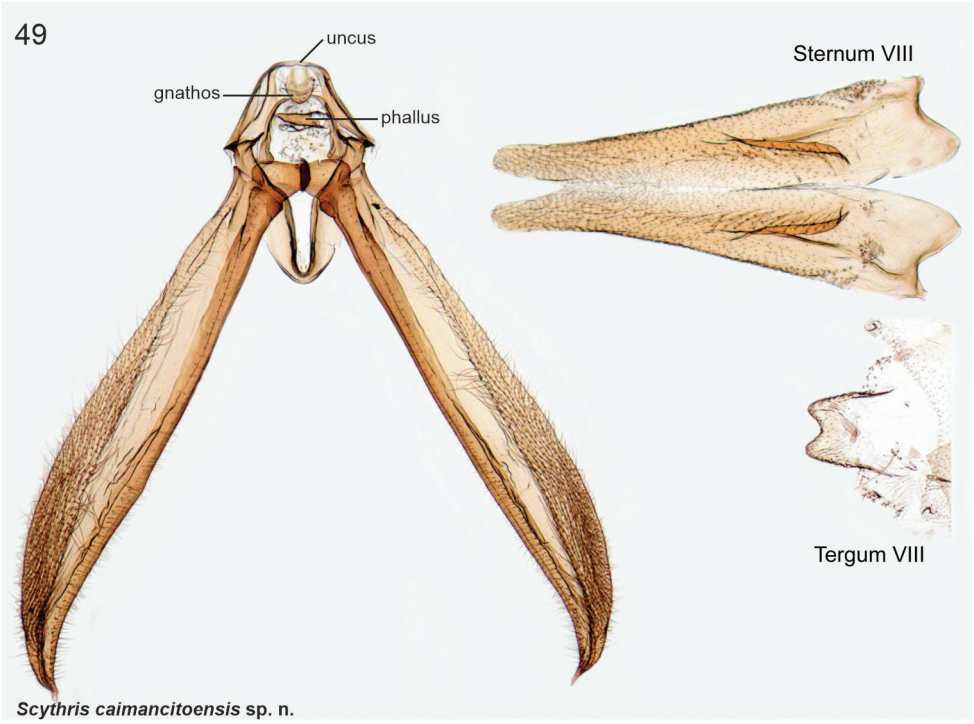

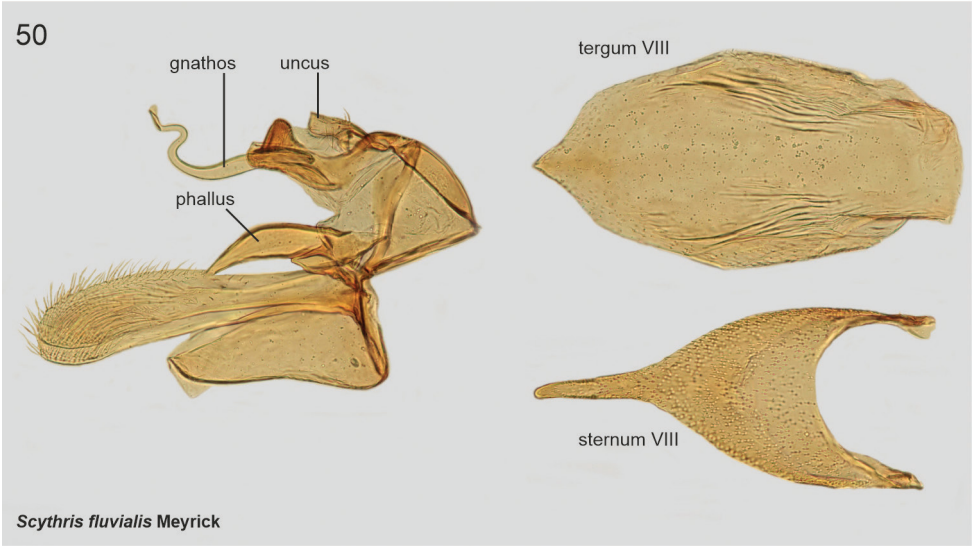

Figures 49–50. Male genitalia of *Scythris* **49** *S. caimancitoensis* Nupponen sp. nov., holotype, slide 3/9 Dec. 2019 KN **50** *S. fluvialis* Meyrick, 1916, lectotype, slide JFGC No. 8052 (genitalia shown in lateral view).

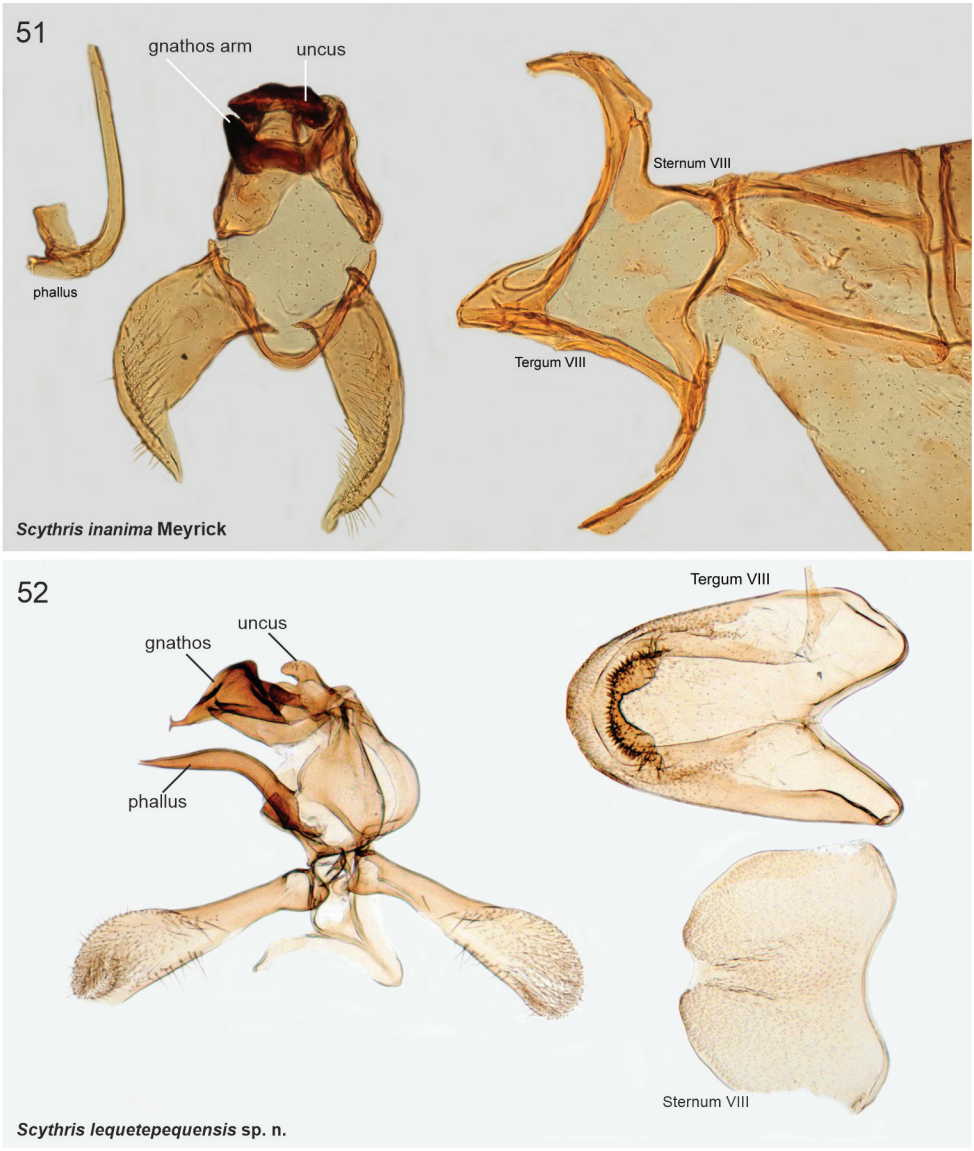

Figures 51–52. Male genitalia of *Scythris* **51** *S. inanima* Meyrick, 1916, holotype, slide JFGC No. 8051 **52** *S. lequetepequensis* Nupponen sp. nov., holotype, slide 2/8 Dec. 2019 KN.

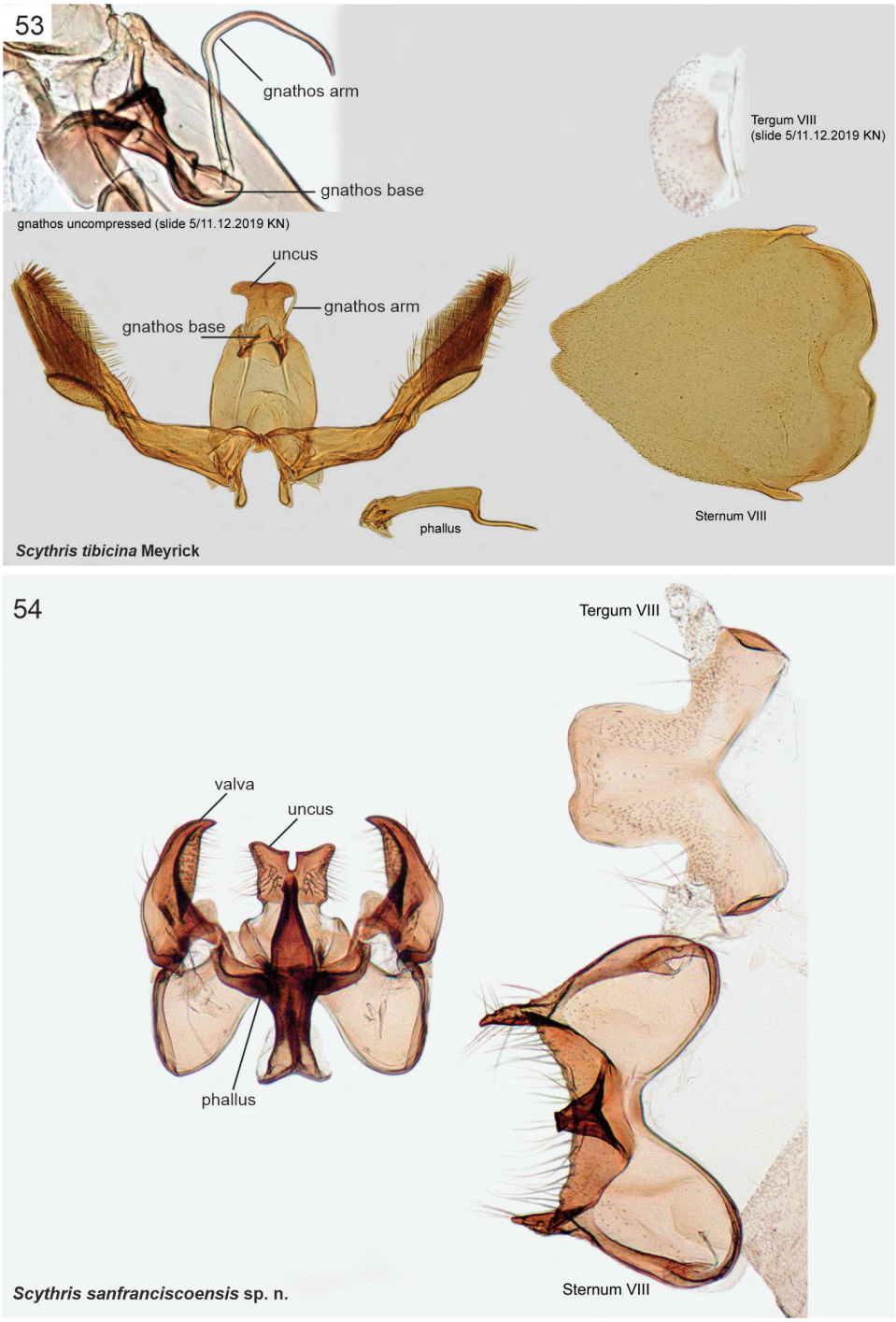

Figures 53–54. Male genitalia of *Scythris* **53** *S. tibicina* Meyrick, 1916, lectotype, slide JFGC No. 8053 (top right corner: tergum VIII and gnathos uncompressed, slide 5/11 Dec. 2019 KN **54** *S. sanfranciscoensis* Nupponen sp. nov., holotype, slide 2/10 Dec. 2019 KN.

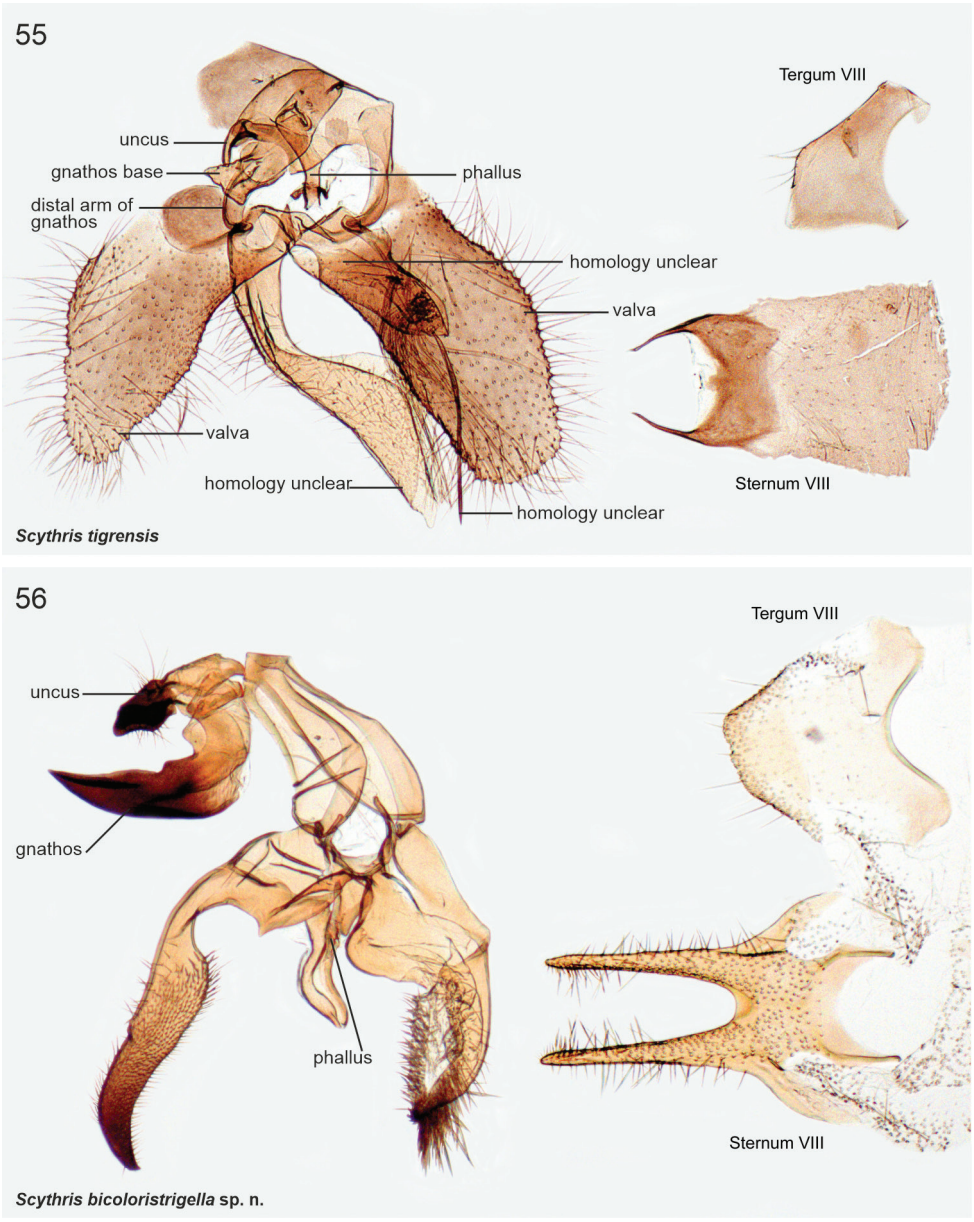

Figures 55–56. Male genitalia of *Scythris* **55** *S. tigrensis* Nupponen sp. nov., holotype, slide 1/08 Dec. 2019 KN **56** *S. bicoloristrigella* Nupponen sp. nov., genus combination incertae sedis, holotype, slide 1/9 Dec. 2019 KN.

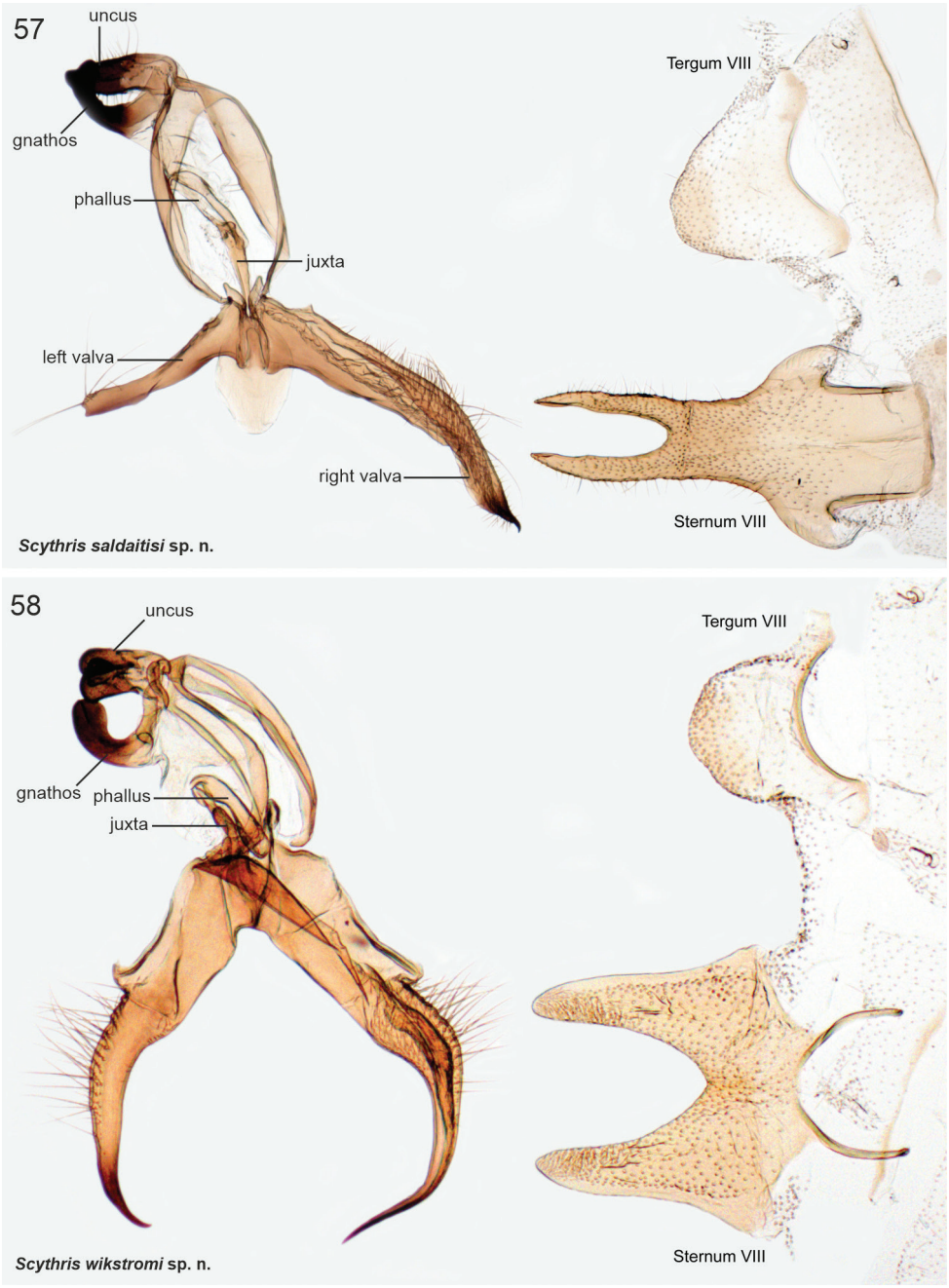

Figures 57–58. Male genitalia of *Scythris* **57** *S. saldaitisi* Nupponen sp. nov., genus combination incertae sedis, holotype, slide 4/11 Dec. 2019 KN **58** *S. wikstromi* Nupponen, sp. nov., genus combination incertae sedis, holotype, slide 2/12 Dec. 2019 KN.

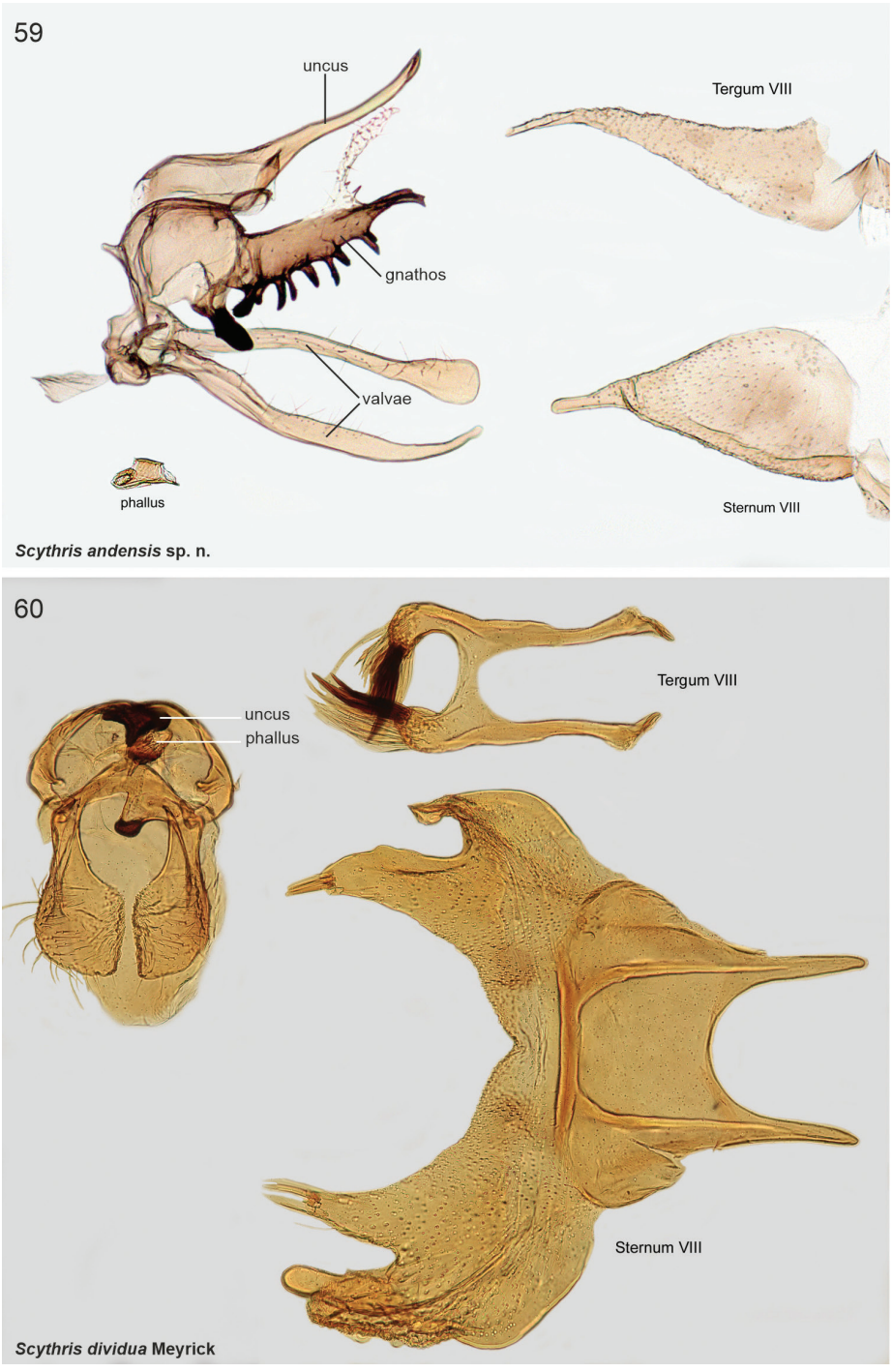

Figures 59–60. Male genitalia of *Scythris* **59** *S. andensis* Nupponen sp. nov., genus combination incertae sedis, holotype, slide 2/15 Dec. 2019 KN (genitalia shown in lateral view) **60** *S. dividua* Meyrick, 1916, genus combination incertae sedis, lectotype, slide JFGC No. 8054.

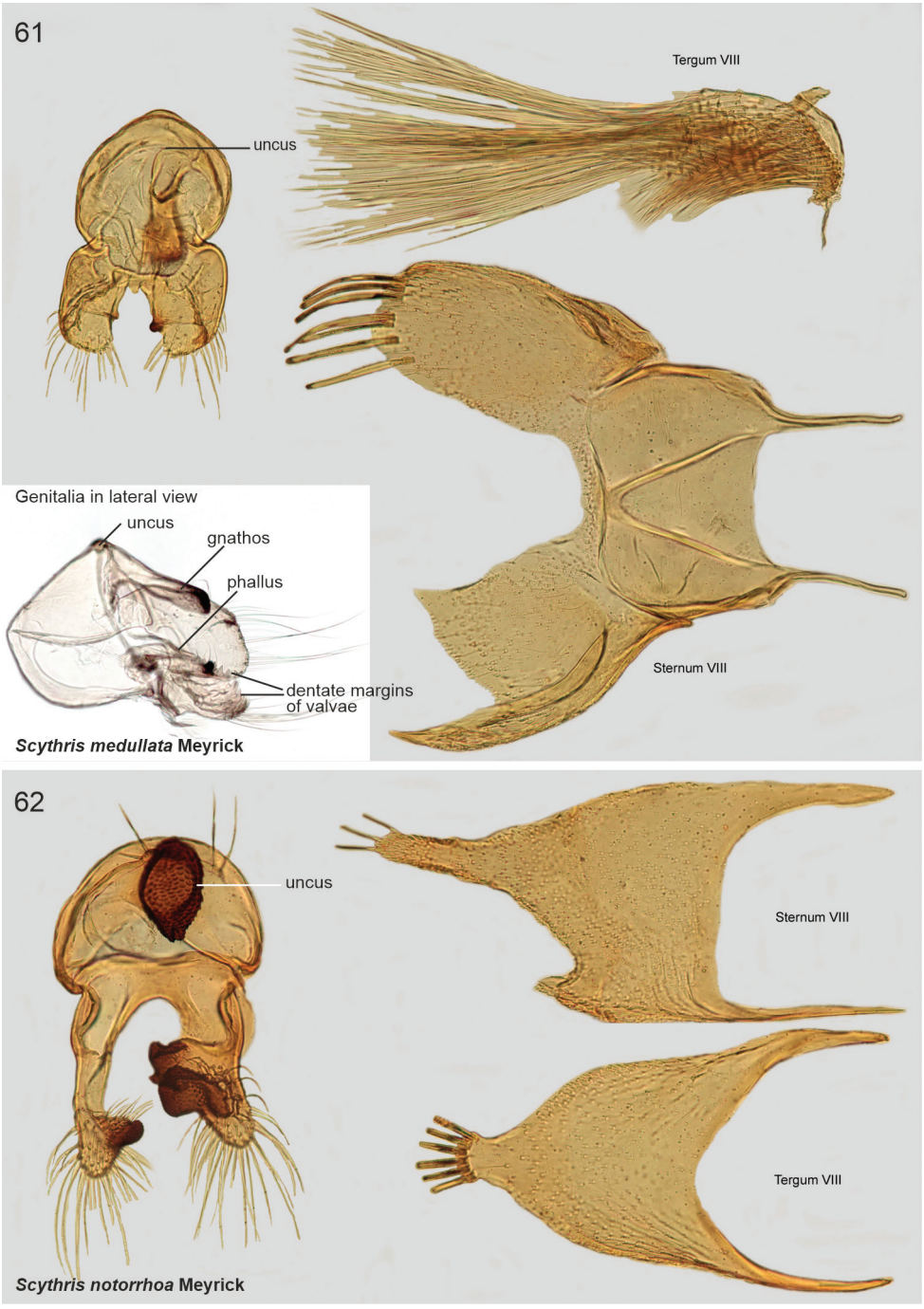

Figures 61–62. Male genitalia of *Scythris* **61** *S. medullata* Meyrick, 1916, genus combination incertae sedis, lectotype, slide JFGC No. 8055 **62** *S. notorrhoa* Meyrick, 1921, genus combination incertae sedis, lectotype, slide JFGC No. 8065.

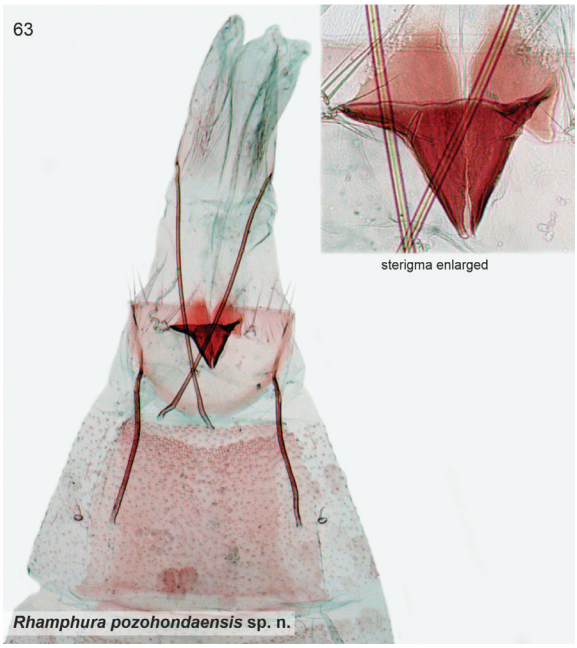

Figure 63. Female genitalia of *Rhamphura pozohondaensis* Nupponen sp. nov., holotype, slide 1/14 Dec. 2019 KN.

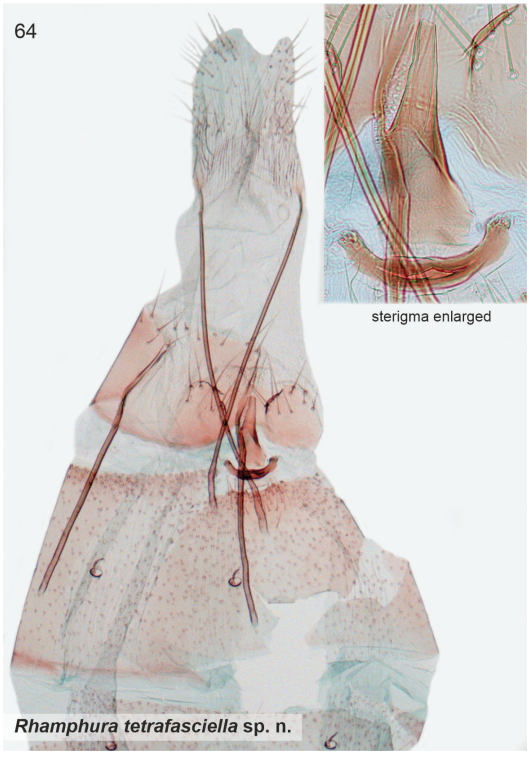

Figure 64. Female genitalia of *Rhamphura tetrafasciella* Nupponen sp. nov., genus combination incertae sedis, holotype, slide 3/13 Dec. 2019 KN.

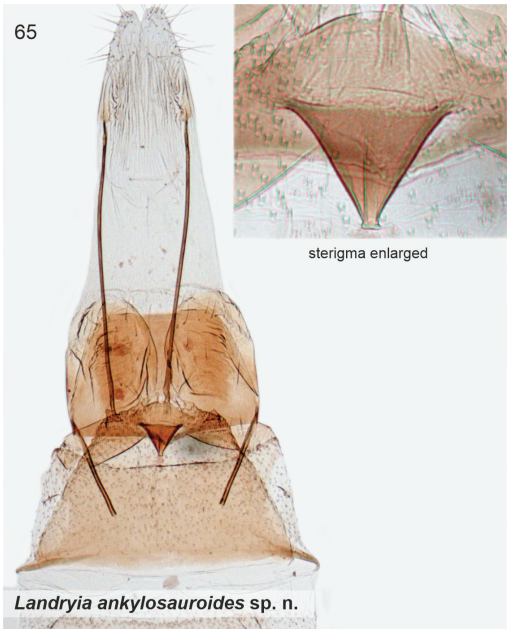

Figure 65. Female genitalia of *Landryia ankylosauroides* Nupponen sp. nov., genus combination incertae sedis, paratype, slide 1/15 Dec.2019 KN.

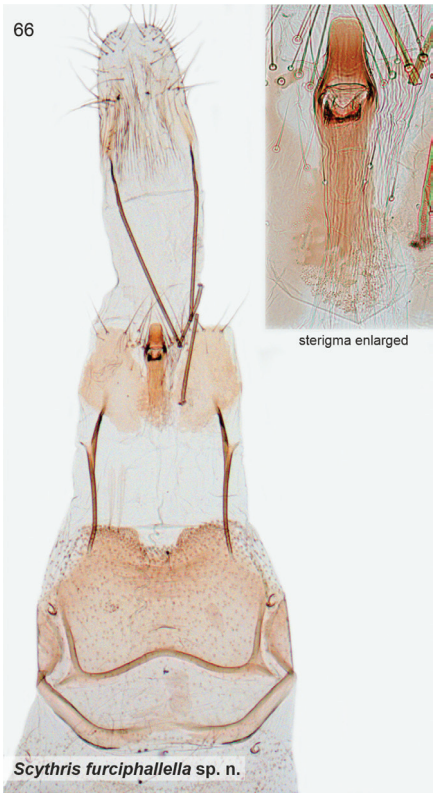

Figure 66. Female genitalia of *Scythris furciphallella* Nupponen sp. nov., paratype, slide 3/16 Dec. 2019 KN.

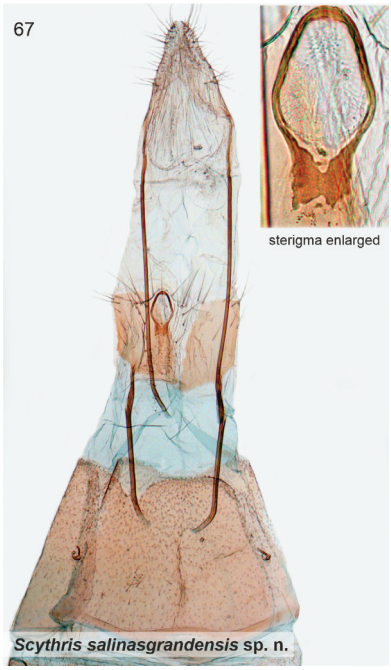

Figure 67. Female genitalia of *Scythris salinasgrandensis* Nupponen sp. nov., holotype, slide 3/11 Dec. 2019 KN.

Figure 68. Female genitalia of *Scythris plocogastra* Meyrick, 1931, holotype, slide J.F.G.C. No. 8063.

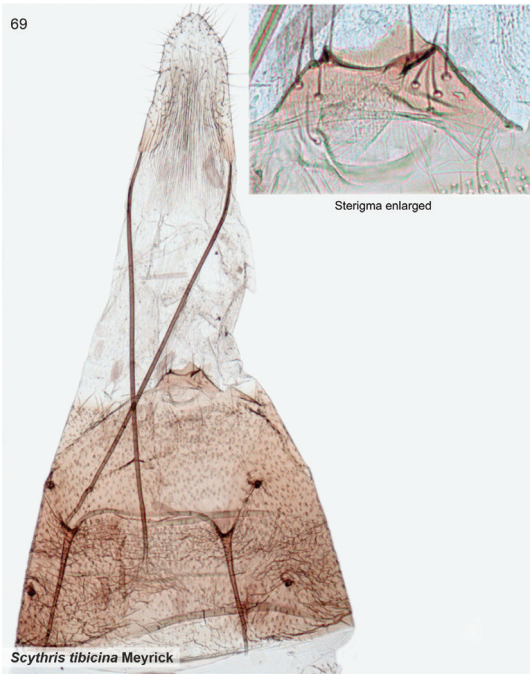

Figure 69. Female genitalia of *Scythris tibicina* Meyrick, 1916, slide 1/18 Dec. 2019 KN.

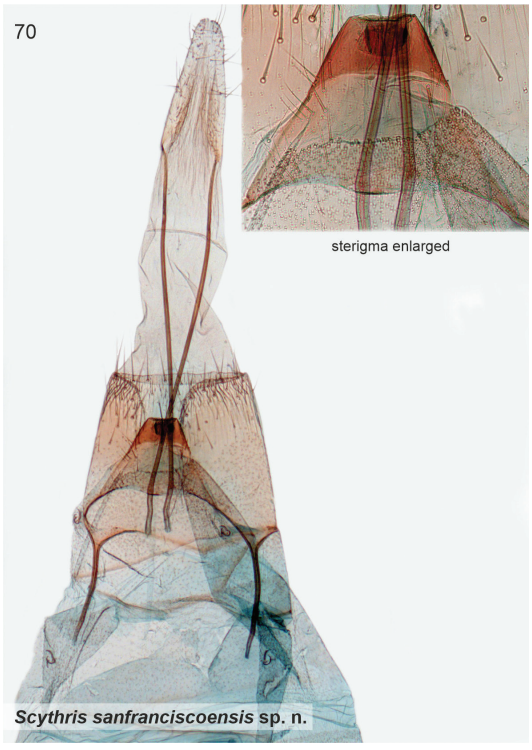

Figure 70. Female genitalia of *Scythris sanfranciscoensis* Nupponen sp. nov., paratype, slide 3/14 Dec. 2019 KN.

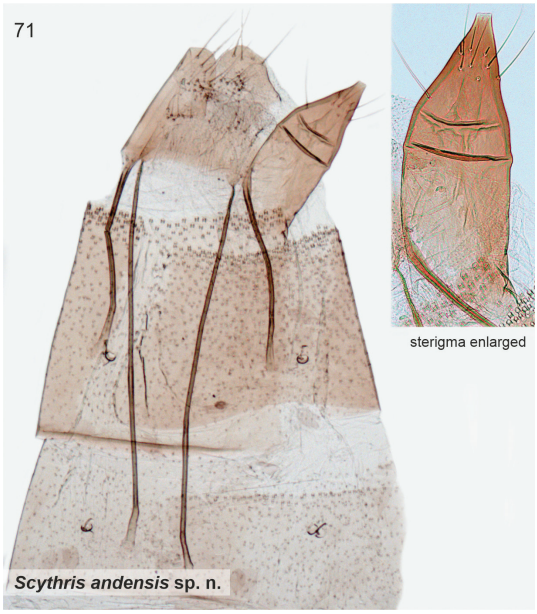

Figure 71. Female genitalia of *Scythris andensis* Nupponen sp. nov., genus combination incertae sedis, paratype, slide 4/14 Dec. 2019 KN.

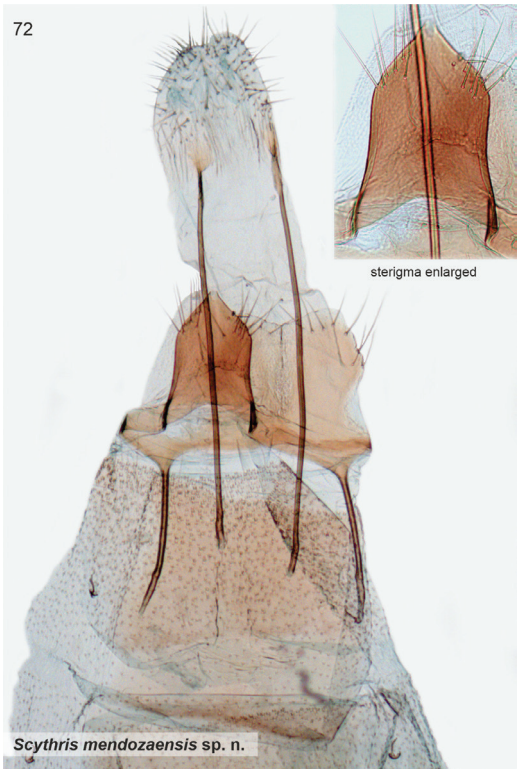

Figure 72. Female genitalia of *Scythris mendozaensis* Nupponen sp. nov., genus combination incertae sedis, holotype, slide 2/14 Dec. 2019 KN.

Figure 73. Female genitalia of *Scythris medullata* Meyrick, 1916, genus combination incertae sedis, slide 2/17 Dec. 2019 KN.

Figure 74. Holotype female of *Syntetrernis neocompsa* Meyrick, 1933, transferred from Scythrididae (Hodges 1997) to Cosmopterigidae incertae sedis (revised classification) **A** adult, Argentina: Alta Grazia (coll. NHMUK) **B** genitalia, slide JFGC No. 6153.

Figure 75. Collecting site of *Scythris andensis* sp. nov. and *S. furciphallella* sp. nov.: Argentina, Andes Mts. (2085 m), Sierra de Famatina, 27 Jan. 2017.

Figure 76. Collecting site of *Scythris manchaoensis* sp. nov.: Argentina, Andes Mts. (1185 m), Sierra de Manchao, 23 Sep. 2017.

Figure 77. Collecting site of *Rhamphura depressa* Meyrick, *R. pozohondaensis* sp. nov., *R. subdimota* sp. nov., *R. curvisociella* sp. nov., *Scythris directiphallella* sp. nov., *S. angustivalvella* sp. nov., *Landryia ankylosauroides* sp. nov. Argentina, Pozo Honda vill. S (259 m), 19 Sep. 2017.

Figure 78. Collecting site of *Scythris bicoloristrigella* sp. nov. and *Rhamphura spiniuncus* sp. nov.: Argentina, Andes Mts. (1620 m), salt lake by Cordillera del Tigre, 26 Jan. 2017.

Figure 79. Collecting site of *Rhamphura angulisociella* sp. nov., *Scythris caimancitoensis* sp. nov. and *S. sanfranciscoi* sp. nov.: Argentina, Rio San Francisco (397 m), 18 Sep. 2017.

Figure 80. Collecting site of *Scythris lequetepequensis* sp. nov. and *S. medullata* Meyr.: Peru, Lequetepeque River shore (200 m), 1 Feb. 2019.

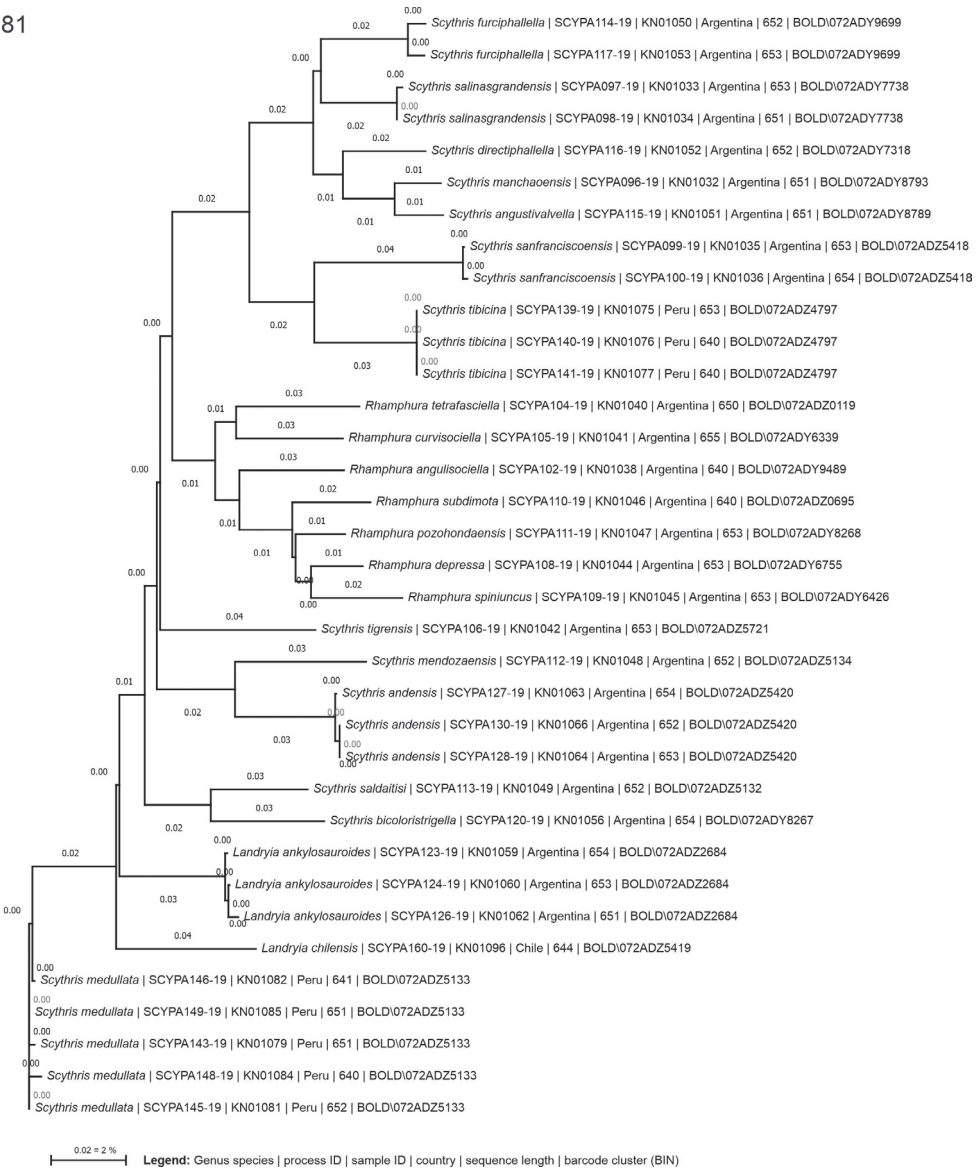

Figure 81. Neighbor-joining tree of 35 barcoded specimens generated from BOLD (Sujeevan and Hebert 2007, https://v4.boldsystems.org/ For each specimen, data are presented as shown at bottom of the tree. BOLD analysis parameters: taxon ID tree, Kimura 2-parameter model, BOLD aligner, contaminants excluded, records with stop codon excluded, records flagged as misidentifications or errors excluded, pairwise deletion, codon positions included: 1st, 2nd, 3rd.

Etymology. Latinised adjective in the nominative singular. The name of the species refers to its geographical origin, the Andes Mountains.

Distribution. NW Argentina.

Habitat. The species was collected in a dry sandy river bed at medium altitude of the Andes Mts., surrounded by dry and xerothermic rocky slopes with low vegetation and sparse shrubs (Fig. 75).

Genetic data. BIN: BOLD:ADZ5420 (*n* = 3 from Argentina). Genetically slightly heterogenous, maximum variation 0.16%. Nearest neighbour: *Scythris mendozaensis* Nupponen sp. nov. from Argentina (Scythrididae, BIN: BOLD:ADZ5134, 5.78%).

Remarks. *Scythris andensis* and *S. mendozaensis* are morphologically similar. In COI maximum likelihood phylogeny these taxa associate next to taxa, which are classified in *Scythris* or without genus combination on BOLD (Suppl. material 2). Structurally these taxa are not easy to combine to any North American Scythrididae genus (Landry 1991)). For these reasons we tentatively classify *andensis* and *mendozaensis* in *Scythris* (incertae sedis), highlighting the need for more research.

Scythris mendozaensis Nupponen, sp. nov., genus combination incertae sedis

http://zoobank.org/158CC3B9-9F3A-40FF-828B-1F515DC38497

Figs 31, 72

Type material. ***Holotype.*** Argentina • ♀; prov. Mendoza, Andes Mts., Cordillera del Tigre, Mendoza River valley near Uspallata village; 32°35.9'S, 69°22.9'W; 1900 m a.s.l.; 25 Jan. 2017; K. Nupponen & R. Haverinen leg.; [BOLD sample ID] KN01048; [genitalia slide] K. Nupponen prep. no. 2/14 Dec. 2019; coll. NUPP (MZH).

Diagnosis. Externally resembles to some extent *S. notorrhoa* and some colour forms of *L. ankylosauroides*. White streak on forewing continues to tornus in *mendozaensis* (to termen in *notorrhoa* and *ankylosauroides*), the streak is narrow and dorsally without interrupted line (streak is broader in *notorrhoa*, and dorsally with interrupted line in *ankylosauroides*). In the female genitalia of *S. mendozaensis*, a large pentagonal sterigma is diagnostic. *Scythris mendozaensis* is known from 1900 metres altitude in the Anders, whereas *S. notorrhoa* is known from the Amazonian lowland rain forest.

Description. Wingspan 13.5 mm. Head, collar, tegula, and thorax beige with scattered white. Few white scales exist around eye. Neck tuft and haustellum white. Scape dorsally beige, ventrally dirty white; pecten longer than diameter of scape. Flagellum dark brown, 0.7 × length of forewing. Labial palp white, except lower surface of palpomeres II and III brown. Legs white, tarsus and tibia mixed with beige. Abdomen dorsally beige, ventrally white. Forewing beige, fold widely white from base to tornus; indistinct brown blotches at dorsal margin of fold at 0.2 and 0.45; dark brown spot at cell end. Hindwing pale fuscous.

Female genitalia. Sterigma large, twice as long as wide, pentagonal; anterior margin concave, posteriorly tapered and pointed. Ostium small, situated at posterior tip of sterigma. Sternum VII rectangular, undifferentiated. Apophyses anteriores 0.35 × length of apophyses posteriores.

Etymology. Latinised adjective in the nominative singular. The species is named after the type locality, valley of the River Mendoza.

Distribution. NW Argentina.

Habitat. The collecting site at the type locality is a dry and xerothermic valley of the River Mendoza at medium altitude of the Andes, surrounded by rocky slopes with sparse and low vegetation.

Genetic data. BIN: BOLD:ADZ5134 (*n* = 1 from Argentina). Nearest neighbour: *Scythris andensis* Nupponen, sp. nov. (BIN: BOLD:ADZ5420, 5.78%).

Remarks. Male unknown. *Scythris andensis* and *S. mendozaensis* are morphologically similar. In COI maximum likelihood phylogeny these taxa associate next to taxa, which are classified in *Scythris* or without genus combination on BOLD (Suppl. material 2). Structurally these taxa are not easy to combine to any North American Scythrididae genus (Landry 1991)). For these reasons we tentatively classify *andensis* and *mendozaensis* in *Scythris* (incertae sedis), highlighting the need for more research.

The *dividua* species group

Phallus short and thick, basally more sclerotised. Valvae short and broad, potentially almost immobile. Male sternum VIII large asymmetrical plate, with stout apical pegs. Species included: *dividua*, *medullata*, *notorrhoa*.

Scythris dividua, *S. notorrhoa*, and *S. medullata* are morphologically similar. The DNA barcode is available for *S. medullata* only, and in COI maximum likelihood phylogeny it associates next to taxa, which are classified in *Landryia* or without genus combination on BOLD (Suppl. material 2). However, structurally these taxa do not have the diagnostic characters of *Landryia* (treated as *Asymmetrura* in Landry 1991), such as the greatly enlarged bulbus ejaculatorius in the male genitalia, or the pincer-like projections on caudal margin of sternum VII on the female abdomen, and these three species are not easy to combine to any North American Scythrididae genus. For these reasons we tentatively classify *Scythris dividua*, *S. notorrhoa*, and *S. medullata* in *Scythris* (incertae sedis). Relationship to *Neoscythris* is also possible, see Genetic data under *S. medullata*.

Scythris dividua (Meyrick, 1916), genus combination incertae sedis

Figs 32, 60

Scythris dividua Meyrick, 1916. Exotic Microlepidoptera, vol. 2 (part 1): 12.

Material examined. ***Lectotype.*** Peru • ♂: Oroya; [11°31'S, 75°53'W]; 12200 feet a.s.l.; 7.14.; Parish leg.; [genitalia slide] JFGC No. 8054; NHMUK ID 010922357; NHMUK slide ID 010316666; coll. NHMUK.

Paralectotypes. Peru • 11 exx.; same data as for lectotype; coll. NHMUK.

Diagnosis. *Scythris dividua*, *S. medullata*, and *S. notorrhoa* are similar externally. Reliable determination can be achieved by genitalia examination (DNA barcodes not

available for all these three taxa yet). Uncus pentagonal, heavily sclerotised in *dividua*; rectangular, small, less sclerotised in *medullata*; oval and heavily sclerotised in *notorrhoa*. Valvae narrow basally, inner margin without sclerotisations in *dividua*; broad basally, inner margin with minute sclerotisation in *medullata*; asymmetrical, inner margin with large sclerotisations in *notorrhoa*. Segment VIII distinct in each three species, see illustrations.

Description. The original description is quoted: "Wingspan 12–15 mm ♂, ♀. Head, palpi and thorax dark bronzy-grey, somewhat sprinkled with whitish. Antennal ciliations of ♂ 1. Abdomen dark grey, in ♂ sprinkled with whitish beneath, in ♀ suffused with ochreous-whitish beneath and towards apex above. Forewings lanceolate; dark bronzy-grey, irregularly strewn with whitish scales, especially posteriorly; a cloudy white median streak from base to near termen, and a slenderer one close beneath it to beyond middle; an undefined subdorsal streak of obscure whitish irroration from base to tornus: cilia grey, mixed with white towards base. Hindwings 0.75, 4 and 5 separate; dark grey, thinly scaled anteriorly; cilia grey."

***Male genitalia*.** Uncus pentagonal, heavily sclerotised plate. Tegumen trapezoid hood; anteriorly attached to broad transverse sclerotisation having anteriorly a rectangular extension with heavily sclerotised blunt tip. Phallus short and thick, basally more sclerotised (homology interpretation tentative, this structure could also be gnathos base). Valva short, basal rather narrow, distally broad and round. Saccus labiate, longer than valva. Sternum VIII large asymmetrical plate; basal portion rectangular with anterior apodemes, arched sclerotisation medially; posteriorly two large bifurcate processes, outer lobes distally asymmetrically extended, inner lobes with three stout apical spikes. Tergum VIII H-shaped; posterior shanks bent inwards, apices with five stout spiniform setae and bunch of thick setae; tip of anterior shanks foot-shaped.

***Female genitalia*.** Not dissected.

Distribution. Peru.

Scythris medullata (Meyrick, 1916), genus combination incertae sedis

Figs 33, 61, 73

Scythris medullata Meyrick, 1916. Exotic Microlepidoptera, vol. 2 (part 1): 13.

Material examined. ***Lectotype*.** Peru • ♂; Lima; 500 feet a.s.l.; 8–14.; Parish leg.; [genitalia slide] JFGC No. 8055; NHMUK ID 010922362; NHMUK slide ID 010316667; coll. NHMUK.

***Paralectotypes*.** Colombia, Equador, Peru • Meyrick (1916) described the species based on 80 specimens, but only 13 remain the NHMUK/Meyrick collection, also reported by Clarke (1965).

Other material. Peru • 1 ♂, 3 ♀; prov. La Libertad, Lequetepeque River, near El Huabal village; 7°16.9'S, 79°18.2'W; 200 m a.s.l.; 1 Feb. 2019; K. Nupponen & R. Haverinen leg.; [BOLD sample IDs] KN01079, KN01080, KN01081, KN01084; [genitalia slide] K. Nupponen prep. no. 2/17 Dec. 2019 ♀; coll. NUPP. • 1 ♂, 1 ♀;

prov. Cajamarca, Lequetepeque River, near Chilete village; 7°13.0'S, 78°45.3'W; 980 m a.s.l.; 4 Feb. 2019; K. Nupponen & R. Haverinen leg.; [BOLD sample IDs] KN01082, KN01083; [genitalia preparations] 2 in glycerol; coll. NUPP. • 1 ♂; prov. Ancash, Fortaleza River, Raquia village 13 km SW; 10°13.1'S, 77°33.6'W; 1180 m a.s.l.; 31 Jan. 2019; K. Nupponen & R. Haverinen leg.; [BOLD sample ID] KN01085; [genitalia slide] K. Nupponen prep. no. 3/17 Dec.2019; coll. NUPP. Argentina • 1 ♂; prov. Salta, Rio San Francisco, by Algarrobal village; 24°38.0'S, 64°54.5'W; 620 m a.s.l.; 16 Sep. 2017; K. Nupponen & R. Haverinen leg.; [BOLD sample ID] KN01039; [genitalia slide] K. Nupponen prep. no. 2/13 Dec. 2019; coll. NUPP.

Diagnosis. *Scythris dividua*, *S. medullata*, and *S. notorrhoa* are similar externally. Reliable determination can be achieved by genitalia examination (DNA barcodes not available for all these three taxa yet). Uncus pentagonal, heavily sclerotised in *dividua*; rectangular, small, less sclerotised in *medullata*; oval and heavily sclerotised in *notorrhoa*. Valvae narrow basally, inner margin without sclerotisations in *dividua*; broad basally, inner margin with minute sclerotisation in *medullata*; asymmetrical, inner margin with large sclerotisations in *notorrhoa*. Segment VIII distinct in each three species, see illustrations.

Description. The original description is quoted: "Wingspan 11–12 mm ♂, ♀. Head, palpi and thorax dark violet-bronzy-grey, somewhat touched with whitish. Antennal ciliations of ♂ 0.75. Abdomen dark grey, suffused with ochreous-white beneath with both sexes. Forewings lanceolate; dark violet-bronzy-grey, either irregularly sprinkled with whitish except towards base, or with two closely adjacent whitish longitudinal streaks from base, upper median; reaching to about 0.75, lower reaching to beyond middle, and with every transitional variation between these two forms, the streaks and irroration varying in development but always one or the other present; plical and second discal stigmata more or less perceptible as obscure spots of dark fuscous suffusion, and sometimes one or two other similar spots in disc: cilia fuscous, variably mixed with whitish towards base. Hindwings 0.66, 4 and 5 separate; dark fuscous, thinly scaled anteriorly; cilia dark grey."

Male genitalia. Uncus rectangular, small. Gnathos base narrow belt; distal arm robust, rectangular with sclerotised tip. Tegumen hood-shaped. Phallus as long as gnathos, slim and shallowly bent, posterior quarter tapered, tip pointed. Valvae short, asymmetrical, broad, as long as gnathos; left valva slightly narrower, inner margin with minute sclerotisation, ventral margin with small sclerotised extension; right valva with semi-circular and heavily sclerotised extension at ventral margin, apical margin dentate. Sternum VIII large asymmetrical plate; basal portion rectangular with anterior apodemes, V-shaped reinforcement at middle; posterior part with two large extensions, left rectangular with horn-shaped lateral extension, right rectangular with rounded corners and posteriorly with seven long pegs. Tergum VIII small asymmetrical plate with bunch of long bristles.

Female genitalia. Sterigma funnel-shaped, broad and rather short. Ostium round. Sternum VII trapezoid, medioposteriorly cleft, anterior margin chitinised. Apophyses anteriores short, one quarter length of apophyses posteriores.

Distribution. Argentina, Colombia, Ecuador, Peru.

Habitat. The moth inhabits moist riverside meadows (Fig. 80).

Genetic data. BIN: BOLD:ADZ5133 (n = 6 from Costa Rica and Peru). Genetically slightly heterogenous, maximum variation 0.49%. Nearest neighbor: North American *Neoscythris* sp. (Scythrididae, BIN: BOLD:ABA1135, 0.29%).

Remarks. New to Argentina. Originally the type series comprise 80 specimens, but only 13 exx. remain in the Meyrick collection (Colombia, Cali, 500 feet; Caldas 4400 feet; La Crumbre 6600 feet, in May. Ecuador, Huigra 4500 feet, in June; Peru, Lima 500 feet, in June; Chosica 2800 feet, in July and August (Parish). In the original description *S. medullata* is mentioned as an externally very variable species, and the variation being to some extent localised, the specimens from one locality being mostly externally similar.

Scythris notorrhoa (Meyrick, 1921), genus combination incertae sedis

Figs 34, 62

Scythris notorrhoa Meyrick, 1921. Exotic Microlepidoptera, vol. 2 (part 14): 441.

Material examined. ***Lectotype*.** Brazil • ♂; Amazonas, Manaos; 11.19.; Parish leg.; [genitalia slide] JFGC No. 8065; NHMUK ID 010922363; NHMUK slide ID 010316671; coll. NHMUK.

***Paralectotype*.** Brazil • 17 exx.; same data as for lectotype; coll. NHMUK.

Diagnosis. *Scythris dividua*, *S. medullata*, and *S. notorrhoa* are similar externally. Reliable determination can be achieved by genitalia examination (DNA barcodes not available for all these three taxa yet). Uncus pentagonal, heavily sclerotised in *dividua*; rectangular, small, less sclerotised in *medullata*; oval and heavily sclerotised in *notorrhoa*. Valvae narrow basally, inner margin without sclerotisations in *dividua*; broad basally, inner margin with minute sclerotisation in *medullata*; asymmetrical, inner margin with large sclerotisations in *notorrhoa*. Segment VIII distinct in each three species, see illustrations.

Description. The original description is quoted: "♂ ♀. 10–12 mm. Head bronzy-fuscous, sides ochreous-whitish, or in ♂ wholly suffused ochreous-whitish. Palpi fuscous more or less suffused ochreous-whitish. Thorax dark bronzy-fuscous, an ochreous-whitish, on inner side of patagia, in ♂ more or less suffused ochreous-whitish. Abdomen dark grey, beneath suffused ochreous-whitish. Forewings ♂ fuscous, ♀ dark bronzy-fuscous: a broad ochreous-whitish median stripe from base to termen, sometimes with slight apical projection above, dorsal area below this stripe in ♂ wholly suffused ochreous-whitish, plical stigma sometimes marked on lower margin of stripe: cilia grey, in ♂ paler and more or less suffused ochreous-whitish on termen. Hindwings 0.6, 4 and 5 separate; dark grey; cilia grey."

***Male genitalia*.** Uncus heavily sclerotised, oval, slightly pointed on apex, surface granulate. Tegumen hood-shaped. Valvae asymmetrical, margins reinforced at basal 1/3: left valva longer, rather narrow, subapically with elongated and heavily sclerotised

ventral extension, apex with long setae; right valva beyond middle with two large and complex heavily sclerotised extensions, apex with long setae. Phallus not detected on the lectotype slide (JFGC No. 8065). Sternum VIII large asymmetrical plate; basal portion rectangular; anteriorly with deep quadrangular concavity; posteriorly with two extensions: one short, the other triangularly extended with three stout apical pegs. Tergum VIII pentagonal, posteriorly extended, apically with six stout pegs; anteriorly with deep U-shaped concavity.

***Female genitalia*.** Not dissected.

Distribution. Brazil.

Remarks. Originally the type series comprised 80 specimens, but only 20 specimens remain in the Meyrick collection (Clarke 1965).

Taxon excluded from Scythrididae

Syntetrernis neocompsa Meyrick, 1933, Cosmopterigidae incertae sedis

Fig. 74

Syntetrernis neocompsa Meyrick, 1933. Exotic Microlepidoptera, vol. 4 (part 14): 428.
Scythris neocompsa (Meyrick, 1933). Transferred from Cosmopterigidae to Scythrididae: *Scythris*, but without evidence to support the transfer (Hodges 1997).

Material examined. ***Holotype*.** Argentina • ♀; Alta Grazia; CB. .32; C. Bruch leg.; [genitalia slide] JFGC No. 6153; NHMUK ID 010922354; NHMUK slide ID 010316673; coll. NHMUK.

Diagnosis. Unmistakeable both externally (wings, thorax and head brownish-grey with white streaks) and by a characteristic ring-shaped sterigma in the female genitalia.

Description. The original description is quoted: "Wingspan 17 mm ♂. Head light brownish-grey, white lateral streaks. Palpi white, second joint with grey subapical ring, terminal joint with grey lateral line. Thorax light brownish-grey, five light lines. Forewings narrow-lanceolate; grey-brownish; markings white; a short very oblique streak from base of costa; a fine line on dorsal edge towards base; an oblique streak from costa at 0.2 to fold; an oblique streak from costa at 0.4 in an even curve through middle of disc to costa at 0.8; a line running from fold at 0.4 to dorsum in middle of wing, thence to disc at 0.66, and returning to termen beyond tornus; a streak from disc at 0.75 to apex: cilia light brownish-grey, a white bar at apex and finer one above tornus. Hindwings and cilia grey."

***Female genitalia*.** The genitalia are partly destroyed by museum pests. Sterigma thick ring-shaped. Ostium round, situated approximately at middle of sterigma, lateral margins reinforced by semi-circular and arched sclerotisations. Apophyses anteriores 0.8 × length of apophyses posteriores.

Distribution. Argentina.

Remarks. Male unknown. *Syntetrernis neocompsa* Meyrick, 1933 is transferred from Scythrididae (Hodges 1997) to Cosmopterigidae incertae sedis, following a consultation with Jean-François Landry (pers. comm.): "An examination of the type,

shown in Fig. 74, strongly suggests that it is not a Scythrididae. The long, sickle-shaped labial palps are not found in scythridids; some spatulate scales are discernible on the head (vertex), and such scales are not found in scythridids but in other gelechioid families such as Cosmopterigidae, Momphidae, and Gelechiidae. The forewing pattern is atypical of scythridids (not trustworthy by itself but significant combined with the other characters). The female genitalia (Fig. 74B) shows a sterigma that is reminiscent of some Cosmopterigidae (e.g. *Triclonella* Busck, 1901, *Hyposmocoma* Butler, 1881, *Asymphorodes* Meyrick, 1929). These features suggest that this is likely a Cosmopterigidae. The original genus *Syntetrernis* was transferred to Parametriotinae (now in Elachistidae) by Hodges (1997), however, the taxon *neocompsa* doubtfully matches that subfamily." The male is unknown.

Discussion

The results of our three expeditions show that the Scythrididae fauna of the study area is mostly unknown. This study brings the total of described species of the family Scythrididae from continental South America to 35. It is difficult to estimate the actual species richness in South America, except to note that it is estimated that the undescribed Scythrididae species outnumber described ones by a factor of ten in the more extensively explored North America (Hodges et al. 1983; Landry 1991). In North America 44 species are included in the family (Pohl et al. 2016), but the actual number of species is possibly between 400 and 500 species (Landry 1991). Bengtsson (2014) reported 307 species from Africa, but Agassiz (2014) speculated the fauna of Africa to be perhaps several times higher. Of the 25 species collected by the first author for the current paper, 22 (91%) were species new to science. With 60% of recorded species represented by a single specimen only, more extensive collecting is obviously needed to document the actual species richness and abundance. This also effects the identification key and the authors expect that the key to males will be out of date as soon as more South American material is examined.

The area with the highest species richness appears to be the eastern slopes of the Andes at medium and low elevations (~ 180–2100 meters). All Scythrididae in the study area were attracted to light, and despite considerable efforts, not a single specimen was found during the day.

Recently, taxonomic revisions that rely on DNA barcodes and photographs of external features alone have started to gain ground. One example of such minimalist approach is the revision of Costa Rican braconid wasps (Sharkey et al. 2021). Such studies are tempting and pragmatic if the fauna is unexplored, because arguably the identities are less subjective, it takes less taxonomists' time to prepare, and those are easier to update. Such approaches have been criticised, particularly because in the long run they do not speed up description of the biodiversity, but rather introduce "superficial taxonomic impediment" for future generations of taxonomists (Meier et al. 2021). We justify our classical approach by the historical Meyrick material, which we included

in the study, because with regard to this material we had to rely on morphology alone. Meyrick's type specimens have not been DNA barcoded yet. Our approach was very time consuming, but by treating the new material in a similar manner, we aimed to make all South American Scythrididae material better accessible for future studies. We managed to provide DNA barcodes for 19 of the 22 new species described in the current paper, and also for three of the 13 species described by Meyrick, the latter being based on fresh material.

On several occasions, it was difficult to combine South American Scythrididae into the existing classification (Landry 1991). Often some morphological similarity is evident, particularly in the genitalia structures, but repeatedly it was doubtful whether the existing genus definitions should be broadened to encompass the observed variation, or should new genera be described to highlight the differences. *Rhamphura* is a case in point: the morphology of the taxa *subdimota*, *depressa*, *pozohondaensis*, and *spiniuncus* agrees well with the morphological definition of *Rhamphura* as in Landry (1991), while the taxa *angulisociella*, *tetrafasciella*, and *curvisociella* are more heterogenous and possess varying degrees of similarities to the North American *Rhamphura*. This finding was also supported by the COI maximum likelihood phylogeny (Suppl. material 2). For practical reasons, we adopted the view used in Landry (1991), and instead of describing new genera we classified such obscure taxa in existing genera with an incertae sedis note, highlighting the need for further research.

Molecular phylogenies focusing on Scythrididae are not yet available, and thus far Scythrididae have been represented in molecular phylogenies by few genera only out of at least 25 genera considered valid globally (Passerin and Roggero 2007). The molecular studies, which have included Scythrididae, have focused on resolving the family-level relationships in Gelechioidea (e.g., Kaila et al. 2011; Heikkilä et al. 2014; Wang and Li 2020). The most detailed phylogenetic analysis focused on supraspecific taxa in the North American fauna, and it is based on morphology (Landry 1991). Even though our COI maximum likelihood phylogeny (Suppl. material 2) is limited in terms of molecular data, and cannot considered but a first pass phylogeny, it agrees with Landry's (1991) hypothesis in several points. This supports the view that DNA barcode sequences can form a highly valuable source of complementary information to supplement morphological data, and could help resolve controversial taxonomic issues not only at the species level, but also at the genus level (Breitling 2019a, b). The genus *Scythris* is the most heterogenic in terms of genital characters in our study, agreeing with similar notion of Landry (1991). This suggests it may not be monophyletic. In our COI phylogeny *Scythris* was recovered as a large monophyletic lineage, but with several genetically distant lineages. This heterogeneity may be better communicated in a classification that includes species groups within *Scythris*, or where separate genera are recognised.

Against this background it is obvious that a global phylogenetic framework for Scythrididae is needed, preferably using an integrative approach to include both molecular and morphological data. Only this will bring stability to the classification and will provide a basis to define homological structures in a group, which is morphologically among the most diverse in Lepidoptera.

We hope our paper could act as a starting point to increase future interest to study the species richness and systematics of Scythrididae in South America, and eventually also life histories.

Acknowledgements

Kari Nupponen is indebted to Risto Haverinen (Vantaa, Finland) for his invaluable help in the field work, as well as development and loan of effective collecting equipment over the years. KN also thanks Aleksander Pototski (Tallinn, Estonia) for assistance and company during the expeditions; Kimmo Silvonen (Espoo, Finland) for his help in adult specimens' photography; Hildebrando Rojas Gonzales (Satipo, Peru), Rainer and Peter Marx (Lima, Peru), and Marko Mutanen (Kiiminki, Finland) for analysing the DNA samples; Elena Nupponen (Espoo, Finland), Timo Nupponen (Espoo, Finland), Nigel and Grace Venters (Cordoba, Argentina), and Faunatica Oy and Ripako Oy for various kinds of support and assistance. We thank Kyung Min Lee (Finnish Museum of Natural History, Finland) for carrying out phylogenetic analyses for molecular data. Louise Allan, David Lees and Peter Wing arranged adult photographs of type specimens housed in the NHMUK, under the Digital Collections Programme, and this is greatly appreciated. Those figures are under the copyright of the Trustees of the Natural History Museum, London (used with permission), made available under CC 4.0 https://creativecommons.org/licenses/by/4.0/. Lauri Kaila (Finnish Museum of Natural History, Finland) is thanked for comments on an earlier version of this manuscript, Axel Hausmann (Bavarian State Collection of Zoology, Germany) is thanked for advising us on Latin grammar and etymology, ZooKeys editor Erik J. van Nieukerken (Naturalis Biodiversity Center, Netherlands) for his valuable comments, editing, and help and reviewers Héctor Vargas (Universidad de Tarapacá, Chile) and Jean-François Landry (Agriculture and Agri-Food Canada, Ottawa Research and Development Centre, Canada) for their helpful comments and constructive criticism. Kari Nupponen acknowledges Suomen Perhostutkijain Seura (The Lepidopterological Society of Finland) for a grant to barcode the specimens. Open access fee of the publication was paid by Helsinki University Library.

References

Agassiz D (2014) Book review: The Afrotropical Scythrididae, Esperiana Memoir 7. Nota Lepidopterologica 37: 183–184. https://doi.org/10.3897/nl.37.8444

Bengtsson BÅ (1997) Scythrididae. Microlepidoptera of Europe, vol. 2. Apollo Books, Stenstrup, 301 pp.

Bengtsson BÅ (2014) The Afrotropical Scythrididae. Bad Staffelstein & Schwanfeld. Esperiana Memoir 7: 5–361. [116 plates]

Bidzilya OV, Budashkin YI, Zhakov AV (2017) Checklist of scythridid moths (Lepidoptera, Scythrididae) of Ukraine with description of two new species. Zootaxa 4291: 481–503. https://doi.org/10.11646/zootaxa.4291.3.3

Breitling R (2019a) Barcode taxonomy at the genus level. Ecologica Montenegrina 21: 17–37. https://doi.org/10.37828/em.2019.21.2

Breitling R (2019b) A little learning is a dangerous thing – on the usefulness of barcode data for genus-level taxonomy. Ecologica Montenegrina 22: 40–49. https://doi.org/10.37828/em.2019.22.4

Bucheli SR (2005) Systematics of the megadiverse superfamily Gelechioidea (Insecta: Lepidoptera). Dissertation, The Ohio State University, 389 pp. http://rave.ohiolink.edu/etdc/view?acc_num=osu1124119415

Clarke JFG (1965) Catalogue of the Type Specimens of Microlepidoptera in the British Museum (Natural History) described by Edward Meyrick, Volume V: 1–581. Trustees of the British Museum (Natural History), London. https://www.biodiversitylibrary.org/page/42780382

deWaard JR, Ivanova NV, Hajibabaei M, Hebert PDN (2008) Assembling DNA barcodes: analytical protocols. In: Martin CC (Ed.) Methods in molecular biology: Environmental genomics. Humana Press, Totowa, NJ, 275–293. https://doi.org/10.1007/978-1-59745-548-0_15

Gatesy J, DeSalle R, Wahlberg N (2007) How many genes should a systematist sample? Conflicting Insights from a phylogenomic matrix characterised by replicated incongruence. Systematic Biology 56: 355–363. https://doi.org/10.1080/10635150701294733

Heikkilä M, Mutanen M, Kekkonen M, Kaila L (2014) Morphology reinforces proposed molecular phylogenetic affinities: a revised classification for Gelechioidea (Lepidoptera). Cladistics 30: 563–589. https://doi.org/10.1111/cla.12064

Hodges RW (1997) A new agonoxenine moth damaging *Araucaria araucana* needles in Western Argentina and notes on the Neotropical Agonoxenine fauna (Lepidoptera: Gelechioidea: Elachistidae). Proceedings of the Entomological Society of Washington 99(2): 267–278. https://www.biodiversitylibrary.org/page/16212934

Hodges RW, Dominick T, Davis DR, Ferguson DC, Franclemont JG, Munroe EG, Powell JA [Eds] (1983) Check list of Lepidoptera of America north of Mexico. E.W. Classey & The Wedge Entomological Research Foundation, London, [xxiv +] 284 pp.

ICZN [International Commission on Zoological Nomenclature] (2000) International Code of Zoological Nomenclature, 4th ed. The Code Online. http://iczn.org/iczn/index.jsp

Jäckh E (1977) Bearbeitung der Gattung *Scythris* Hübner (Lepidoptera, Scythrididae). 1. Die '*grandipennis*-Gruppe'. Deutsche Entomologische Zeitschrift 24: 261–271. https://doi.org/10.1002/mmnd.19770240117

Kaila L (2004) Phylogeny of the superfamily Gelechioidea (Lepidoptera: Ditrysia): an exemplar approach. Cladistics 20: 303–340. https://doi.org/10.1111/j.1096-0031.2004.00027.x

Kaila L, Mutanen M, Nyman T (2011) Phylogeny of the mega-diverse Gelechioidea (Lepidoptera): Adaptations and determinants of success. Molecular phylogenetics and evolution 61: 801–809. https://doi.org/10.1016/j.ympev.2011.08.016

Kalyaanamoorthy S, Minh BQ, Wong TKF, Von Haeseler A, Jermiin LS (2017) ModelFinder: Fast model selection for accurate phylogenetic estimates. Nature Methods 14: 587–589. https://doi.org/10.1038/nmeth.4285

Kemal M, Koçak AÖ (2006) Nomenclatural notes on the Nearctic Lepidoptera. Centre for Entomological Studies Ankara, Miscellaneous Papers 100: 7–8.

Klots AB (1970) Lepidoptera. In: Tuxen SL (Ed.) Taxonomists' glossary of genitalia in insects. Munksgaard, Copenhagen, 115–130. http://antbase.org/ants/publications/21060/21060.pdf

Kristensen NP (2003) Skeleton and muscles: adults. In: Kristensen NP (Ed.) Handbook of Zoology, vol. IV, Arthropoda, Insecta, part 36, Lepidoptera, Moths and Butterflies, vol. 2, Morphology, physiology, and development. de Gruyter, Berlin, 39–131. https://doi.org/10.1515/9783110893724

Landry JF (1991) Systematics of Nearctic Scythrididae (Lepidoptera: Gelechioidea): phylogeny and classification of supraspecific taxa, with a review of described species. Memoirs of the Entomological Society of Canada 160: 1–341. https://doi.org/10.4039/entm123160fv

Meier R, Blaimer BB, Buenaventura, Hartop E, vonRintelen T, Srivathsan A, Yeo D (2021) A re-analysis of the data in Sharkey et al.'s (2021) minimalist revision reveals that BINs do not deserve names, but BOLD Systems needs a stronger commitment to open science. Cladistics (early view): 1–12. https://doi.org/10.1111/cla.12489

Meyrick E (1912–1916) Exotic Microlepidoptera, vol. 1. Taylor and Francis, Red Lion Court, Fleet Street, 640 pp. https://doi.org/10.5962/bhl.title.9241

Meyrick E (1916) Exotic Microlepidoptera vol. 2 (part 1). Taylor and Francis, Red Lion Court, Fleet Street, 32 pp. https://www.biodiversitylibrary.org/page/9808406

Meyrick E (1916–1923) Exotic Microlepidoptera, vol. 2. Taylor and Francis, Red Lion Court, Fleet Street, 640 pp. https://doi.org/10.5962/bhl.title.9241

Meyrick E (1921) Exotic Microlepidoptera vol. 2 (part 14). Taylor and Francis, Red Lion Court, Fleet Street: 417–448. https://www.biodiversitylibrary.org/page/9808837

Meyrick E (1923–1930) Exotic Microlepidoptera, vol. 3. Taylor and Francis, Red Lion Court, Fleet Street, 723 pp. https://doi.org/10.5962/bhl.title.9241

Meyrick E (1928) Exotic Microlepidoptera vol. 3 (part 13). Taylor and Francis, Red Lion Court, Fleet Street, 385–416. https://www.biodiversitylibrary.org/page/60297745

Meyrick E (1930–1936) Exotic Microlepidoptera, vol. 4. Taylor and Francis, Red Lion Court, Fleet Street, 685 pp. https://doi.org/10.5962/bhl.title.9241

Meyrick E (1931) Exotic Microlepidoptera, vol. 4 (part 6). Taylor and Francis, Red Lion Court, Fleet Street, 161–192. https://www.biodiversitylibrary.org/page/60386609

Meyrick E (1931) Reports of an expedition to Brazil and Paraguay in 1926–7, supported by the trustees of the Percy Sladen Memorial Fund and the executive committee of the Carnegie Trust for Scotland. Zoological Journal of the Linnean Society 37: 277–284. https://doi.org/10.1111/j.1096-3642.1930.tb02069.x

Meyrick E (1933) Exotic Microlepidoptera vol. 4 (part 14). Taylor and Francis, Red Lion Court, Fleet Street, 417–448. https://www.biodiversitylibrary.org/page/60387089

Meyrick E (1936–1937) Exotic Microlepidoptera, vol. 5. Taylor and Francis, Red Lion Court, Fleet Street, 723 pp.

Minh BQ, Nguyen MAT, von Haeseler A (2013) Ultrafast approximation for phylogenetic bootstrap. Molecular Biology and Evolution 30: 1188–1195. https://doi.org/10.1093/molbev/mst024

Nupponen K (2009) *Scythris antisymmetrica* Nupponen, sp. n. from Central Spain, an example of antisymmetric male genitalia in the order Lepidoptera (Lepidoptera: Scythrididae). SHILAP Revista de Lepidopterologia 38: 439–444. https://www.redalyc.org/pdf/455/45515028004.pdf

Nupponen K, Saldaitis A (2013) Recent records of scythridids from the islands of Socotra and Maldives in the Indian Ocean, with descriptions of two new species (Lepidoptera: Gelechioidea, Scythrididae). Zootaxa 3626(2): 288–294. https://doi.org/10.11646/zootaxa.3626.2.6

Pohl GR, Patterson B, Pelham JP (2016) Annotated taxonomic checklist of the Lepidoptera of North America, North of Mexico. Working paper published online by the authors at ResearchGate.net, 766 pp. http://dx.doi.org/10.13140/RG.2.1.2186.3287

Passerin d'Entrèves P, Roggero A (2007) Scythrididae. 44. In: Heppner JB (Ed.) Lepidopterorum Catalogus (New Series). Vol. 3. Association for Tropical Lepidoptera, Gainesville, 85 pp.

Rambaut A (2015) FigTree, v1. 4.2: tree figure drawing tool. Molecular evolution, phylogenetics and epidemiology. http://tree.bio.ed.ac.uk/software/figtree/

Ratnasingham S, Hebert PDN (2007) BOLD: The Barcode of Life Data System www.barcodinglife.org Molecular Ecology Notes. https://doi.org/10.1111/j.1471-8286.2007.01678.x

Ratnasingham S, Hebert PDN (2013) A DNA-Based registry for all animal species: The Barcode Index Number (BIN) System. PLoS ONE 8(7): e66213. https://doi.org/10.1371/journal.pone.0066213

Robinson GS (1976) The preparation of slides of Lepidoptera genitalia with special reference to the Microlepidoptera. Entomologist´s Gazette 27: 127–132. http://idtools.org/id/leps/tortai/Robinson_1976.pdf

Sharkey MJ, Janzen DH, Hallwachs W, Chapman EG, Smith MA, Dapkey T, Brown A, Ratnasingham S, Naik S, Manjunath R, Perez K, Milton M, Hebert P, Shaw SR, Kittel RN, Solis MA, Metz MA, Goldstein PZ, Brown JW, Quicke DLJ, van Achterberg C, Brown BV, Burns JM (2021) Minimalist revision and description of 403 new species in 11 subfamilies of Costa Rican braconid parasitoid wasps, including host records for 219 species. ZooKeys 1013: 1–665. https://doi.org/10.3897/zookeys.1013.55600

Tamura K, Stecher G, Peterson D, Filipski A, Kumar S (2013) MEGA6: Molecular Evolutionary Genetics Analysis Version 6.0. Molecular Biology and Evolution 30: 2725–2729. https://doi.org/10.1093/molbev/mst197

Trifinopoulos J, Nguyen L-T, von Haeseler A, Quang Minh B (2016) W-IQ-TREE: a fast online phylogenetic tool for maximum likelihood analysis. Nucleic Acids Research 44: W232–W235. https://doi.org/10.1093/nar/gkw256

Walsingham L (1907) Microlepidoptera. In: Sharp D (Ed.) Fauna Hawaiiensis. Vol. 1, Part V. Cambridge University Press. Cambridge, 469–759. http://hbs.bishopmuseum.org/pubs-online/pdf/fh1-5.pdf

Wang QY, Li HH (2020) Phylogeny of the superfamily Gelechioidea (Lepidoptera: Obtectomera), with an exploratory application on geometric morphometrics. Zoologica Scripta 49: 307–328. https://doi.org/10.1111/zsc.12407

Supplementary material 1

Supplementary file 1

Authors: Kari Nupponen, Pasi Sihvonen

Data type: GenBank accession numbers (xslx. file)

Explanation note: DNA barcodes developed for this article (35 specimens), the associated GenBank accession numbers and other metadata.

Link: https://doi.org/10.3897/zookeys.1087.64382.suppl1

Supplementary material 2

Supplementary file 2

Authors: Kari Nupponen, Pasi Sihvonen

Data type: Phylogenetic hypothesis (pdf. file)

Explanation note: Maximum likelihood phylogeny based on 728 COI barcode sequences (including 3 outgroups). Parameters: minimum 500 bp per each sample, W-IQ-TREE (Trifinopoulos et al. 2016), ultrafast bootstrap (1000 replicates), GTR+F+I+G4 model. Data includes all public COI samples available on BOLD in September 2001 with taxon name "Scythrididae" from North, Central and South America. New COI barcodes published in this paper are highlighted with red. Right margin includes tentative genus classification for the included samples.

Link: https://doi.org/10.3897/zookeys.1087.64382.suppl2

ZooKeys 1087: 105–122 (2022)
doi: 10.3897/zookeys.1087.78998
https://zookeys.pensoft.net

RESEARCH ARTICLE

A peer-reviewed open-access journal
ZooKeys
Launched to accelerate biodiversity research

Comparative mitogenomic analysis of two earwigs (Insecta, Dermaptera) and the preliminary phylogenetic implications

Zhi-Teng Chen[1]

1 *School of Grain Science and Technology, Jiangsu University of Science and Technology, Zhenjiang 212004, China*

Corresponding author: Zhi-Teng Chen (741208116@qq.com)

Academic editor: Fabian Haas | Received 7 December 2021 | Accepted 15 February 2022 | Published 23 February 2022

http://zoobank.org/6CB2BEF7-3FA3-40AD-A76D-B2F868301538

Citation: Chen Z-T (2022) Comparative mitogenomic analysis of two earwigs (Insecta, Dermaptera) and the preliminary phylogenetic implications. ZooKeys 1087: 105–122. https://doi.org/10.3897/zookeys.1087.78998

Abstract

The phylogenetic position and inner relationships of Dermaptera remain unresolved despite the numerous efforts using morphological and molecular data. To facilitate the resolution of problems, this study sequenced the complete mitogenome of *Apachyus feae* de Bormans, 1894 (Apachyidae) and the nearly complete mitogenome of *Diplatys flavicollis* Shiraki, 1907 (Diplatyidae). The 19,029-bp long mitogenome of *A. feae* exhibited an extra *trnV* gene and two control regions in addition to the typical set of 37 genes including 13 protein-coding genes (PCGs), 22 transfer RNA (tRNA) genes, and two ribosomal RNA (rRNA) genes. The 12,950-bp long partially sequenced mitogenome of *D. flavicollis* was composed of 10 and a partial fragment of PCGs, 18 tRNA genes, two rRNA genes, and a control region. Comparative analysis of available earwig mitogenomes revealed variable mitogenomic structure and extensive gene rearrangements in Dermaptera. The preliminary phylogenetic analyses using Bayesian inference and maximum likelihood methods showed identical results, but the limited sampling and different types of molecular data lead to an apparent incongruence with previous phylogenetic studies.

Keywords

Apachyidae, Dermaptera, Diplatyidae, mitochondrial genome, phylogeny

Introduction

Dermaptera (earwigs) are a small group of ancient insects in Polyneoptera, with more than 1900 extant species within 11 families known worldwide (Haas 2018). The characteristics such as forceps-like, unsegmented cerci in the adults of this group are functional in predation, defense, wingfolding and mating (Haas et al. 2000). Most earwigs are free-living and commonly found in damp areas feeding on plant materials, spores, fungi, or insects (Haas 2018). With the exception of Arixeniidae and Hemimeridae, these two families are distinctly epizoic and live non-parasitically on cavernicolous bats and hamster rats, respectively (Nakata and Maa 1974; Haas and Gorb 2004). The majority of earwigs are oviparous, whereas the epizoic groups are viviparous, i.e., directly giving birth to nymphs. Besides, unusual maternal care behavior is found in all studied earwig species, with the female protecting eggs and first-instar nymphs (Suzuki et al. 2005; Staerkle and Koelliker 2008).

The extant Dermaptera is traditionally divided into three suborders, i.e., Arixeniina, Hemimerina, and Forficulina (Gullan and Cranston 2010). Arixeniidae and Hemimeridae are sometimes considered to be derived members of Forficulina (nonparasitic Dermaptera) in several studies (Popham 1985; Klass 2001; Engel and Haas 2007). The most recent reclassification of Dermaptera was established by Engel and Haas (2007), which included all extant earwigs in the suborder Neodermaptera. Protodermaptera and Epidermaptera are recognized as two infraorders in Neodermaptera, and Epidermaptera comprises the two epizoic families.

The phylogenetic position of Dermaptera in Insecta and the inner relationship within Dermaptera remain controversial (Beutel et al. 2013). Different research using morphological characteristics or molecular data from nuclear and mitochondrial genes generated different phylogenies of Dermaptera (Wan et al. 2012; Naegle et al. 2016). Wan et al. (2012) sequenced and analyzed the first earwig mitochondrial genome (mitogenome) and investigated the phylogeny of Polyneoptera. To date, *Challia fletcheri* Burr, 1904 and *Euborellia arcanum* Matzke & Kocarek, 2015 are the only two complete earwig mitogenomes available in GenBank, and only the mitogenomic structure of *C. fletcheri* has been analyzed (Wan et al. 2012). To better resolve the phylogeny of earwigs using mitogenomic data, this study sequenced and analyzed two new mitogenomes for Dermaptera. A preliminary phylogenetic tree of Dermaptera is constructed based on the newly sequenced and the known mitogenomic data to provide a basic topology for the relationships among families.

Materials and methods

Sample preparation and DNA extraction

The specimen of *Apachyus feae* de Bormans, 1894 was collected from Laibin, Guangxi Province of China (24.1402°N, 110.1844°E) in October of 2019; the specimen of *Diplatys flavicollis* Shiraki, 1907 was collected from Jurong, Jiangsu Province of China

(32.1325°N, 119.0743°E) in February of 2020. The specimens were identified by the author, preserved in 100% ethanol, and stored in the Insect Collection of Jiangsu University of Science and Technology (**ICJUST**). The total genomic DNA of the two earwigs was isolated using the E.Z.N.A. Tissue DNA Kit (Omega Bio-Tek, Inc.) and preserved at −20 °C before the sequencing process.

Sequencing, assembly, annotation, and analysis

The Illumina TruSeq short-insert libraries (size = 450 bp) were constructed using 1 μg of purified DNA fragments and were sequenced by Illumina Hiseq 4000 (Shanghai Biozeron Biotechnology Co., Ltd). Raw reads were filtered prior to assembly; high-quality reads were retained and assembled into contigs by SOAPdenovo2.04 (Luo et al. 2012). The assembled contigs were then aligned to the reference mitogenomes of Dermaptera using BLAST. Subsequently, the aligned contigs (≥80% similarity and query coverage) were arranged according to the reference mitogenomes. Finally, the clean reads were mapped to the assembled draft mitogenomes to fix the wrong bases; gaps were filled using GapFiller v. 2.1.1 (https://sourceforge.net/projects/gapfiller/). The mitogenome sequences of *A. feae* and *D. flavicollis* were deposited in GenBank under the accession numbers MW291948 and MW291949, respectively. Mitochondrial gene analyses of *A. feae* and *D. flavicollis* were compared to four additional species of Dermaptera with available mitogenomes (Table 1). The gene order was compared with *Drosophila yakuba* Burla, 1954, which was considered to possess the ancestral arthropod mitochondrial gene arrangement (Clary and Wolstenholme 1985).

All protein-coding genes (**PCGs**) and ribosomal RNA (**rRNA**) genes were identified by homology alignments. Gene boundaries of each PCG were further confirmed by ORF finder (https://www.ncbi.nlm.nih.gov/orffinder/). All transfer RNA (**tRNA**) genes were predicted and illustrated by the MITOS online server (Bernt et al. 2013). The visual structure of the mitogenomes were depicted using CGView Server (http://stothard.afns.ualberta.ca/cgview_server/) (Grant and Stothard 2008). Nucleotide composition of each gene and codon usage of PCGs were calculated using MEGA v. 6.0 (Tamura et al. 2013). The composition skew values were calculated by AT-skew

Table 1. List of species used in this study.

Infraorder	Parvorder	Family	Species	Length (bp)	A+T%	Accession number
Protodermaptera		Diplatyidae	**Diplatys flavicollis*	12,950	73.5	MW291949
		Pygidicranidae	*Challia fletcheri*	20,456	72.6	NC_018538
Epidermaptera	Paradermaptera	Apachyidae	*Apachyus feae*	19,029	61.2	MW291948
	Metadermaptera	Anisolabididae	*Euborellia arcanum*	16,087	68.3	KX673196
	Eteodermaptera	Forficulidae	**Eudohrnia metallica*	16,324	58.7	KX091853
			**Paratimomenus flavocapitatus*	15,677	67.4	KX091861
Outgroup	Outgroup	Outgroup	*Kamimuria chungnanshana*	—	—	NC_028076

* Incomplete mitogenomes.

= [A – T] / [A + T] and GC-skew = [G – C] / [G + C] formulas (Perna and Kocher 1995). The synonymous substitution rate (Ks) and nonsynonymous substitution rate (Ka) were computed by DnaSP v. 5.10 (Librado and Rozas 2009). Presumed secondary structures in the control regions were predicted by the online tool Tandem Repeats Finder (http://tandem.bu.edu/trf/trf.advanced.submit.html), DNAMAN v. 6.0.3 and ARWEN (http://mbio-serv2.mbioekol.lu.se/ARWEN/) (Laslett and Canbäck 2008).

Phylogenetic analysis

Nucleotide sequences of PCGs derived from six species of Dermaptera, including *A. feae* and *D. flavicollis* sequenced in this study, were used in the phylogenetic analysis (Table 1). The stonefly *Kamimuria chungnanshana* Wu, 1938 (Plecoptera, Perlidae; GenBank accession no. NC_028076) was used as the outgroup. The 13 PCGs were respectively aligned by MAFFT and concatenated as a combined dataset using SequenceMatrix v. 1.7.8 (Katoh and Standley 2013). The optimal nucleotide substitution models and partitioning schemes for the dataset was determined by PartitionFinder v. 2.1.1 using the Bayesian Information Criterion (BIC) and a greedy search algorithm (Lanfear et al. 2016). Bayesian inferences (BI) and Maximum likelihood (ML) analyses were conducted with the optimal partition schemes. The BI analysis was conducted by MrBayes v. 3.2.7, with 20 million generations sampling every 1000 generations, running one cold chain and three hot chains with a burn-in of 25% trees (Ronquist and Huelsenbeck 2003). TRACER v. 1.5 was used to examine the stability of the results of the BI analysis. The ML analysis was performed by RAxML v. 8.2.12 with 1000 bootstrap replicates (Stamatakis 2014). FigTree v. 1.4.2 was used to adjust and visualize the tree files generated by both BI and ML inferences.

Results

Mitogenome annotation and nucleotide composition

The complete mitogenome of *A. feae* is a typical double-strand circular molecule with a length of 19,029 bp (Fig. 1). The obtained partial mitogenome of *D. flavicollis* is 12,950 bp in length (Fig. 1). The completely sequenced three mitogenomes of Dermaptera range in size from 16,087 bp in *E. arcanum* to 20,456 bp in *C. fletcheri*. In the mitogenome of *A. feae*, an extra *trnV* gene and two control regions are found in addition to the standard set of 37 genes (13 PCGs, 22 tRNA genes and two rRNA genes) (Table 2). In the partial mitogenome of *D. flavicollis*, 10 and a partial fragment of PCGs, 18 tRNA genes, two rRNA genes, and a control region are annotated (Table 3). In *A. feae*, there are 56 overlapping nucleotides located in three pairs of neighboring genes, and the longest overlap is 41-bp long and located between *trnT* and *ND4L* (Table 2). A total of 296 intergenic nucleotides (IGNs) are dispersed in 19 locations for *A. feae*. In *D. flavicollis*, 17 overlapping nucleotides and 504 IGNs are found, including a 227-bp long IGN between *trnS2* (*UCN*) and *ND1* (Table 3).

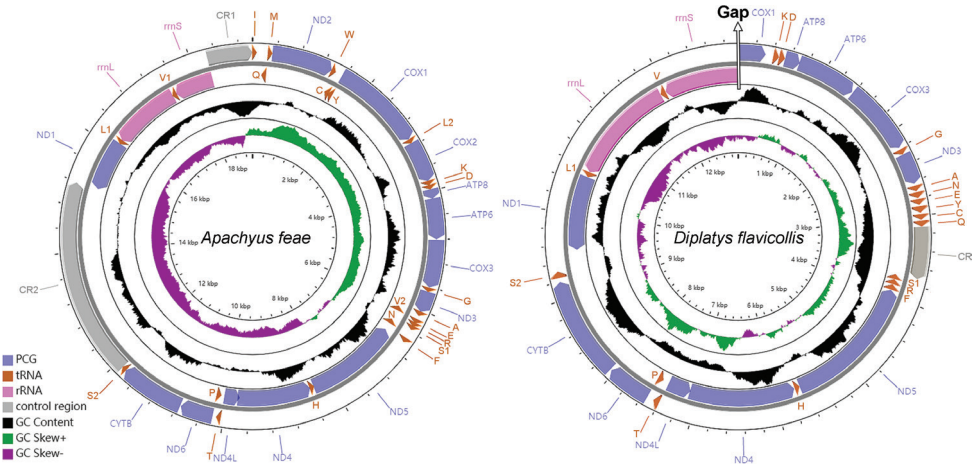

Figure 1. Mitochondrial maps of *Apachyus feae* and *Diplatys flavicollis*. Genes outside the map are transcribed clockwise, whereas those inside the map are transcribed counterclockwise. Names and other details of the genes are listed in Tables 2 and 3. The inside circles show the GC content and the GC skew. GC content and GC skew are plotted as the deviation from the average value of the entire sequence.

The mitogenomes of *A. feae* and *D. flavicollis* are biased toward A and T nucleotides (61.2% and 73.5%, respectively), which is consistent with other earwigs (Table 1). The A+T contents were also rich in each mitochondrial gene, showing the highest in *trnD* of *A. feae* and *trnF* of *D. flavicollis*.

Gene rearrangement

In the sequenced earwigs, no PCG rearrangement are found (Fig. 2). In *A. feae*, most tRNA genes in the gene cluster *trnA-R-N-S1-E-F* are rearranged, and an extra *trnV* is present in the gene cluster. In *D. flavicollis*, the gene cluster *trnA-R-N-S1-E-F* is also rearranged and incorporates *trnY*, *trnC* and *trnQ* from other locations. In *C. fletcheri*, *trnI*, *trnC*, *trnY*, *trnQ*, and *trnE* are rearranged (Wan et al. 2012). In *E. arcanum*, *trnQ*, *trnC*, *trnY*, *trnR*, and *trnS1* are rearranged, and *trnY* is lost. In *E. metallica* and *P. flavocapitatus*, both *trnR* and *trnS1* are absent. These tRNA rearrangements mainly occur in the *trnA-R-N-S1-E-F* gene cluster. The two rRNA genes are located in the same location for all sequenced earwigs; however, they are variable in size interspecifically. In addition to the tRNA rearrangements, the control region of *D. flavicollis* transfers to the new location between *ND3* and *ND5*; an extra control region is also found in *A. feae* and *C. fletcheri* (Wan et al. 2012).

Protein-coding genes (PCGs)

All PCGs of *A. feae* are annotated, whereas *ND2*, *COX2*, and partial *COX1* of *D. flavicollis* are not sequenced. The PCGs of *A. feae* are similar in size to those of *D. flavicollis* and other earwigs. Most PCGs of *A. feae* and all PCGs of *D. flavicollis* utilize the

Table 2. Mitochondrial genome structure of *Apachyus feae*.

Gene	Position (bp)	Size (bp)	Direction	Intergenic nucleotides	Anti- or start/stop codons	A+T%
trnIle (*I*)	1–62	62	Forward	0	GAT	64.5
trnGln (*Q*)	171–240	70	Reverse	108	TTG	65.7
trnMet (*M*)	257–326	70	Forward	16	CAT	61.4
ND2	328–1347	1020	Forward	1	ATT/TAA	62.3
trnTrp (W)	1350–1415	66	Forward	2	TCA	63.6
trnCys (*C*)	1408–1474	67	Reverse	–8	GCA	62.7
trnTyr (*Y*)	1476–1539	64	Reverse	1	GTA	67.2
COX1	1540–3075	1536	Forward	0	ATG/TAG	58.1
trnL2 (*UUR*)	3081–3147	67	Forward	5	TAA	62.7
COX2	3148–3831	684	Forward	0	ATG/TAG	58.0
trnLys (*K*)	3832–3901	70	Forward	0	CTT	61.4
trnAsp (*D*)	3903–3971	69	Forward	1	GTC	79.7
ATP8	3972–4133	162	Forward	0	GTG/TAG	57.4
ATP6	4127–4807	681	Forward	–7	ATG/TAG	58.1
COX3	4813–5607	795	Forward	5	TTG/TAA	56.7
trnGly (*G*)	5620–5680	61	Forward	12	TCC	78.7
ND3	5681–6034	354	Forward	0	ATG/TAG	56.8
trnAla (*A*)	6036–6099	64	Forward	1	TGC	45.3
trnVal2 (*GUU*)	6109–6168	60	Reverse	9	AAC	60.0
trnGlu (*E*)	6177–6238	62	Forward	8	TTC	74.2
trnArg (*R*)	6241–6301	61	Forward	2	TCG	68.9
trnSer1 (*AGN*)	6303–6363	61	Forward	1	GCT	70.5
trnAsn (*N*)	6385–6448	64	Reverse	21	GTT	58.5
trnPhe (*F*)	6533–6598	66	Forward	84	GAA	77.3
ND5	6599–8347	1749	Reverse	0	ATG/TAA	57.5
trnHis (*H*)	8348–8414	67	Reverse	0	GTG	61.2
ND4	8415–9795	1381	Reverse	0	ATG/T–	59.9
ND4L	9755–10045	291	Reverse	–41	ATG/TAA	60.8
trnThr (*T*)	10,053–10,115	63	Forward	7	TGT	73.0
trnPro (*P*)	10,116–10,179	64	Reverse	0	TGG	64.1
ND6	10,182–10,730	549	Forward	2	ATT/TAA	62.8
CYTB	10,741–11,818	1078	Forward	10	ATT/T–	58.2
trnSer2 (*UCN*)	11,819–11,887	69	Forward	0	TGA	73.9
CR2	11,888–15,172	3285	Forward	0	—	59.5
ND1	15,173–16,120	948	Reverse	0	ATG/TAG	62.3
trnLeu1 (*CUN*)	16,121–16,187	67	Reverse	0	TAG	70.1
rrnL	16,188–17,467	1280	Reverse	0	—	67.9
trnV1 (*GUA*)	17,468–17,534	67	Reverse	0	TAC	67.2
rrnS	17,535–18,273	739	Reverse	0	—	66.0
CR1	18,274–19,029	756	Forward	0	—	74.2

standard ATN start codon (ATT, ATC, and ATG), whereas *ATP8* and *COX3* of *A. feae* start with special start codons (GTG and TTG, respectively) (Tables 2, 3). Most PCGs of *A. feae* and all PCGs of *D. flavicollis* have the complete termination codon TAN (TAA or TAG), whereas *ND4* and *CYTB* of *A. feae* end with an incomplete stop codon

Table 3. Mitochondrial genome structure of *Diplatys flavicollis*.

Gene	Position (bp)	Size (bp)	Direction	Intergenic nucleotides	Anti- or start/stop codons	A+T%
COX1 (*partial*)	1–310	310	Forward	0	?/TAA	64.5
trnLys (*K*)	398–463	66	Forward	87	CTT	68.2
trnAsp (*D*)	464–532	69	Forward	0	GTC	87.0
ATP8	533–706	174	Forward	0	ATT/TAG	75.9
ATP6	700–1377	678	Forward	–7	ATG/TAA	72.5
COX3	1388–2200	813	Forward	10	ATT/TAA	68.5
trnGly (*G*)	2222–2286	65	Forward	21	TCC	75.4
ND3	2287–2637	351	Forward	0	ATT/TAA	74.3
trnAla (*A*)	2660–2724	65	Forward	22	TGC	77.6
trnAsn (*N*)	2736–2803	68	Forward	11	GTT	78.5
trnGlu (*E*)	2815–2879	65	Forward	11	TTC	77.5
trnTyr (*Y*)	2895–2969	75	Forward	15	GTA	80.0
trnCys (*C*)	2985–3051	67	Forward	15	GCA	79.7
trnGln (*Q*)	3059–3127	69	Forward	7	TTG	76.8
CR	3128–3719	592	Forward	0	—	82.6
trnSer1 (*AGN*)	3720–3784	65	Reverse	0	GCT	69.2
trnArg (*R*)	3785–3852	68	Reverse	0	TCG	78.3
trnPhe (*F*)	3854–3925	72	Reverse	1	GAA	90.5
ND5	3928–5673	1746	Reverse	2	ATC/TAA	71.5
trnHis (*H*)	5674–5739	66	Reverse	0	GTG	83.6
ND4	5747–7099	1353	Reverse	7	ATC/TAA	72.0
ND4L	7090–7386	297	Reverse	–10	ATT/TAA	74.3
trnThr (*T*)	7394–7464	71	Forward	7	TGT	74.6
trnPro (*P*)	7465–7537	73	Reverse	0	TGG	80.0
ND6	7540–8043	504	Forward	2	ATT/TAG	76.4
CYTB	8056–9198	1143	Forward	12	ATG/TAG	69.8
trnSer2 (*UCN*)	9246–9318	73	Forward	47	TGA	77.0
ND1	9546–10487	942	Reverse	227	ATT/TAA	69.9
trnLeu1 (*CUN*)	10,488–10,554	67	Reverse	0	TAG	79.1
rrnL	10,555–11,918	1364	Reverse	0	—	76.1
trnVal (*V*)	11,919–11,990	72	Reverse	0	TAC	72.2
rrnS	11,991–12,950	960	Reverse	0	—	76.9

T (Tables 2, 3). The relative synonymous codon usage (RSCU) values were calculated for the six earwig mitogenomes (Fig. 3). The most frequently used codon is TCT (Ser) for *A. feae*, TTG (Leu) for *E. metallica*, TTA (Leu) for *D. flavicollis*, *C. fletcheri*, *E. arcanum*, and *P. flavocapitatus*.

The ratio of Ka/Ks was calculated for each PCG of the six earwig mitogenomes to evaluate the evolutionary rates of the PCGs (Fig. 4). The results showed that *COX1* of *E. metallica* has the highest evolutionary rate, followed by *ND5* of *A. feae* and *ND2* of *P. flavocapitatus*, whereas *COX1* of *A. feae* and *E. arcanum* appear to be the lowest. The genes with ratios of Ka/Ks above 1 are evolving under positive selection. Other genes with ratios of Ka/Ks below 1 are expected to evolve under purifying selection.

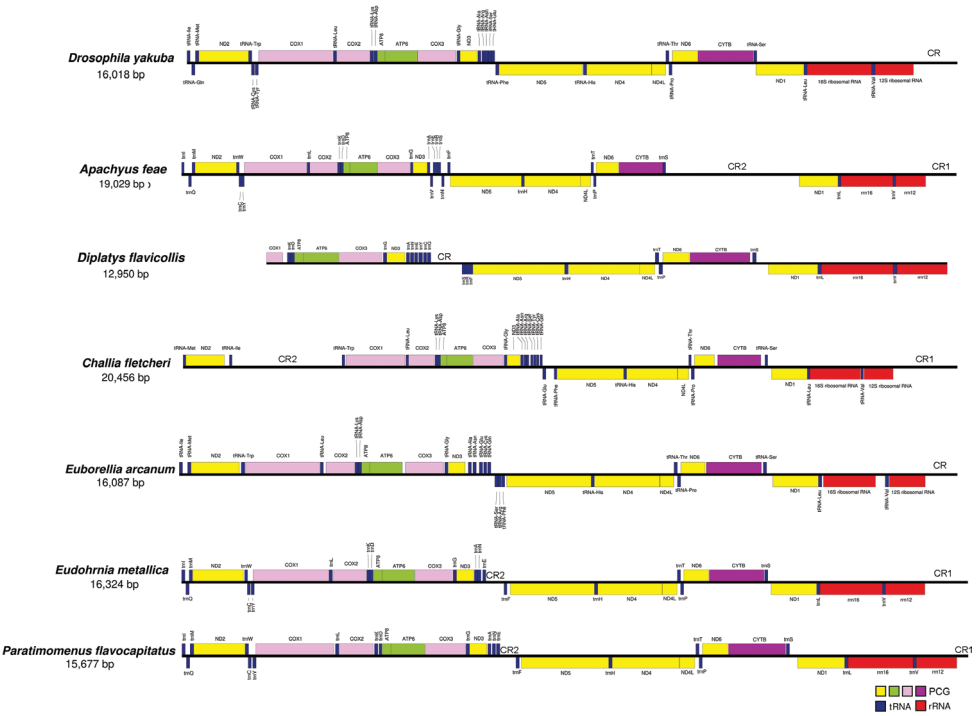

Figure 2. Mitochondrial gene arrangement of six earwigs in comparison with *Drosophila yakuba*.

Transfer RNA (tRNA) genes

The typical set of 22 tRNA genes and an extra *trnV* gene are detected in the mitogenome of *A. feae* (Fig. 5). In *D. flavicollis*, 18 tRNA genes are recognized and the four tRNA genes *trnI*, *trnM*, *trnW*, *trnL* are absent due to the incomplete sequencing of 5′ end (Fig. 6). In other sequenced earwigs, *C. fletcheri* has all 22 tRNA genes (Wan et al. 2012), *E. arcanum* lacks *trnY*, and *E. metallica* and *P. flavocapitatus* lack *trnR* and *trnS1*. Individual tRNA gene of the two newly sequenced mitogenomes range in size from 60 to 75 bp; the longest tRNA gene is *trnY* in *D. flavicollis*, and the shortest tRNA gene is the extra *trnV* in *A. feae*. In the mitogenomes of *A. feae* and *D. flavicollis*, most of the tRNA genes exhibit cloverleaf secondary structures, but the dihydrouridine (DHU) arm is lost for the extra *trnV* of *A. feae* and is reduced for *trnS1* of both species. The anticodons of the tRNA genes were identical among the earwigs. In the tRNA genes of *A. feae* and *D. flavicollis*, a total of 48 and 25 mismatched base pairs are respectively recognized and all of them are G-U pairs.

Ribosomal RNA (rRNA) genes

Two rRNA genes are consistently found in all sequenced mitogenomes. Locations of the two rRNA genes are conserved among earwig species and similar to *D. yakuba*, but

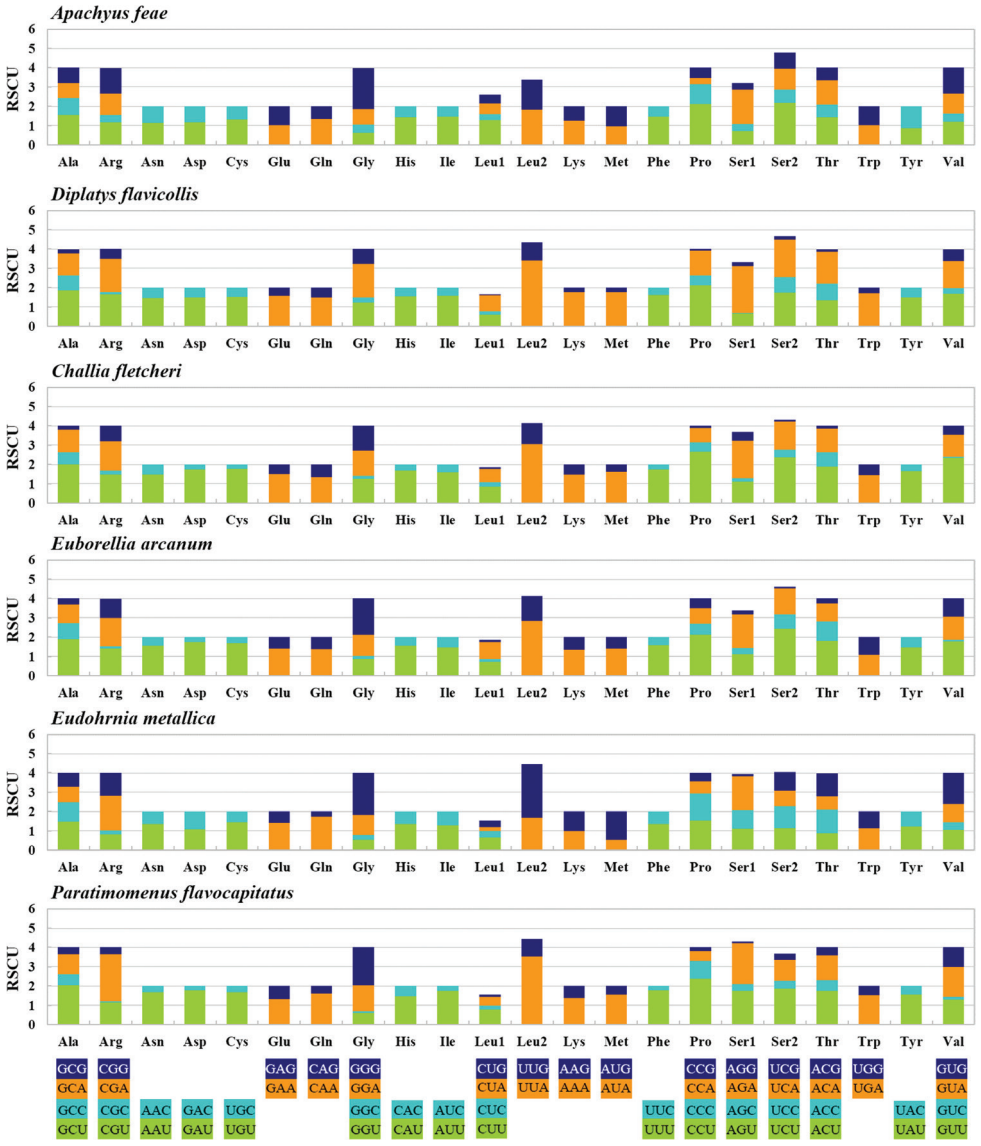

Figure 3. Relative synonymous codon usage (RSCU) of PCGs in six species of earwigs.

the lengths are variable. In *A. feae*, the large ribosomal RNA (*rrnL*) gene is 1280 bp in length with an A+T content of 67.9%; the small ribosomal RNA (*rrnS*) gene is 739 bp with an A+T content of 66.0%. In *D. flavicollis*, the *rrnL* gene is 1364 bp with an A+T content of 76.1%; the *rrnS* gene is 960 bp with an A+T content of 76.9%.

Control region

Two putative control regions (CRs) are found in the mitogenomes of *A. feae*, *E. metallica* and *P. flavocapitatus*. The CR1 of *A. feae* is 756 bp and located after *rrnS*, containing a

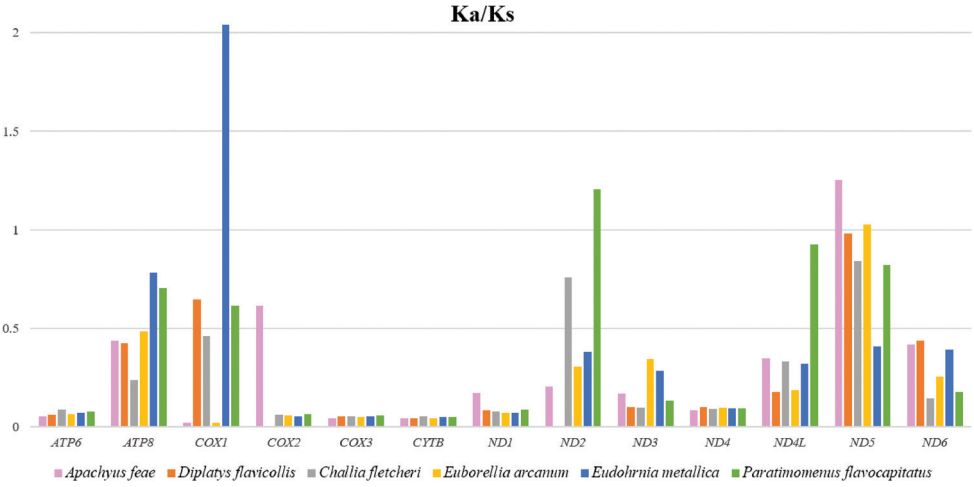

Figure 4. Evolutionary rates of PCGs in six species of earwigs. The bar indicates each gene's Ka/Ks value.

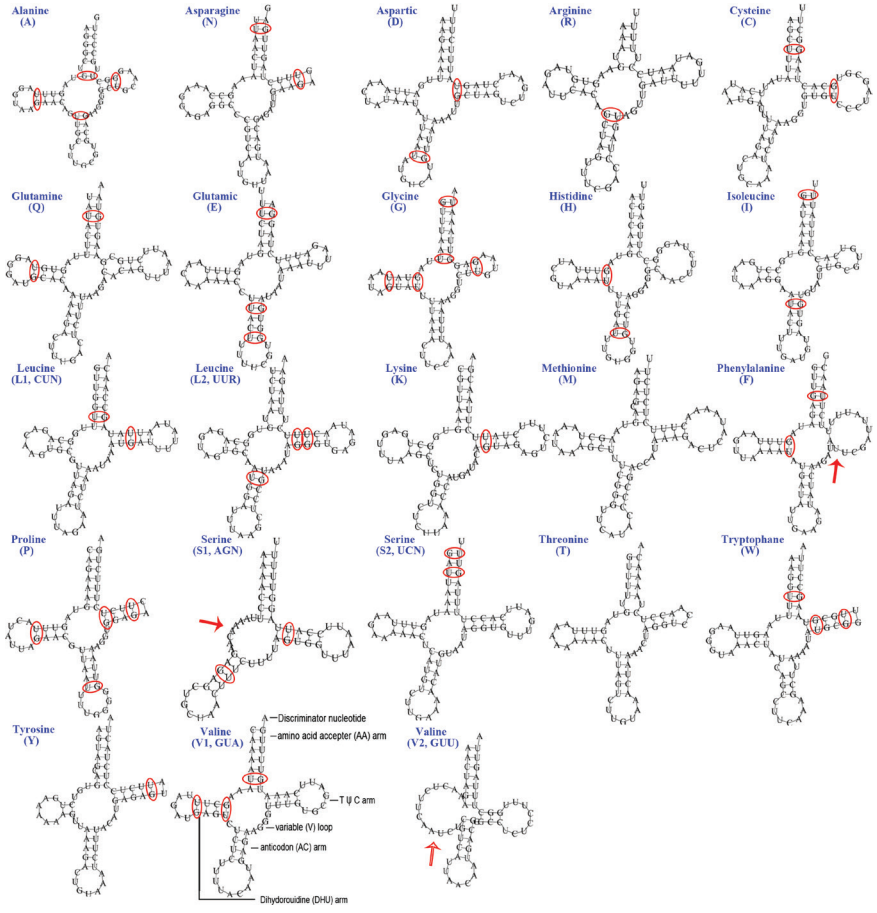

Figure 5. Secondary structures of tRNA genes in the mitogenome of *Apachyus feae*. Mismatched base pairs are indicated by red circles; reduced arms are indicated by red arrowheads.

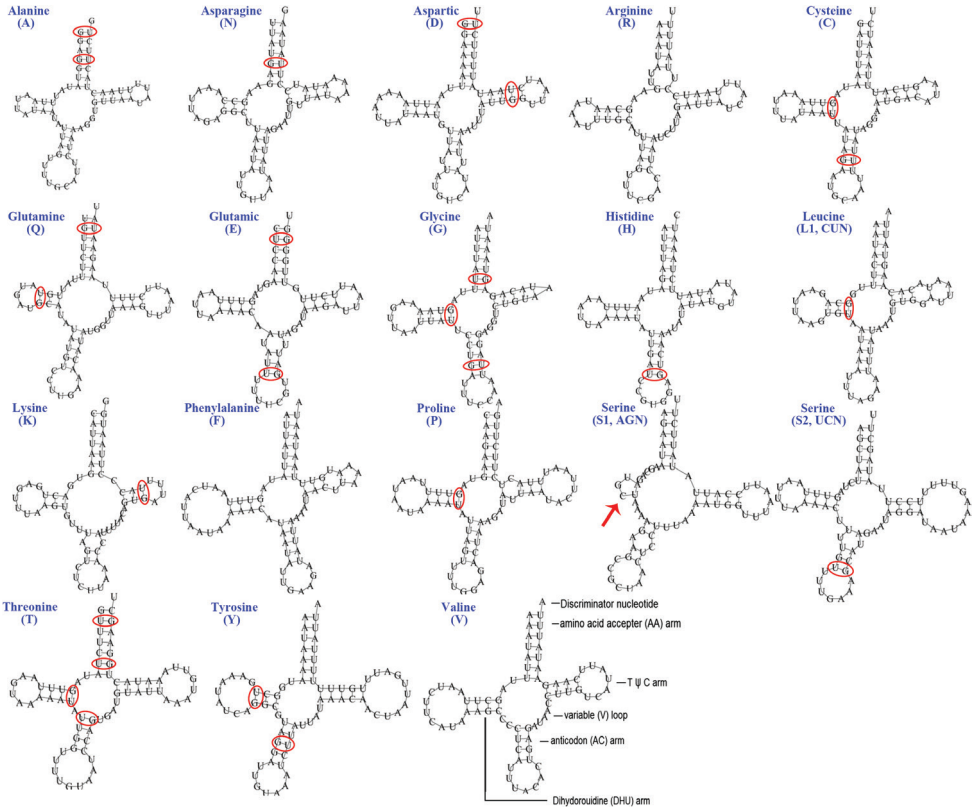

Figure 6. Secondary structures of tRNA genes in the mitogenome of *Diplatys flavicollis.* Mismatched base pairs are indicated by red circles; reduced arms are indicated by red arrowheads.

stem-loop (SL) structure and a poly-[TA]n like stretch (Fig. 7). The CR2 of *A. feae* is 3285-bp long and located between *trnS2* (*UCN*) and *ND1*, being composed of five SL structures and three copies of tandem repeats. The CR of *D. flavicollis* is 592 bp and located between *trnQ* and *trnS1*, comprising two and partial copies of tandem repeats, two tRNA-like structures, and a poly-[T]n stretch (Fig. 8). In *C. fletcheri*, the 1816-bp long CR1 contains a SL structure and two regions of tandem repeats; the entire 2856-bp long CR2 comprises 21.1 copies of tandem repeats (Fig. 9). The CR of *E. arcanum* is 686 bp in size, containing a SL structure, a poly-[TA]n stretch and a tandem repeats region (Fig. 9). The 891-bp long CR of *E. metallica* comprises four SL structures (Fig. 9). The CR of *P. flavocapitatus* is short, 227-bp in size, and contains one SL structure (Fig. 9).

Phylogenetic analyses

The phylogenetic analyses use the nucleotide sequences of six available earwig mitogenomes to investigate the mitochondrial phylogenetic relationships within Dermaptera. The two phylogenetic trees using BI and ML analyses generated identical topological structures for Dermaptera (Fig. 10). The monophyly of Forficulidae is

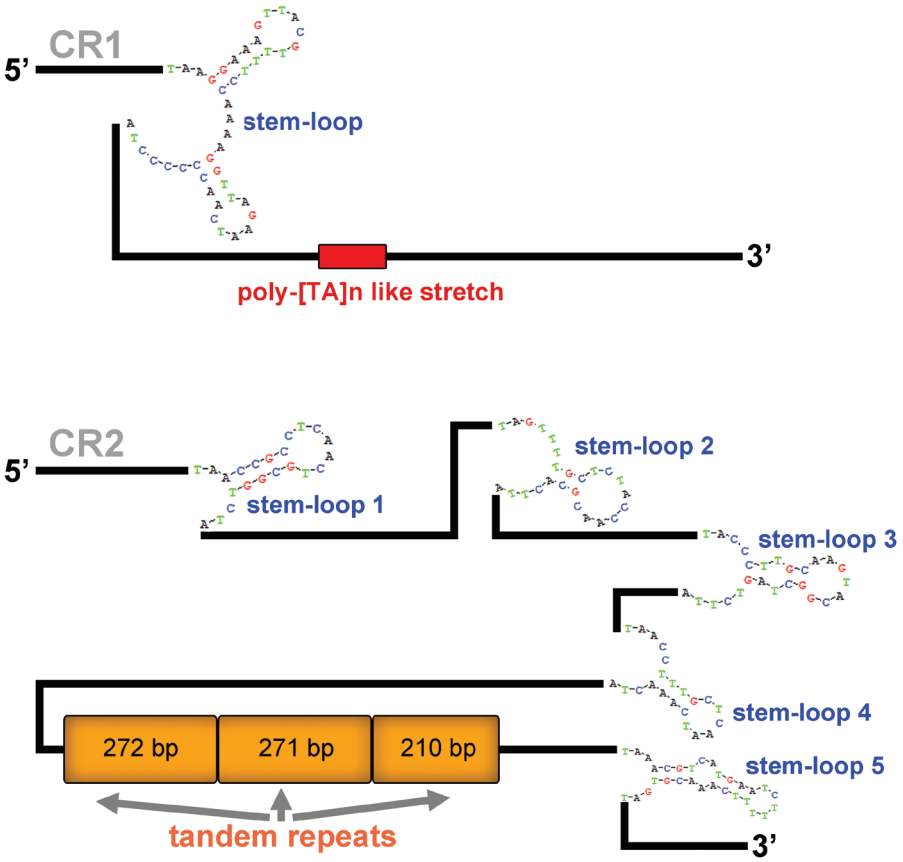

Figure 7. Predicted structural elements in the control regions of *Apachyus feae*.

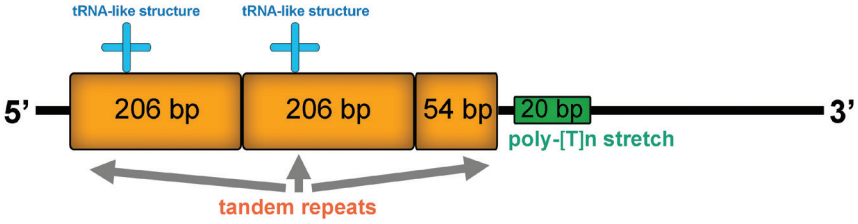

Figure 8. Predicted structural elements in the control region of *Diplatys flavicollis*.

supported with high values. Diplatyidae is recovered as the sister group of Anisolabididae and their combined clade is grouped with Pygidicranidae. Apachyidae is supported as the sister group to other sequenced families. Monophyly of the two infraorders Protodermaptera and Epidermaptera cannot be supported by either analysis. The three parvorders Paradermaptera, Metadermaptera, and Eteodermaptera are each represented by single family and their relationship was recovered as Paradermaptera + (Eteodermaptera + Metadermaptera).

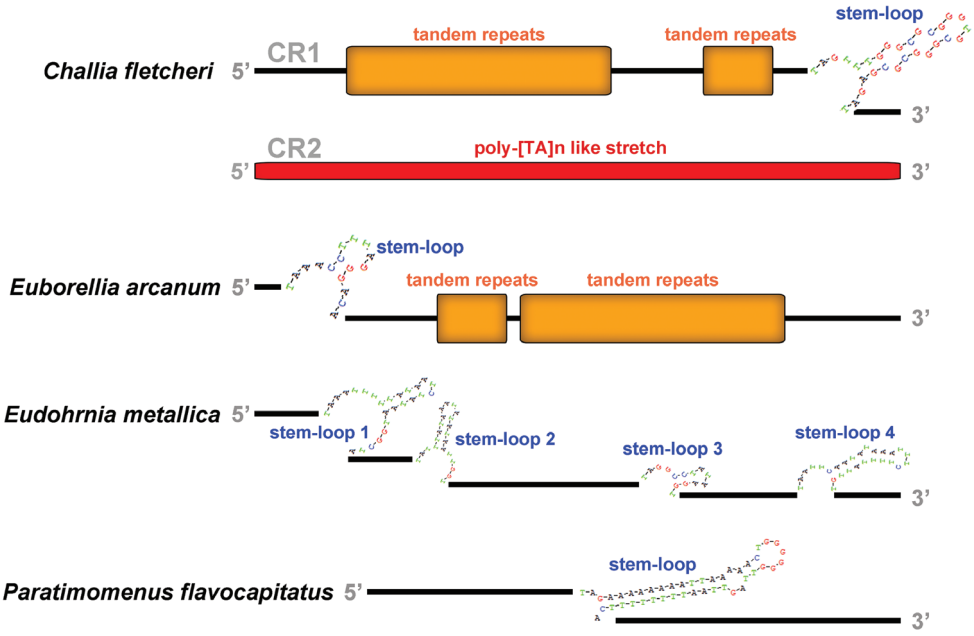

Figure 9. Predicted structural elements in the control regions of *Challia fletcheri*, *Euborellia arcanum*, *Eudohrnia metallica*, and *Paratimomenus flavocapitatus*.

Discussion

This study sequenced and comparatively analyzed two earwig mitogenomes with other available public data. The mitogenomes of *A. feae* and *D. flavicollis* were slightly smaller in size than that of *C. fletcheri* (20,456 bp) (Wan et al. 2012). Unlike most other insects (Wei et al. 2010), the *A. feae* mitogenome has both negative AT-skew and GC-skew values as in *E. metallica* and *P. flavocapitatus*, whereas *D. flavicollis* exhibits negative AT-skew and positive GC-skew values as in *C. fletcheri* (Wan et al. 2012) and *E. arcanum*. The number of mitochondrial genes and control regions were variable in Dermaptera, either with the addition or loss of several tRNA genes. In other four completely or partially sequenced mitogenomes of Dermaptera, the presence of typical 37 genes and two elongated control regions is found in *C. fletcheri* (Wan et al. 2012), the lack of *trnY* is found in *E. arcanum*, and the absence of *trnR* and *trnS1* (*AGN*) occurs in both *E. metallica* and *P. flavocapitatus*. The presence of an elongated control region or an extra control region is temporarily considered a common phenomenon in earwig mitogenomes. The elongated non-coding regions in Dermaptera (as found in *A. feae* and *C. fletcheri*) could contribute to the frequently large mitogenomic size (Wan et al. 2012), which is also common in other insect orders, such as in Plecoptera (Chen and Du 2017). Multiple IGNs were present in all available mitogenomes of Dermaptera, indicating a loose mitogenomic structure for the earwigs. No PCG rearrangements were found in all sequenced earwigs (Fig. 2). The PCGs and rRNA genes of Dermaptera seemed

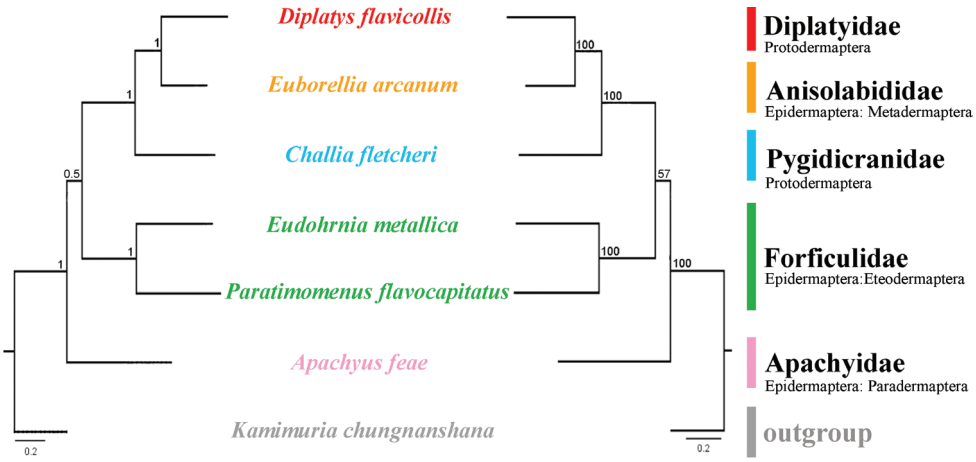

Figure 10. Phylogenetic relationships within Dermaptera inferred by Bayesian inference and maximum likelihood analysis. Numbers at the nodes are posterior probabilities (left) and bootstrap values (right). The family names are listed after the species. Infraorders and parvorders are indicated below each family name.

conserved in arrangements, but this should be confirmed by more mitogenomic data. Rearrangement of tRNA genes were detected in all sequenced earwig species (Fig. 2). The rearrangements concerning tRNA genes occur very frequently in the sequenced earwigs and mainly focus on the *trnA-R-N-S1-E-F* gene cluster, which is similar to the arrangement in Lepidoptera (Cao et al. 2012; Gong et al. 2012; Wang et al. 2014; Park et al. 2016). Extensive mitochondrial rearrangement events are expected to occur in other unsequenced earwigs.

The Ka/Ks calculation revealed the fast-evolving *COX1* and slow-evolving *CYTB* in earwigs. The fast-evolving genes are potential candidates as molecular markers for future genetic studies of Dermaptera. Among the very few molecular studies of Dermaptera, Naegle et al. (2016), Stuart et al. (2019), and Kirstová et al. (2020) supported the efficiency of *COX1* gene in species delimitation and phylogenetic reconstruction. In tRNA genes, reductions of *trnS1* DHU arms was very common in other metazoans (Garey and Wolstenholme 1989). The shortened DHU arm of *trnS1* found in *A. feae* and *D. flavicollis* was also found in *C. fletcheri* but absent in other earwigs (Wan et al. 2012).

The control regions of Dermaptera were highly variable in size, location, and secondary structures. The putative structural elements in the CRs included SL structure, poly-[TA]n like stretch, tandem repeats, tRNA-like structure and poly-[T]n stretch, and they were highly variable in both size and numbers, which implied that the earwig mitogenomes are likely to be regulated in apparent different ways during the mitogenomic replication and transcription processes.

In the phylogenetic analyses, the monophyly of Forficulidae was supported with high values The basal phylogenetic position of Apachyidae was also recovered based on nuclear single-copy genes (Wipfler et al. 2020). However, the current relationship between the five earwig families is entirely incongruent with all previous phylogenetic

studies using either morphological data, other types of molecular markers, or combined data (Haas 1995; Guillet and Vancassel 2001; Haas and Kukalova-Peck 2001; Colgan et al. 2003; Jarvis et al. 2005; Kocarek et al. 2013; Naegle et al. 2016; Wipfler et al. 2020). The preliminary phylogenetic analyses in current study included very few representatives from only five earwig families and thus insufficient for comparison with previous studies. The currently available mitogenomic data could not resolve the relationship within Dermaptera. More comprehensive sampling and sequencing work are necessary to clarify the mitogenomic features and mitogenomic phylogeny of Dermaptera.

Conclusions

The mitochondrial genomes of *A. feae* and *D. flavicollis* were sequenced, analyzed, and compared with other sequenced earwigs. The phylogenetic reconstructions with BI and ML methods generated identical topology but differed from previous phylogenetic studies using morphological data or other molecular markers. Due to the limited sample size, the relationships found here must be treated with caution. More mitogenomes should be obtained in future works to resolve the phylogeny of earwigs.

Acknowledgements

This work was supported by the Natural Science Foundation of Jiangsu Province (grant no. BK20201009) and the Start-up Funding of Jiangsu University of Science and Technology (grant no. 1182931901). The author thanks the editor and reviewers for valuable comments and manuscript improvement.

References

Bormans ADE (1894) Viaggio di Leonardo Fea in Birmaniae regioni vicne. LXI. Dermapters (2nd Partie). Annali di Museo Civico di Storia Naturale di Giacomo Doria 14(2): 371–409.

Burr M (1904) Observations on the Dermatoptera, including revisions of several genera, and descriptions of new genera and species. Transactions of the American Entomological Society 52(2): 277–322. https://doi.org/10.1111/j.1365-2311.1904.tb02747.x

Bernt M, Donath A, Jühling F, Externbrink F, Florentz C, Fritzsch G, Pütz J, Middendorf M, Stadler PF (2013) MITOS: improved de novo metazoan mitochondrial genome annotation. Molecular Phylogenetics and Evolution 69(2): 313–319. https://doi.org/10.1016/j.ympev.2012.08.023

Beutel R, Wipfler B, Gottardo M, Dallai R (2013) Polyneoptera or "Lower Neoptera"-New light on old and difficult phylogenetic problems. Atti Accademia Nazionale Italiana di Entomologia 61: 113–142.

Colgan DJ, Cassis G, Beacham E (2003) Setting the molecular phylogenetic framework for the Dermaptera. Insect Systematics and Evolution 34(1): 65–79. https://doi.org/10.1163/187631203788964935

Clary DO, Wolstenholme DR (1985) The ribosomal RNA genes of *Drosophila* mitochondrial DNA. Nucleic Acids Research 13: 4029–4045. https://doi.org/10.1093/nar/13.11.4029

Cao YQ, Ma C, Chen JY, Yang DR (2012) The complete mitochondrial genomes of two ghost moths, *Thitarodes renzhiensis* and *Thitarodes yunnanensis*: the ancestral gene arrangement in Lepidoptera. BMC Genomics 13(1): 1–13. https://doi.org/10.1186/1471-2164-13-276

Chen ZT, Du YZ (2017) First mitochondrial genome from Nemouridae (Plecoptera) reveals novel features of the elongated control region and phylogenetic implications. International Journal of Molecular Sciences 18(5): e996. https://doi.org/10.3390/ijms18050996

Engel MS, Haas F (2007) Family-group names for earwigs (Dermaptera). American Museum Novitates 3567: 1–20. https://doi.org/10.1206/0003-0082(2007)539[1:FNFED]2.0.CO;2

Grant JR, Stothard P (2008) The CGView server: a comparative genomics tool for circular genomes. Nucleic Acids Research 36: 181–184. https://doi.org/10.1093/nar/gkn179

Garey JR, Wolstenholme DR (1989) Platyhelminth mitochondrial DNA: evidence for early evolutionary origin of a tRNAserAGN that contains a dihydrouridine arm replacement loop, and of serine-specifying AGA and AGG codons. Journal of Molecular Evolution 28: 374–387. https://doi.org/10.1007/BF02603072

Gullan PJ, Cranston PS (2010) The Insect: an Outline of Entomology, 4th edn. John Wiley & Sons, Oxford, 565 pp.

Guillet S, Vancassel M (2001) Dermapteran life-history evolution and phylogeny with special reference to the Forficulidae family. Evolutionary Ecology Research 3: 477–486.

Gong YJ, Shi BC, Kang ZJ, Zhang F, Wei SJ (2012) The complete mitochondrial genome of the oriental fruit moth *Grapholita molesta* (Busck) (Lepidoptera: Tortricidae). Molecular Biology Reports 39(3): 2893–2900. https://doi.org/10.1007/s11033-011-1049-y

Haas F (1995) The phylogeny of the Forficulina, a suborder of the Dermaptera. Systematic Entomology 20: 85–98. https://doi.org/10.1111/j.1365-3113.1995.tb00085.x

Haas F (2018) Biodiversity of Dermaptera. Insect Biodiversity: Science and Society 2: 315–334. https://doi.org/10.1002/9781118945582.ch12

Haas F, Gorb SN (2004) Evolution of locomotory attachment pads in the Dermaptera (Insecta). Arthropod Structure and Development 33: 45–66. https://doi.org/10.1016/j.asd.2003.11.003

Haas F, Gorb SN, Wootton RJ (2000) Elastic joints in dermapteran hind wings: materials and wing folding. Arthropod Structure and Development 29: 137–146. https://doi.org/10.1016/S1467-8039(00)00025-6

Haas F, Kukalová-Peck J (2001) Dermaptera hindwing structure and folding: new evidence for familial, ordinal and superordinal relationships within Neoptera (Insecta). European Journal of Entomology 98: 445–510. https://doi.org/10.14411/eje.2001.065

Jarvis KJ, Haas F, Whiting MF (2005) Phylogeny of earwigs (Insecta: Dermaptera) based on molecular and morphological evidence: reconsidering the classification of Dermaptera. Systematic Entomology 30(3): 442–453. https://doi.org/10.1111/j.1365-3113.2004.00276.x

Katoh K, Standley DM (2013) MAFFT multiple sequence alignment software version 7: improvements in performance and usability. Molecular Biology and Evolution 30: 772–780. https://doi.org/10.1093/molbev/mst010

Klass KD (2001) The female abdomen of the viviparous earwig *Hemimerus vosseleri* (Insecta: Dermaptera: Hemimeridae), with a discussion of the postgenital abdomen of Insecta. Zoological Journal of the Linnean Society 131: 251–307. https://doi.org/10.1111/j.1096-3642.2001.tb02239.x

Kirstová M, Kundrata R, Kočárek P (2020) Molecular phylogeny and classification of *Chelidurella* Verhoeff, stat. restit. (Dermaptera: Forficulidae). Insect Systematics and Evolution 52(3): 335–371. https://doi.org/10.1163/1876312X-bja10004

Kocarek P, John V, Hulva P (2013) When the body hides the ancestry: phylogeny of morphologically modified epizoic earwigs based on molecular evidence. PLoS ONE 8: e66900. https://doi.org/10.1371/journal.pone.0066900

Laslett D, Canbäck B (2008) ARWEN, a program to detect tRNA genes in metazoan mitochondrial nucleotide sequences. Bioinformatics 24: 172–175. https://doi.org/10.1093/bioinformatics/btm573

Librado P, Rozas J (2009) DnaSP v5: a software for comprehensive analysis of DNA polymorphism data. Bioinformatics 25: 1451–1452. https://doi.org/10.1093/bioinformatics/btp187

Lanfear R, Frandsen PB, Wright AM, Senfeld T, Calcott B (2016) PartitionFinder 2: new methods for selecting partitioned models of evolution for molecular and morphological phylogenetic analyses. Molecular Biology and Evolution 34: 772–773. https://doi.org/10.1093/molbev/msw260

Luo RB, Liu BH, Xie YL, Li Z, Huang W, Yuan J, He G, Chen Y, Pan Q, Liu Y, Tang J, Wu G, Zhang H, Shi Y, Liu Y, Yu C, Wang B, Lu Y, Han C, Cheung DW, Yiu SM, Peng S, Zhu XQ, Liu G, Liao X, Li Y, Yang H, Wang J, Lam TW, Wang J (2012) SOAPdenovo2: an empirically improved memory-efficient short-read de novo assembler. GigaScience 1: 1–18. https://doi.org/10.1186/2047-217X-1-18

Matzke D, Kocarek P (2015) Description and biology of *Euborellia arcanum* sp. nov., an alien earwig occupying greenhouses in Germany and Austria (Dermaptera: Anisolabididae). Zootaxa 3956(1): 131–139. https://doi.org/10.11646/zootaxa.3956.1.8

Naegle MA, Mugleston JD, Bybee SM, Whiting MF (2016) Reassessing the phylogenetic position of the epizoic earwigs (Insecta: Dermaptera). Molecular Phylogenetics and Evolution 100: 382–390. https://doi.org/10.1016/j.ympev.2016.03.012

Nakata S, Maa TC (1974) A review of the parasitic earwigs (Dermaptera: Arixeniina; Hemimerina). Pacific Insects 16: 307–374.

Popham EJ (1985) The mutual affinities of the major earwig taxa (Insecta, Dermaptera). Zeitschrift fur Zoologische Systematik und Evolutionforschung 23: 199–214. https://doi.org/10.1111/j.1439-0469.1985.tb00583.x

Park JS, Kim MJ, Jeong SY, Kim SS, Kim I (2016) Complete mitochondrial genomes of two gelechioids, *Mesophleps albilinella* and *Dichomeris ustalella* (Lepidoptera: Gelechiidae), with a description of gene rearrangement in Lepidoptera. Current Genetics 62(4): 809–826. https://doi.org/10.1007/s00294-016-0585-3

Perna NT, Kocher TD (1995) Patterns of nucleotide composition at fourfold degenerate sites of animal mitochondrial genomes. Journal of Molecular Evolution 41: 353–358. https://doi.org/10.1007/BF01215182

Ronquist F, Huelsenbeck JP (2003) MrBayes 3: Bayesian phylogenetic inference under mixed models. Bioinformatics 19: 1572–1574. https://doi.org/10.1093/bioinformatics/btg180

Stamatakis A (2014) RAxML version 8: a tool for phylogenetic analysis and postanalysis of large phylogenies. Bioinformatics 30: 1312–1313. https://doi.org/10.1093/bioinformatics/btu033

Staerkle M, Koelliker M (2008) Maternal food regurgitation to nymphs in earwigs (*Forficula auricularia*). Ethology 114(9): 844–850. https://doi.org/10.1111/j.1439-0310.2008.01526.x

Stuart OP, Binns M, Umina PA, Holloway J, Severtson D, Nash M, Heddle T, van Helden M, Hoffmann AA (2019) Morphological and molecular analysis of Australian earwigs (Dermaptera) points to unique species and regional endemism in the Anisolabididae family. Insects 10(3): e72. https://doi.org/10.3390/insects10030072

Suzuki S, Kitamura M, Matsubayashi K (2005) Matriphagy in the hump earwig, *Anechura harmandi* (Dermaptera: Forficulidae), increases the survival rates of the offspring. Journal of Ethology 23(2): 211–213. https://doi.org/10.1007/s10164-005-0145-7

Shiraki T (1907) Neue Blattiden und Forficuliden Japans. Transactions of the Sapporo Natural History Society 2: 103–111.

Tamura K, Stecher G, Peterson D, Filipski A, Kumar S (2013) MEGA6: Molecular Evolutionary Genetics Analysis version 6.0. Molecular Biology and Evolution 30: 2725–2729. https://doi.org/10.1093/molbev/mst197

Wipfler B, Koehler W, Frandsen PB, Donath A, Liu S, Machida R, Misof B, Peters RS, Shimizu S, Zhou X, Simon, S (2020) Phylogenomics changes our understanding about earwig evolution. Systematic Entomology 45(3): 516–526. https://doi.org/10.1111/syen.12420

Wu CF (1938) The stoneflies of China (Order Plecoptera). Peking Natural History Bulletin 13(1): 53–87.

Wei SJ, Shi M, Chen XX, Sharkey MJ, van Achterberg C, Ye GY, He JH (2010) New views on strand asymmetry in insect mitochondrial genomes. PLoS ONE 5: e12708. https://doi.org/10.1371/journal.pone.0012708

Wang W, Meng ZQ, Shi FX, Li F (2013) Advances in comparative studies of Lepidoptera (Arthropoda: Insecta). Chinese Science Bulletin 30: 3017–3029.

Wan X, Kim MI, Kim MJ, Kim I (2012) Complete mitochondrial genome of the free-living earwig, *Challia fletcheri* (Dermaptera: Pygidicranidae) and phylogeny of Polyneoptera. PLoS ONE 7: e42056. https://doi.org/10.1371/journal.pone.0042056

ZooKeys 1087: 123–139 (2022)
doi: 10.3897/zookeys.1087.76668
https://zookeys.pensoft.net

RESEARCH ARTICLE

A peer-reviewed open-access journal
ZooKeys
Launched to accelerate biodiversity research

Redescription of *Tylos maindroni* Giordani Soika, 1954 (Crustacea, Isopoda, Oniscidea) based on SEM and molecular data

Valiallah Khalaji-Pirbalouty[1], Hamzeh Oraie[1], Carlos A. Santamaria[2], Johann Wolfgang Wägele[3]

1 *Department of Biology, Faculty of Basic Science, Shahrekord University, Shahrekord, Iran* **2** *Department of Biology, University of Tampa, 401 W Kennedy Blvd, Tampa, FL 33606, USA* **3** *Leibniz-Institut zur Analyse des Biodiversitätwandels, Museum Koenig, Adenauerallee 160, 53113 Bonn, Germany*

Corresponding author: Valiallah Khalaji-Pirbalouty (vkhalaji@sci.sku.ac.ir, khalajiv@yahoo.com)

Academic editor: Saskia Brix | Received 17 October 2021 | Accepted 26 January 2022 | Published 23 February 2022

http://zoobank.org/C09E59BC-55B2-4FAA-AD9A-7D05CA6F827F

Citation: Khalaji-Pirbalouty V, Oraie H, Santamaria CA, Wägele JW (2022) Redescription of *Tylos maindroni* Giordani Soika, 1954 (Crustacea, Isopoda, Oniscidea) based on SEM and molecular data. ZooKeys 1087: 123–139. https://doi.org/10.3897/zookeys.1087.76668

Abstract

The woodlouse species *Tylos maindroni* Giordani Soika, 1954 (Crustacea, Isopoda, Oniscidea) is redescribed from the Persian Gulf based on light and scanning electron microscopy. This species differs from the closely related *T. exiguus* Stebbing, 1910, from the Red Sea (coasts of Sudan and Eritrea), and Socotra Island, by pereopod 1 superior margin without a prominent projection and pleopod 2 endopod 2.3 times as long as exopod, vs. 3.6 in *T. exiguus*. A distribution map for *T. maindroni* is provided. In addition, we studied the molecular differentiation of five populations of *T. maindroni* from the Persian Gulf, based on partial *cytochrome c oxidas*e subunit I (*COI*) gene sequences. The results revealed low levels of population structuring between the analyzed populations.

Keywords

DNA barcoding, haplotype network, Isopoda, Persian Gulf, Redescription, SEM

Introduction

The isopod genus *Tylos* Audouin, 1826 has a worldwide distribution, with 21 species currently considered as valid (Boyko et al. 2008 onwards). Species in this genus are found in the marine sandy supralittoral zone, where animals can feed on algae and other organic material washed up on the beach by the waves (Kensley 1974). To avoid excessive predation by daytime predators (birds, crabs), feeding occurs at night (Schmalfuss and Vergara 2000). These animals are able to roll up into a perfect ball, with the antennae remaining inside the ball. Endoantennal conglobation can be also observed in Armadilliidae, Eubelidae, and Scleropactidae. Rolling up is not only a response to predators, but it can also help reduce water loss by about 35% (Schmalfuss and Vergara 2000; Sfenthourakis et al. 2020). According to Schmalfuss (2003), only two species of *Tylos* have been recorded from the northwestern areas of the Indian Ocean: *T. exiguus* Stebbing, 1910 from the Red Sea (coasts of Sudan and Eritrea) and the coasts of Socotra Island (Schmalfuss and Vergara 2000; Taiti and Ferrara 2004; Taiti and Checcucci 2010); and *T. maindroni* Giordani Soika, 1954 from the Gulf of Oman and the Persian Gulf. The original description of *T. maindroni* is brief and based on a single female from Muscat, Oman. Taiti and Ferrara (1991) later reported this species from Kuwait, Oman, and Iran (Busher coast), with illustrations of specimens from Kuwait. Recently, a molecular phylogenetic study including various species of the genus *Tylos* clearly revealed the existence of two distinct *Tylos* species along the coastal zones of the Arabian Peninsula (northwestern Indian Ocean): *T. maindroni* and *T. exiguus* (Hurtado et al. 2014).

Herein, we redescribe *T. maindroni* based on material from the Persian Gulf and provide new *COI* mtDNA sequence data.

Materials and methods

Morphological analyses

Specimens used in this study were collected from four coastal sites in the Persian Gulf, Iran during field expeditions from 2006 to 2021 (Fig. 1; Table 1). All specimens are held in the isopod collection of the Zoological Museum of Shahrekord University (**ZMSU**).

Specimens prepared for SEM were washed in a chilled 1% sodium acetate solution for 10 minutes, then cleaned for 10–20 seconds in an ultrasound cleaner in a weak solution of jewelry soap and distilled water to remove sediment and debris adhering to the cuticle. Specimens were dehydrated in an ethanol series (70, 75, 80, 85, 90, 95, 100%; 20 minutes per treatment). Specimens were transferred through ethanol and hexamethyldisilazane (**HMDS**) solutions (ethanol: HMDS ratios were 2:1, 1:1, 1:2) and finally into 100% HMDS (20 minutes per treatment). All samples were transferred to fresh HMDS, which evaporated overnight. Specimens were mounted on stubs using double adhesive carbon spots before being coated with gold in a

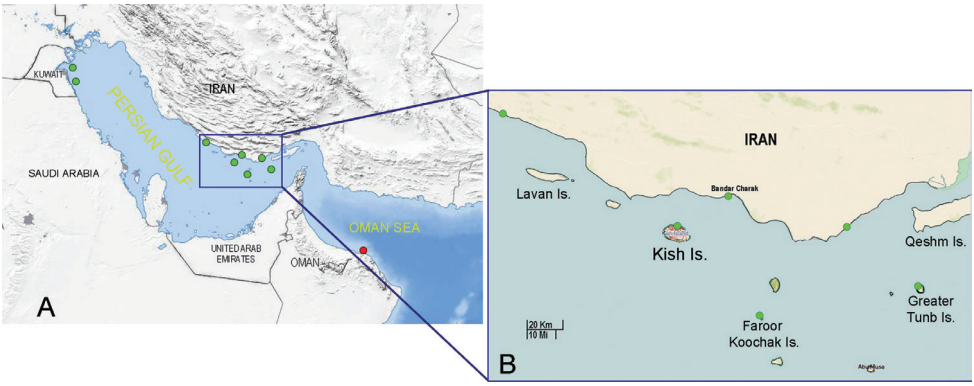

Figure 1. Map showing geographic distribution of *Tylos maindroni* Giordani Soika, 1954 **A** the Persian Gulf and Gulf of Oman **B** the Persian Gulf. Green circles = in the Persian Gulf, Red circle = type locality.

Table 1. Samples of the *Tylos maindroni* from the Persian Gulf used in this study.

Museum number	Voucher numbers	Coordinates	Collection date	Locality	GenBank Accession number COI
ZSMU 1206	1043	26°16'20.48"N, 55°17'28.00"E	03.01.2021	Greater Tunb Island	OK513061
ZSMU 1206	1044	26°16'20.48"N, 55°17'28.00"E	03.01.2021	Greater Tunb Island	OK513060
ZMSU 1205	1051	26°6'59.99"N, 54°26'10.88"E	30.12.2017	Faroor Koochak Island	OK513062
ZMSU 1201	1098	26°42'555"N, 54°14'329"E	05.12.2008	Bandar-e-Charak	OK513063
ZMSU 1201	C2	26°42'555"N, 54°14'329"E	05.12.2008	Bandar-e-Charak	OK513064
ZMSU 1202	B1	27°07'113"N, 53°01'418"E	30.01.2006	Banda-e Bostaneh	OK513065
ZMSU 1202	B2	27°07'113"N, 53°01'418"E	30.01.2006	Banda-e Bostaneh	OK513066

sputter coater to 40 nm thickness. Micrographs were taken using a Hitachi S-2460N SEM at Zoologisches Forschungsmuseum Alexander Koenig in Bonn, Germany. Color images were taken using a Zeiss AxioCam ERc5s camera mounted on a Zeiss Stereomicroscope (Stemi 508).

Molecular analyses

We extracted genomic DNA from the legs of seven specimens, 1–2 individuals per locality, using the Aron-Gene Tissue DNA Extraction kit (Aron-Gene, Iran) following the manufacturer's protocol. A 536 base pair fragment of the mitochondrial *Cytochrome Oxidase I* (COI) gene was PCR-amplified using the LCO-1490 and HCO-2198 primer pair under standard conditions (Folmer et al. 1994). The PCR solution consisted of a 10 µl PCR Master Mix (SinaClon BioScience, Iran), 2 µl of template DNA (~50 ng), 1 µl of each primer (concentration 10 pm/ml), and 6 µl of nuclease-free water for a total volume of 20 µl. PCR products were examined using gel electrophoresis on 1% agarose gels, with positive PCR amplifications sequenced on an ABI 3130XL automated sequencer. We assembled, inspected, and edited sequences using Bioedit v.7.0.5.3.

Once assembled and edited, sequences produced in this study were combined with previously published COI sequences of *T. maindroni* as well as other *Tylos* species, provided that these sequences were > 500-bp long. Information for publicly available sequences included in this study can be found in Table 2. Sequences were aligned using the online MAFFT server (Katoh et al. 2019) and default settings. The resulting alignment was trimmed to remove end gaps. No evidence suggestive of pseudo-genes was observed in the final alignment. Given the high levels of divergence amongst *Tylos* species and differences in sequence lengths across studies, we re-aligned the COI sequences for *T. maindroni* individuals separately.

We used ASAP (Puillandre et al. 2021), a distance-based species delimitation approach, to determine if all *T. maindroni* sequences were assigned to a single species cluster. This analysis was carried out on the ASAP web portal (https://bioinfo.mnhn.fr/abi/public/asap/) under the Kimura (K80 or K2P) model (Kimura 1980) and a ts/tv ratio of 2.0. All other settings were as default. We estimated pairwise genetic distances with the Kimura-2-Parameter (K2P) correction in MEGA v11.0.10 (Tamura et al. 2021).

Lastly, we visualized relationships between *T. maindroni* COI haplotypes by reconstructing branch connections using the TCS network option (Clement et al. 2002) of PopArt v1.7 (Leigh and Bryant 2015), with a 95% connection limit.

Table 2. GenBank Accession information for sequences used in this study. Accession numbers of sequences produced in this study are in bold.

	Number of individuals	GenBank Acc. No
T. maindroni	8	KJ468116; **OK513060 – OK513066**
T. capensis	33	MZ540108-MZ540140
T. chilensis	1	KJ468109
T. exiguous	1	KJ468112
T. granulatus	179	MK603245-MK603423
T. granuliferus	123	AB763432-AB763552; KJ468113-KJ468114
T. marcuzzii	1	KJ468118
T. niveus	1	KJ468120
T. opercularis	1	KJ468121
T. punctatus	23	KF007550-KF007555; KF007571-KF007574; KF007582-KF007586; KF007596-KF007598; KF007607-KF007608; KF007686-KF007688
Tylos sp. BOLD:ACM2291	1	KJ592778
Tylos sp. clade B*	1	KF007644
Tylos sp. clade C*	1	KF007626
Tylos sp. clade D*	1	KF007575
Tylos sp. clade F*	2	KF007689-KF007690
Tylos sp. clade G*	13	KF007576; KF007654; KF007657; KF007669-KF007671; KF007679-KF007680; KF007685; KF007698; KF007711-KF007712; KF007718
Tylos sp. clade H*	9	KF007599; KF007609-KF007611; KF007615-KF007616; KF007646-KF007648
Tylos sp. clade I*	7	KF007569; KF007664; KF007667-KF007668; KF007705; KF007713; KF007715
Tylos sp. hachijoMN12	1	AB763553
Tylos sp. outgroup*	1	KF007724
T. spinulosus	1	KJ468125
T. wegeneri	1	KJ468126

* = Clades reported by Hurtado et al. (2014).

Systematic account

Order Isopoda Latreille, 1817
Suborder Oniscidea Latreille, 1802
Family Tylidae Milne-Edwards, 1840

Genus *Tylos* Audouin, 1826

Type species. *Tylos latreillii* Audouin, 1826; from an unspecified location in Egypt (type locality); but current status is a nomen dubium (Taiti and Ferrara 1996: 460).

Diagnosis. A diagnosis for the genus was published by Schmalfuss (2000).

***Tylos maindroni* Giordani Soika, 1954**
Figs 2–6

Tylos maindroni Giordani Soika, 1954: 76, figs 8, 9, pl. 10, Oman Sea, Muscat (type locality); Ferrara and Taiti 1986: 94; Taiti and Ferrara 1991: 213, fig. 3; Taiti et al. 2000: 148; Hurtado et al. 2014: 3, fig. 1.

Material examined. 7 ♂♂ (5.1 to 9.8 mm), 3 ♀♀ (5.5, 8.5, 10 mm), the Persian Gulf, Bandar-e-Charak, sandy shore, under wood block and rubbish on sand, 05 Dec. 2008, 26°42'555"N, 54°14'329"E, coll. V. Khalaji (ZMSU 1201); 8 ♂♂ (5 to 8 mm), 6 ♀♀ (6 to 9.2 mm), Bandar-e-Bostaneh, sandy shore, 03 Jan. 2006, 27°07'113"N, 53°01'418"E, coll. R. Naderloo (ZMSU 1202); 1 ♀ (12.2 mm), Bandar-e-Lengeh, sandy beach, beneath wood, 03 May 2010, 26°34'10"N, 54°54'21"E, coll. V. Khalaji (ZMSU 1203); 2 ♀♀ (9 and 10 mm), Kish Island, northern coast, Derakht-e-Sabz, 24 Jun. 2006, 26°34'102"N, 53°58'098"E, coll. V. Khalaji (ZMSU 1204); 3 ♂♂ (9 to 11mm); 8 ♀♀ (8 to 10 mm), Faroor Koochak Island, rocky, sandy western coast, 30 Dec. 2017, 26°65'999"N, 54°26'108"E, coll. V. Khalaji (ZMSU 1205); 10 ♀♀ (7 to 11mm), 5 ♂♂ (7.7 to 11 mm), Greater Tunb Island, sandy beach, 03 Jan. 2021, 26°16'20.48"N, 55°17'28.00"E, coll. V. Khalaji and M. Majidi (ZSMU 1206).

Redescription of male (from the Persian Gulf). Color yellowish, or light brown dorsally with small, dark, pigmented dots of various densities (Fig. 2A–D), about 2.5 times as long as greatest width. ***Cephalon*** with a weak domed process on each side between eyes. ***Epistome*** triangular with narrowly rounded apex, labrum with rows of small tubercles, as figured (Fig. 3B). ***Eyes*** composed of 36–38 ommatidia in adults (Fig. 3E). Coxal plates 2–5 with rounded margin, coxal plates 6–7 rectangular with strait margin. ***Pleotelson*** framed by pleonite 5 laterally, distal margin with small setae, length about 0.55 times width (Fig 3F, G).

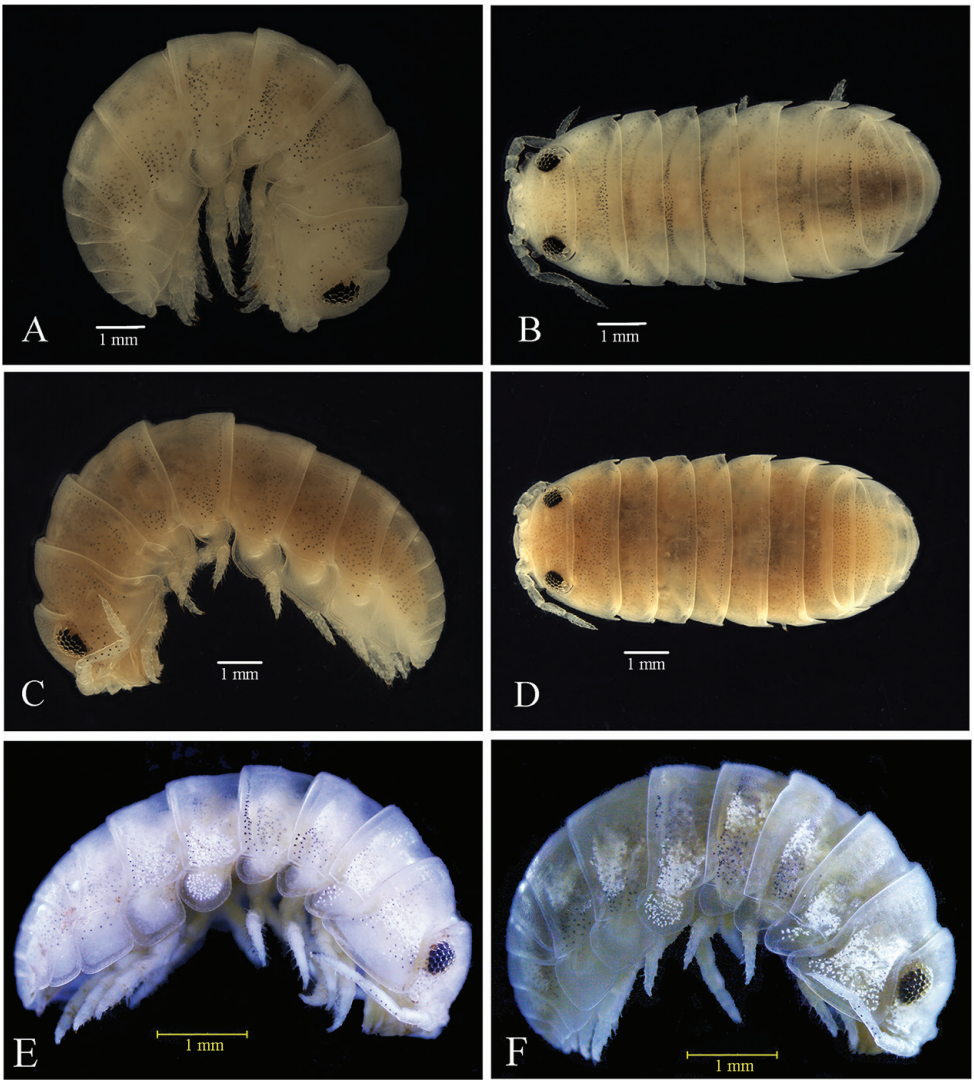

Figure 2. *Tylos maindroni* Giordani Soika, 1954 **A, B** male from the Persian Gulf, Bandar-e-Charak (ZMSU 1201) **C, D** female from the Persian Gulf, Bandar-e-Charak (ZMSU 1201) **E** female from Faroor Koochak Island (ZMSU 1205) **F** male from Greater Tunb Island (ZSMU 1206).

Antennula (Fig. 3C). Small, disolateral and apical margins straight, medial margin concave, covered with cuticular scales, about 1.3 times as long as greatest width.

Antenna (Fig. 3D). Extending to posterior margin of pereonite 1, basal peduncular articles 2–5 increasing in length; article 5 about 1.3 times as long as article 4; flagellum with 4 articles, distal article smallest, apex with cone-like tuft of setae.

Left mandible (Fig. 4D). Pars incisiva with three cusps; lacinia mobilis with three cusps and 2 penicils; pars molaris with flat grinding surface and with a tuft of numerous hair-like setae on margin.

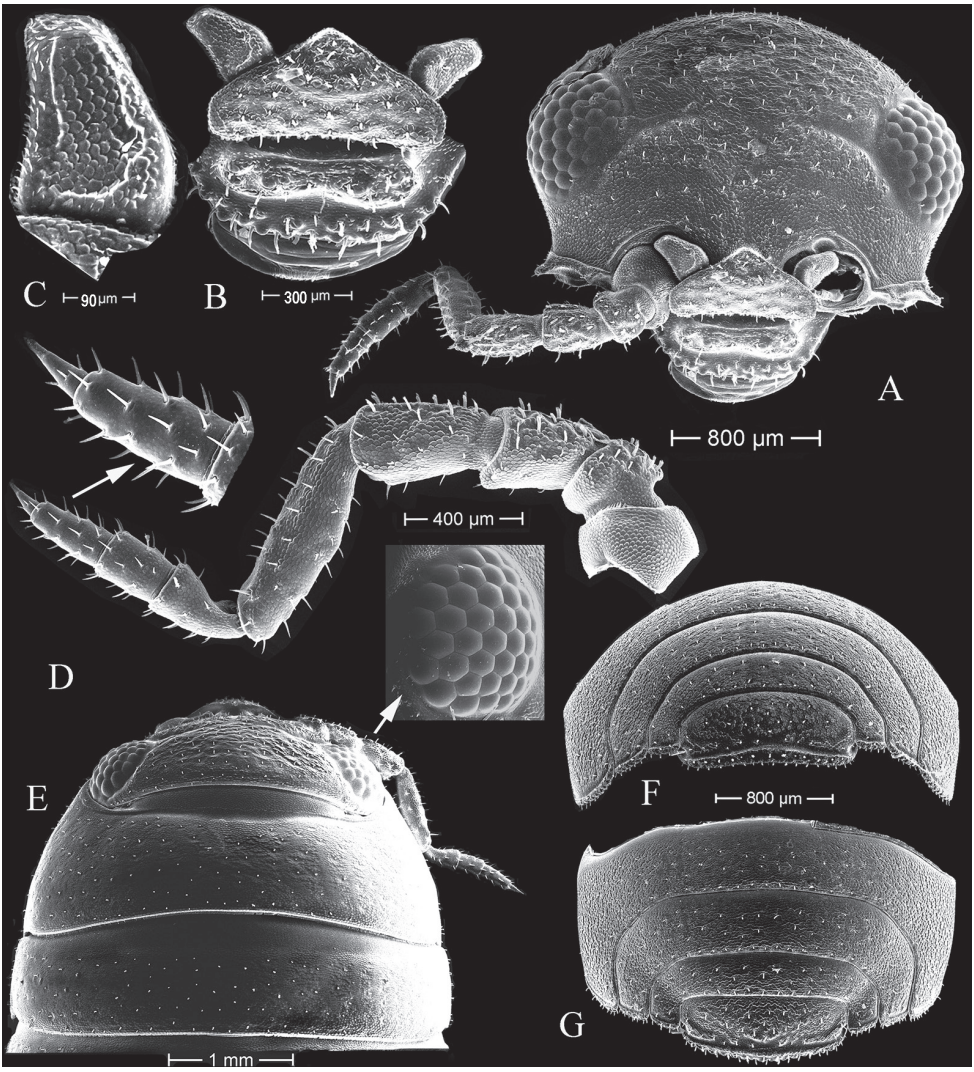

Figure 3. *Tylos maindroni* Giordani Soika, 1954, male from the Persian Gulf, Bandar-e-Charak, scanning electron micrographs **A** head, frontal view **B** epistome **C** antennule **D** antenna **E** head, dorsal view **F** pleon and pleotelson, caudal view **G** pleon and pleotelson, dorsal view.

Right mandible (Fig. 4E). Pars incisiva with three cusps; lacinia mobilis with some small, sharp cusps (about 8) and 2 penicils; pars molaris grinding surface smaller than on left mandible, with a tuft of numerous hair-like setae on proximal margin.

Maxillule (Fig. 4A, B). Lateral endite with 12 robust, simple or serrate setae; mesial endite with 2 subapical and 1 apical penicils.

Maxilla (Fig. 4C). Apical margin round, densely setose.

Maxilliped (Fig. 4F). Endite apical margin with 6 robust, simple setae, 3 large penicils, and 2 smaller penicils; palp of five articles, articles 2–5 each bearing a tuft of marginal, rod-like setae.

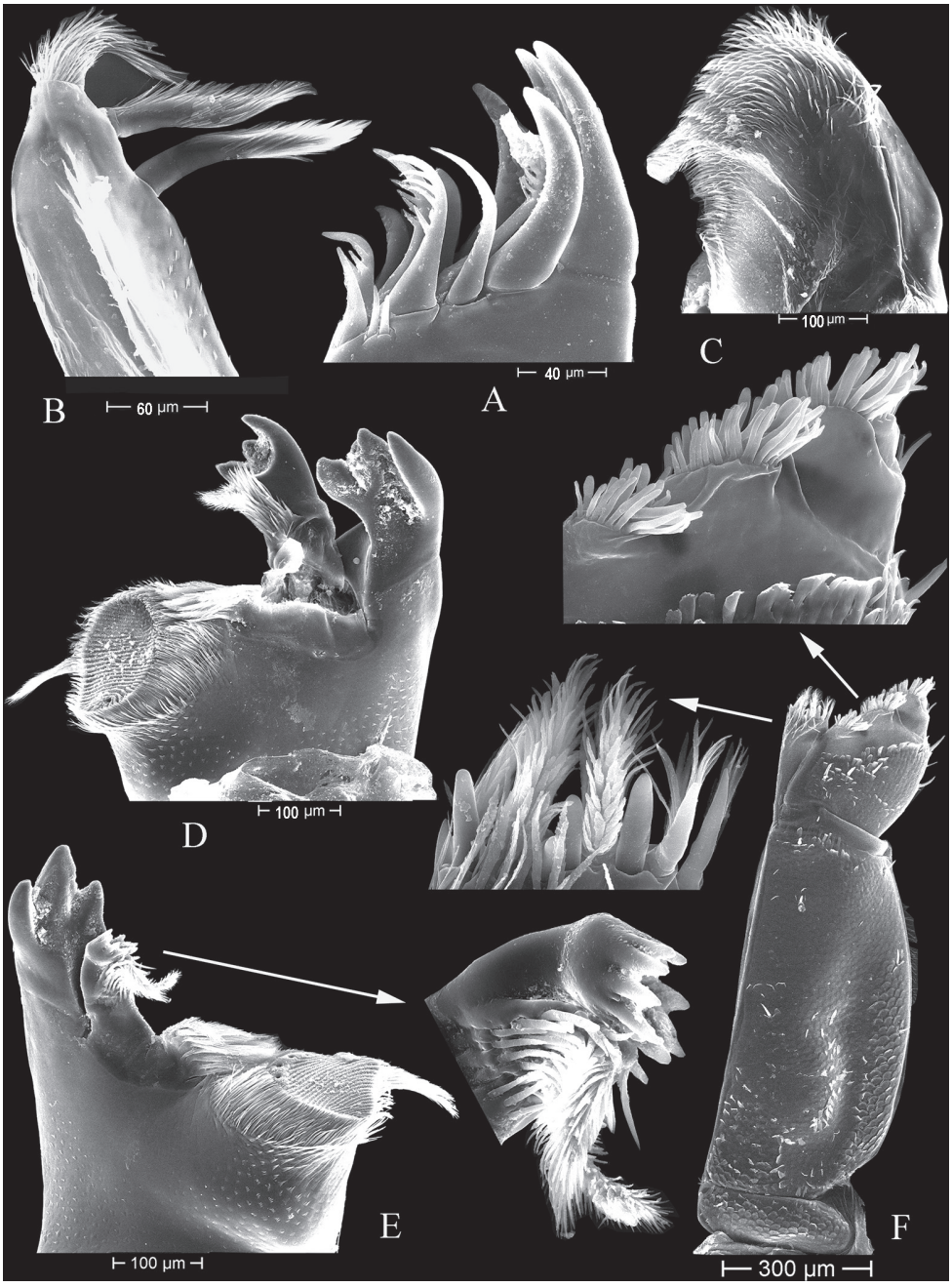

Figure 4. *Tylos maindroni* Giordani Soika, 1954, male from the Persian Gulf, Bandar-e-Charak, scanning electron micrographs **A** maxillule, lateral endite **B** maxillule, medial endite **C** maxilla **D** left mandible **E** right mandible **F** maxilliped.

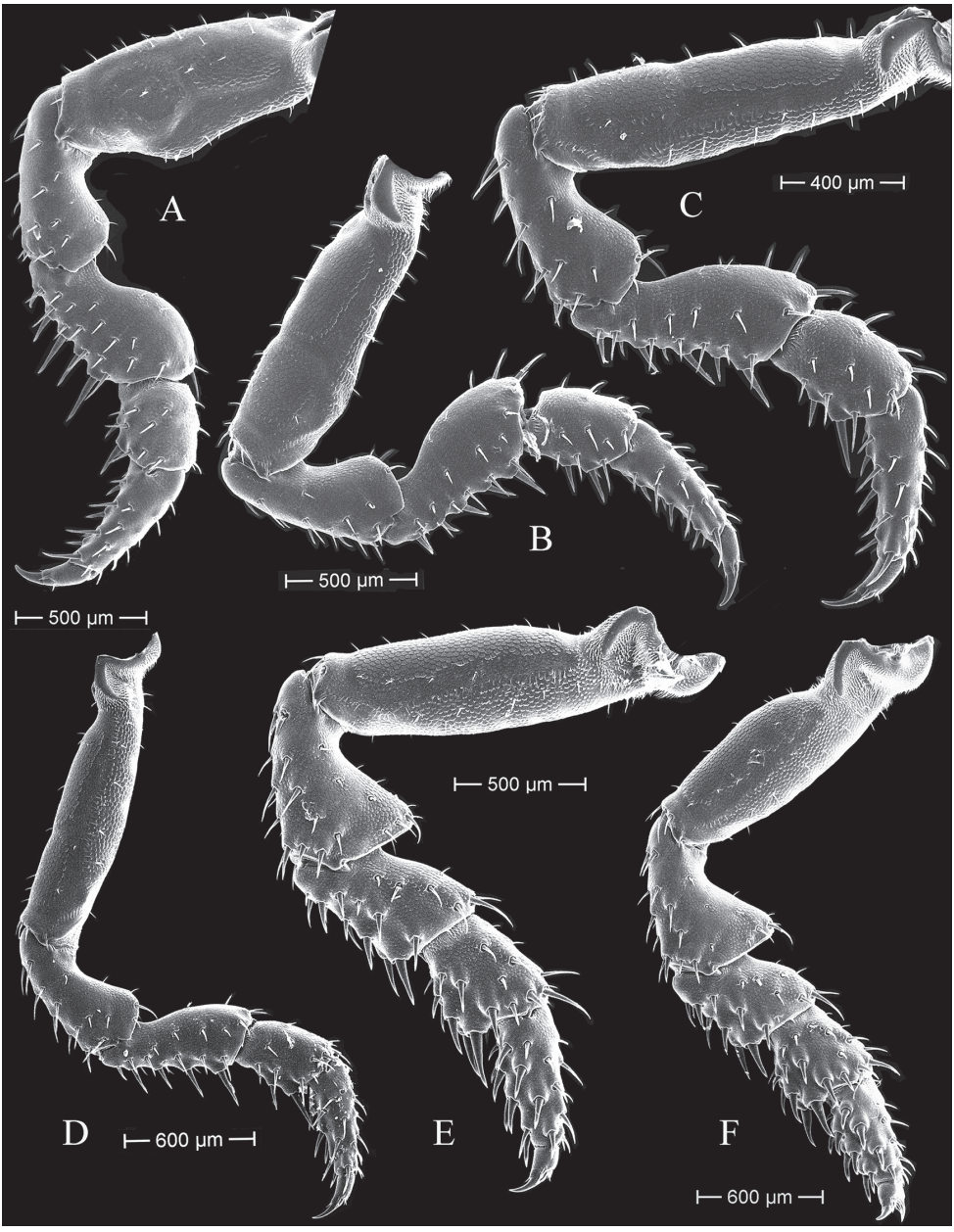

Figure 5. *Tylos maindroni* Giordani Soika, 1954, male from the Persian Gulf, Bandar-e- Charak, scanning electron micrographs **A–F** pereopods 1–7, respectively.

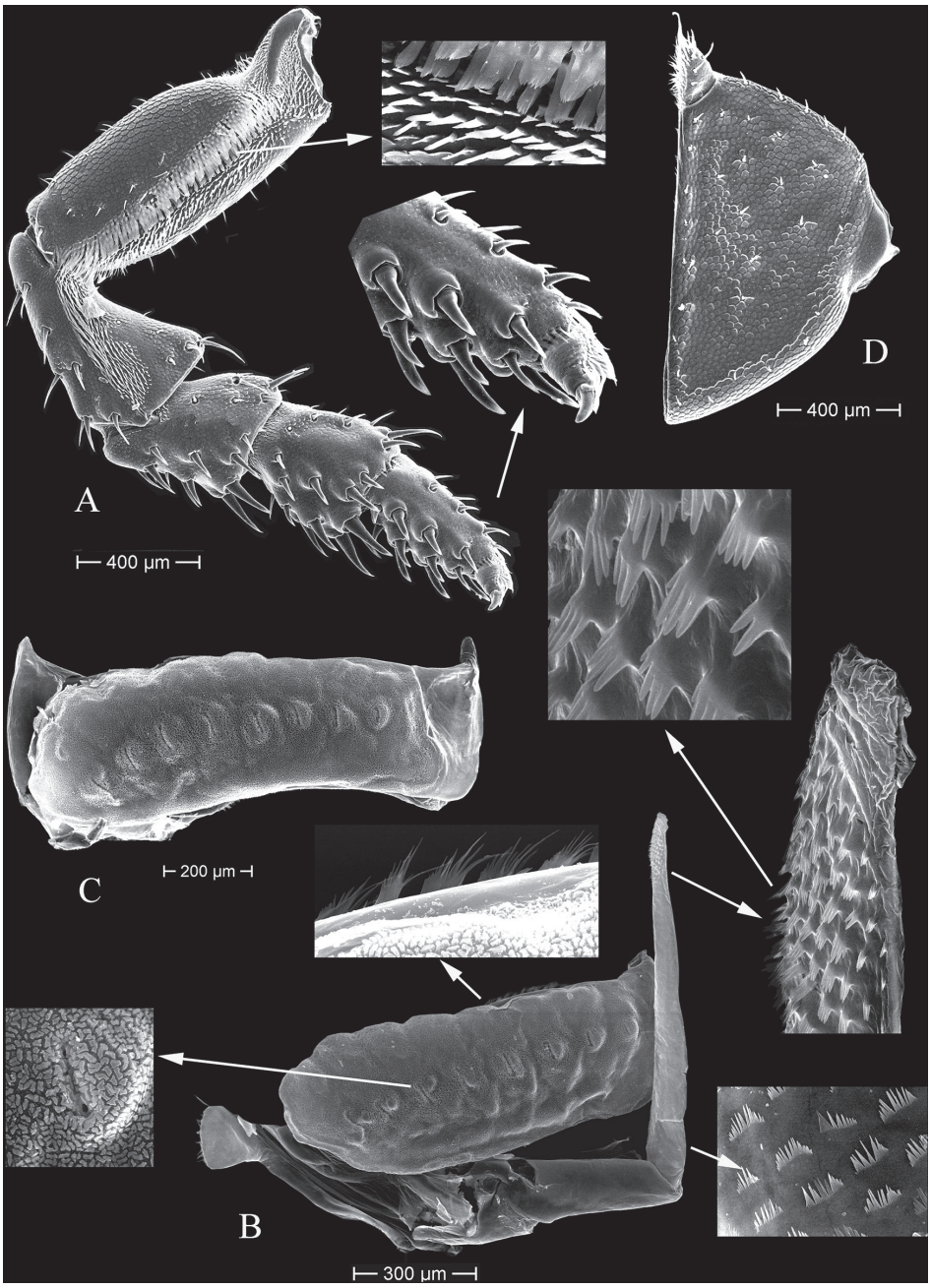

Figure 6. *Tylos maindroni* Giordani Soika, 1954, male from the Persian Gulf, Bandar-e- Charak, scanning electron micrographs **A** pereopod 7 **B** pleopod 2 **C** pleopod 3 **D** uropod.

Pereopod 1–7 (Figs 5A–F, 6A). All with a rich armature of robust setae; pereopod 1 basis about 2.1 times as long as wide, ventral margin with a weak extension; pereopods 2–5 with longer basis; pereopod 7 (Fig. 6A) basis about 2.3 times as long as wide, with water conducting scale-rows.

Pleopod 2 (Fig. 6B). Exopod equipped with open lungs consisting of 8 pores, distal margin with cuticular scale. Endopod elongated, well extended beyond exopod distal margin, apical part bearing hand-like scales with 2–7 "fingers" that are directed proximally, proximal third covered with cuticular scales.

Pleopod 3 (Fig. 6C). Exopod equipped with open lungs consisting of 9 pores.

Uropod (Fig. 6D). Protopod (peduncle) with straight medial margin, disto-lateral margin with 6 small marginal setae, length about 1.62 greatest width; exopod small, about 0.23 times length of protopod, covered with small setae medially.

Female (Fig. 2C, D). Apart from sexual characters, similar to male.

Distribution. Oman, the Persian Gulf (Kuwait; Bandar-e-Charak, Bandar-e-Bostaneh, Bandar-e-Lengeh, Kish, Greater Tunb, and Faroor Koochak Islands, Iran)

Results

Genetic differentiation

We obtained seven 534-bp long *COI* sequences from *T. maindroni* individuals from four locations across the Persian Gulf coastline of Iran. These sequences were combined with a previously published *COI* sequence of *T. maindroni* from Kuwait (GenBank Acc. KJ468116; BIN: BOLD: ACQ3230). We identified four highly similar COI haplotypes as indicated by K2P divergences (0.0–0.4%, 1–3 nucleotide differences, Fig. 7). These haplotypes, however, were highly divergent from those found in other *Tylos* species (16.2–33.9% COI K2P divergences, Table 3).

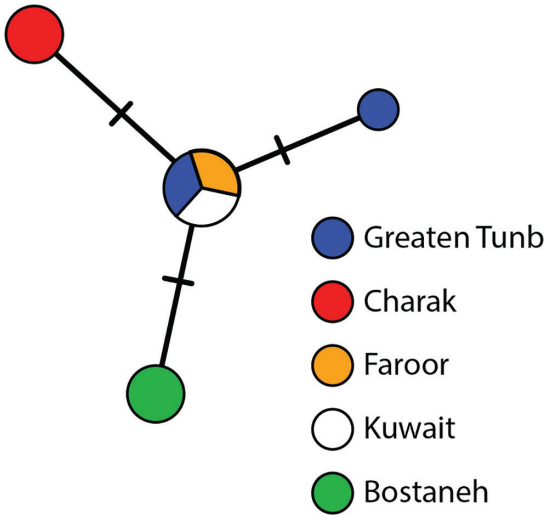

Figure 7. Haplotype networks for the COI mitochondrial gene fragment of *Tylos* from the Persian Gulf. Colors correspond to locations as indicated in figure. Dashes along branches represent the number of nucleotide differences between haplotypes. Frequency of haplotype recovery represented through relative sizes of circles.

Table 3. Average COI K2P divergences amongst *Tylos* species included in this study.

	T. maindroni	*T. punctatus*	***Tylos* sp. BOLD:**ACM2291	***Tylos* sp. clade F***	***Tylos* sp. clade D***	***Tylos* sp. clade G***	***Tylos* sp. clade H***	***Tylos* sp. clade I***	***Tylos* sp. clade C***	***Tylos* sp. clade B***	***Tylos* sp. outgroup***	*T. niveus*	*T. granulatus*	*T. capensis*	*T. marcuzzii*	*T. exiguus*	*T. opercularis*	*T. chilensis*	*T. spinulosus*	***Tylos* sp. hachijoMN12**	*T. granuliferus*	*T. wegeneri*
T. maindroni	<0.5																					
T. punctatus	20.5	<5.8																				
Tylos sp. BOLD: ACM2291	20.5	0.1	N/A																			
Tylos sp. clade F*	19.2	14.9	14.8	0.0																		
Tylos sp. clade D*	17.7	12.5	12.4	11.0	N/A																	
Tylos sp. clade G*	18.2	13.6	13.6	13.2	12.5	<6.2																
Tylos sp. clade H*	18.6	14.0	14.1	12.6	12.2	4.6	0.0															
Tylos sp. clade I*	18.9	14.2	14.3	13.6	13.0	5.6	4.5	0.0														
Tylos sp. clade C*	21.2	15.6	15.5	12.1	14.2	13.5	14.0	13.9	N/A													
Tylos sp. clade B*	20.4	12.9	12.8	14.5	13.1	13.4	13.1	13.4	13.1	N/A												
Tylos sp. outgroup*	19.9	16.0	15.9	16.7	18.2	15.8	15.9	16.3	18.4	14.7	N/A											
T. niveus	17.7	16.0	15.8	15.1	16.8	15.5	17.1	16.8	16.6	15.9	15.6	N/A										
T. granulatus	17.4	15.9	15.9	15.7	15.0	15.2	15.9	15.8	18.5	16.7	19.1	15.8	<13.2									
T. capensis	19.5	16.3	16.3	17.9	17.7	17.5	18.4	17.7	20.8	17.8	19.0	19.8	12.2	<2.8								
T. marcuzzii	21.5	17.8	17.8	21.6	22.7	20.2	20.9	21.3	19.9	17.3	18.0	20.6	19.4	19.6	N/A							
T. exiguus	20.7	21.3	21.2	20.5	19.2	18.7	18.8	19.2	21.9	20.5	21.0	22.9	18.9	19.1	23.1	N/A						
T. opercularis	25.4	25.5	25.5	21.9	25.2	25.1	25.2	25.2	27.3	25.8	23.6	19.2	23.3	23.3	26.0	23.0	N/A					
T. chilensis	25.6	23.7	23.6	26.2	25.4	24.9	25.0	24.6	24.8	25.1	24.3	25.5	22.7	24.8	24.4	24.1	29.1	N/A				
T. spinulosus	23.2	21.1	21.0	22.6	22.2	21.0	21.4	22.7	22.8	21.3	23.5	23.0	20.9	22.1	27.0	22.0	31.3	13.7	N/A			
Tylos sp. hachijoMN12	23.9	27.3	27.3	25.1	26.6	25.2	27.4	27.0	25.7	24.9	26.2	21.2	25.2	25.8	29.7	28.2	24.1	33.5	28.3	N/A		
T. granuliferus	28.9	30.5	30.4	27.1	25.6	27.6	27.2	27.2	28.0	27.5	31.5	27.3	25.6	26.2	32.0	26.3	24.4	32.2	30.3	24.4	<25.2	
T. wegeneri	26.2	28.7	28.7	27.3	27.2	26.3	25.4	27.7	26.2	26.0	27.7	27.4	25.9	26.0	25.7	27.1	26.4	27.8	27.3	26.5	29.2	N/A

* = Clades reported by Hurtado et al. (2014).

Combining the *T. maindroni* sequences with other previously published sequences of the genus *Tylos* resulted in a 517-bp long alignment containing 410 sequences. ASAP analyses of this dataset identified two partitioning schemes with nearly similar numbers of hypothetical species groups (23 and 24), threshold distances (0.068107 and 0.051440), and low ASAP scores (7 and 8). This last measure reflects both the p-value and the relative barcode gap width rank for a given partitioning scheme, with lower values reflecting stronger support for a given partitioning scheme. All COI haplotypes from *T. maindroni* individuals were placed in a single cluster that included no sequences from other *Tylos* species, regardless of the partitioning scheme.

Discussion

Tylos maindroni was first described by Giordani Soika in 1954; however, the original description was brief and did not include a discussion or illustration of characters used in the taxonomy of this genus. A later work by Taiti and Ferrara (1991) suggested that *T. maindroni*'s geographic range extends into the Persian Gulf, including locations on the coasts of Kuwait and Iran, but additional work remains necessary to clarify the status of this species and its geographic range. Additionally, considering the high levels of genetic divergence reported in several coastal isopod taxa (Hurtado et al. 2013; Khalaji-Pirbalouty and Raupach 2014, 2016; Raupach et al. 2014; Hurtado et al. 2017; Santamaria et al. 2017; Greenan et al. 2018; Hurtado et al. 2018; Santamaria 2019), it would be important to determine if *T. maindroni* harbors cryptic diversity in its native range.

Our Persian Gulf specimens correspond morphologically quite well to the brief description and illustrations of *T. maindroni* from Oman by Giordani Soika (1954) and from Kuwait by Taiti and Ferrara (1991). Nevertheless, there is a slight difference in the number of lung pores on the exopod of the pleopods: the exopod of pleopod 2 has 8 pores rather than 7 and the exopod of pleopod 3 has 9 pores rather than 8. *Tylos maindroni* is morphologically most similar to *T. exiguus* Stebbing, 1910, a Red Sea species shown by Hurtado et al. (2014) to be a sister taxon to *T. maindroni* based on several mitochondrial markers. The former species differs from *T. maindroni* by having pereonite 1 posterior margin with a distinctly deeper concavity at the lateral side, pereopod 1 superior margin with a prominent projection, and pleopod 2 endopod 3.6 times as long as exopod (vs. 2.3 times in *T. maindroni*).

Molecular data are in concordance with the above findings. All *Tylos* specimens that were morphologically identified as *T. maindroni* have highly similar COI haplotypes differing by a maximum of three positions (K2P distances amongst haplotypes < 0.5%). Furthermore, sequences recovered from *T. maindroni* individuals were highly divergent from all other COI sequences recovered from other *Tylos* species including *T. exiguus* (16.2–33.9% COI K2P). Not surprisingly, all *T. maindroni* haplotypes were assigned to a single species cluster in species delimitation analyses carried out in ASAP, regardless of the partitioning scheme.

The low level of diversification herein reported between individuals of *T. maindroni* collected at Persian Gulf locations stands in contrast with those reported for other coastal oniscid taxa (Khalaji-Pirbalouty and Raupach 2014, 2016; Raupach et al. 2014; Hurtado et al. 2017; Santamaria et al. 2017; Greenan et al. 2018; Hurtado et al. 2018; Santamaria 2019), including other *Tylos* species (Hurtado et al. 2013). For instance, the molecular characterizations of *Tylos* populations from the Gulf of California showed genetic differentiation in COI sequences ranging from 3.6 to 17.3%, indicating long-standing isolation of the populations in the region as well as the possible presence of cryptic species (Hurtado et al. 2013). Similarly, *T. granulatus* populations in South Africa have shown to harbor two highly divergent mitochondrial

lineages (Mbongwa et al. 2019). In contrast to this, the COI K2P divergences observed in *T. maindroni* were less than 0.5%.

The low levels of genetic divergence within *T. maindroni* in the Persian Gulf is likely a reflection of the young age of this marine waterbody. Although there is disagreement on the extent of the Persian Gulf coastline during the Holocene and Late Pleistocene (Sissakian et al. 2020), the Gulf Basin is thought to have been free of marine influence up until the last glacial maximum ~18,000 ya., with marine flooding due to rising sea levels and glacial displacement starting ~14,000 ya (Lambeck 1996). Thus, the geology of the region suggests that the ancestor to *T. maindroni* populations in the Persian Gulf area invaded the Gulf in the past ~14,000 years. Alternatively, the low divergence levels between COI sequences reported herein may be the result of infection with *Wolbachia*. Infection with this endosymbiotic bacterium has been proposed to reduce mitochondrial polymorphisms in arthropods, including isopods (Marcadé et al. 2009; Xiao et al. 2012; Delhoumi et al. 2019; but see Tang et al. 2019). We cannot determine whether *Wolbachia* have reduced mitochondrial diversity in *T. maindroni* in the Persian Gulf as we did not test for the presence of *Wolbachia* in our specimens. However, given the recent geological and hydrological history of the Persian Gulf, we propose that the low levels of divergence in *T. maindroni* reported herein are likely the result of the young age of the modern Persian Gulf. Nevertheless, future work remains needed to conclusively discern between these explanations. Future studies also remain needed to clarify the origins and evolution of *T. maindroni* in the region. The closest extant relative of *T. maindroni* in the Persian Gulf is *T. exiguus* (Hurtado et al. 2014), suggesting that the Persian Gulf populations of *T. maindroni* likely originated from an ancestor inhabiting coastal habitats in the Indian Ocean basin. As our sampling did not include *T. maindroni* populations from the Indian Ocean, future work would be best served by incorporating these populations.

Acknowledgements

We would like to thank Dr. Saskia Brix (Senckenberg Research Institute, Germany), Dr. Michael Raupach (Bavarian State Collection of Zoology, Munich, Germany) and one anonymous reviewer for their constructive suggestions and helpful comments. This study is a part of the Biodiversity and Conservation project under a joint program by the Ministry of Science, Research and Technology of Iran and the Leibniz Association, Germany. Financial support for this study was provided by the Iran University of Science and Technology, International Affairs, Shahrekord University, Iran and the Leibniz Association, Germany.

References

Boyko C, Bruce N, Hadfield K, Merrin K, Ota Y, Poore G, Taiti S, Schotte M, Wilson G (2008 onwards) World Marine, Freshwater and Terrestrial Isopod Crustaceans. Database. http://www.marinespecies.org/aphia.php?p=taxdetails&id=147192 [Accessed 12 Ocotber 2021].

Clement M, Snell Q, Walker P, Posada D, Crandall K (2002) TCS: Estimating gene genealogies. Proceedings of the 16th International Parallel and Distributed Processing Symposium. 311 pp. IEEE Computer Society. https://doi.org/10.1109/IPDPS.2002.1016585

Delhoumi M, Zaabar W, Bouslama MF, Zayani D, Achouri MS (2019) High level of genetic variation in mitochondrial 16S rDNA among populations of *Porcellionides pruinosus* (Brandt, 1833) (Crustacea: Isopoda: Oniscidea) in Tunisia. The European Zoological Journal 86(1): 1–8. https://doi.org/10.1080/24750263.2018.1540669

Folmer O, Black M, Hoeh W, Lutz R, Vrijenhoek R (1994) DNA primers for amplification of mitochondrial cytochrome c oxidase subunit I from diverse metazoan invertebrates. Molecular Marine Biology and Biotechnology 3: 294–299.

Giordani Soika A (1954) Ecologia, sistematica, biogeografia ed evoluzione del *Tylos latreillei* Auct.(Isop. Tylidae). Bollettino del Museo civico di storia naturale di Venezia 7: 63–83.

Greenan TM, Griffiths CL, Santamaria CA (2018) Molecular approaches uncover cryptic diversity in intertidal *Ligia* isopods (Crustacea, Isopoda, Ligiidae) across the southern Africa coastline. PeerJ 6: e4658. https://doi.org/10.7717/peerj.4658

Hurtado LA, Lee EJ, Mateos M (2013) Contrasting phylogeography of sandy vs. rocky supralittoral isopods in the megadiverse and geologically dynamic Gulf of California and adjacent areas. PLoS ONE 8(7): e67827. https://doi.org/10.1371/journal.pone.0067827

Hurtado LA, Lee EJ, Mateos M, Taiti S (2014) Global diversification at the harsh sea-land interface: Mitochondrial phylogeny of the supralittoral isopod genus *Tylos* (Tylidae, Oniscidea). PLoS ONE 9(4): e94081. https://doi.org/10.1371/journal.pone.0094081

Hurtado LA, Mateos M, Liu S (2017) Phylogeographic patterns of a lower intertidal isopod in the Gulf of California and the Caribbean and comparison with other intertidal isopods. Ecology and Evolution 7(1): 346–357. https://doi.org/10.1002/ece3.2599

Hurtado LA, Mateos M, Wang C, Santamaria CA, Jung J, Khalaji-Pirbalouty V, Kim W (2018) Out of Asia: mitochondrial evolutionary history of the globally introduced supralittoral isopod *Ligia exotica*. PeerJ 6: e4337. https://doi.org/10.7717/peerj.4337

Katoh K, Rozewicki J, Yamada KD (2019) MAFFT online service: multiple sequence alignment, interactive sequence choice and visualization. Briefings in Bioinformatics 20(4): 1160–1166. https://doi.org/10.1093/bib/bbx108

Kensley BF (1974) Aspects of the biology and ecology of the genus *Tylos latreille*. Annals of the South African Museum 65: 401–471.

Khalaji-Pirbalouty V, Raupach MJ (2014) A new species of *Cymodoce* Leach, 1814 (Crustacea: Isopoda: Sphaeromatidae) based on morphological and molecular data, with a key to the Northern Indian Ocean species. Zootaxa 3826(1): 230–254. https://doi.org/10.11646/zootaxa.3826.1.7

Khalaji-Pirbalouty V, Raupach MJ (2016) DNA barcoding and morphological studies confirm the occurrence of three *Atarbolana* (Crustacea: Isopoda: Cirolanidae) species along the coastal zone of the Persian Gulf and Gulf of Oman. Zootaxa 4200(1): 4201–4207. https://doi.org/10.11646/zootaxa.4200.1.7

Kimura M (1980) A simple method for estimating evolutionary rates of base substitutions through comparative studies of nucleotide sequences. Journal of Molecular Evolution 16(2): 111–120. https://doi.org/10.1007/BF01731581

Lambeck K (1996) Shoreline reconstructions for the Persian Gulf since the last glacial maximum. Earth and Planetary Science Letters 142(1): 43–57. https://doi.org/10.1016/0012-821X(96)00069-6

Leigh JW, Bryant D (2015) popart: Full-feature software for haplotype network construction. Methods in Ecology and Evolution 6(9): 1110–1116. https://doi.org/10.1111/2041-210X.12410

Marcadé I, Souty-Grosset C, Bouchon D, Rigaud T, Raimond R (1999) Mitochondrial DNA variability and *Wolbachia* infection in two sibling woodlice species. Heredity 83(1): 71–78. https://doi.org/10.1038/sj.hdy.6885380

Mbongwa NA, Hui C, Pulfrich A, von der Heyden S (2019) Every beach an island deep population divergence and possible loss of genetic diversity in *Tylos granulatus*, a sandy shore isopod. Marine Ecology Progress Series 614: 111–123. https://doi.org/10.3354/meps12882

Puillandre N, Brouillet S, Achaz G (2021) ASAP: Assemble species by automatic partitioning. Molecular Ecology Resources 21(2): 609–620. https://doi.org/10.1111/1755-0998.13281

Raupach MJ, Bininda-Emonds OR, Knebelsberger T, Laakmann S, Pfaender J, Leese F (2014) Phylogeographical analysis of Ligia oceanica (Crustacea: Isopoda) reveals two deeply divergent mitochondrial lineages. Biological Journal of the Linnean Society 112(1): 16–30. https://doi.org/10.1111/bij.12254

Santamaria CA (2019) Molecular taxonomy of endemic coastal *Ligia* isopods from the Hawaiian Islands: re-description of *L. hawaiensis* and description of seven novel cryptic species. PeerJ 7: e7531. https://doi.org/10.7717/peerj.7531

Santamaria CA, Bluemel JK, Bunbury N, Curran M (2017) Cryptic biodiversity and phylogeographic patterns of Seychellois Ligia isopods. PeerJ 5: e3894. https://doi.org/10.7717/peerj.3894

Schmalfuss H (2003) World catalog of terrestrial isopods (Isopoda: Oniscidea). Stuttgarter Beiträge zur Naturkunde, Serie A (Biologie) 654: 1–341.

Schmalfuss H, Vergara K (2000) The isopod genus *Tylos* (Oniscidea: Tylidae) in Chile, with bibliographies of all described species of the genus. Stuttgarter Beiträge zur Naturkunde, Serie A (Biologie) 612: 1–42.

Sfenthourakis S, Myers A A, Taiti S, Lowry JK (2020) Terrestrial Environments. In: Poore GCB, Thiel M (Eds) The Natural History of the Crustacea: Evolution and Biogeography. Vol. 8, Oxford University Press, New York, 552 pp. https://doi.org/10.1093/oso/9780190637842.003.0014

Sissakian VK, Adamo N, Al-Ansari N, Abdullah M, Laue J (2020) Sea level changes in the Mesopotamian plain and limits of the Arabian gulf: A critical review. Journal of Earth Sciences and Geotechnical Engineering 10(4): 87–110.

Taiti S, Checcucci I (2010) New species and records of terrestrial Isopoda (Crustacea, Oniscidea) from Socotra Island, Yemen. ZooKeys 31: 73–103. http://doi.org/10.3897/zookeys.31.140.

Taiti S, Ferrara F (1991) New species and records of terrestrial isopods (Crustacea) from the Arabian Peninsula. Fauna of Saudi Arabia 12: 209–224.

Taiti S, Ferrara F (1996) The terrestrial Isopoda of Corsica (Crustacea, Oniscidea). Bulletin du Muséum national d'histoire naturelle. Paris (4e Sér.) Sect A (3–4): 459–545.

Taiti S, Ferrara F (2004) The terrestrial Isopoda (Crustacea: Oniscidea) of the Socotra Archipelago. Fauna of Arabia 20: 211–326.

Tamura K, Stecher G, Kumar S (2021) MEGA11: Molecular evolutionary genetics analysis version 11. Molecular Biology and Evolution 38(7): 3022–3027. https://doi.org/10.1093/molbev/msab120

Tang XT, Xu J, Lu MX, Du YZ (2019) No evidence for an effect of *Wolbachia* on mtDNA variation and evolution in natural populations of *Sesamia inferens* (Lepidoptera: Noctuidae). Journal of Integrative Agriculture 18(5): 1050–1063. https://doi.org/10.1016/S2095-3119(18)62019-2

Xiao JH, Wang NX, Murphy RW, Cook J, Jia LY, Huang DW (2012) *Wolbachia* infection and dramatic intraspecific mitochondrial DNA divergence in a fig wasp. Evolution: International Journal of Organic Evolution 66(6): 1907–1916. https://doi.org/10.1111/j.1558-5646.2011.01561

ZooKeys 1087: 141–161 (2022)
doi: 10.3897/zookeys.1087.78707
https://zookeys.pensoft.net

RESEARCH ARTICLE

A peer-reviewed open-access journal
ZooKeys
Launched to accelerate biodiversity research

DNA barcoding of the horsefly fauna (Diptera, Tabanidae) of Croatia with notes on the morphology and taxonomy of selected species from Chrysopsinae and Tabaninae

Stjepan Krčmar[1], Mladen Kučinić[2], Marco Pezzi[3], Branka Bruvo Mađarić[4]

1 *Department of Biology, Josip Juraj Strossmayer University of Osijek, Cara Hadrijana 8/A, 31000 Osijek, Croatia* **2** *Department of Biology, Faculty of Science, University of Zagreb, 10000 Zagreb, Croatia* **3** *Department of Life Sciences and Biotechnology, University of Ferrara, Via Luigi Borsari 46, 44121 Ferrara, Italy* **4** *Ruđer Bošković Institute, Bijenička cesta 54, 10000 Zagreb, Croatia*

Corresponding authors: Stjepan Krčmar (stjepan@biologija.unios.hr), Branka Bruvo Mađarić (branka.bruvo.madjaric@irb.hr)

Academic editor: T. Dikow | Received 2 December 2021 | Accepted 4 February 2022 | Published 23 February 2022

http://zoobank.org/F65D91F7-029D-436B-9501-6E229DA495D2

Citation: Krčmar S, Kučinić M, Pezzi M, Bruvo Mađarić B (2022) DNA barcoding of the horsefly fauna (Diptera, Tabanidae) of Croatia with notes on the morphology and taxonomy of selected species from Chrysopsinae and Tabaninae. ZooKeys 1087: 141–161. https://doi.org/10.3897/zookeys.1087.78707

Abstract

In the Croatian fauna, horseflies (Tabanidae) are represented by 78 species belonging to two subfamilies, five tribes, and 10 genera. Identification of these species is based on morphological characteristics. In this study, 43 species of horseflies were analyzed. The highest number of species (19) belongs to the genus *Tabanus*, followed by the genera *Hybomitra* with seven species, *Haematopota* with six species, *Chrysops* with four species, *Atylotus* and *Philipomyia* with two species each, and the genera *Silvius*, *Dasyrhamphis*, and *Heptatoma* with one species each. The standard DNA barcoding region of the mitochondrial cytochrome c oxidase gene, subunit I (COI), was sequenced and compared to the Barcode of Life Database (BOLD). Our analyses confirmed our morphological identifications and added 16 new Barcode Index Numbers (BINs) for Tabanidae to BOLD. Potential problems in the systematics and taxonomy of this family are highlighted.

Keywords

Barcode Index Number (BIN), cytochrome c oxidase gene subunit I (COI), Molecular Operational Taxonomic Unit (MOTU), species delimitation, vector species

Introduction

The Tabanidae comprise about 4400 species and include some of the largest biting flies, commonly called horseflies, deer flies, and clegs (Pape et al. 2011; Morita et al. 2016; Ježek et al. 2017). The females of horseflies are known worldwide as important mechanical vectors of viruses, bacteria, protozoa, and helminths that cause disease in wild and domestic animals (Foil 1989; Desquesnes and Dia 2004). Horseflies are important pests of livestock because of the blood loss and nuisance caused by their bites, so they have been associated with losses in livestock production (Baldacchino et al. 2014). The known human pathogens transmitted by horsefly species *Chrysops dimidiatus* Wulp, 1885 and *C. silaceus* Austen, 1907 are *Loa loa* Cobbold, 1864 (Spirulida, Onchocercidae) in Africa (Chippaux et al. 2000; Cheke et al. 2003) and *Bacillus anthracis* Cohn, 1872 (Bacillales, Bacillaceae) (Chainey 1993). About 550 species of horseflies are known in the Palaearctic region (Chvála 1988), with 220 occurring in Europe (Pape et al. 2015).

Currently, the identification of horsefly species is mainly based on morphological features, but it requires a lot of experience and is extremely time-consuming. Some morphological features, i.e., colouration of the abdomen, antennae, maxillary palpi, and notopleural lobes, as well as the shape and colour of frontal calli (the lower callus, located at the lower part of the frons and the upper callus, often present on the middle of the frons), the width of the vertex, or post ocular margins, are considered important taxonomic characters for the identification of horseflies (Chvála et al. 1972). Distinguishing these morphological features can be difficult, leading to misidentifications. Therefore, many recent studies utilize DNA barcoding to verify/supplement their findings (Banerjee et al. 2015; Nitiyamatawat et al. 2017; Changbunjong et al. 2018; Mugasa et al. 2018; Morinière et al. 2019; Changbunjong et al. 2020; Mazumdar et al. 2021). DNA barcoding is established as a universal tool in biodiversity research, ensuring rapid and accurate species identification independent of the developmental stage (Hebert et al. 2003). In addition to species identification, DNA barcoding is also used to reveal genetic diversity and determine the presence of biotypes, and it can help to point out taxonomic ambiguities at species level and within species complexes (Votýpka et al. 2019).

The horsefly fauna is still poorly studied in the western and central Balkans. In Bosnia and Herzegovina, 62 species have been recorded (Mikuška et al. 2008), followed by Serbia with 45 species (Krčmar 2011; Aibulatov et al. 2012), Slovenia with 44 species (Krčmar and Bogdanović 2001), Montenegro with 42 species, North Macedonia with 40 species (Krčmar et al. 2002), and Kosovo with six species (Krčmar et al. 2002), while in Hungary 61 species have been recorded (Majer 2001).

In Croatia, 78 species classified in 10 genera and two subfamilies of horseflies have been recorded, many with differing requirements in habitat preference for larval and adult stages in the feeding area and annual periodicity (Krčmar et al. 2011). The subfamily Chrysopsinae comprises the genera *Silvius* Meigen, 1820 and *Chrysops* Meigen, 1803 with two and seven species, respectively. The majority of Croatian tabanid species belong to the subfamily Tabaninae, which is represented by eight genera. The genus *Tabanus* Linnaeus, 1758 includes the majority of species (30), followed by the genera *Hybomitra* Enderlein, 1922 with 17, *Haematopota* Meigen, 1803 with nine,

Atylotus Osten-Sacken, 1876 with five, *Dasyrhamphis* Enderlein, 1922 with three, *Therioplectes* Zeller, 1842 and *Philipomyia* Olsufjev, 1964 with two species each, while for the genus *Heptatoma* Meigen, 1803 only one species is recorded (Krčmar et al. 2011). Molecular studies of horseflies in Croatia and surrounding countries are very limited (Biruš 2006), so this study represents the first comprehensive use of DNA barcoding for the identification and delimitation of species belonging to the Croatian, as well as regional, horsefly fauna.

Materials and methods

Horseflies were collected on 14 localities (Fig. 1) during the summer months of 2015–2018 using Malaise traps (design by Townes 1972), Nzi traps according to the design of Mihok (2002), and canopy traps according to the design of Hribar et al. (1991). Identification, morphological description of analysed species, and nomenclature followed that of Chvála et al. (1972), Chvála (1988), Zeegers (2018), and Andreeva (2004). Several analysed species of *Tabanus*, *Hybomitra*, and *Haematopota* have a high morphological similarity. Morphological characteristics of females important for their identification are presented in Suppl. material 1 according to Chvála et al. (1972) and Zeegers (2018). All analysed species were identified using a stereomicroscope (Carl Zeiss, Jena, Germany) under magnification of 40×. The list of specimens analysed in this study is presented in Table 1. The horseflies were kept individually in 20 ml plastic tubes in 96% ethanol.

Genomic DNA was extracted from a single leg for each individual using the GenEluteTM Mammalian Genomic DNA Miniprep Kit (Sigma, St. Louis, MO, USA), following the protocol for rodent tail preparation with slight modifications (incubation in proteinase K overnight; DNA eluted in 100 µl of elution solution). Barcoded specimens are kept as vouchers in the Tabanidae collection of the Department of Biology of the Josip Juraj Strossmayer University of Osijek (listed in Table 1).

Standard barcoding region of mitochondrial cytochrome c oxidase I (COI) gene (Hebert et al. 2003) was successfully amplified for all horsefly specimens. Amplification mixtures included 1× DreamTaq reaction buffer with 2 mM $MgCl_2$ (Thermo Scientific, Waltham, MA, USA), 0.2 mM dNTP mix (Qiagen, Hilden, Germany), 0.5 µM each primer (LCO1490 / HCO2198), 1.0 U DreamTaq polymerase (Thermo Scientific, Waltham, MA, USA) and 3 µl of DNA in 20 µl reaction volume. PCR products were enzymatically purified using the ExoI-rSAP system (NEB, Ipswich, MA, USA) following the manufacturer's protocol and bidirectionally sequenced in Macrogen Europe Inc. (Amsterdam, the Netherlands) using amplification primers. Sequences were checked and edited in Geneious v. 8.1.4. (https://www.geneious.com) and subsequently deposited in NCBI GenBank and the Barcode of Life Database (BOLD) (NCBI GenBank acc. numbers MZ563329–MZ563371 and OM502029; BOLD ID numbers listed in Table 1; BOLD project CROTA). The BIN-RESL algorithm (Ratnasingham and Hebert 2013) assigned the new sequences to particular BINs in BOLD, corresponding to putative Molecular Operational Taxonomic Units (MOTUs).

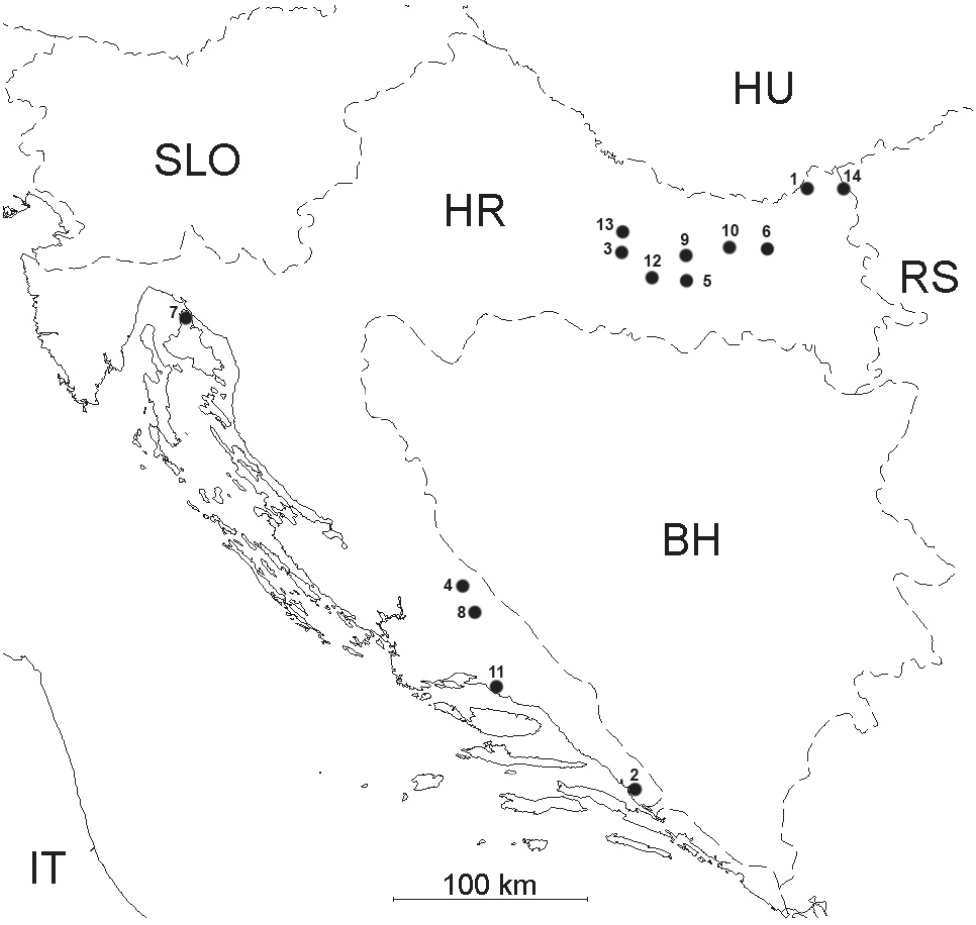

Figure 1. Sampling sites of horseflies (Diptera: Tabanidae) in Croatia: 1 – Branjina, 2 – Desne, 3 – Djedovica (Papuk Mountain), 4 – Donje Maovice, 5 – Kutjevo, 6 – Normanci, 7 – Njivice (Krk Island), 8 – Peruča, 9 – Petrov vrh (Papuk Mountain), 10 – Seona (Našice), 11 – Tugare, 12 – Velika, 13 – Voćin, 14 – Zmajevac. The details about localities can be found in BOLD project CROTA. Acronyms for the countries: HR: Croatia; SLO: Slovenia; HU: Hungary; RS: Republic of Serbia; BH: Bosnia and Herzegovina: IT: Italy.

The BOLD identification tool (http://www.boldsystems.org/index.php/IDS_OpenIdEngine; accessed on 2021-6-6) was used to compare DNA barcode sequences amplified from our samples with the public barcode data available in BOLD. The NCBI GenBank database was searched using the BLAST tool via MegaBlast algorithm (https://blast.ncbi.nlm.nih.gov/Blast.cgi; accessed on 2021-6-6). Publicly available COI sequences of conspecific and congeneric tabanid specimens (preferentially of the species confined to the Palaearctic region) were downloaded from BOLD and used in all subsequent analyses. As outgroups, three species from the family Rhagionidae were used: *Rhagio maculatus* (De Geer, 1776), *Chrysopilus nubecula* (Fallén, 1814) and *Symphoromyia crassicornis* (Panzer, 1806).

The COI sequences were analysed in the three following datasets: 1. tribe Chrysopsini; 2. tribes Haematopotini and Heptatomini united in a single dataset (because

Heptatoma was long considered part of the tribe Haematopotini); 3. tribes Tabanini and Diachlorini united in a single dataset (because the genus *Philipomyia* was until recently considered part of the genus *Tabanus*). Multiple sequence alignments were conducted with MAFFT v. 7, using the "Auto" strategy (Katoh et al. 2019) (https://mafft.cbrc.jp/alignment/server/index.html). Final alignments are given in Suppl. material 2.

Table 1. List of analysed horsefly species from Croatian fauna.

Tribe	Species	locality/region	sample ID/voucher nr.	BOLD process ID nr.	BOLD hit (>98% identity)
Chrysopsini	*Chrysops caecutiens*	Djedovica/CO	SK-4/CROBB288	CROTA004-20	*C. caecutiens*
	Chrysops parallelogrammus	Zmajevac/CO	SK-3/CROBB287	CROTA003-20	*C. parallelogrammus* *
	Chrysops relictus	Zmajevac/CO	SK-1/CROBB285	CROTA001-20	*C. relictus* *
	Chrysops viduatus	Zmajevac/CO	SK-2/CROBB286	CROTA002-20	*C. viduatus*
	Silvius alpinus	Velika/CO	SK-31/CROBB315	CROTA031-20	*S. alpinus* *
Diachlorini	***Dasyrhamphis umbrinus***	Njivice/ME	**SK-28/CROBB312**	CROTA028-20	-
	Philipomyia aprica	Peruča/ME	SK-30/CROBB314	CROTA030-20	*T. bovinus* *
	Philipomyia graeca	Desne/ME	SK-29/CROBB313	CROTA029-20	*T. bovinus* *
Haematopotini	***Haematopota grandis***	Donje Maovice/ME	**SK-42/CROBB326**	CROTA042-20	-
	Haematopota italica	Zmajevac/CO	SK-35/CROBB319	CROTA035-20	*Ha. italica*
	Haematopota pandazisi	Branjina/CO	**SK-34/CROBB318**	CROTA034-20	-
	Haematopota pluvialis	Kutjevo/CO	SK-32/CROBB316	CROTA032-20	*Ha. pluvialis*
	Haematopota scutellata	Djedovica/CO	SK-36/CROBB320	CROTA036-20	*Ha. scutellata* *
	Haematopota subcylindrica	Zmajevac/CO	**SK-33/CROBB317**	CROTA033-20	-
Heptatomini	*Heptatoma pellucens*	Zmajevac/CO	SK-40/CROBB324	CROTA040-20	*He. pellucens* *
Tabanini	*Atylotus loewianus*	Branjina/CO	SK-38/CROBB322	CROTA038-20	*A. loewianus* *
	Atylotus rusticus	Peruča/ME	SK-37/CROBB321	CROTA037-20	*A. rusticus* *
	Hybomitra acuminata	Njivice/ME	**SK-22/CROBB306**	CROTA022-20	-
	Hybomitra bimaculata	Normanci/CO	SK-23/CROBB307	CROTA023-20	*H. bimaculata*
	Hybomitra solstitialis	Zmajevac/CO	**SK-24/CROBB308**	CROTA024-20	-
	Hybomitra distinguenda	Djedovica/CO	SK-25/CROBB309	CROTA025-20	*H. distinguenda* *
	Hybomitra muehlfeldi	Zmajevac/CO	SK-26/CROBB310	CROTA026-20	*H. muehlfeldi* *
	Hybomitra pilosa	Seona/CO	**SK-27/CROBB311**	CROTA027-20	-
	Hybomitra ukrainica	Zmajevac/CO	SK-39/CROBB323	CROTA039-20	*H. solstitialis*
	Tabanus autumnalis	Zmajevac/CO	SK-5/CROBB289	CROTA005-20	*T. autumnalis* *
	Tabanus bifarius	Njivice/ME	**SK-7/CROBB291**	CROTA007-20	-
	Tabanus bovinus	Zmajevac/CO	SK-8/CROBB292	CROTA008-20	*T. sudeticus*
	Tabanus briani	Voćin/CO	**SK-45/ CROBB882**	CROTA045-21	-
	Tabanus bromius	Zmajevac/CO	SK-6/CROBB290	CROTA006-20	*T. bromius*
	Tabanus cordiger	Voćin/CO	SK-9/CROBB293	CROTA009-20	*T. cordiger* *
	Tabanus darimonti	Desne/ME	**SK-10/CROBB294**	CROTA010-20	-
	Tabanus eggeri	Desne/ME	**SK-11/CROBB295**	CROTA011-20	-
	Tabanus exclusus	Tugare/ME	**SK-12/CROBB296**	CROTA012-20	-
	Tabanus glaucopis	Voćin/CO	SK-13/CROBB297	CROTA013-20	*T. glaucopis* *
	Tabanus lunatus	Tugare/ME	**SK-14/CROBB298**	CROTA014-20	-
	Tabanus maculicornis	Normanci/CO	SK-15/CROBB299	CROTA015-20	*T. maculicornis*
	Tabanus miki	Desne/ME	**SK-16/CROBB300**	CROTA016-20	-
	Tabanus quatuornotatus	Donje Maovice/ME	**SK-21/CROBB305**	CROTA021-20	-
	Tabanus rupium	Petrov vrh/CO	SK-17/CROBB301	CROTA017-20	*T. rupium*
	Tabanus shannonellus	Donje Maovice/ME	**SK-43/CROBB327**	CROTA043-20	-
	Tabanus spodopterus	Peruča/ME	SK-41/CROBB325	CROTA041-20	*T. spodopterus* *
	Tabanus sudeticus	Zmajevac/CO	SK-18/CROBB302	CROTA018-20	*T. sudeticus* *
	Tabanus tergestinus	Zmajevac/CO	SK-19/CROBB303	CROTA019-20	*T. tergestinus* *

Region: Continental = CO; Mediterranean = ME. Asterisks (*) denote hits with private records from BOLD database; entries constituting new BINs in BOLD are shown in bold font.

Intraspecific and interspecific *p*-distances were calculated in MEGA v. 7.0.25 (Kumar et al. 2016). Neighbor-joining (NJ) trees based on the *p*-distance model were calculated in MEGA v. 7.0.25, and the robustness of the clades was assessed through 1000 bootstrap replicates. Maximum likelihood (ML) trees were constructed on PhyML 3.0 webserver (Guindon et al. 2010) (http://www.atgc-montpellier.fr/phyml), with automatic model selection by SMS (Smart Model Selection algorithm) (Lefort et al. 2017) determined through Akaike selection criterion, and with aLRT SH-like support (Anisimova and Gascuel 2006). The resulting trees were edited in FigTree v. 1.4.3. (http://tree.bio.ed.ac.uk/software/figtree).

Three species delimitation methods were employed to confirm the assignment of specimens to particular MOTUs. bPTP (Zhang et al. 2013) is a tree-based method using the Poisson tree processes model to infer putative species boundaries on a given phylogenetic input tree. As input for the bPTP (https://species.h-its.org/ptp/), the inferred PhyML trees were used; MCMC (Markov Chain Monte Carlo) analyses were run for 10^6 generations, with a thinning of 200 and burn-in proportion of 0.1; species delimitation was inferred by maximum likelihood solution.

ABGD (Puillandre et al. 2012) and ASAP (Puillandre et al. 2021) are distance-based methods that use threshold values for differentiation between inter- and intraspecific divergences. Both methods indicate the presence of a "barcode gap", thus clustering the samples into putative MOTUs within partitions. ASAP additionally ranks the partitions according to an ad-hoc score computed using the probabilities of groups to be panmictic species and the barcode gap widths (Puillandre et al. 2021). ABGD and ASAP were performed online (https://bioinfo.mnhn.fr/abi/public/abgd/abgdweb.html and https://bioinfo.mnhn.fr/abi/public/asap/asapweb.html, respectively) under default parameters, based on *p*-distances.

Results

In this study, 43 of the 78 Croatian species of horseflies (55%), belonging to the subfamilies Chrysopsinae (genera *Chrysops* and *Silvius*) and Tabaninae (genera *Tabanus*, *Hybomitra*, *Atylotus*, *Haematopota*, *Dasyrhamphis*, *Philipomyia*, and *Heptatoma*), were morphologically identified and their identification was checked by DNA barcoding and species delimitation methods (Table 1). Most of the analysed species belong to the genus *Tabanus* (19 out of 30 recorded species), followed by *Hybomitra* (seven of 17), *Haematopota* (six of nine), *Chrysops* (four of seven), *Atylotus* (two of five), *Philipomyia* (two of two), *Silvius* (one of two), *Heptatoma* (one of one), and *Dasyrhamphis* (one of three species) (Table 1). No species for the genus *Therioplectes* (zero of two recorded) were analysed.

The results of the BOLD identification tool are shown in Table 1. Most of the newly sequenced records have species-level matches in BOLD, but among the matched sequences many are private and therefore not available for further analysis. Among our specimens, 16 have no species-level matches to either public or private data in BOLD

and, thus, constitute new BINs (Barcode Index Numbers, roughly corresponding to MOTUs) in BOLD. These are *Dasyrhamphis umbrinus* (Meigen, 1820), *Haematopota grandis* Meigen, 1820, *Ha. pandazisi* (Kröber, 1936), *Ha. subcylindrica* Pandellé 1883, *Hybomitra acuminata* (Loew, 1858), *H. pilosa* (Loew, 1858), *H. solstitialis* (Meigen, 1820) nec Lyneborg (1959), *Tabanus bifarius* Loew, 1858, *T. briani* Leclercq, 1962, *T. darimonti* Leclercq, 1964, *T. eggeri* Schiner, 1868, *T. exclusus* Pandellé, 1883, *T. lunatus* Fabricius, 1794, *T. miki* Brauer in Brauer & Bergenstamm, 1880, *T. quatuornotatus* Meigen, 1820, and *T. shannonellus* (Kröber, 1936). For 17 additional MOTUs, no public data are available in BOLD (as of July 2021), so these sequences represent the first public entries for the respective species. These are *Atylotus loewianus* (Villeneuve, 1920), *A. rusticus* (Linnaeus, 1767), *C. parallelogrammus* Zeller, 1842, *C. relictus* Meigen, 1820, *Silvius alpinus* (Scopoli, 1763), *Ha. scutellata* (Olsufjev, Moucha & Chvála, 1964), *Heptatoma pellucens* (Fabricius, 1776), *H. distinguenda* (Verrall, 1909), *H. muehlfeldi* (Brauer in Brauer & Bergenstamm, 1880), *Philipomyia aprica* (Meigen, 1820), *P. graeca* (Fabricius, 1794), *T. autumnalis* Linnaeus, 1761, *T. cordiger* Meigen, 1820, *T. glaucopis* Meigen, 1820, *T. spodopterus* Meigen, 1820, *T. sudeticus* Zeller, 1842, and *T. tergestinus* Egger, 1859. Three species of the tribe Diachlorini, sequenced here (*D. umbrinus*, *P. aprica*, and *P. graeca*) represent the first records for this tribe deposited in the BOLD database.

It must be emphasized that under the names of some of these species there are previous BOLD records with sequences that do not match our new entries (i.e., they are classified in separate BOLD BINs, e.g., for *H. solstitialis* and *Ha. pandazisi*), most likely due to misidentification or possible species complexes.

On the other hand, several of our records match the data from BOLD, but these matched sequences were deposited under different species names. For example, our sample of *T. bovinus* Linnaeus, 1758 matches a public BOLD record deposited as *T. sudeticus*, while our sample of *T. sudeticus* matches a public BOLD record of *T. bovinus*; however, the private BOLD database contains high-score hit sequences stored under the matching names for both of our samples (*T. bovinus* and *T. sudeticus*). Our sample of *H. ukrainica* (Olsufjev, 1952) matches several samples deposited in BOLD under the name *H. solstitialis*. Another example is the case of species *P. aprica* and *P. graeca*, for which there are no high-score matches in the public BOLD database, but which have high-score matches with *T. bovinus* from private BOLD records. These cases most likely represent misidentifications of the specimens deposited in BOLD. The results of species delimitation methods for the three datasets are presented in Figs 2–4 and in Suppl. materials 3–5.

The bPTP, ABGD, and ASAP species delimitation methods yielded mostly concordant results, in turn in agreement with BIN-RESL classifications of our newly sequenced specimens (marked on Figs 2–4), with only a few exceptions (namely, for the species pairs *Ha. pluvialis* (Linnaeus, 1758) / *Ha. subcylindrica* and *P. aprica* / *P. graeca*). Most of our records are placed within conspecific MOTUs, except for those that represent new BOLD species entries and therefore form separate MOTUs / BINs (Figs 2–4; Suppl. materials 3–5). In addition, the exceptions are also our samples of

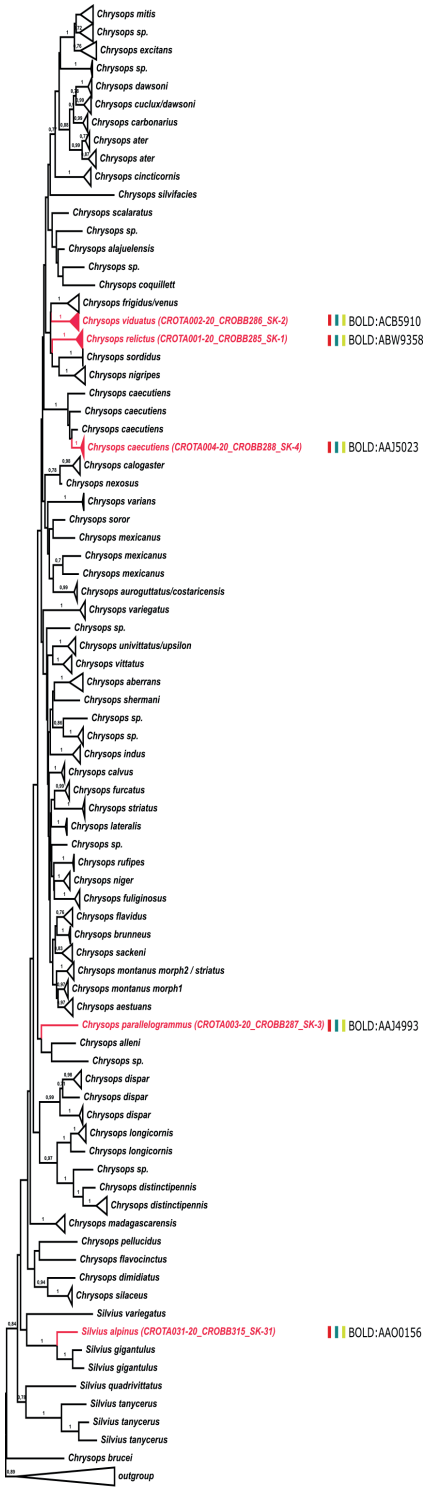
Chrysops mitis
Chrysops sp.
Chrysops excitans
Chrysops sp.
Chrysops dawsoni
Chrysops cuclux/dawsoni
Chrysops carbonarius
Chrysops ater
Chrysops ater
Chrysops cincticornis
Chrysops silvifacies
Chrysops scalaratus
Chrysops sp.
Chrysops alajuelensis
Chrysops sp.
Chrysops coquillett
Chrysops frigidus/venus
Chrysops viduatus (CROTA002-20_CROBB286_SK-2)
BOLD:ACB5910
Chrysops relictus (CROTA001-20_CROBB285_SK-1)
BOLD:ABW9358
Chrysops sordidus
Chrysops nigripes
Chrysops caecutiens
Chrysops caecutiens
Chrysops caecutiens
Chrysops caecutiens (CROTA004-20_CROBB288_SK-4)
BOLD:AAJ5023
Chrysops calogaster
Chrysops nexosus
Chrysops varians
Chrysops soror
Chrysops mexicanus
Chrysops mexicanus
Chrysops mexicanus
Chrysops auroguttatus/costaricensis
Chrysops variegatus
Chrysops sp.
Chrysops univittatus/upsilon
Chrysops vittatus
Chrysops aberrans
Chrysops shermani
Chrysops sp.
Chrysops sp.
Chrysops indus
Chrysops calvus
Chrysops furcatus
Chrysops striatus
Chrysops lateralis
Chrysops sp.
Chrysops rufipes
Chrysops niger
Chrysops fuliginosus
Chrysops flavidus
Chrysops brunneus
Chrysops sackeni
Chrysops montanus morph2 / striatus
Chrysops montanus morph1
Chrysops aestuans
Chrysops parallelogrammus (CROTA003-20_CROBB287_SK-3)
BOLD:AAJ4993
Chrysops alleni
Chrysops sp.
Chrysops dispar
Chrysops dispar
Chrysops dispar
Chrysops longicornis
Chrysops longicornis
Chrysops sp.
Chrysops distinctipennis
Chrysops distinctipennis
Chrysops madagascarensis
Chrysops pellucidus
Chrysops flavocinctus
Chrysops dimidiatus
Chrysops silaceus
Silvius variegatus
Silvius alpinus (CROTA031-20_CROBB315_SK-31)
BOLD:AAO0156
Silvius gigantulus
Silvius gigantulus
Silvius quadrivittatus
Silvius tanycerus
Silvius tanycerus
Silvius tanycerus
Chrysops brucei
outgroup

T. quatuornotatus and *Ha. pandazisi*, which constitute MOTUs / BINs separate from other samples of these two species from BOLD. The MOTUs determined by species delimitation methods are highly supported in the phylogenetic trees, but the relationships between the MOTUs are largely unresolved and generally have much lower support values. In addition, there are cases of inconsistency between formal species designations and positioning within MOTUs. In all three datasets, some of the species are split into more than one MOTU (for example *A. agrestis* (Wiedemann, 1828), *C. caecutiens* (Linnaeus, 1758), *Ha. pandazisi*, *T. bromius* Linnaeus, 1758, *T. quatuornotatus*, etc.). In addition, several MOTUs contain samples that are designated by different names, for example a clade containing samples of *A. agrestis*, *A. diurnus* (Walker, 1850), and *A. nigromaculatus* Ricardo, 1900, or a clade composed of *T. taiwanus* Hayakawa & Takahasi, 1983 and *A. miser* (Szilády, 1915). These cases represent discordant BINs.

All genera within the tribes Chrysopsini and Tabanini appear to be paraphyletic, as well as the tribe Tabanini with respect to the tribe Diachlorini (although with low support).

The range of *p*-distances within MOTUs is 0–2.1%, while the range of those among MOTUs within the tribes is 1.7–14%. The highest intraspecific value of *p*-distances is observed for the species *T. bromius* (2.1%), while the lowest interspecific *p*-distances are recorded for the species pairs *Ha. pluvialis* / *Ha. subcylindrica* (1.8–2.7%) and *P. aprica* / *P. graeca* (1.7%).

Discussion

Studies on vector ecology are crucial for understanding, predicting, and controlling insect-borne diseases. In that instance, national collections of DNA barcodes are particularly useful in cases of medically or veterinary, as well as economically important species. For example, in the recently published DNA barcode collection of German Diptera (Morinière et al. 2019), the authors emphasized the importance of monitoring vector species by metabarcoding. However, COI barcodes for only about 550 out of more than 4400 described tabanid species are presently available in BOLD, and relatively few molecular-level studies have been conducted on the European horsefly fauna (Morinière et al. 2019). Regarding the horsefly species from Croatia, no DNA barcoding data have been available in BOLD up to date.

The high degree of variability in the colouration of the frontal calli, antennae, notopleural lobes, legs, and abdomen in some horsefly species very often leads to confusion,

Figure 2. Maximum likelihood (ML) phylogenetic tree for the tribe Chrysopsini based on COI sequences of specimens sampled in this work and congeneric sequences from BOLD database of public records. The clades corresponding to MOTUs (as determined by species delimitation methods) are collapsed for simplicity; numbers on the nodes denote ML aLRT support (values lower than 0.70 are not shown). MOTUs containing sequences obtained in this study are marked in red; the results of the species delineation methods for the newly sequenced samples are presented as vertical bars beside the respective MOTU clades (bPTP in red; ABGD in green; ASAP in yellow; classification into BOLD BINs as assigned by BIN-RESL).

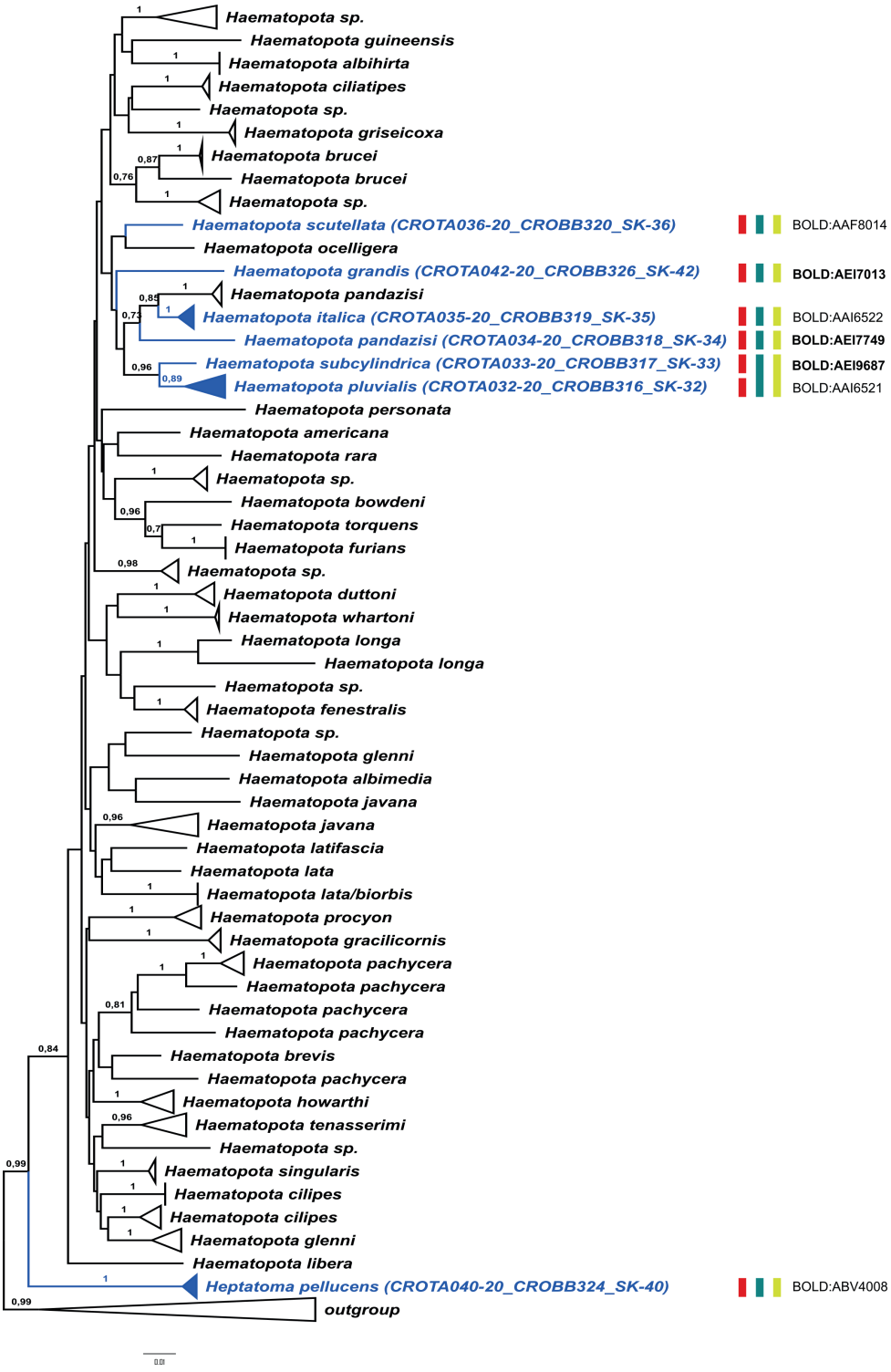
Haematopota sp.
Haematopota guineensis
Haematopota albihirta
Haematopota ciliatipes
Haematopota sp.
Haematopota griseicoxa
Haematopota brucei
Haematopota brucei
Haematopota sp.
Haematopota scutellata (CROTA036-20_CROBB320_SK-36)
Haematopota ocelligera
Haematopota grandis (CROTA042-20_CROBB326_SK-42)
Haematopota pandazisi
Haematopota italica (CROTA035-20_CROBB319_SK-35)
Haematopota pandazisi (CROTA034-20_CROBB318_SK-34)
Haematopota subcylindrica (CROTA033-20_CROBB317_SK-33)
Haematopota pluvialis (CROTA032-20_CROBB316_SK-32)
Haematopota personata
Haematopota americana
Haematopota rara
Haematopota sp.
Haematopota bowdeni
Haematopota torquens
Haematopota furians
Haematopota sp.
Haematopota duttoni
Haematopota whartoni
Haematopota longa
Haematopota longa
Haematopota sp.
Haematopota fenestralis
Haematopota sp.
Haematopota glenni
Haematopota albimedia
Haematopota javana
Haematopota javana
Haematopota latifascia
Haematopota lata
Haematopota lata/biorbis
Haematopota procyon
Haematopota gracilicornis
Haematopota pachycera
Haematopota pachycera
Haematopota pachycera
Haematopota pachycera
Haematopota brevis
Haematopota pachycera
Haematopota howarthi
Haematopota tenasserimi
Haematopota sp.
Haematopota singularis
Haematopota cilipes
Haematopota cilipes
Haematopota glenni
Haematopota libera
Heptatoma pellucens (CROTA040-20_CROBB324_SK-40)
outgroup
BOLD:AAF8014
BOLD:AEI7013
BOLD:AAI6522
BOLD:AEI7749
BOLD:AEI9687
BOLD:AAI6521
BOLD:ABV4008

making correct identification very difficult. In addition, when specimens are old and damaged or missing parts such as antennae, legs, palpi, or hairs on eyes, identification is even more difficult, and errors are quite common. Such misidentifications can also cause incorrect record entries into public databases such as NCBI and BOLD, as we observed in this study. The use of new literature data and DNA sequencing is therefore important for correct insect taxonomy and systematic studies, in order to avoid errors in species identification (Schmidt and Polaszek 2007).

Most European horsefly species belong to the tribe Tabanini, and their representatives are found in all terrestrial zoogeographical regions except those permanently covered with ice (Chvála et al. 1972; Trojan 2001). Within this tribe, the genus *Tabanus* in Europe comprises 4% of all known *Tabanus* species worldwide (Chvála et al. 1972), and it is represented in Croatian horsefly fauna by about 38% of all recorded species. The taxonomy of this genus is quite complex. It is divided into several groups of species according to their morphological characteristics; separation is based mainly on female morphology (Chvála et al. 1972; Suppl. material 1). Some species described as *Tabanus* in the older literature are now referred to other genera (Chvála et al. 1972; Andreeva 2004). For example, the tribe Diachlorini includes several European species of the genus *Philipomyia*, and some genera from the Neotropics have been synonymized with *Tabanus* (Chvála et al. 1972). These taxonomic changes often lead to confusion in tabanid nomenclature, especially among researchers who study medical significance or vector role of this family. A recent study (Werszko et al. 2020) reported vector horsefly species *T. distinguendus* Verrall, 1909 and *T. apricus* Meigen, 1820, although the valid name for *T. distinguendus* is *H. distinguenda* (Verrall, 1909) and that for *T. apricus* is *P. aprica*. Another study, reporting skin lesions caused by bites of *T. bovinus* in Bolivia (Veraldi and Esposito 2017), caught the attention of Dr Stephen M. Smith who reported that the skin damage could not have been caused by bites from *T. bovinus*, since the species does not belong to the Neotropical fauna (Smith 2018). Probably a very high morphological similarity between the Palaearctic species *T. bovinus* and some Neotropical species from the genus *Tabanus* was the reason for these errors. In the European fauna, *T. bovinus* and *T. sudeticus* are morphologically very similar, which often leads to erroneous identification, especially when performed by non-specialists.

In the present study, the COI barcoding region was used for species confirmation. The sequence data enabled us to unequivocally identify some of the horsefly species

Figure 3. ML phylogenetic tree for the tribes Haematopotini and Heptatomini based on COI sequences of specimens sampled in this work and congeneric sequences from BOLD database of public records. The clades corresponding to MOTUs (as determined by species delimitation methods) are collapsed for simplicity; numbers on the nodes denote ML aLRT support (values lower than 0.70 are not shown). MOTUs containing sequences obtained in this study are marked in blue; the results of the species delineation methods for the newly sequenced samples are presented as vertical bars beside the respective MOTU clades (bPTP in red; ABGD in green; ASAP in yellow; classification into BOLD BINs as assigned by BIN-RESL, with newly established BINs marked in bold font).

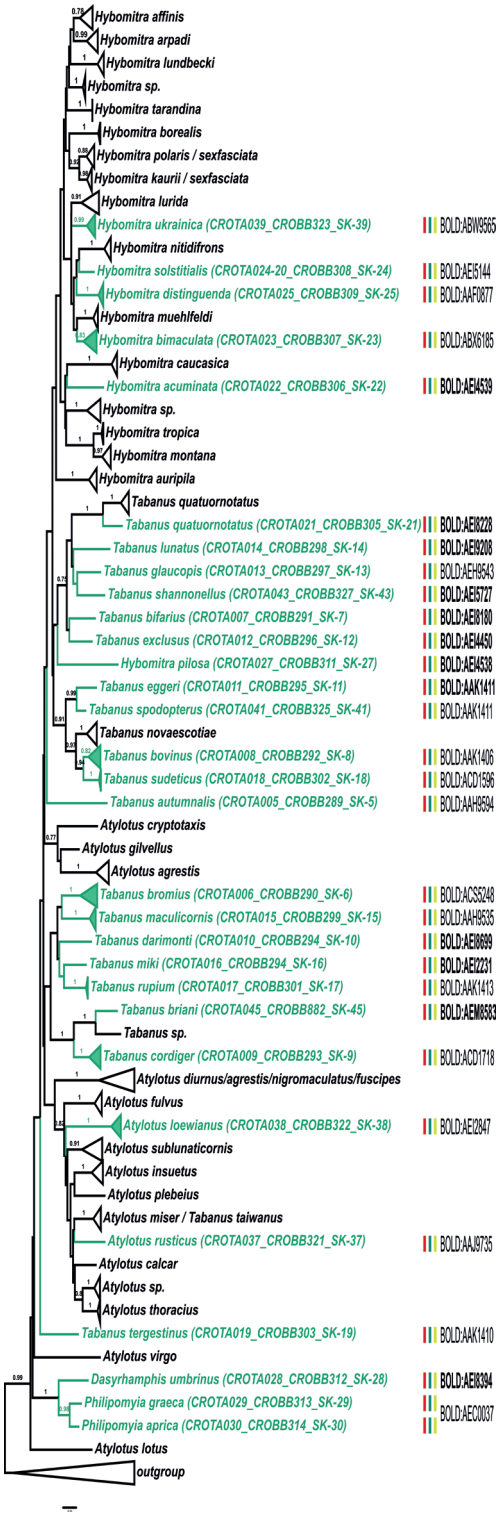
Hybomitra affinis
Hybomitra arpadi
Hybomitra lundbecki
Hybomitra sp.
Hybomitra tarandina
Hybomitra borealis
Hybomitra polaris / sexfasciata
Hybomitra kaurii / sexfasciata
Hybomitra lurida
Hybomitra ukrainica (CROTA039_CROBB323_SK-39) BOLD:ABW9965
Hybomitra nitidifrons
Hybomitra solstitialis (CROTA024-20_CROBB308_SK-24) BOLD:AEI6144
Hybomitra distinguenda (CROTA025_CROBB309_SK-25) BOLD:AAF0877
Hybomitra muehlfeldi
Hybomitra bimaculata (CROTA023_CROBB307_SK-23) BOLD:ABX6185
Hybomitra caucasica
Hybomitra acuminata (CROTA022_CROBB306_SK-22) BOLD:AEI4539
Hybomitra sp.
Hybomitra tropica
Hybomitra montana
Hybomitra auripila
Tabanus quatuornotatus
Tabanus quatuornotatus (CROTA021_CROBB305_SK-21) BOLD:AEI8228
Tabanus lunatus (CROTA014_CROBB298_SK-14) BOLD:AEI9208
Tabanus glaucopis (CROTA013_CROBB297_SK-13) BOLD:AEH9543
Tabanus shannonellus (CROTA043_CROBB327_SK-43) BOLD:AEI5727
Tabanus bifarius (CROTA007_CROBB291_SK-7) BOLD:AEI8180
Tabanus exclusus (CROTA012_CROBB296_SK-12) BOLD:AEI4450
Hybomitra pilosa (CROTA027_CROBB311_SK-27) BOLD:AEI4538
Tabanus eggeri (CROTA011_CROBB295_SK-11) BOLD:AAK1411
Tabanus spodopterus (CROTA041_CROBB325_SK-41) BOLD:AAK1411
Tabanus novaescotiae
Tabanus bovinus (CROTA008_CROBB292_SK-8) BOLD:AAK1406
Tabanus sudeticus (CROTA018_CROBB302_SK-18) BOLD:ACD1596
Tabanus autumnalis (CROTA005_CROBB289_SK-5) BOLD:AAH0594
Atylotus cryptotaxis
Atylotus gilvellus
Atylotus agrestis
Tabanus bromius (CROTA006_CROBB290_SK-6) BOLD:ACS5248
Tabanus maculicornis (CROTA015_CROBB299_SK-15) BOLD:AAH9535
Tabanus darimonti (CROTA010_CROBB294_SK-10) BOLD:AEI8699
Tabanus miki (CROTA016_CROBB294_SK-16) BOLD:AEI2231
Tabanus rupium (CROTA017_CROBB301_SK-17) BOLD:AAK1413
Tabanus briani (CROTA045_CROBB882_SK-45) BOLD:AEM9583
Tabanus sp.
Tabanus cordiger (CROTA009_CROBB293_SK-9) BOLD:ACD1718
Atylotus diurnus/agrestis/nigromaculatus/fuscipes
Atylotus fulvus
Atylotus loewianus (CROTA038_CROBB322_SK-38) BOLD:AEI2847
Atylotus sublunaticornis
Atylotus insuetus
Atylotus plebeius
Atylotus miser / Tabanus taiwanus
Atylotus rusticus (CROTA037_CROBB321_SK-37) BOLD:AAJ9735
Atylotus calcar
Atylotus sp.
Atylotus thoracius
Tabanus tergestinus (CROTA019_CROBB303_SK-19) BOLD:AAK1410
Atylotus virgo
Dasyrhamphis umbrinus (CROTA028_CROBB312_SK-28) BOLD:AEI8394
Philipomyia graeca (CROTA029_CROBB313_SK-29) BOLD:AEC0037
Philipomyia aprica (CROTA030_CROBB314_SK-30)
Atylotus lotus
outgroup

which are morphologically very similar, for instance, the already mentioned *T. bovinus* and *T. sudeticus*, but also some others, like *H. solstitialis* / *H. ukrainica* and *T. maculicornis* / *T. bromius* (mentioned in Suppl. material 1). In the Palaearctic region, identification of species from the genus *Hybomitra* is often difficult due to variability in colouration and uncertainty about structural features (Zeegers 2018; see Suppl. material 1). When the occurrence of *H. ukrainica* in the Croatian fauna was first reported (Krčmar and Majer 1994), a revision of the horsefly collections in Croatian Natural History Museum in Zagreb in 2001 revealed that this species had already been collected in Croatia in 1982, 1987, 1988, and 1989 (Krčmar and Mikuska 2001) but had been incorrectly identified as *H. solstitialis*, formerly called *H. ciureai* (Séguy, 1937). Since the 1950s, the name *H. solstitialis* has been misinterpreted in the European literature, although *H. ciureai* was originally described as a variety of *H. solstitialis* (Zeegers 2018). Despite well-illustrated morphological characters relevant for identification of *H. ukrainica* and *H. ciureai* (now *H. solstitialis*) (Mally 1985), mistakes are still possible due to high morphological similarity. Therefore, for the identification of these two species belonging to "*bimaculata*" group, molecular analyses are necessary. The results of our analyses confirm a significant genetic divergence in the standard COI barcoding region between these two species (*H. solstitialis* and *H. ukrainica*) and prove that DNA barcoding is informative enough for their unequivocal distinction. Moreover, our results reveal high levels of genetic variability within some of the currently recognized tabanid taxa, reflected through their splitting in multiple separate MOTUs. This finding is also consistent with previous studies (Morita et al. 2016; Morinière et al. 2019) and indicates the possibility of cryptic diversity or the existence of species complexes not yet recognized. In that context, it is interesting to note that our specimens of *T. quatuornotatus* and *Ha. pandazisi* constitute new BINs in BOLD, genetically diverged from other samples denoted with the same names. Other evident examples are *A. agrestis*, which appears in several clearly separated OTUs scattered in the phylogenetic tree, or several species of *Chrysops*, which appear in multiple OTUs each.

On the other hand, our data suggests high genetic similarity in the DNA barcoding region between some of the species, leading to incongruence between the results of the different species delimitation methods. For example, the range of *p*-distances for *Ha. pluvialis* and *Ha. subcylindrica* is 1.8–2.7%, and both the BIN-RESL algorithm and bPTP recognized them as separate MOTUs. In contrast, the ABGD and ASAP methods recovered these two species in a single MOTU (Fig. 3). *Ha. pluvialis* is very

Figure 4. ML phylogenetic tree for the tribes Tabanini and Diachlorini based on COI sequences of specimens sampled in this work and congeneric sequences from BOLD database of public records. The clades corresponding to MOTUs (as determined by species delimitation methods) are collapsed for simplicity; numbers on the nodes denote ML aLRT support (values < 0.70 are not shown). MOTUs containing sequences obtained in this study are marked in green; the results of the species delineation methods for the newly sequenced samples are presented as vertical bars beside the respective MOTU clades (bPTP in red; ABGD in green; ASAP in yellow; classification into BOLD BINs as assigned by BIN-RESL, with newly established BINs marked in bold font).

similar to *Ha. subcylindrica* so the identification and separation of these two species is sometimes very difficult on morphological basis (see Suppl. material 1). A similar situation is observed for *P. aprica* and *P. graeca*. These two species are mainly distinguished by the colouration of the abdomen and the shape and colouration of antennae. The inferred *p*-distances for these two species (1.7%) are below the standard threshold for BIN separation in BOLD and they have been classified within the same BIN; however, species delimitation methods bPTP, ABGD, and ASAP all recovered them in two separate MOTUs (Fig. 4). Besides a high degree of morphological similarity, the species within each of these two species pairs (*Ha. pluvialis* / *Ha. subcylindrica* and *P. aprica* / *P. graeca*) also share some ecological characteristics: they inhabit the same regions, occur at the same time, and their flight period is almost the same; however, *P. aprica* prefers mountainous habitats. Therefore, the high genetic similarity of the species within these two species pairs could also be indicative of their close evolutionary relationship. Other than in these two cases of high genetic similarity which caused the incongruence between various species-delimitation methods, other investigated MOTUs are clearly distinguished through non-overlapping low intraspecific and high interspecific variability, indicating the existence of a barcoding gap which is a prerequisite for efficient and reliable DNA barcoding (Hebert et al. 2003).

Analyses of various molecular markers have been used worldwide in the study of the taxonomy, phylogeography and phylogenetics of horseflies (Sofield et al. 1984; Wiegmann et al. 2000; Iranpour et al. 2004; Cywinska et al. 2010; Morita et al. 2016; Sanal Demirci et al. 2021); however, many phylogenetic aspects of this family still remain unclear (Morita et al. 2016; Votýpka et al. 2019). One of the most comprehensive studies of phylogenetic relationships within the family Tabanidae and its subfamilies and tribes was conducted using several genetic markers: mitochondrial COI, nuclear 28S rRNA, CAD (carbamoyl-phosphate synthetase 2, aspartate transcarbamylase and dihydroorotase), and AATS (alanyl-tRNA synthetase) (Morita et al. 2016). The authors reported that the classification of Tabanidae should be reconsidered based on the new data obtained by molecular techniques. Their main finding was the paraphyly of the Chrysopsinae, as already proposed by Mackerras (1954). However, the tribes Pangoniini and Tabanini could also be paraphyletic, although the support for this is weak. In addition, most genera within the tribes Chrysopsini and Tabanini appear to be paraphyletic. For example, the large genus *Tabanus*, which is one of the most diversified genera in Diptera, is most likely paraphyletic with respect to several other genera (Morita et al. 2016).

Although our analyses are based on a single mitochondrial locus, most of the results are consistent with previous studies (Morita et al. 2016; Changbunjong et al. 2018). Analysis of the tribes Tabanini and Diachlorini resulted in Diachlorini embedded within the Tabanini, with *A. lotus* Burton, 1978 positioned as basal to all other Tabanini and Diachlorini, suggesting the paraphyly of the tribe Tabanini. In addition, all genera within the tribes Chrysopsini and Tabanini—*Chrysops* and *Silvius* in Chrysopsinae, and *Hybomitra*, *Atylotus*, and *Tabanus* in Tabaninae—appear to be mutually paraphyletic. However, most of these results have low support, similar to previous studies, and further work is required to obtain useful data for correct classification.

Molecular markers for phylogenetic studies of horseflies in Croatian fauna were first used in 2006 (Biruš 2006). In that study, the phylogenetic relationships between several species of the horsefly genera *Philipomyia*, *Dasyrhamphis* (both from the tribe Diachlorini), and *Tabanus* (from the tribe Tabanini) were investigated using 16S rRNA and COI mitochondrial genes. The sequence-based phylogenetic data supported the recent morphology-based classification of two horsefly species, *P. aprica* and *P. graeca*, within the new genus *Philipomyia* (these two species were previously classified in the genus *Tabanus*) and the placement of this genus in the tribe Diachlorini rather than in the tribe Tabanini (Biruš 2006). Our results are consistent with these data: both species of *Philipomyia* are positioned in a highly supported monophyletic clade along with *D. umbrinus*.

Among all representatives of the subfamily Tabaninae, *He. pellucens* is the only species with a unique morphological feature, a totally bare subcostal vein (Trojan 1994). Moreover, the differences in larval forms between species of the genera *Heptatoma* and *Haematopota* confirm the necessary separation of the genus *Heptatoma* into a separate tribe (Andreeva 2004). The results of our analysis also support that conclusion, with *Heptatoma* being positioned basally to all species of Haematopotini, thus rendering the former tribe monophyletic.

Conclusion

In this paper, 55% of the horsefly species known from Croatia were analysed by DNA barcoding, which proved to be an effective tool for their identification. The obtained data provide a basis for a reference library of Tabanidae DNA barcodes for the investigated region and contribute to BOLD through the addition of 16 new BINs. The presented results also indicate some inconsistencies in the taxonomy and systematics of horseflies, mostly in line with previous systematic studies. However, considering the shortcomings of a single-locus approach for systematic studies, a more comprehensive integrative approach covering a broader range of taxa and additional molecular markers is needed to address these issues.

Acknowledgements

The authors wish to thank Prof. Chiara Scapoli, University of Ferrara, for critical reading of the manuscript and valuable suggestions. Comments from an anonymous reviewer significantly improved the manuscript.

This research was funded by Department of Biology, Josip Juraj Strossmayer University of Osijek (to Prof. S.K.) and by the Croatian Science Foundation under the projects IP-2016-06-9988 “DNA Barcoding of Biodiversity of Croatian Fauna” (P.I. Prof. M.K.) and IP-2019-04-6915 “Alpha Satellite DNA in Evolution of Gene Modulatory Networks” (P.I. Prof. Đurđica Ugarković).

References

Aibulatov S, Chetverikova T, Chetverikov P (2012) List of horseflies (Diptera: Tabanidae) from Belgrade neighbourhoods (Serbia). Acta Entomologica Serbica 17: 167–169.

Andreeva RV (2004) Additions and comments to the Catalogue of Palearctic Diptera (Tabanidae). Zeitschrift der Arbeitsgemeinschaft Österreichischer Entomologen 56: 93–106.

Anisimova M, Gascuel O (2006) Approximate likelihood-ratio test for branches: a fast, accurate, and powerful alternative. Systematic Biology 55: 539–552. https://doi.org/10.1080/10635150600755453

Baldacchino F, Desquesnes M, Mihok S, Foil LD, Duvallet G, Jittapalapong S (2014) Tabanids: neglected subjects of research, but important vectors of disease agents! Infection, Genetics and Evolution 28: 596–615. https://doi.org/10.1016/j.meegid.2014.03.029

Banerjee D, Kumar V, Maity A, Ghosh B, Tyagi K, Singha D, Kundu S, Laskar BA, Naskar A, Rath S (2015) Identification through DNA barcoding of Tabanidae (Diptera) vectors of surra disease in India. Acta Tropica 150: 52–58. https://doi.org/10.1016/j.actatropica.2015.06.023

Biruš I (2006) Phylogenetic analysis of horseflies (Diptera: Tabanidae) belonging to genera *Tabanus* and *Philipomyia* by comparison of mitochondrial DNA. Master of Science thesis, University of Zagreb.

Chainey JE (1993) Horse-flies, deer-flies and clegs (Tabanidae). In: Lane RP, Crosskey RW (Eds) Medical Insects and Arachnids. Springer Netherlands, Dordrecht, 310–332. https://doi.org/10.1007/978-94-011-1554-4_8

Changbunjong T, Bhusri B, Sedwisai P, Weluwanarak T, Nitiyamatawat E, Chareonviriyaphap T, Ruangsittichai J (2018) Species identification of horse flies (Diptera: Tabanidae) in Thailand using DNA barcoding. Veterinary Parasitology 259: 35–43. https://doi.org/10.1016/j.vetpar.2018.07.002

Changbunjong T, Weluwanarak T, Sedwisai P, Ruangsittichai J, Duvallet G, Chareonviriyaphap T (2020) New records and DNA barcoding of deer flies, *Chrysops* (Diptera: Tabanidae) in Thailand. Acta Tropica 210: e105532. https://doi.org/10.1016/j.actatropica.2020.105532

Cheke RA, Mas J, Chainey JE (2003) Potential vectors of loiasis and other tabanids on the island of Bioko, Equatorial Guinea. Medical and Veterinary Entomology 17: 221–223. https://doi.org/10.1046/j.1365-2915.2003.00436.x

Chippaux J-P, Bouchité B, Demanou M, Morlais I, Le Goff G (2000) Density and dispersal of the loaiasis vector *Chrysops dimidiata* in southern Cameroon. Medical and Veterinary Entomology 14: 339–344. https://doi.org/10.1046/j.1365-2915.2000.00249.x

Chvála M (1988) Family Tabanidae. In: Soós Á (Ed.) Catalogue of Palaearctic Diptera, Athericidae – Asilidae. Akadémiai Kiadó, Budapest, 97–171.

Chvála M, Lyneborg L, Moucha J (1972) The horse flies of Europe (Diptera, Tabanidae). Entomological Society of Copenhagen, Copenhagen.

Cywinska A, Hannan MA, Kevan PG, Roughley RE, Iranpour M, Hunter FF (2010) Evaluation of DNA barcoding and identification of new haplomorphs in Canadian deerflies and horseflies. Medical and Veterinary Entomology 24: 382–410. https://doi.org/10.1111/j.1365-2915.2010.00896.x

Desquesnes M, Dia ML (2004) Mechanical transmission of *Trypanosoma vivax* in cattle by the African tabanid *Atylotus fuscipes*. Veterinary Parasitology 119: 9–19. https://doi.org/10.1016/j.vetpar.2003.10.015

Foil LD (1989) Tabanids as vectors of disease agents. Parasitology Today 5: 88–96. https://doi.org/10.1016/0169-4758(89)90009-4

Guindon S, Dufayard J-F, Lefort V, Anisimova M, Hordijk W, Gascuel O (2010) New algorithms and methods to estimate maximum-likelihood phylogenies: assessing the performance of PhyML 3.0. Systematic Biology 59: 307–321. https://doi.org/10.1093/sysbio/syq010

Hebert PDN, Cywinska A, Ball SL, deWaard JR (2003) Biological identifications through DNA barcodes. Proceedings of the Royal Society B: Biological Sciences 270: 313–321. https://doi.org/10.1098/rspb.2002.2218

Hribar LJ, Leprince DJ, Foil LD (1991) Design for a canopy trap for collecting horse flies (Diptera: Tabanidae). Journal of the American Mosquito Control Association 7: 657–659.

Iranpour M, Schurko AM, Klassen GR, Galloway TD (2004) DNA fingerprinting of tabanids (Diptera: Tabanidae) and their respective egg masses using PCR—restriction fragment profiling. The Canadian Entomologist 136: 605–619. https://doi.org/10.4039/n03-076

Ježek J, Tkoč M, van Harten A (2017) Order Diptera, family Tabanidae. In: van Harten A (Ed.) Arthropod Fauna of the UAE. Department of the President's Affairs, United Arab Emirates 6: 477–537.

Katoh K, Rozewicki J, Yamada KD (2019) MAFFT online service: multiple sequence alignment, interactive sequence choice and visualization. Briefings in Bioinformatics 20: 1160–1166. https://doi.org/10.1093/bib/bbx108

Krčmar S (2011) Preliminary list of horse flies (Diptera: Tabanidae) of Serbia. ZooKeys 117: 73–81. https://doi.org/10.3897/zookeys.117.1328

Krčmar S, Majer J (1994) *Hybomitra ukrainica* (Olsufjev, 1952) a new species in the fauna of horse flies (Diptera, Tabanidae) in Croatia. Natura Croatica 3: 261–264.

Krčmar S, Bogdanović T (2001) List of Tabanidae (Diptera) in Slovenia. Folia Entomologica Hungarica 62: 257-262.

Krčmar S, Mikuska J (2001) The horseflies of Eastern Croatia (Diptera: Tabanidae). Anali Zavoda za znanstveni i umjetnički rad u Osijeku 17: 91–146.

Krčmar S, Mikuska J, Chvála M (2002) Tabanidae (Diptera) of Western and Central Balkans—Bosnia and Herzegovina, Serbia, Montenegro, Vojvodina, Kosovo and Macedonia. Acta Universitatis Carolinae Biologica 46: 305–320.

Krčmar S, Hackenberger DK, Hackenberger BK (2011) Key to the horse flies fauna of Croatia (Diptera, Tabanidae). Periodicum Biologorum 113: 1–61.

Kumar S, Stecher G, Tamura K (2016) MEGA7: Molecular Evolutionary Genetics Analysis version 7.0 for bigger datasets. Molecular Biology and Evolution 33: 1870–1874. https://doi.org/10.1093/molbev/msw054

Lefort V, Longueville J-E, Gascuel O (2017) SMS: Smart Model Selection in PhyML. Molecular Biology and Evolution 34: 2422–2424. https://doi.org/10.1093/molbev/msx149

Mackerras IM (1954) Classification and distribution of Tabanidae (Diptera). Australian Journal of Zoology 2: 431–454. https://doi.org/10.1071/ZO9540431

Majer J (2001) Tabanidae. In: Papp L, Ádám L, Černý M, Darvas B, Dely-Draskovits Á, Déval Gy, Földvári M, Krzemińska E, Majer J, Martinovský J, Merz B, Mohrig W, Móra A, Rulik B, Ševčik J, Skuhravá M, Starý J, Tóth S, van der Weele R, Zatwarnicki T (Eds) Checklist of the Diptera of Hungary. Hungarian Natural History Museum, Budapest, 142-145.

Mally M (1985) *Hybomitra ucrainica* (Olsufjev, 1952) und *Hybomitra ciureai* (Séguy, 1937) – morphologische Differenzen (Diptera, Tabanidae). Zeitschrift der Arbeitsgemeinschaft Österreichen Entomologen 37: 121–125.

Mazumdar S, Hebert PDN, Bhuiya BA (2021) A survey of true flies (Insecta: Diptera) by DNA barcoding of Malaise trap collection in Bangladesh. Journal of Insect Biodiversity and Systematics 7: 15–42. https://doi.org/10.52547/jibs.7.1.15

Mihok, S (2002) The development of a multipurpose trap (the Nzi) for tsetse and other biting flies. Bulletin of Entomological Research 92: 385–403. https://doi.org/10.1079/BER2002186

Mikuška A, Krčmar S, Mikuska J (2008) Horse flies (Tabanidae) of Bosnia and Herzegovina. Journal of Vector Ecology 33: 365–369. https://doi.org/10.3376/1081-1710-33.2.365

Morinière J, Balke M, Doczkal D, Geiger MF, Hardulak LA, Haszprunar G, Hausmann A, Hendrich L, Regalado L, Rulik B, Schmidt S, Wägele J-W, Hebert PDN (2019) A DNA barcode library for 5,200 German flies and midges (Insecta: Diptera) and its implications for metabarcoding-based biomonitoring. Molecular Ecology Resources 19: 900–928. https://doi.org/10.1111/1755-0998.13022

Morita SI, Bayless KM, Yeates DK, Wiegmann BM (2016) Molecular phylogeny of the horse flies: a framework for renewing tabanid taxonomy: horsefly phylogeny. Systematic Entomology 41: 56–72. https://doi.org/10.1111/syen.12145

Mugasa CM, Villinger J, Gitau J, Ndungu N, Ciosi M, Masiga D (2018) Morphological redescription and molecular identification of Tabanidae (Diptera) in East Africa. ZooKeys 769: 117–144. https://doi.org/10.3897/zookeys.769.21144

Nitiyamatawat E, Changbunjong T, Sumruayphol S, Sriwichai P, Thaenkham U, Ruangsitichai J (2017) DNA barcoding for identification of cleg flies, *Haematopota* spp. (Diptera: Tabanidae) in Thailand. Thai Journal of Veterinary Medicine 47: 303–305.

Pape T, Blagoderov V, Mostovski MB (2011) Order Diptera Linnaeus, 1758. Zootaxa 3148: 222–229. https://doi.org/10.11646/zootaxa.3148.1.42

Pape T, Beuk P, Pont A, Shatalkin A, Ozerov A, Woźnica A, Merz B, Bystrowski C, Raper C, Bergström C, Kehlmaier C, Clements D, Greathead D, Kameneva E, Nartshuk E, Petersen F, Weber G, Bächli G, Geller-Grimm F, Van de Weyer G, Tschorsnig H, de Jong H, van Zuijlen J, Vaňhara J, Roháček J, Ziegler J, Majer J, Hurka K, Holston K, Rognes K, Greve-Jensen L, Munari L, de Meyer M, Pollet M, Speight M, Ebejer M, Martinez M, Carles-Tolrá M, Földvári M, Chvála M, Barták M, Evenhuis N, Chandler P, Cerretti P, Meier R, Rozkosny R, Prescher S, Gaimari S, Zatwarnicki T, Zeegers T, Dikow T, Korneyev V, Richter V, Michelsen V, Tanasijtshuk V, Mathis W, Hubenov Z, de Jong Y (2015) Fauna Europaea: Diptera-Brachycera. Biodiversity Data Journal 3: e4187. https://doi.org/10.3897/BDJ.3.e4187

Puillandre N, Brouillet S, Achaz G (2021) ASAP: assemble species by automatic partitioning. Molecular Ecology Resources 21: 609–620. https://doi.org/10.1111/1755-0998.13281

Puillandre N, Lambert A, Brouillet S, Achaz G (2012) ABGD, Automatic Barcode Gap Discovery for primary species delimitation: ABGD, Automatic Barcode Gap Discovery. Molecular Ecology 21: 1864–1877. https://doi.org/10.1111/j.1365-294X.2011.05239.x

Ratnasingham S, Hebert PDN (2013) A DNA-based registry for all animal species: the Barcode Index Number (BIN) system. PLoS ONE 8: e66213. https://doi.org/10.1371/journal.pone.0066213

Sanal Demirci SN, Kilic V, Mutun S, Kilic AY (2021) Population genetics and phylogeography of *Tabanus bromius* (Diptera: Tabanidae). Parasites & Vectors 14: e453. https://doi.org/10.1186/s13071-021-04970-5

Schmidt S, Polaszek A (2007) *Encarsia* or *Encarsiella*?—redefining generic limits based on morphological and molecular evidence (Hymenoptera, Aphelinidae). Systematic Entomology 32: 81–94. https://doi.org/10.1111/j.1365-3113.2006.00364.x

Smith SM (2018) *Tabanus bovinus* in Bolivia? Journal of Travel Medicine 25: e1. https://doi.org/10.1093/jtm/tax088

Sofield RK, Douglas ME, Hansens EJ, Vrijenhoek RC (1984) Diagnosis and detection of cryptic species: the *Tabanus nigrovittatus* complex (Diptera: Tabanidae) in coastal New Jersey. Annals of the Entomological Society of America 77: 587–591. https://doi.org/10.1093/aesa/77.5.587

Townes H (1972) A light-weight Malaise trap. Entomological News 83: 239–247.

Trojan P (1994) Supraspecific taxa of Tabaninae (Diptera, Tabanidae). I. The definition of the subfamily and its tribes. Annals of the Upper Silesian Museum (Entomology) 5: 53–67.

Trojan P (2001) Supraspecific taxa of Tabaninae (Diptera: Tabanidae) IV. The tribe Tabanini and its taxonomic division. Annals of the Upper Silesian Museum (Entomology) 10–11: 31–62.

Veraldi S, Esposito L (2017) Skin lesions caused by *Tabanus bovinus* bites. Journal of Travel Medicine 24(5): 1–3. https://doi.org/10.1093/jtm/tax049

Votýpka J, Brzoňová J, Ježek J, Modrý D (2019) Horse flies (Diptera: Tabanidae) of three West African countries: a faunistic update, barcoding analysis and trypanosome occurrence. Acta Tropica 197: e105069. https://doi.org/10.1016/j.actatropica.2019.105069

Werszko J, Szewczyk T, Steiner-Bogdaszewska Ż, Wróblewski P, Karbowiak G, Laskowski Z (2020) Molecular detection of *Megatrypanum* trypanosomes in tabanid flies. Medical and Veterinary Entomology 34: 69–73. https://doi.org/10.1111/mve.12409

Wiegmann BM, Tsaur S-C, Webb DW, Yeates DK, Cassel BK (2000) Monophyly and relationships of the Tabanomorpha (Diptera: Brachycera) Based on 28S ribosomal gene sequences. Annals of the Entomological Society of America 93: 1031–1038. https://doi.org/10.1603/0013-8746(2000)093[1031:MAROTT]2.0.CO;2

Zeegers T (2018) A new synonymy in the horsefly genus *Hybomitra* (Diptera: Tabanidae). Nederlandse Faunistische Mededelingen 50: 89–92.

Zhang J, Kapli P, Pavlidis P, Stamatakis A (2013) A general species delimitation method with applications to phylogenetic placements. Bioinformatics 29: 2869–2876. https://doi.org/10.1093/bioinformatics/btt499

Supplementary material 1

Morphological characteristics of females of some horseflies from subfamily Tabaninae and Chrysopsinae

Author: Stjepan Krčmar

Data type: pdf file

Explanation note: Morphological characteristics of females of some horseflies from subfamily Tabaninae and Chrysopsinae, important for species identification (presented according to Chvála et al. (1972) and Zeegers (2018)).

Link: https://doi.org/10.3897/zookeys.1087.78707.suppl1

Supplementary material 2

COI multiple sequence alignments

Author: Branka Bruvo Mađarić

Data type: docx file

Explanation note: MAFFT multiple alignments of COI nucleotide sequences (in fasta format) for the tree datasets: 1. Chrysopsini; 2. Haematopotini and Heptatomini; 3. Tabanini and Diachlorini.

Link: https://doi.org/10.3897/zookeys.1087.78707.suppl2

Supplementary material 3

Figure S1. NJ tree for the tribe Chrysopsini

Author: Branka Bruvo Mađarić

Data type: pdf file

Link: https://doi.org/10.3897/zookeys.1087.78707.suppl3

Supplementary material 4

Figure S2. NJ tree for the tribes Haematopotini and Heptatomini
Author: Branka Bruvo Mađarić
Data type: pdf file

Link: https://doi.org/10.3897/zookeys.1087.78707.suppl4

Supplementary material 5

Figure S3. NJ tree for the tribes Tabanini and Diachlorini
Author: Branka Bruvo Mađarić
Data type: pdf file

Link: https://doi.org/10.3897/zookeys.1087.78707.suppl5

ZooKeys 1087: 163–198 (2022)
doi: 10.3897/zookeys.1087.78193
https://zookeys.pensoft.net

RESEARCH ARTICLE

A peer-reviewed open-access journal
ZooKeys
Launched to accelerate biodiversity research

Molecular phylogeny of *Nipponacmea* (Patellogastropoda, Lottiidae) from Japan: a re-evaluation of species taxonomy and morphological diagnosis

Shinnosuke Teruya[1,2], Davin H. E. Setiamarga[2,3], Tomoyuki Nakano[4], Takenori Sasaki[2]

1 *Okinawa Prefectural Deep Sea Water Research Center, 500-1 Maja, Kumejima-cho, Okinawa 901-3104, Japan* **2** *The University Museum, The University of Tokyo, 7-3-1 Hongo, Bunkyo-ku, Tokyo 113-0033, Japan* **3** *Department of Applied Chemistry and Biochemistry / Ecosystem Engineering, National Institute of Technology (KOSEN), Wakayama College, 77 Noshima, Nada-cho, Gobo-shi, Wakayama, 644-0023, Japan* **4** *Seto Marine Biological Laboratory, Field Science Education and Research Centre, Kyoto University, 459 Shirahama, Wakayama, 649-2211, Japan*

Corresponding author: Shinnosuke Teruya (shi.teruya@gmail.com)

Academic editor: E. Gittenberger | Received 24 November 2021 | Accepted 21 January 2022 | Published 25 February 2022

http://zoobank.org/DB9F75BC-4C7F-4679-B327-43C977C6B31C

Citation: Teruya S, Setiamarga DHE, Nakano T, Sasaki T (2022) Molecular phylogeny of *Nipponacmea* (Patellogastropoda, Lottiidae) from Japan: a re-evaluation of species taxonomy and morphological diagnosis. ZooKeys 1087: 163–198. https://doi.org/10.3897/zookeys.1087.78193

Abstract

The patellogastropod limpet genus *Nipponacmea* is widely distributed in Japan and adjacent East Asia. Species identification within *Nipponacmea* is challenging due to the high variation in shell morphology. In this study, we examined the taxonomy of this genus represented by nine nominal species from 43 localities (including type localities). Results of the molecular phylogenetic analysis revealed that: (1) *N. gloriosa*, the sole species in this genus inhabiting the subtidal zone, represents the most basal independent branch; (2) the remaining species are divided into two large clades with lower- and higher-apex shell profiles; and (3) the high-apex morphology was derived from the low-apex type. The terminal clades defined using the molecular data were consistent with nine morphospecies and had 100% bootstrap values, strongly supporting the conventional taxonomy of *Nipponacmea*. Although morphological similarities do not always reflect phylogeny, the set of morphological characters used in the current taxonomy were proven to be adequate for diagnosis. In conclusion, this study provided solid evidence to uphold the monophyly of known species of *Nipponacmea* in Japan and demonstrated the usefulness of morphological characters for species diagnosis.

Keywords

Lottiidae, morphology, *Nipponacmea*, phylogeny, taxonomy

Introduction

Limpets belonging to the clade Patellogastropoda are abundant in the intertidal rocky shores globally and are important in marine biology (Branch 1985a, b). Species taxonomy of patellogastropods has historically been based on the morphology of the shell and radula (Pilsbry 1891; Suter 1907; Oliver 1926; Powell 1973; Ponder and Creese 1980). However, identification of the members of this group is difficult due to the simplicity and high variability of shell morphology (Sasaki 1999a, b; Nakano and Spencer 2007; Nakano et al. 2009a). Therefore, corroboration with molecular phylogenetic analysis is required to establish reliable species taxonomy (Koufopanou et al. 1999), and this approach has resulted in the identification of cryptic species or polymorphisms in certain groups (Nakano and Ozawa 2005; Nakano and Spencer 2007; de Aranzamendi et al. 2009; Nakano et al. 2009a; González-Wevar et al. 2011).

Molecular phylogenetic analysis and comparison of morphological characters have previously been performed for limpets with ambiguous taxonomies (*Lottia*: Simison and Lindberg 2003; *Notoacmea*: Nakano and Spencer 2007; Nakano et al. 2009a; *Patella*: Mauro et al. 2003; *Patelloida*: Nakano and Ozawa 2005; *Nacella*: de Aranzamendi et al. 2009; González-Wevar et al. 2011; *Cellana*: Reisser et al. 2011 and 2012). Use of molecular and morphological characters have led to consistent conclusions in most cases in the genera *Lottia*, *Notoacmea*, and *Patelloida*, whereas species monophyly was rejected in *Nacella* and *Cellana* (see above references). The genetic distances within and among species are variable across taxonomic groups. Previous studies have revealed that the genetic distances within species based on the cytochrome oxidase I gene (COI) are estimated to be less than 4%; however, the values are highly variable among species, ranging from 4% to 44.4% (Mauro et al. 2003; Nakano and Ozawa 2005; Nakano and Spencer 2007; Nakano et al. 2009a). Therefore, there is no fixed threshold for species delimitation using genetic distances, and species taxonomy must also be based on the level of continuity of the morphological characters.

COI is used most frequently in molecular phylogenetic analyses at the population and species levels (Mauro et al. 2003; Simison and Lindberg 2003; Nakano and Ozawa 2005; Nakano and Spencer 2007; de Aranzamendi et al. 2009; Nakano et al. 2009a; González-Wevar et al. 2011; Reisser et al. 2011). In addition, phylogenetic estimation has been based on the 12S rRNA (Goldstien et al. 2009), 16S rRNA (Simison and Lindberg 2003; Nakano and Ozawa 2005; Goldstien et al. 2009), cytochrome b mitochondrial gene (Cytb) (de Aranzamendi et al. 2009; Goldstien et al. 2009), and the ITS1 region from nuclear DNA (Nakano and Spencer 2007; Nakano et al. 2009a). Previous studies have shown that COI is a fast-evolving gene that is suitable for investigation of the validity of species designations (Hebert et al. 2003).

Species delineations have been completed by comparing shell morphology (de Aranzamendi et al. 2009) and radulae (Simison and Lindberg 2003; Nakano and Ozawa 2005; Nakano and Spencer 2007; Nakano et al. 2009a), and through quantitative

analysis of shell morphometry (Mauro et al. 2003; González-Wevar et al. 2011; Reisser et al. 2012). Determining the morphology of the radula is often considered one of the most effective means for species identification of patellogastropods (Lindberg 1998; Sasaki 1999a; Nakano and Ozawa 2005, 2007); however, the radular character can vary considerably in some species (e.g., *Notoacmea scapha*; Nakano and Spencer 2007). Therefore, species distinction and identification based solely on the radula is not always reliable. Quantitative analysis of shells may not clearly reveal species boundaries since different species of limpets frequently yield similar shapes. Comparative anatomy using features from the entire animal should be used for species recognition in patellogastropods (Lindberg 1988; Sasaki and Okutani 1993, 1994a, b; Sasaki 1999a); however, comprehensive analysis including both anatomical and molecular characteristics has rarely been conducted with this group.

The genus *Nipponacmea* of the family Lottiidae is widely distributed in East Asia (Nakano and Ozawa 2004, 2007; Nakano and Sasaki 2011), and there are nine known species in Japan (Sasaki 2000, 2017), and at least three more species outside of Japan (Christiaens 1980; Chernyshev and Chernova 2002; Chernyshev 2008; Bouchet 2015, see discussion for details). Before the discovery of specific anatomical characteristics and DNA sequences, the taxonomy of the genus was indistinct (Kira 1954; Habe and Kosuge 1967; Kuroda et al. 1971; Okutani and Habe 1975; Nakamura 1986; Asakura and Nishihama 1987; Takada 1992). Problems in taxonomic classification using morphological characteristics were caused by extensive variation of shell morphology within species. Sasaki and Okutani (1993) observed shell morphology and microstructure as well as anatomy in detail and utilized these features to redefine each species of *Nipponacmea*. As a result, new characters were found in the soft parts of the body, such as snout pigmentation, foot and cephalic tentacles, radula, radula sac configuration, and ovary color.

Molecular phylogenetic analyses of *Nipponacmea* have been undertaken by both Nakano and Ozawa (2004, 2007) and Yu et al. (2014). Nakano and Ozawa (2004, 2007) completed a phylogenetic analysis of the entire patellogastropod clade based on the sequences of the COI, 12S rRNA, 16S rRNA, 18S rRNA, and 28S rRNA genes, in which *Nipponacmea* was supported as a monophyletic lineage, independent of *Notoacmea* and *Tectura.* However, the monophyly of each *Nipponacmea* species could not be tested since only a single individual was used of each. Yu et al. (2014) performed identifications by barcoding and phylogeographic analysis of three *Nipponacmea* species in China, using the COI, 28S rRNA, and histone H3 genes. Currently, phylogenetic and taxonomic classification has only been attempted for selected *Nipponacmea* species in Asia.

The purposes of this study were to: (1) assess the taxonomy of *Nipponacmea* species from Japan using an integrative approach, with distance-based and tree-based methods for molecular data, and testing the utility of morphological diagnostic characters using type specimens and sequenced specimens from type localities or adjacent regions; and (2) phylogenetically analyze the relationships among species.

Materials and methods

Collection of samples

We collected *Nipponacmea* samples from 43 localities on the Japanese coast (Fig. 1, Table 1). The type localities or nearby areas are included for nine nominal species in this study (see Table 2). In addition, three species of *Lottia* (*L. kogamogai* (southern population), *L. tenuisculpta*, and *L. lindbergi*) described by Sasaki and Okutani (1994c), were used as outgroups.

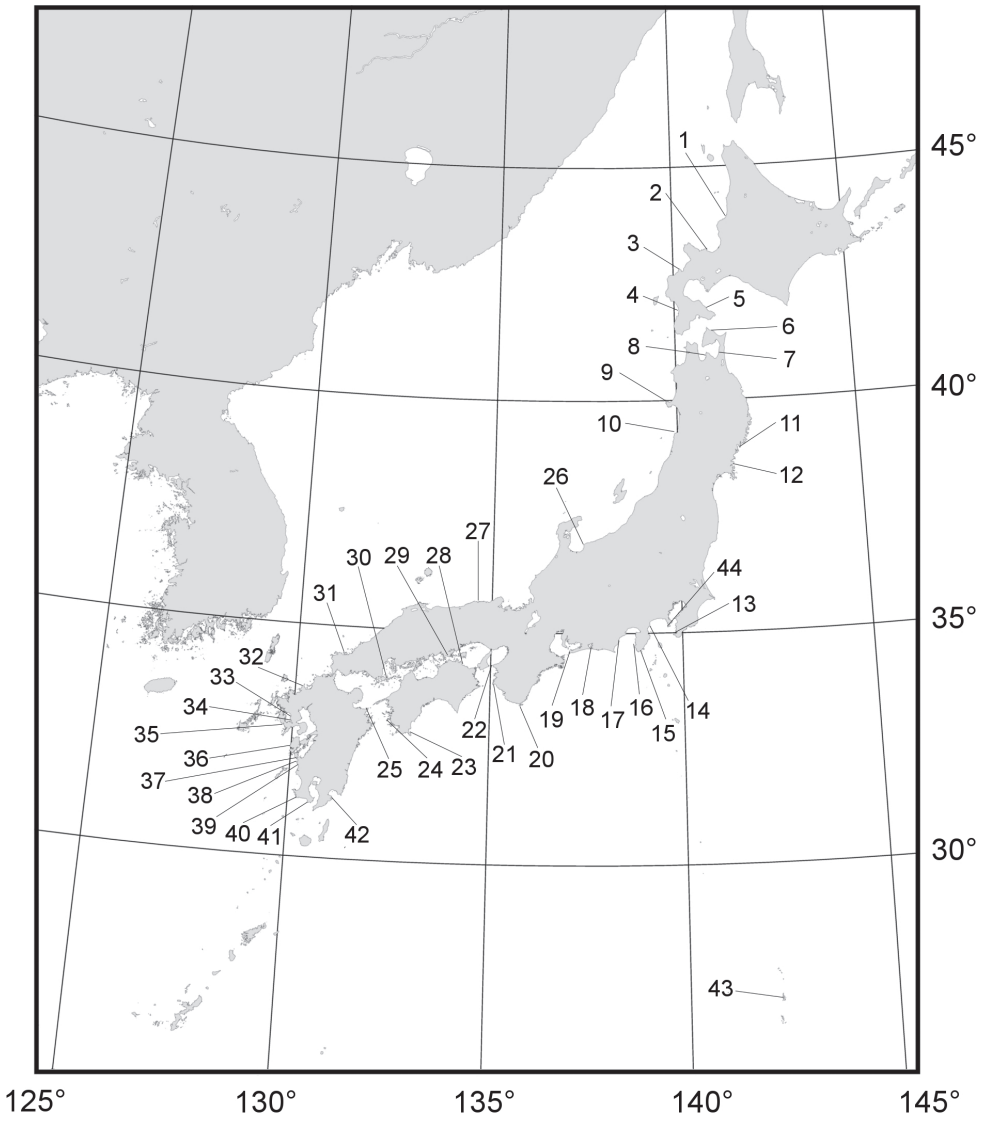

Figure 1. Collection localities of the specimens used in this study. The numbers are shown in Table 1.

Table 1. List of localities. See also Fig. 1 for map and Table 2 for list of specimens. All localities are in Japan.

No.	Locality	Coordinates (Latitude, Longitude)
1	Omachi, Rumoi, Hokkaido	43°56'45"N, 141°37'41"E
2	Shukutsu, Otaru, Hokkaido	43°14'09"N, 141°00'57"E
3	Masadomari, Suttu, Hokkaido	42°49'28"N, 140°11'15"E
4	Genna, Otobe, Hokkaido	42°00'24"N, 140°06'15"E
5	Usujiri, Hokkaido	41°56'11"N, 140°56'57"E
6	Hebiura, Kazamaura, Aomori Prefecture	41°29'42"N, 140°58'55"E
7	Arito, Noheji, Aomori Prefecture	40°54'25"N, 141°10'50"E
8	Tsuchiya, Hiranai, Aomori Prefecture	40°54'13"N, 140°51'46"E
9	Togashiohama, Oga, Akita Prefecture	39°56'40"N, 139°42'14"E
10	Kisakata, Nikaho, Akita Prefecture	39°12'34"N, 139°53'34"E
11	Masakicho, Ofunato, Iwate Prefecture	39°01'23"N, 141°42'36"E
12	Karakuwa, Ishinomaki, Miyagi Prefecture	38°30'47"N, 141°28'45"E
13	Okinoshima, Tateyama, Chiba Prefecture	34°59'27"N, 139°49'51"E
14	Mitsuishi, Manazuru, Kanagawa Prefecture	35°08'25"N, 139°09'41"E
15	Irouzaki, Minamiizu, Shizuoka Prefecture	34°36'47"N, 138°50'57"E
16	Futo, Nishiizu, Shizuoka Prefecture	34°47'36"N, 138°45'26"E
17	Iwashigashima, Yaizu, Shizuoka Prefecture	34°51'30"N, 138°19'40"E
18	Yutocho, Hamamatsu, Shizuoka Prefecture	34°42'13"N, 137°36'48"E
19	Iragocho, Tahara, Aichi Prefecture	34°34'56"N, 137°01'01"E
20	Shionomisaki, Kushimoto, Wakayama Prefecutre	33°26'11"N, 135°45'23"E
21	Mio, Mihamacho, Wakayama Prefecture	33°53'15"N, 135°04'31"E
22	Kada, Wakayama Prefecture	34°16'21"N, 135°03'54"E
23	Oki, Tosashimizu, Kochi Prefecture	32°51'00"N, 132°57'21"E
24	Ajiro, Ainancho, Ehime Prefecture	33°02'00"N, 132°24'19"E
25	Ohira, Oita, Oita Prefecture	33°14'50"N, 131°49'40"E
26	Suwacho, Uozu, Toyama Prefecture	36°48'40"N, 137°23'33"E
27	Yoroi, Kazumi, Hyogo Prefecture	35°39'10"N, 134°34'37"E
28	Tsudacho, Sanuki, Kagawa Prefecture	34°17'16"N, 134°16'04"E
29	Shibukawa, Tamano, Okayama Prefecture	34°27'23"N, 133°53'51"E
30	Hirano, Suo-Oshima, Yamaguchi Prefecture	33°53'59"N, 132°21'51"E
31	Higashifukawa, Nagato, Yamaguchi Prefecture	34°22'32"N, 131°10'33"E
32	Nishinoura, Nishi-ku, Fukuoka Prefecture	33°39'20"N, 130°12'28"E
33	Hiranitago, Higashisonogi, Nagasaki Prefecture	33°00'26"N, 129°56'47"E
34	Kujima, Omura, Nagasaki Prefecture	32°53'42"N, 129°57'11"E
35	Nagatamachi, Nagasaki Prefecture	32°50'00"N, 129°43'01"E
36	Odatoko Bay, Amakusa, Kumamoto Prefecture	32°24'07"N, 130°00'09"E
37	Wakimoto, Akune, Kagoshima Prefecture	32°05'03"N, 130°11'26"E
38	Sagata, Akune, Kagoshima Prefecture	31°59'31"N, 130°10'54"E
39	Okawa, Akune, Kagoshima Prefecture	31°56'47"N, 130°12'58"E
40	Bonotsu, Minamisatsuma, Kagoshima Prefecture	31°16'26"N, 130°13'19"E
41	Kaimon, Ibusuki, Kagoshima Prefecture	31°11'28"N, 130°30'30"E
42	Kishira, Kimotsuki, Kagoshima Prefecture	31°13'41"N, 131°01'04"E
43	Chichijima, Ogasawara Islands	27°05'36"N, 142°11'39"E
44	Koajiro, Misaki, Miura, Kanagawa Prefecture	35°09'27"N, 139°36'40"E

Animals were preserved in 99% ethanol. Preliminary identification of specimens prior to DNA sequencing was based on shell characters (Sasaki and Okutani 1993; Sasaki 2000, 2017). All voucher specimens were deposited in the Department of Historical Geology and Paleontology at The University Museum, University of Tokyo (UMUT RM31815–31935, 32353–32364).

Table 2. List of specimens used in this study. UMUT: The University Museum, The University of Tokyo. *Type locality, ** locality close to type locality.

Species	UMUT no.	Loc. no. (Fig. 1)	Accession no.				Figure(s)
			COI	Cytb	12S	16S	
N. boninensis	RM31815	43*	LC138228	LC142818	LC142951	LC143084	Figs 3N, 7G
	RM31816	43*	LC138229	LC142819	LC142952	LC143085	Figs 3O, 5C
	RM31817	43*	LC138230	LC142820	LC142953	LC143086	Figs 3K–M, 6C, 7F
N. concinna	RM31818	10	LC138231	LC142821	LC142954	LC143087	
	RM31819	10	LC138232	LC142822	LC142955	LC143088	
	RM31820	11	LC138233	LC142823	LC142956	LC143089	Fig. 3U–W
	RM31821	11	LC138234	LC142824	LC142957	LC143090	
	RM31822	17	LC138235	LC142825	LC142958	LC143091	
	RM31823	19	LC138236	LC142826	LC142959	LC143092	Fig. 7M
	RM31824	21	LC138237	LC142827	LC142960	LC143093	Fig. 3X
	RM31825	21	LC138238	LC142828	LC142961	LC143094	
	RM31826	29	LC138239	LC142829	LC142962	LC143095	
	RM31827	30	LC138240	LC142830	LC142963	LC143096	
	RM31828	30	LC138241	LC142831	LC142964	LC143097	Fig. 3Y
	RM31829	32	LC138242	LC142832	LC142965	LC143098	
	RM31830	34	LC138243	LC142833	LC142966	LC143099	Fig. 5E
	RM31831	34	LC138244	LC142834	LC142967	LC143100	Fig. 7K
	RM32353	35*	LC138349	LC142939	LC143072	LC143205	Figs 6E, 7L
N. fuscoviridis	RM31832	1	LC138245	LC142835	LC142968	LC143101	
	RM31833	1	LC138246	LC142836	LC142969	LC143102	
	RM31834	1	LC138247	LC142837	LC142970	LC143103	Fig. 7E
	RM31835	1	LC138248	LC142838	LC142971	LC143104	
	RM31836	1	LC138249	LC142839	LC142972	LC143105	
	RM31837	4	LC138250	LC142840	LC142973	LC143106	
	RM31838	4	LC138251	LC142841	LC142974	LC143107	
	RM31839	4	LC138252	LC142842	LC142975	LC143108	
	RM31840	8	LC138253	LC142843	LC142976	LC143109	
	RM31841	10	LC138254	LC142844	LC142977	LC143110	
	RM31842	10	LC138255	LC142845	LC142978	LC143111	
	RM31843	10	LC138256	LC142846	LC142979	LC143112	
	RM31844	10	LC138257	LC142847	LC142980	LC143113	
	RM31845	10	LC138258	LC142848	LC142981	LC143114	
	RM31846	10	LC138259	LC142849	LC142982	LC143115	Fig. 3I
	RM31847	13	LC138260	LC142850	LC142983	LC143116	Fig. 5B
	RM31848	32	LC138261	LC142851	LC142984	LC143117	
	RM31849	32	LC138262	LC142852	LC142985	LC143118	
	RM31850	32	LC138263	LC142853	LC142986	LC143119	
	RM31851	32	LC138264	LC142854	LC142987	LC143120	
	RM31852	32	LC138265	LC142855	LC142988	LC143121	
	RM31853	36	LC138266	LC142856	LC142989	LC143122	
	RM31854	36	LC138267	LC142857	LC142990	LC143123	
	RM31855	36	LC138268	LC142858	LC142991	LC143124	
	RM31856	36	LC138269	LC142859	LC142992	LC143125	
	RM31857	39*	LC138270	LC142860	LC142993	LC143126	
	RM32354	39*	LC138350	LC142940	LC143073	LC143206	Figs 6B, 7D
	RM31858	42	LC138271	LC142861	LC142994	LC143127	Figs 3F–H, 7C
	RM31859	42	LC138272	LC142862	LC142995	LC143128	Fig. 3J
N. gloriosa	RM31860	13	LC138273	LC142863	LC142996	LC143129	Figs 3D, 7B
	RM31861	14	LC138274	LC142864	LC142997	LC143130	Fig. 5A
	RM31862	14	LC138275	LC142865	LC142998	LC143131	Fig. 3E
	RM31863	14	LC138276	LC142866	LC142999	LC143132	
	RM31864	16	LC138277	LC142867	LC143000	LC143133	
	RM31865	27	LC138278	LC142868	LC143001	LC143134	
	RM31866	27	LC138279	LC142869	LC143002	LC143135	

Species	UMUT no.	Loc. no. (Fig. 1)	Accession no.				Figure(s)
			COI	Cytb	12S	16S	
N. gloriosa	RM31867	27	LC138280	LC142870	LC143003	LC143136	
	RM31868	40	LC138281	LC142871	LC143004	LC143137	
	RM31869	41	LC138282	LC142872	LC143005	LC143138	Fig. 3A–C
	RM32355	41	LC138351	LC142941	LC143074	LC143207	Figs 6A, 7A
N. habei	RM31870	2	LC138283	LC142873	LC143006	LC143139	Fig. 5H
	RM31871	3	LC138284	LC142874	LC143007	LC143140	
	RM31872	3	LC138285	LC142875	LC143008	LC143141	Fig. 7U
	RM31873	5**	LC138286	LC142876	LC143009	LC143142	Figs 4T, 7V
	RM32357	5**	LC138353	LC142943	LC143076	LC143209	Fig. 7W
	RM31874	12	LC138287	LC142877	LC143010	LC143143	Fig. 4P–R
	RM31875	13	LC138288	LC142878	LC143011	LC143144	Fig. 4S
	RM32356	13	LC138352	LC142942	LC143075	LC143208	Figs 6H, 7X
	RM32364	13	LC138360	LC142950	LC143083	LC143216	Fig. 7T
N. nigrans	RM31876	1	LC138289	LC142879	LC143012	LC143145	
	RM31877	3	LC138290	LC142880	LC143013	LC143146	
	RM31878	3	LC138291	LC142881	LC143014	LC143147	
	RM31879	3	LC138292	LC142882	LC143015	LC143148	
	RM31880	3	LC138293	LC142883	LC143016	LC143149	
	RM31881	4	LC138294	LC142884	LC143017	LC143150	
	RM31882	4	LC138295	LC142885	LC143018	LC143151	
	RM31883	7	LC138296	LC142886	LC143019	LC143152	
	RM31884	11	LC138297	LC142887	LC143020	LC143153	
	RM31885	12	LC138298	LC142888	LC143021	LC143154	
	RM31886	15	LC138299	LC142889	LC143022	LC143155	Fig. 4N
	RM31887	15	LC138300	LC142890	LC143023	LC143156	Fig. 4K–M
	RM32358	20*	LC138354	LC142944	LC143077	LC143210	Fig. 7S
	RM32359	20*	LC138355	LC142945	LC143078	LC143211	Fig. 7R
	RM32360	20*	LC138356	LC142946	LC143079	LC143212	Fig. 7Q
	RM32361	20*	LC138357	LC142947	LC143080	LC143213	Fig. 5G
	RM32362	20*	LC138358	LC142948	LC143081	LC143214	Fig. 6G
	RM31888	22	LC138301	LC142891	LC143024	LC143157	
	RM31889	22	LC138302	LC142892	LC143025	LC143158	
	RM31890	22	LC138303	LC142893	LC143026	LC143159	
	RM31891	26	LC138304	LC142894	LC143027	LC143160	
	RM31892	32	LC138305	LC142895	LC143028	LC143161	Fig. 4F–H
	RM31893	33	LC138306	LC142896	LC143029	LC143162	
	RM31894	33	LC138307	LC142897	LC143030	LC143163	
	RM31895	33	LC138308	LC142898	LC143031	LC143164	Fig. 4J
	RM31896	33	LC138309	LC142899	LC143032	LC143165	
	RM31897	33	LC138310	LC142900	LC143033	LC143166	Fig. 4O
N. radula	RM31898	18	LC138311	LC142901	LC143034	LC143167	Fig. 7N
	RM31899	31	LC138312	LC142902	LC143035	LC143168	Fig. 4E
	RM31900	31	LC138313	LC142903	LC143036	LC143169	Fig. 5F
	RM31901	34	LC138314	LC142904	LC143037	LC143170	
	RM31902	34	LC138315	LC142905	LC143038	LC143171	Fig. 4D
	RM31903	34	LC138316	LC142906	LC143039	LC143172	
	RM31904	34	LC138317	LC142907	LC143040	LC143173	Figs 4A–C, 7O
	RM32363	37*	LC138359	LC142949	LC143082	LC143215	Figs 6F, 7P
N. schrenckii	*RM31905*	6	LC138318	LC142908	LC143041	LC143174	
	RM31906	6	LC138319	LC142909	LC143042	LC143175	Figs 3P–R, 6D, 7I
	RM31907	6	LC138320	LC142910	LC143043	LC143176	
	RM31908	6	LC138321	LC142911	LC143044	LC143177	Figs 3S, 5D
	RM31909	9	LC138322	LC142912	LC143045	LC143178	
	RM31910	9	LC138323	LC142913	LC143046	LC143179	
	RM31911	9	LC138324	LC142914	LC143047	LC143180	
	RM31912	14	LC138325	LC142915	LC143048	LC143181	

Species	UMUT no.	Loc. no. (Fig. 1)	Accession no.				Figure(s)
			COI	Cytb	12S	16S	
N. schrenckii	RM31913	14	LC138326	LC142916	LC143049	LC143182	
	RM31914	23	LC138327	LC142917	LC143050	LC143183	
	RM31915	30	LC138328	LC142918	LC143051	LC143184	Fig. 7H
	RM31916	35*	LC138329	LC142919	LC143052	LC143185	Figs 3T, 7J
N. teramachii	RM31917	13	LC138330	LC142920	LC143053	LC143186	Fig. 5I
	RM31918	13	LC138331	LC142921	LC143054	LC143187	
	RM31919	21	LC138332	LC142922	LC143055	LC143188	
	RM31920	21	LC138333	LC142923	LC143056	LC143189	
	RM31921	24	LC138334	LC142924	LC143057	LC143190	
	RM31922	24	LC138335	LC142925	LC143058	LC143191	Fig. 4Y
	RM31923	25	LC138336	LC142926	LC143059	LC143192	
	RM31924	25	LC138337	LC142927	LC143060	LC143193	Fig. 7Z
	RM31925	28	LC138338	LC142928	LC143061	LC143194	Fig. 4X
	RM31926	28	LC138339	LC142929	LC143062	LC143195	Fig. 7Y
	RM31927	30	LC138340	LC142930	LC143063	LC143196	
	RM31928	30	LC138341	LC142931	LC143064	LC143197	Fig. 6I
	RM31929	32	LC138342	LC142932	LC143065	LC143198	
	RM31930	32	LC138343	LC142933	LC143066	LC143199	Fig. 4U–W
	RM31931	38*	LC138344	LC142934	LC143067	LC143200	
	RM31932	38*	LC138345	LC142935	LC143068	LC143201	
L. kogamogai	RM31933	44	LC138346	LC142936	LC143069	LC143202	
L. tenuisculpta	RM31934	44	LC138347	LC142937	LC143070	LC143203	
L. lindbergi	RM31935	44	LC138348	LC142938	LC143071	LC143204	

DNA extraction, amplification, and sequencing

Total genomic DNA was extracted from the mantle using the cetyltrimethylammonium bromide (CTAB) method (Doyle and Doyle 1990). The mtDNA cytochrome c oxidase I (COI), cytochrome b (Cytb), the small-subunit ribosomal RNA (12S rRNA), and the large-subunit ribosomal RNA (16S rRNA) were used as the molecular markers in this study. PCR products of each gene was amplified with universal primers (Table 3). PCR amplification was performed in a reaction volume of 25 μL containing 10 μM Tris HCl at pH 8.3, 50 μM KCL, 1.5 μM $MgCl_2$, 200 μM dNTPs, 0.2 μM of each primer, 2 units of Taq polymerase (Takara), and 1 μL of template DNA. The amplification cycle consisted of an initial denaturation for 3 min at 94 °C, followed by 30 cycles of denaturation for 45 s at 94 °C, annealing for 90 s at a gene-specific annealing temperature (50 °C for COI, 52 °C for Cytb, and 55 °C for the 12S) and extension for 120 s at 72 °C, followed by a 5 min final extension at 72 °C. The PCR products

Table 3. List of PCR primers.

Gene	Primer name	Sequence (5'→3')	Source
COI	LCO1490 (F)	GGTCAACAAATCATAAAGATATTGG	Folmer et al. (1994)
	HCO2198 (R)	TAAACTTCAGGGTGACCAAAAAATCA	Folmer et al. (1994)
Cytb	cobF (F)	GGWTAYGTWYTWCCWTGRGGWCARAT	Boore and Brown 2000
	cobR (R)	GCRTAWGCRAAWARRAARTAYCAYTCWGG	Boore and Brown 2000
12S	12Sma (F)	CTGGGATTAGATACCCTGTTAT	Koufopanou et al. (1999)
	12Smb (R)	CAGAGAGTGACGGGCGATTTGT	Koufopanou et al. (1999)
16S	16LRN13398 (F)	CGCCTGTTTAACAAAAACAT	Koufopanou et al. (1999)
	16SRHTB (R)	ACGCCGGTTTGAACTCAGATC	Koufopanou et al. (1999)

were purified with Illustra ExoStar (GE Healthcare), and used as the template DNA for cycle sequencing reactions from both directions with the DTCS-Quick Start Kit (Beckman Coulter) following standard protocols using the CEQ 2000 XL (Beckman Coulter) automatic sequencer.

Datasets

All sequences were aligned using MEGA 6.06 (Tamura et al. 2011) and multiple sequence alignments were constructed using MAFFT (Katoh and Toh 2008). Ambiguous regions were removed with Gblocks (Talavera and Castresana 2007) to allow for smaller final blocks and less strict flanking positions.

Phylogenetic analyses

Phylogenetic analyses were conducted using a maximum-likelihood (ML) approach via GARLI v. 2.0 (Zwickl 2006) and a Bayesian approach via MrBayes v3.1.2 (Ronquist and Huelsenbeck 2003) with appropriate substitution models for each partition. MrModeltest v2.3 (Nylander 2004) was applied to obtain appropriate substitution models using the Akaike information criterion (Akaike 1974). The substitution models chosen were GTR+I+G for the 12S rRNA, 16S rRNA and Cytb genes, and HKY+I+G for the COI gene.

ML bootstrap values were calculated from 1000 replicates. MrBayes was utilized with the following settings: six substitution types were employed (nst = 6); rate variation across sites was modeled using a gamma distribution with a proportion of the sites as invariant (rate = invgamma); and finally, the shape, invariable site proportion, state frequency, and substitution rate parameters were estimated.

Bayesian analysis was performed for 4,000,000 generations (for the four genes concatenated), 4,500,000 generations (COI), 4,000,000 generations (Cytb), 3,500,000 generations (12S rRNA), and 6,000,000 generations (16S rRNA) with a sample frequency of 100 and the first 25% generations discarded as the burn-in; convergence was determined when the average standard deviation of the split frequencies value (ASDSF) was below 0.01.

The genetic distances among and within species were calculated using the Kimura-2-Parameter (K2P) in MEGA 6.06.

Morphological characters

Sequenced specimens were dissected under a binocular microscope. After observations of the animal including the snout pigmentation, cephalic tentacles, and foot lateral wall, the visceral mass was dissected to reveal the configuration of the radular sac. Removed radulae were cleaned in diluted commercial bleach, coated with platinum vanadium, and observed with a scanning electron microscope (Keyence VE-8800). The color of the ovary was recorded before ethanol fixation for specimens collected in breeding season, since gonad color fades when stored in ethanol.

Three shell characters were measured for a total of 130 sequenced specimens: shell length (L), shell width (W), and shell height (H). All individuals were measured with a digital caliper (to 0.01 mm). Allometric analyses were performed among species and genetic groups to determine relationships among length, width, and height using Welch's t-test. Canonical discriminant analysis was performed among species using the three shell characters (L, W, and H). Discriminant functions also calculated the percentage of individuals that were classified correctly. Canonical discriminant analysis was conducted using R software package version 3.1.0 (R Core Team 2014).

Results

Molecular data

A total of 130 *Nipponacmea* individuals morphologically identified as *N. schrenckii* (12), *N. fuscoviridis* (29), *N. concinna* (15), *N. radula* (8), *N. boninensis* (3), *N. habei* (9), *N. teramachii* (16), *N. nigrans* (27), and *N. gloriosa* (11) were sequenced (Table 2). The lengths of the COI, Cytb, 12S rRNA, and 16S rRNA gene sequences were 648, 410, 443, and 604 bp, respectively. After removal of ambiguous regions and trimming the ends of poor quality sequences, final lengths of 506, 404, 324, and 575 bp were used for the analysis, respectively. The sequences of the four genes were combined into a total of 1809 bp for constructing phylogenetic trees. All nucleotide sequences in this study were deposited in GenBank (Accession numbers LC138228–LC138360, LC14818–LC143216).

Molecular phylogenetic analysis

The resultant phylogenetic tree using the four genes is shown in Fig. 2. The monophyly of the genus *Nipponacmea* was supported with a bootstrap value (BS) = 100% and posterior probability (PP) = 1.00. There are nine terminal clades, and morphological characters of the sequenced specimens confirmed that these clades corresponded to the *Nipponacmea* species previously defined by Sasaki and Okutani (1993, 1994a) (see below for more notes on the morphology). The relationships among species indicated that: (1) *N. gloriosa* is the sister to the remaining lineages, (2) the remaining species form a large clade supported with BS = 99% and PP = 1.00, and (3) the large clade is divided into two subclades, which we have referred to as Clades A and B. The monophyly of Clade A was well supported with BS = 100% and PP = 1.00. The topology within Clade A was: (*N. radula*, *N. concinna*, *N. schrenckii*, (*N. boninensis*, *N. fuscoviridis*)). BS values for interspecific relationships within this clade were less than 70%, and its branches were not well supported. The highest value within Clade A was between *N. fuscoviridis* and *N. boninensis* (BS = 66%, PP = 0.96). Clade B was supported with BS = 58% and PP = 0.94, and the

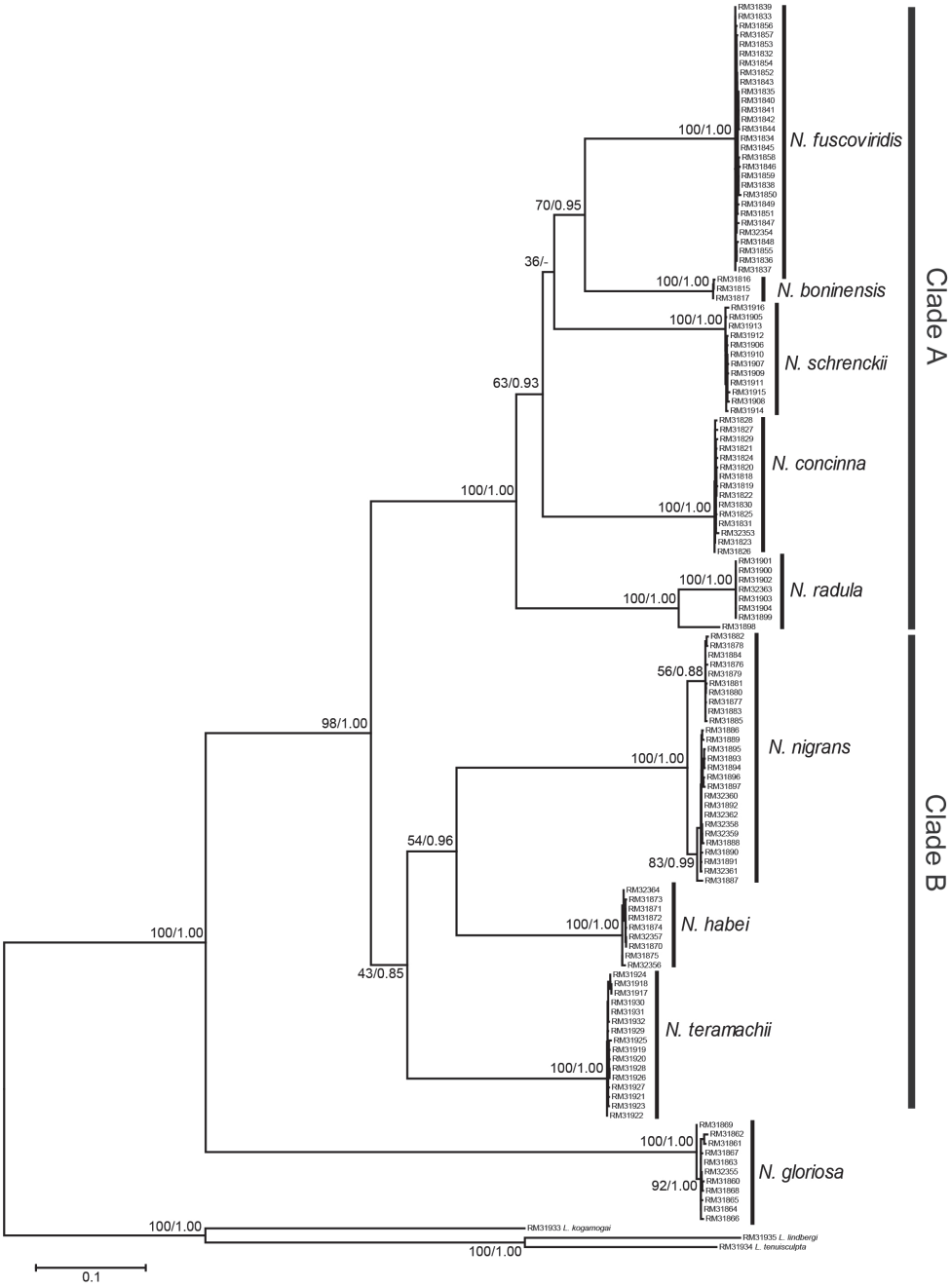

Figure 2. Maximum likelihood phylogenetic tree generated from 1809 bp constructed from the concatenated COI, Cytb, 12S rRNA, and 16S rRNA gene sequences from *Nipponacmea* representatives. Numbers above or below the branches are ML bootstrap values and Bayesian posterior probabilities, respectively. See Table 2 for sample numbers.

topology within this group was: (*N. teramachii*, (*N. nigrans*, *N. habei*)). The highest supported values within Clade B were BS = 61% and PP = 0.99 between *N. nigrans* and *N. habei*.

Separate analyses of the four genes resulted in slightly different phylogenetic relationships that are described below. The divergence within *Nipponacmea* in the COI tree (Suppl. material 1: Fig. S1) was expressed as: (Clade A, (Clade B, *N. gloriosa*)), whereas in the tree constructed with combined sequences, *N. gloriosa* was a sister to the other lineages. The topology within Clade A, unlike what was revealed with the combined sequence tree, was: ((*N. fuscoviridis*, *N. concinna*), (*N. schrenckii*, (*N. radula*, *N. boninensis*))), whereas that for Clade B was the same as that of the combined tree. Phylogenetic relationships within *Nipponacmea* species were different from those of the combined tree in the Cytb analysis (Suppl. material 2: Fig. S2). The topology within Clade A was: (*N. boninensis*, (*N. fuscoviridis*, (*N. concinna*, (*N. schrenckii*, *N. radula*)))), while Clade B showed: (*N. teramachii*, (*N. nigrans*, (*N. habei*, *N. gloriosa*))). Relationships among species were similar to those of the combined tree in the analysis of 12S rRNA gene (Suppl. material 3: Fig. S3). The result of phylogenetic analysis of 16S rRNA gene is shown in Suppl. material 4: Fig. S4. As in the combined tree, *N. gloriosa* was the sister to the remaining *Nipponacmea*, Clade A was well supported, and the topology within that clade was the same as that of the tree of combined sequences. In comparison to the combined tree, the monophyly of Clade B was not supported in the analysis of the 16S rRNA.

Although the monophyly of Clade A was well supported, branching order within the clade was not (BS values < 70%). In contrast, the monophyly of clade B was not strongly supported, nor was the monophyly of *N. nigrans* and *N. habei* (BS = 54%). Perhaps not surprisingly, separate analyses of the four genes resulted in slightly different trees (Suppl. material 1: Fig. S1, Suppl. material 2: Fig. S2, Suppl. material 3: Fig. S3, Suppl. material 4: Fig. S4).

Morphological characters

In this study, we tested the identification of *Nipponacmea* species based only on sequences, and the results revealed nine phylogenetic groups, which confirmed the nine species currently described. In addition, scientific names were verified by comparison between type and sequenced specimens according to morphological traits. Among numerous possible morphological and anatomical characters, the following six characters were revealed to be most reliable for *Nipponacmea* species identification (Table 5).

(1) Granules: Granules on the shell exterior exhibited five character states: (a) rounded (*N. concinna*), (b) pointed (*N. radula*), (c) smooth (*N. boninensis*), (d) thickly elongated (*N. nigrans*), and (e) thinly elongated (the remaining species). These results corroborate previous observations by Sasaki and Okutani (1993; fig. 15). The phylogeny suggests granules were differentiated according to species-specific types in Clade A, such as the elongate type seen in *N. gloriosa*, and Clade B.

(2) Riblets: Exterior riblets were either fine, rough, or absent, depending on species. In Clade A, the riblets were fine and sparse in *N. fuscoviridis*, *N. schrenckii*, *N. radula*, while they were fine and dense in *N. boninensis*, and absent in *N. concinna*. In Clade B, the riblets were thick and dense in *N. nigrans*, fine and dense in *N. habei*, and absent in *N. teramachii*. The topology of the molecular phylogenetic trees indicated that the riblets do not reflect phylogeny.

(3) Animal pigmentation: Pigmentation in the snout, cephalic tentacles, and side of the foot was divergent among species, including black, grey, or non-pigmented types (Fig. 5). The snout was not pigmented in *N. gloriosa*, *N. fuscoviridis*, or *N. boninensis*; lightly pigmented in *N. radula* and *N. nigrans*; and blackened in the remaining four species. The pigmentation of the snout did not reflect phylogenetic relationships. Only *N. gloriosa* lacked pigmentation in the cephalic tentacles, whereas the other eight species had darkly pigmented tentacles. The side of the foot was not pigmented in *N. gloriosa* or *N. fuscoviridis*, lightly pigmented in *N. boninensis*, *N. radula*, and *N. nigrans*, and finally darkly pigmented in the remaining four species. Relationships between pigmentation patterns and phylogeny were not detected.

(4) Radular sac: The configuration of the radular sac was different among the species (Fig. 6). *Nipponacmea concinna* and *N. radula* had two loops, the anterior and posterior loops, while the other species formed a single shorter loop. Again, this character did not correspond with the defined phylogenetic relationships.

(5) Radular teeth: The lateral teeth were short and blunt in *N. gloriosa*, long and slightly blunt in *N. boninensis*, and long and acute in the rest of the species (Fig. 7). The radular morphology of *N. habei* teeth showed a wider range of variation than that of the remaining species in regard to the acuteness of the middle lateral teeth.

(6) Ovary: The color of the ovary can be classified into three categories: green in *N. fuscoviridis* and *N. schrenckii*, red in *N. boninensis* and *N. gloriosa*, and brown in *N. concinna*, *N. radula*, *N. teramachii*, *N. nigrans*, and *N. habei.* The ovaries of all species in Clade B were pigmented brown, whereas those of Clade A were variable and are characterized by one of the three color patterns outlined above.

Morphometric analysis

The relationships among length, width, and height are indicated in Fig. 8 and were similar among species; however, the correlations between length and height, and between width and height differed. The results of Welch's t-test using the proportion of length and height indicated that the apex height of Clade B (average H/L ratio = 0.27) was significantly higher than that of Clade A (average H/L ratio = 0.22; $t = 5.24$, $P = 0.001$). Applying the canonical discriminant analysis, only 51.9% of the original 130 individuals were assigned to the correct species (Fig. 9, Table 6). Therefore, it is difficult to distinguish between the nine genetic species solely from shell morphometry. *Nipponacmea nigrans* was discriminated best, with 23 out of 27 correctly matched individuals, while *N. boninensis* was the least discriminated, with 0 out of 3 individuals classified correctly.

Discussion

Monophyly of species

The monophyly of Japanese *Nipponacmea* species has not been previously tested using molecular characters; however, it was strongly supported by the data obtained from the present study (Fig. 2). The taxonomy of patellogastropod species based on morphological characters can be frustrated due to polyphenism (*Patelloida*: Nakano and Ozawa 2005, *Notoacmea scapha*: Nakano and Spencer 2007; Nakano et al. 2009a) or the existence of cryptic species (*Notoacmea* species: Nakano and Spencer 2007; Nakano et al. 2009a, *Nacella* species; de Aranzamendi et al. 2009; González-Wevar et al. 2011). In the present study, neither polyphenism nor cryptic species were found in *Nipponacmea*.

In this study, the maximum genetic distance within species was noticeably smaller than the minimum among species; therefore, the genetic distances were consistent with morphology-based species taxonomy. The maximum genetic distance within Japanese *Nipponacmea* species was 9.9% in COI in *N. radula* (Table 4). The minimum genetic distance was 17.8% in COI between *N. boninensis* and *N. schrenckii*. The genetic distances among species in *Notoacmea* in New Zealand ranged from 3.94% to 44.4% for COI, and distances within species were from 0.00% to 2.96% (Nakano and Spencer 2007; Nakano et al. 2009a). Thus, genetic distances are greatly variable among species in the New Zealand *Notoacmea* and the Japanese *Nipponacmea*.

A comparison of holotype and sequenced specimens from type localities (topotypes) is useful to confirm species identity. We investigated holotypes of seven species (*N. radula*, *N. boninensis*, *N. habei*, *N. teramachii*, *N. nigrans*, *N. gloriosa*, and *N. formosa*), excluding *N. schrenckii*, *N. concinna*, and *N. fuscoviridis* whose type materials are currently missing (Table 6). Morphological comparisons between sequenced specimens and holotypes were possible when considering characters related to shell surface sculpture (riblets and granules). In addition, sequence data of topotypes are important to precisely identify sequenced specimens. In this study, genetic variation was not significant among individuals of the four species collected from their type localities (*N. boninensis*, *N. fuscoviridis*, *N. nigrans*, and *N. teramachii*). The maximum genetic distances among COI sequences of topotypes of these species were 0.4% for *N. boninensis*, and 0.2% for *N. fuscoviridis*, *N. nigrans*, and *N. teramachii*. Thus, the molecular phylogeny corroborated the morphology-based taxonomy originally defined in the 1990s.

Phylogenetic relationships among *Nipponacmea* species

The results of the molecular phylogenetic analysis in this study revealed three major clades (*N. gloriosa*, Clade A, and Clade B), with *N. gloriosa* as sister to the other *Nipponacmea* species. This relationship is consistent with delineations observed based on major differences observed in radular morphology, food preference, and habitat. *Nipponacmea gloriosa* grazes exclusively on coralline algae, while the other species

Table 4. Genetic distances among *Nipponacmea* species using COI, Cytb, and the 12S rRNA gene. Numbers in bold typeface indicated the intraspecific.

	1	2	3	4	5	6	7	8	9	10
COI										
1 *N. nigrans*	**0.0–5.5**									
2 *N. habei*	21.5–23.7	**0.0–0.8**								
3 *N. teramachii*	22.1–25.1	21.7–22.9	**0.0–0.8**							
4 *N. fuscoviridis*	24.9–28.1	22.1–23.1	22.1–23.1	**0.0–1.2**						
5 *N. boninensis*	23.5–24.7	23.7–24.1	24.1–25.1	19.6–20.8	**0.0–0.4**					
6 *N. schrenckii*	23.1–25.1	22.5–23.1	23.3–24.5	18.6–19.6	17.8–18.4	**0.0–1.0**				
7 *N. concinna*	22.9–24.9	24.3–25.3	23.7–24.3	19.4–20.9	19.6–20.2	20.8–21.9	**0.0–0.8**			
8 *N. radula*	25.1–27.3	23.1–26.9	25.7–26.9	23.3–24.9	18.8–21.7	21.5–23.1	21.7–23.7	**0.0–9.9**		
9 *N. gloriosa*	26.7–29.2	27.5–28.1	26.3–27.5	26.5–27.5	26.9–27.9	26.5–27.7	24.9–26.3	29.4–32	**0.0–0.8**	
10 *L. kogamogai*	25.0–27.0	24.5–24.7	24.7–25.1	25.9–26.9	26.9–27.1	25.7–26.3	25.3–25.9	25.3–27.5	28.1–28.5	**0.0**
Cytb										
1 *N. nigrans*	**0.0–4.7**									
2 *N. habei*	20.5–22.0	**0.0–0.7**								
3 *N. teramachii*	24.8–27.0	23.8–24.5	**0.0–1.2**							
4 *N. fuscoviridis*	23.0–24.8	24.0–24.8	23.3–24.3	**0.0–0.5**						
5 *N. boninensis*	21.3–22.8	20.5–20.8	21.8–22.5	17.1–17.3	**0.0**					
6 *N. schrenckii*	24.8–27.0	22.0–22.8	23.0–24.8	19.8–21.0	21.0–21.8	**0.0–1.0**				
7 *N. concinna*	26.0–27.5	26.2–27.0	23.0–23.8	18.8–19.8	19.1–19.8	21.5–22.3	**0.0–0.7**			
8 *N. radula*	24.5–30.0	22.0–24.0	21.8–22.5	21.0–21.5	21.0–22.3	18.6–20.0	21.8–22.3	**0.0–7.7**		
9 *N. gloriosa*	21.8–23.8	20.3–21.3	23.8–25.2	23.3–24.8	24.0–24.5	23.3–24.3	24.5–26.5	23.5–25.0	**0–2.5**	
10 *L. kogamogai*	26.2–27.0	32.4–32.4	28.2–28.7	28.0–28.2	28.7–28.7	31.2–31.4	29.7–30.2	30.0–30.4	30.2–31.2	**0.0**
12S rRNA										
1 *N. nigrans*	**0.0–1.2**									
2 *N. habei*	10.5–11.1	**0.0**								
3 *N. teramachii*	12.7–13.6	13.0	**0.0**							
4 *N. fuscoviridis*	15.4–16.0	14.8–15.1	14.2–14.5	**0.0–0.3**						
5 *N. boninensis*	16.0–16.7	14.8	14.8	5.6–5.9	**0.0**					
6 *N. schrenckii*	16.0–16.7	14.8	16.4	7.7–8.0	9.0	**0.0**				
7 *N. concinna*	14.8–15.4	12.7	14.5	8.6–9.0	7.7	9.6	**0.0**			
8 *N. radula*	20.1–21.3	16.7–17.6	14.5	9.6–11.1	12.0–12.7	12.0–13.0	14.2–14.5	**0.0–2.2**		
9 *N. gloriosa*	21.6–23.1	21.3–22.5	22.2–23.5	24.4–25.0	23.5–24.1	21.9–22.2	22.2–22.5	25.0–25.9	**0.0–1.2**	
10 *L. kogamogai*	23.8–24.1	23.1	25.3	25.3–25.6	24.7	25.3	25.3	28.1–28.4	24.4–25	**0.0**
16S rRNA										
1 *N. nigrans*	**0.0–0.7**									
2 *N. habei*	9.3–9.5	**0.0**								
3 *N. teramachii*	8.7–9.4	8.9–9.1	**0.0–0.2**							
4 *N. fuscoviridis*	12.6–13.4	14.9–15.2	11.1–11.6	**0–0.2**						
5 *N. boninensis*	11–11.7	14.3–14.3	11.3–11.5	9.3–9.5	**0.0**					
6 *N. schrenckii*	12.8–13.5	13.8–14.3	12.5–13.2	10.7–11.4	8.2–8.4	**0.2–0.3**				
7 *N. concinna*	11.2–12.1	11.7–12	10.4–10.9	9.0–9.5	7.9–8.2	8.0–8.4	**0.0–0.2**			
8 *N. radula*	11.5–12.6	12.7–13.4	11.3–12.3	9.3–9.7	8.7–10.7	8.9–10.7	8.2–9.3	**0.0–2.0**		
9 *N. gloriosa*	26.1–26.4	22.4–22.7	24.3–24.9	28.1–28.5	24.9–25.2	22.3–23.2	26.4–27.0	25.8–26.1	**0.0–0.2**	
10 *L. kogamogai*	25.2–25.5	22.8–22.8	26.2–26.5	29.9–30.0	27.9–27.9	28.8–29.5	27.8–28.1	28.5–29.9	28.8–28.8	**0.0**

consume different materials, for example, *N. concinna* is known to graze on *Ulva* spp. (Kawakami and Habe 1986). Additionally, *N. gloriosa* is the only species that inhabits the subtidal zone; the others are restricted to the intertidal zone (Sasaki and Okutani 1993; Sasaki 2000, 2017).

Clade A was robustly supported with high bootstrap values by Nakano and Ozawa (2007) (BS = 99%) as well as in this study (BS = 100%). Branching order within the

Table 5. Diagnostic characters of *Nipponacmea* species distributed in Japan.

Species	Shell sculpture		Animal pigmentation			Radula sac	Radular teeth	Ovary
	Granules	Riblets	Snout	Cephalic tentacles	Foot			
N. gloriosa	Elongate and thin	Fine and sparse	Non-pigmented	Non-pigmented	Non-pigmented	Short	Blunt	Red
N. fuscoviridis	Elongate and thin	Fine and sparse	Non-pigmented	Black	Non-pigmented	Long, posterior and right loops	Acute	Green
N. boninensis	Absent	Fine and dense	Non-pigmented	Black	Gray	Intermediate	Slightly blunt	Red
N. schrenckii	Elongate and thin	Fine and sparse	Black	Black	Black	Intermediate	Acute	Green
N. concinna	Rounded	Absent	Black	Black	Black	Long, posterior and right loops	Acute	Brown
N. radula	Pointed	Fine and sparse	Gray	Black	Gray	Long, posterior and right loops	Acute	Brown
N. nigrans	Elongate and thcik	Thick and dense	Gray	Black	Gray	Short	Acute	Brown
N. habei	Elongate and thin	Fine and dense	Black	Black	Black	Variable from long to short loops	Acute to blunt	Brown
N. teramachii	Elongate and thin	Absent	Black	Black	Black	Short	Acute	Brown

Table 6. Canonical discriminant analysis for individuals of *Nipponacmea* species identified with mtDNA sequences.

Observed classification	Predicted classification									
	1	2	3	4	5	6	7	8	9	% correct
1 *N. gloriosa*	8	0	0	3	0	0	0	0	0	72.7
2 *N. fuscoviridis*	0	23	0	0	1	1	2	0	2	79.3
3 *N. boninensis*	0	1	0	1	0	0	0	0	1	0.0
4 *N. schrenckii*	3	0	0	8	0	0	0	0	1	66.7
5 *N. concinna*	0	7	0	0	7	0	0	1	0	46.7
6 *N. radula*	0	4	0	0	2	1	0	1	0	12.5
7 *N. nigrans*	0	3	0	0	0	0	23	1	0	85.2
8 *N. habei*	0	1	0	0	0	0	6	2	0	66.7
9 *N. teramachii*	0	9	0	1	0	0	0	0	6	37.5

clade is as follows: *N. radula*, *N. concinna*, *N. schrenckii*, and *N. fuscoviridis*, with the latter as the most derived species in this clade. *Nipponacmea boninensis* was recently included in the phylogenetic analysis in this study and formed a clade with *N. fuscoviridis*. Asakura and Nishihama (1987) compared *N. boninensis* to *N. schrenckii*, but Nakano (2007) mentioned similarities between *N. boninensis* and *N. fuscoviridis* regarding morphological and ecological characters. In this study, the latter hypothesis was clearly supported.

The monophyly of Clade B was supported with relatively lower bootstrap values than that of Clade A (BS = 80% by Nakano and Ozawa (2007); and BS = 67% in this study). Phylogenetic relationships within Clade B were inconstant among different analyses. In this study, *N. teramachii* diverges first, and *N. nigrans* and *N. habei* are more closely related (BS = 75%). Previous studies revealed that *N. nigrans* is separated first, and *N. habei* and *N. teramachii* form a clade (BS = 80%) (Nakano and Ozawa 2007).

Differences exist in the aims and taxa sampled between our studies and previous research focused on *Nipponacmea*; however, the results are not contradictory. Compared to previous studies, we improved the phylogenetic analyses and validation of species taxonomy and taxonomic characters by: (1) obtaining novel sequence data from *N. boninensis* for the first time; (2) using the most diverse taxon sampling for *Nipponacmea* to date, including multiple specimens (ranging from 3 to 29) for each species, for a total of 130 specimens from 43 localities and 9 species; and (3) obtaining sequence data for Cytb in addition to other three mitochondrial (COI, 12S, and 16S rRNA) genes. The Cytb gene was used in this study since it evolves at higher rates than the 16S and is better for investigation of among-species and among-populations relationships.

Nipponacmea species taxonomy

The species taxonomy of *Nipponacmea* had long been confused prior to revision by Sasaki and Okutani (1993). The chief cause of this confusion and misidentification was an overemphasis of the importance of shell color pattern. Four to seven species occur sympatrically in temperate Japanese waters, and the distinction and taxonomic rank of these species or subspecies has been contested by various authors (see Sasaki and Okutani 1993 for details). A similar situation also existed in the New Zealand genus *Notoacmea*, before a phylogenetic analysis and taxonomic revision of this genus was performed by Nakano and Spencer (2007) and Nakano et al. (2009) reporting cryptic species and phenotypic polymorphisms. These anomalies were not found in the present study with *Nipponacmea*, and the DNA-based clades were consistent with the morphological species recognized by Sasaki and Okutani (1993). Based on the results of phylogenetic analysis, we discuss the validity and current issues concerning the definition of each species below.

(1) *Nipponacmea gloriosa*: *N. gloriosa* is the exclusive species living in the subtidal zone that grazes on coralline algae (Sasaki and Okutani 1993; Sasaki 2000, 2017). This species was originally described based on shell morphology, shell color, and radula (Habe 1944). The shell is reddish, while the head, cephalic tentacles, and side of the foot are not pigmented (Table 5). Juveniles of *N. gloriosa* can be easily distinguished from those of other *Nipponacmea* species by their reddish-brown radial lines (Sasaki 2006). On morphological grounds, Sasaki and Okutani (1994b) regarded *Collisella cellanica* from Hong Kong as a junior synonym of *N. gloriosa*; this species should be investigated using molecular phylogenetic analysis in the future. It is unclear whether *N. gloriosa* is present outside of Japan in places such as South Korea or Taiwan.

(2) *Nipponacmea fuscoviridis*: The holotype of *N. fuscoviridis* (Teramachi, 1949) was apparently held in the Toba Aquarium's Teramachi Collection, but its location cannot be confirmed. Currently, the identity of this species is based on the topotype specimens collected by Teramachi and preserved in the Kira Collection (Sasaki et al. 2014). For an unclear reason *N. fuscoviridis* was previously regarded as a subspecies of *N. concinna* (Kira 1954; Habe and Kosuge 1967; Kuroda et al. 1971; Okutani and

Habe 1975). *Nipponacmea fuscoviridis* is the only species of the genus found in the Ryukyu Islands (Sasaki and Okutani 1993; Sasaki and Nakano 2007), and it is also distributed in South Korea (Min 2001; Noseworthy et al. 2007) and China (Yu et al. 2014).

Two morphologically similar species are known from Taiwan and Vietnam. Christiaens (1980) described *Collisella formosa* from northern Taiwan based on shell and radula morphology, and Sasaki and Okutani (1994b) suggested that *C. formosa* belongs to *Nipponacmea.* We examined the holotype specimen and concluded that *N. formosa* is most similar to *N. fuscoviridis* based on color pattern and features of the shell sculpture. The validity of *N. formosa* should be verified by molecular characters in future studies. Chernyshev (2008) described *N. vietnamensis* from the Gulf of Tonkin, located in northern Vietnam. *Nipponacmea vietnamensis* is very similar to *N. fuscoviridis*, but it has a different shell color and a characteristic reddish ovary (Chernyshev 2008). The distribution of *N. formosa* and *N. vietnamensis* is geographically separate, but similarity in morphological features suggest they are phylogenetically close and, therefore, these species should also be compared using molecular makers.

(3) *Nipponacmea boninensis*: In the original description, *N. boninensis* was compared to *N. schrenckii* based on shell and radula morphology (Asakura and Nishihama 1987). However, Nakano (2007) highlighted that *N. boninensis* is more similar to *N. fuscoviridis* based on shell color patterns and habitat. In this study, we confirmed that *N. boninensis* is more closely related to *N. fuscoviridis* than *N. schrenckii* genetically. Morphologically this relationship is supported by the outline, apex height, and color pattern of the shell, as well as the pigmentation on the side of the foot, and arrangement of the radular sac (Table 5). The genetic distances indicate that *N. boninensis* is closely related to *N. fuscoviridis* according to the Cytb and 12S rRNA genes (17.1% and 5.6%, respectively). Therefore, *N. boninensis* is clearly differentiated from the other species morphologically and genetically, and should be regarded as an independent species.

Nipponacmea boninensis is an endemic species to the southern Izu Islands (Hachijo Island), Ogasawara Islands, and the northernmost part of the Northern Mariana Islands (Asuncion and Maug Islands: Asakura and Kurozumi 1991: figs 1–3). There are no other *Nipponacmea* species recorded in the Izu-Ogasawara Islands or southward of this region. Fukuda (1993, 1994, 1995a, b) stated that temperate mollusks in the Ogasawara Islands are conveyed by Kuroshio currents from southern Honshu. In the genus *Cellana*, ancestral species possibly reached the Ogasawara Islands through the Izu Islands as stepping-stones (Nakano et al. 2009b). Similar to *Cellana*, the ancestral species of *N. boninensis* was assumed to have migrated from Honshu to the Ogasawara Islands through the Izu Islands.

(4) *Nipponacmea schrenckii*: *N. schrenckii* has the lowest shell apex among *Nipponacmea* species (Takada 1992). Lischke's (1868) holotype is apparently lost, but illustrations from the original literature are clear, leading to few challenges concerning the taxonomic status of the species (Table 6; Lischke 1869). *Nipponacmea schrenckii* also occurs in South Korea (Noseworthy et al. 2007) and China (Huang 2008; Liu 2008), but not in Taiwan.

(5) *Nipponacmea concinna*: Lischke's (1870) type is also missing; however, we used the original illustration for identification purposes. Similar to examples of distinct color polymorphism in patellogastropods (Sasaki 1999a, b; Lindberg 2008; Nakano et al. 2010), *N. concinna* has two color forms (solid and spotted) with occasional intermediate variations (Fig. 3U–Y; Sasaki and Okutani 1993; Sasaki 2000, 2017). The results of this study revealed that these two morphs are intermingled in a single clade; thus, the color forms were proven to be intraspecific variations. The spotted form of *N. concinna* and *N. radula* are the most readily confused phenotypes; however, *N. concinna* can be distinguished by rounded granules and black pigmentation in the snout and the side of the foot. The presence of *N. concinna* outside of Japan and in South Korea has been confirmed (Min 2001; Noseworthy et al. 2007); however, no specimens have been found in China or Taiwan.

(6) *Nipponacmea radula*: The distribution of *N. radula* is limited to the southwest area of Japan, which is a small area compared to that of other *Nipponacmea* species. However, intraspecific genetic divergence is high for this genus. *Nipponacmea radula* tends to prefer sheltered environments, and its distribution areas are often isolated. This specialized habitat may lead to the large genetic distances across the entire geographic range of *N. radula* (within species 9.9% for COI: Table 4). Populations with large genetic distances are completely indistinguishable according to morphological features. The shell height for *N. radula* is relatively low for the genus, and the color pattern is considerably variable (Fig. 4A–E). In the past, this species was misidentified as *N. concinna* or regarded as a subspecies of *N. concinna* (Habe and Kosuge 1967; Nakamura 1986; Takada 1992). *Nipponacmea radula* was found outside of Japan, in South Korea (Min 2001; Noseworthy et al. 2007) and China (Yu et al. 2014), but not in Taiwan.

(7) *Nipponacmea nigrans*: The shell height of *N. nigrans* is relatively high, and the color patterns and shell shape are highly variable (Fig. 3K–T). The individuals from northeastern Japan are more darkly colored, whereas southwestern Japanese populations are lighter. Like *N. radula*, *N. nigrans* has been confused with *N. concinna* (or regarded as a subspecies of *N. concinna*) (Habe and Kosuge 1967; Kuroda et al. 1971; Nakamura 1986). *Collisella mortoni*, Christiaens, 1980 is possibly a junior synonym of this species (Sasaki & Okutani, 1994b). Another similar-looking species, *N. moskalevi* Chernyshev & Chernova, 2002 was described from Sukhoputnaya Bay, Russia based on differences in the sculpture of shell surfaces. In this species, arrangement of the radular sac and radula morphology is similar to that of *N. nigrans*. Relationships among *N. nigrans* and *N. moskalevi* should be tested using molecular makers in future studies. Nipponacmea *nigrans* also occurs in South Korea (Min 2001), China (Christiaens 1980; Yu et al. 2014), and Taiwan (Teruya pers. obs.).

(8) *Nipponacmean habei*: This species is distributed mainly in the cold-water region from the Izu Peninsula to southern Hokkaido on the Pacific coast and from Niigata Prefecture to southern Hokkaido in the Sea of Japan (Sasaki and Okutani 1994a; Sasaki 2000, 2017). *Nipponacmea habei* can be distinguished by its high shell-apex, the lack of a greenish hue inside of the shell, and dark pigmentation.

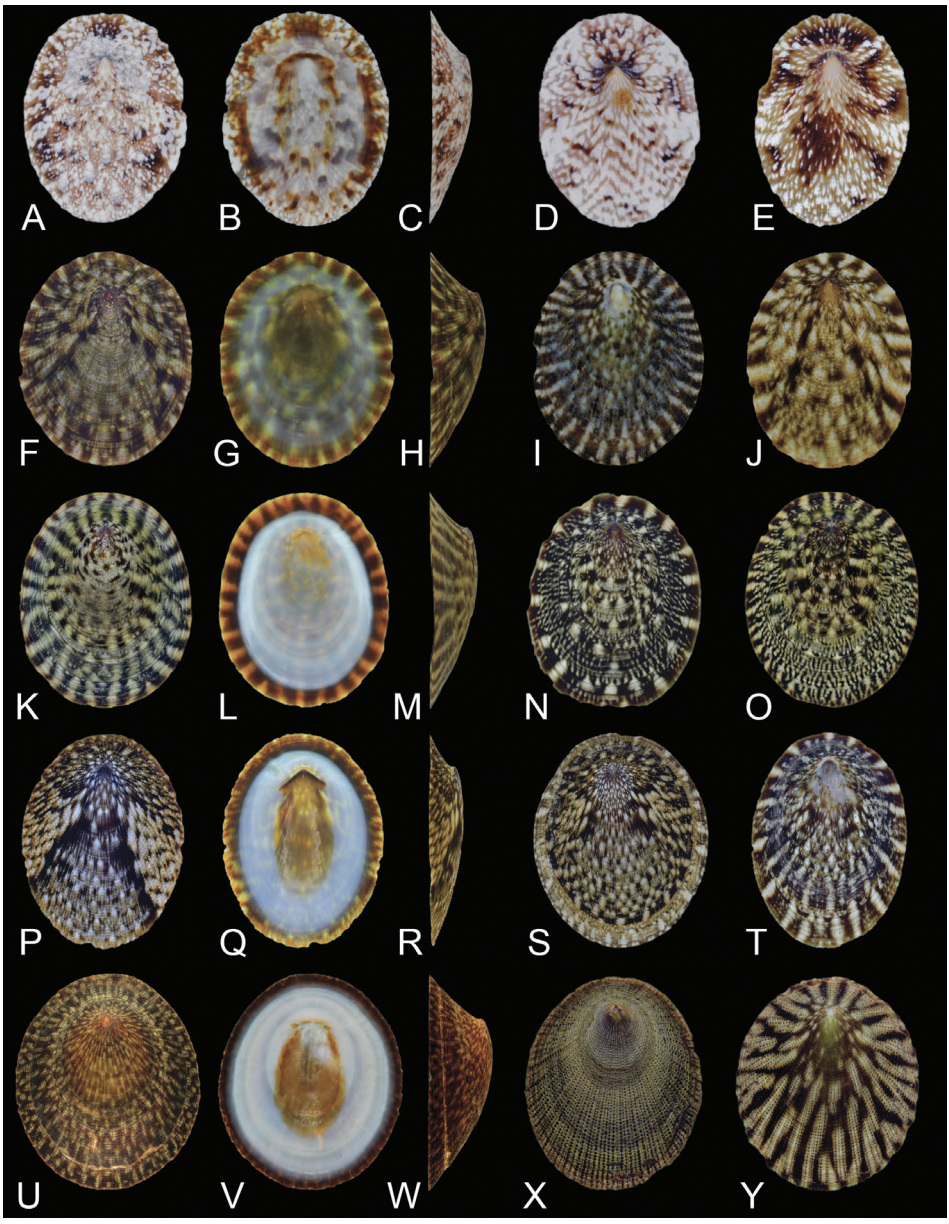

Figure 3. Shell morphology and color pattern of *Nipponacmea gloriosa* and four species of Clade A **A–C** *N. gloriosa*, RM31869, Ibusuki, Kagoshima (41) **D** *N. gloriosa*, RM31860, Tateyama, Chiba (13) **E** *N. gloriosa*, RM31862, Manazuru, Kanagawa (14) **F–H** *N. fuscoviridis*, RM31858, Kimotsuki, Kagoshima (42) **I** *N. fuscoviridis*, RM31846, Nikaho, Akita (10) **J** *N. fuscoviridis*, RM31859, Kimotsuki, Kagoshima (42) **K–M** *N.boninensis*, RM31817, Chichijima Is., Ogasawara (43) **N** *N.boninensis*, RM31815, Chichijima Is., Ogasawara (43) **O** *N.boninensis*, RM31816, Chichijima Is., Ogasawara (43) **P–R** *N. schrenckii*, RM31906, Kazamaura, Aomori (6) **S** *N. schrenckii*, RM31908, Kazamaura, Aomori (6) **T** *N. schrenckii*, RM31916, Nagatamachi, Nagasaki (35) **U–W** *N. concinna*, RM31820, Ofunato, Iwate (11) **X** *N. concinna*, RM31824, Mihamacho, Wakayama (21) **Y** *N. concinna*, RM31828, Suo-Oshima, Yamaguchi (30). Scale bars: 5 mm.

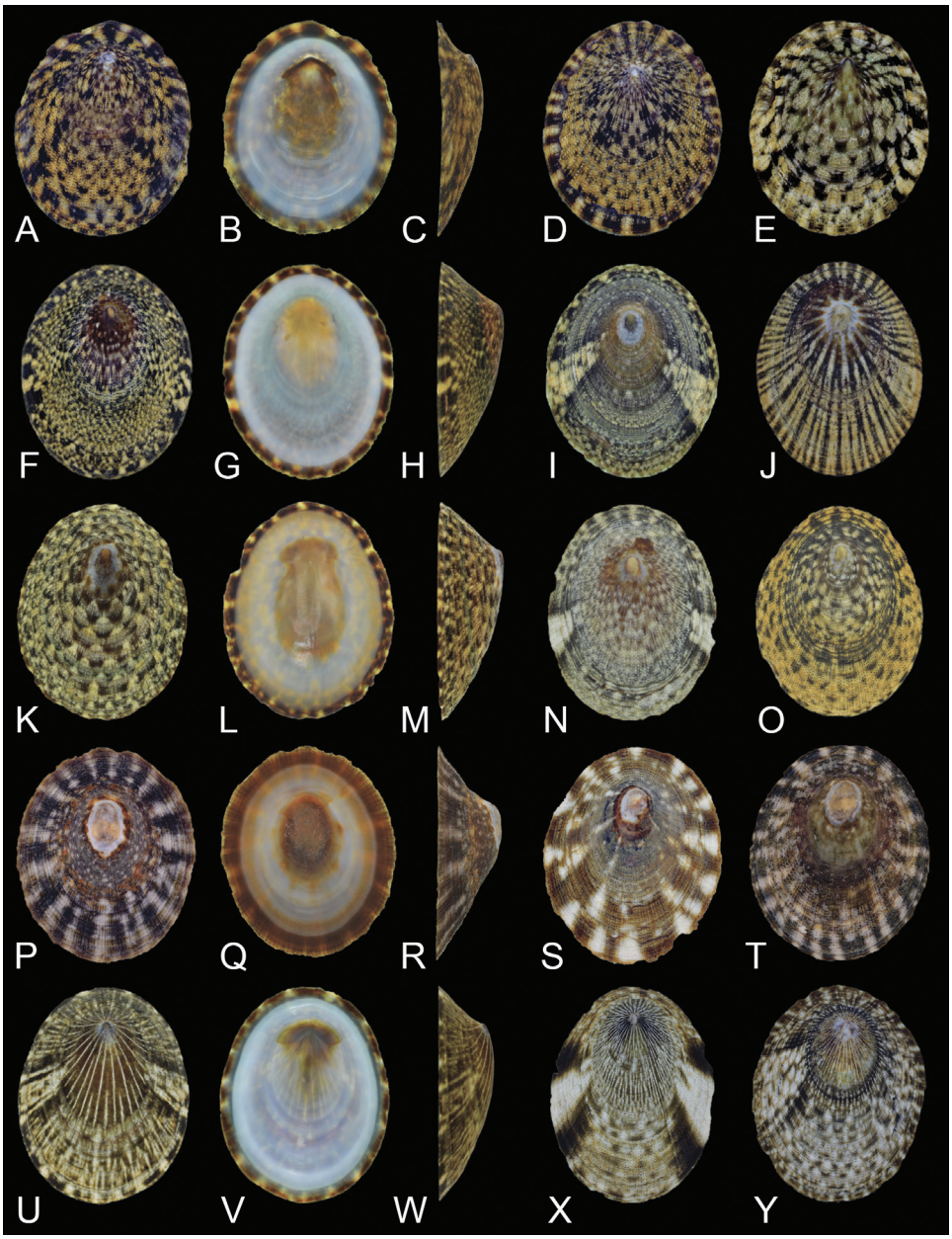

Figure 4. Shell morphology and color pattern of *N. radula* and three species of clade B **A–C** *N. radula*, RM31904, Omura, Nagasaki (34) **D** *N. radula*, RM31902, Omura, Nagasaki (34) **E** *N. radula*, RM31899, Nagato, Yamaguchi (31) **F–H** *N. nigrans*, RM31892, Nishiku, Fukuoka (32) **I** *N. nigrans*, RM31888, Kada, Wakayama (22) **J** *N. nigrans*, RM31895, Higashisonogi, Nagasaki (33) **K–M** *N. nigrans*, RM31887, Minamiizu, Shizuoka (15) **N** *N. nigrans*, RM31886, Minamiizu, Shizuoka (15) **O** *N. nigrans*, RM31897, Higashisonogi, Nagasaki (33) **P–R** *N. habei*, RM31874, Ishinomaki, Miyagi (12) **S** *N. habei*, RM31875, Tateyama, Chiba (13) **T** *N. habei*, RM31873, Usujiri, Hokkaido (5) **U–W** *N. teramachii*, RM31930, Nishiku, Fukuoka (32) **X** *N. teramachii*, RM31925, Sanuki, Kagawa (28) **Y** *N. teramachii*, RM31922, Ainancho, Ehime (24). Scale bars: 5 mm.

Figure 5. Pigmentation of side of foot **A** *N. gloriosa*, RM31861, Manazuru, Kanagawa (14) **B** *N. fuscoviridis*, RM31847, Tateyama, Chiba (13) **C** *N. boninensis*, RM31816, Chichijima Is., Ogasawara (43) **D** *N. schrenckii*, RM31908, Kazamaura, Aomori (6) **E** *N. concinna*, RM31830, Omura, Nagasaki (34) **F** *N. radula*, RM31900, Nagato, Yamaguchi (31) **G** *N. nigrans*, RM32361, Kushimoto, Wakayama (20) **H** *N. habei*, RM31870, Otaru, Hokkaido (2) **I** *N. teramachii*, RM31917, Tateyama, Chiba (13). Scale bars: 5 mm.

The arrangement of the radular sac and the morphology of the lateral teeth are more variable in *N. habei* than in other *Nipponacmea* species (Sasaki and Okutani 1994a), and molecular analysis confirmed that the variants belong to the same clade. The lateral teeth have two main forms (blunt and acute), but can also have an intermediate morphology. Sasaki and Okutani (1994a) presumed that the geographic distribution of the two radular forms is controlled by oceanic currents and different food biota, and a similar case was reported in *Notoacmea scapha* in New Zealand (Nakano and Spencer 2007; Nakano et al. 2009a). However, here we could not sufficiently test the hypothesis using molecular phylogenetic analyses due to the small number of localities and sequenced specimens (Fig. 2, Suppl. material 1: Fig. S1, Suppl. material 2: Fig. S2, Suppl. material 3: Fig. S3). Population genetic structure and morphological tendency should be examined in more detail in the future. *Nipponacmea habei* has not yet been found outside of Japan.

(9) *Nipponacmea teramachii*: Although the name of this species was originally proposed for a form with white radial rays, the shell color pattern of *N. teramachii* is highly variable (Fig. 4). Interestingly, *N. teramachii* juveniles are unexceptionally striated with white radial rays, and most individuals abruptly change their color pattern during ontogeny. According to this juvenile character, *N. teramachii* can easily be distinguished from other *Nipponacmea* species (Sasaki and Okutani 1993; Sasaki 2000, 2017). The variants of *N. nigrans* (e.g., Fig. 4J) with radial rays are similar to *N. teramachii*, but such specimens can be distinguished by the granules on the exterior shell surface. The habitat of *N. teramachii* is limited to slightly sheltered environments. The presence of *N. teramachii* outside of Japan was confirmed in South Korea (Noseworthy et al. 2007), China (Yu et al. 2014), but not in Taiwan.

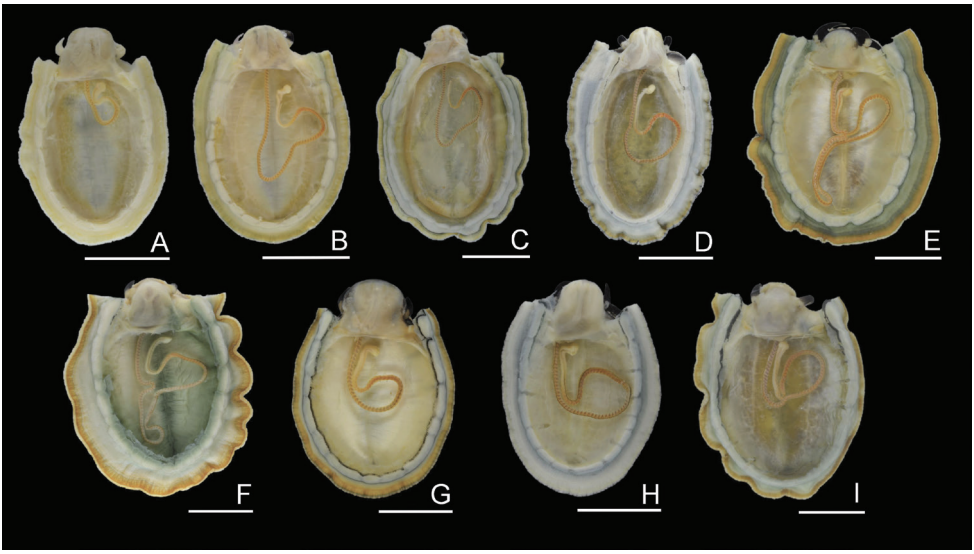

Figure 6. Configuration of radula sac of nine species of *Nipponacema* **A** *N. gloriosa*, RM32355, Ibusuki, Kagoshima (41) **B** *N. fuscoviridis*, RM32354, Akune, Kagoshima (39) **C** *N. boninensis*, RM31817, Chichijima Is., Ogasawara (43) **D** *N. schrenckii*, RM31906, Kazamaura, Aomori (6) **E** *N. concinna*, RM32353, Nagatamachi, Nagasaki (35) **F** *N. radula*, RM32363, Akune, Kagoshima (37) **G** *N. nigrans*, RM32362, Kushimoto, Wakayama (20) **H** *N. habei*, RM32356, Tateyama, Chiba (13) **I** *N. teramachii*, RM31928, Suo-Oshima, Yamaguchi (30). Scale bars: 5 mm.

Validity of morphological characters

Morphology-based studies of patellogastropods have explored various animal characteristics (Lindberg 1981, 1988; Sasaki and Okutani 1993; Ridgway et al. 1998; Sasaki 1998) in addition to the basics of shells and radulae (Pilsbry 1891; Suter 1907; Oliver 1926; Thiele 1929; Powell 1973; Ponder and Creese 1980). Comparison with molecular phylogeny confirmed the utility of shell and soft-part characters in *Nipponacmea*, as discussed below.

(1) Shell color pattern: the degree of variability in the shell color pattern is different among species, and the patterns are categorized into three types: (i) striking variations (*N. radula*, *N. habei*, *N. nigrans*, and *N. teramachii*), (ii) faint variations (*N. schrenckii*, *N. gloriosa*, *N. boninensis*, and *N. fuscoviridis*), and (iii) dimorphisms of solid or spotted patterns (*N. concinna*). In *N. concinna*, the distribution of color forms has a geographic bias maintained by unknown factors: the solid type is common to northeastern Japan, while the spotted type is frequently found in southwestern Japan. Northern individuals of *N. nigrans* and *N. habei* also tend to have dark colored shells. Another similar example is the Japanese mud snail, *Batillaria attramentaria*, which exhibits a shell color polymorphism in which darker morphs are distributed in colder regions and lighter morphs are more commonly found in warmer regions (Miura et al. 2007). The authors

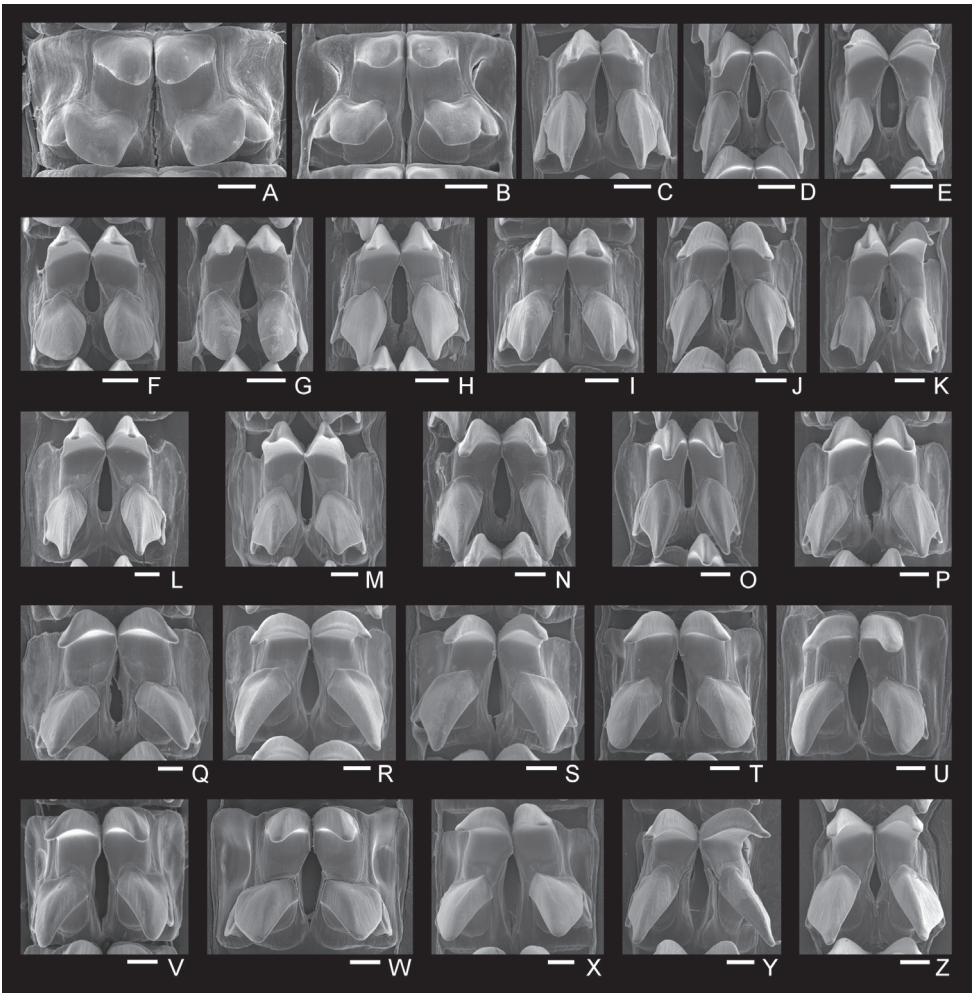

Figure 7. Scanning micrographs of radular teeth of of *Nipponacmea* **A** *N. gloriosa*, RM32355, Ibusuki, Kagoshima (41) **B** *N. gloriosa*, RM31860, Tateyama, Chiba (13) **C** *N. fuscoviridis*, RM31858, Kimotsukicho, Kagoshima (42) **D** *N. fuscoviridis*, RM32354, Akune, Kagoshima (39) **E** *N. fuscoviridis*, RM31834, Rumoi, Hokkaido (1) **F** *N. boninensis*, RM31817, Chichijima Is., Ogasawara (43) **G** *N. boninensis*, RM31815, Chichijima Is., Ogasawara (43) **H** *N. schrenckii*, RM31915, Suo-Oshima, Yamaguchi (30) **I** *N. schrenckii*, RM31906, Kazamaura, Aomori (6) **J** *N. schrenckii*, RM31916, Nagatamachi, Nagasaki (35) **K** *N. concinna*, RM31831, Omura, Nagasaki (34) **L** *N. concinna*, RM32353, Nagatamachi, Nagasaki (35) **M** *N. concinna*, RM31823, Tahara, Aichi (19) **N** *N. radula*, RM31898, Hamamatsu, Shizuoka (18) **O** *N. radula*, RM31904, Omura, Nagasaki (34) **P** *N. radula*, RM32363, Akune, Kagoshima (37) **Q** *N. nigrans*, RM32360, Kushimoto, Wakayama (20) **R** *N. nigrans*, RM32359, Kushimoto, Wakayama (20) **S** *N. nigrans*, RM32358, Kushimoto, Wakayama (20) **T** *N. habei*, RM32364, Tateyama, Chiba (13) **U** *N. habei*, RM31872, Suttu, Hokkaido (3) **V** *N. habei*, RM31873, Usujiri, Hokkaido (5) **W** *N. habei*, RM32357, Usujiri, Hokkaido (5) **X** *N. habei*, RM32356, Tateyama, Chiba (13) **Y** *N. teramachii*, RM31926, Sanuki, Kagawa (28) **Z** *N. teramachii*, RM31924, Ohira, Oita (25). Scale bars: 50 μm.

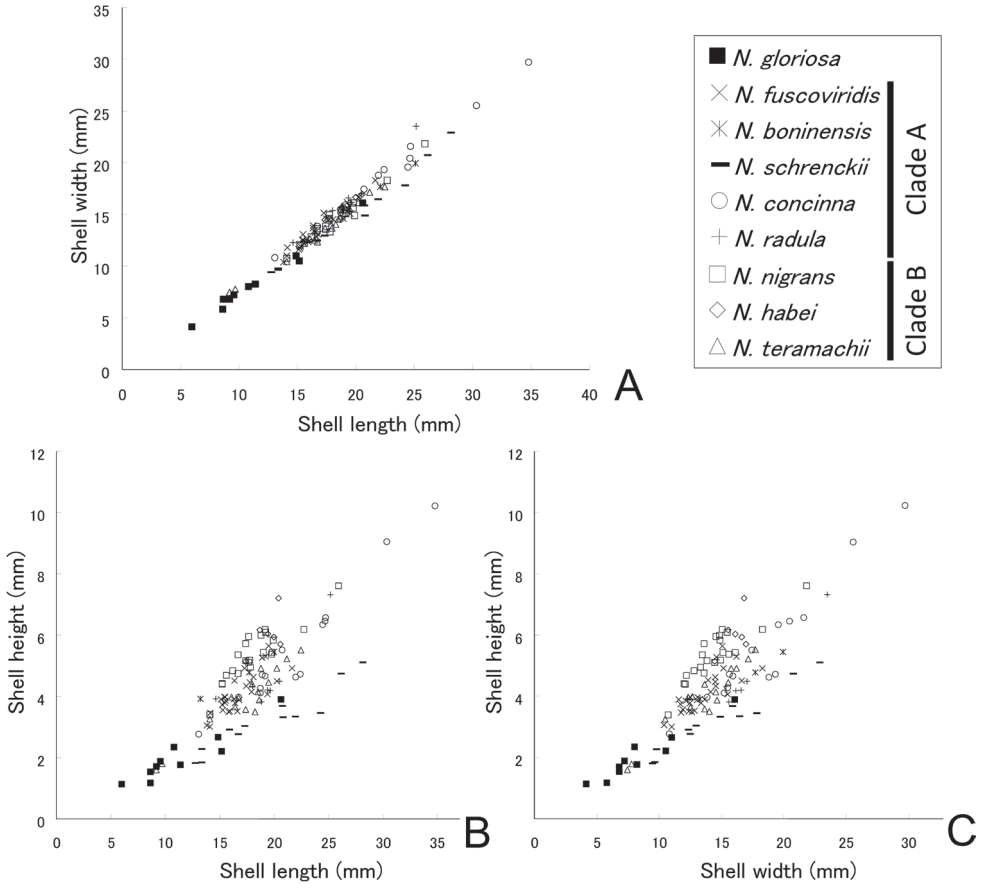

Figure 8. Relationships among shell length, width, and height.

suggested that shell color polymorphism is caused by climatic selection, which could be the case for the shell color patterns of *N. concinna*, *N. nigrans*, and *N. habei*.

The shell of *N. gloriosa* is reddish brown and completely different from other *Nipponacmea* species (Fig. 3A–E). Patellogastropod species associated with coralline algae in the subtidal zone are generally known to have reddish or white shells (e.g., *Niveotectura pallida*, *Tectura emydia*, and *Erginus sybariticus*; Lindberg 2008), and *N. gloriosa* appears to follow this trend. In this case, the color of the shell might be derived from the pigment of the grazed algae.

(2) Shell sculpture: concerning shell sculpture, ribs and granules on the shell exterior are differentiated among species (Table 5). In multiple limpet groups, species living in sun-exposed rocky surfaces tend to have more prominent sculptures than those in shaded habitats (Vermeij 1973). However, this is not observed in *Nipponacmea* species. For instance, *N. fuscoviridis* is attached to the exposed surface during the highest tidal level, but has a delicately sculptured shell, while *N. nigrans* has the most remarkably ornamented ribs and granules, but prefers relatively sheltered environments, and

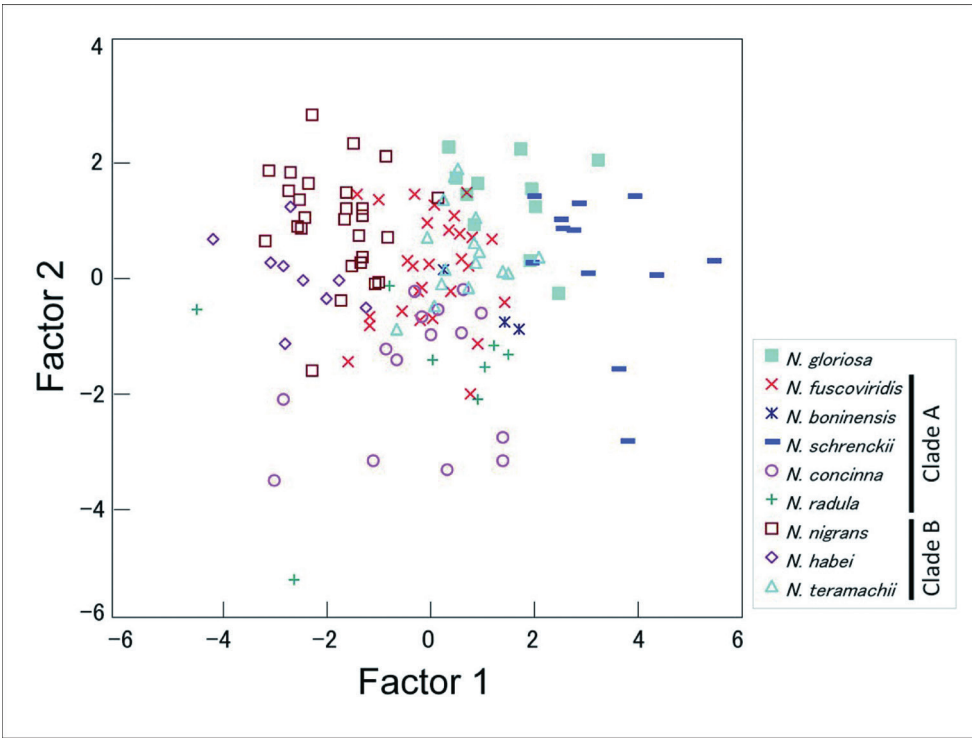

Figure 9. Plot of the results of discriminant function analysis of shell length, width, and height for individuals of *Nipponacmea* species.

N. concinna has notable granules, but is nocturnal and prefers shaded areas in the daytime (Sasaki pers. obs.). Hence, we cannot detect any fixed ecological pattern linked to microscopic shell sculpture within *Nipponacmea*.

(3) Apex height: Takada (1992) indicated quantitatively that there are variations in height among *Nipponacmea* species. For example, in the ratio of shell length to height, *N. schrenckii* has the lowest apex and *N. nigrans* had the highest among *Nipponacmea* species (fig. 2 in Takada 1992). Japanese species are separated into two groups: *N. gloriosa* and Clade A constitute the low-apex group, and Clade B comprises the high-apex one.

In *Nipponacmea*, the shell height is not relevant to the vertical distribution (Sasaki and Okutani 1993: fig. 28) in the tidal zone. It was previously assumed that variation in limpet apex height is correlated with habitat tidal level (Ino 1935; Vermeij 1973), whereby species with a higher shell apex are assumed to store a larger amount of seawater, which might be an adaptation to prevent desiccation (Vermeij 1973; Branch 1975). In this study, we confirmed that the shell height among *Nipponacmea* species is not correlated with tidal level distributions in the intertidal zone.

The topology of the phylogenetic tree implies that the high-apex group could be derived from the low-apex species, since the most basal species, *N. gloriosa*, and Clade A share a low apex. In the genus *Notoacmea* in New Zealand, 13 species formed two

Table 7. Holotype specimens, type localities, and geographic distribution of *Nipponacmea* species.

Species	Holotype	Type locality	Geographic distribution
N. gloriosa (Habe, 1944)	National Museum of Nature and Science,Tsukuba, NSMT-Mo 100675	Urado, Kochi Prefecture	Pacific coast from Choshi to Kyushu, the Sea of Japan from Oga Peninsula to Kyushu, and rare in Seto Inland Sea; China.
N. fuscoviridis (Teramachi, 1949)	Teramachi Collection in Toba Aquarium, missing	Akune, Kagoshima Prefecture	Pacific coast and the Sea of Japan from southern Hokkaido to Kyushu, and Ryukyu Islands; Korea, China.
N. boninensis (Asakura & Nishihama, 1987)	National Museum of Nature and Science,Tsukuba, NSMT-Mo 64445	Yagyu-san, Chichijima Island, Ogasawara Islands	Hachijo Island, Ogasawara Islands, and Northern Mariana Islands (Asuncion and Maug Islands)
N. schrenckii (Lischke, 1868)	Unknown	Nagasaki City	Tsugaru Strait to Kyushu, and Seto Inland Sea; Korea, China.
N. concinna (Lischke, 1870)	Unknown	Nagasaki City	Pacific coast and the Sea of Japan from Hokkaido to Kyushu, and Seto Inland Sea; Korea.
N. radula (Kira, 1961)	Osaka Museum of Natural History, Kira Collection 525	Akune, Kagoshima Prefecture	Pacific coast from Shizuoka Prefecture to Kyushu, the Sea of Japan from Yamaguchi Prefecture to Kyushu, and Seto Island Sea; Korea, China.
N. nigrans (Kira, 1961)	Osaka Museum of Natural History, Kira Collection 540	Shionomisaki, Kii Peninsula	Pacific coast and the Sea of Japan from Hokkaido to Kyushu, and Seto Inland Sea; Korea, China, Taiwan.
N. habei Sasaki & Okutani, 1994	National Museum of Nature and Science,Tsukuba, NSMT-Mo 69985	Shiragami-misaki, Matsumae, Hokkaido	Pacific coast from Hokkaido to Izu Peninsula, the Sea of Japan from Hokkaido to Niigata Prefecutre
N. teramachii (Kira, 1961)	Osaka Museum of Natural History, Kira Collection 554	Akune, Kagoshima Prefecture	Pacific coast from Ojika Peninsula to Kyushu, western and northern Kyushu, and Seto Inland Sea; Korea, China.
N. formosa (Christiaens, 1977)	Natural History Museum, London, No. 1977167	Northern Taiwan	Taiwan
N. vietnamensis Chernyshev, 2008	Zoological Museum of Far East State University, No. 18852	Gulf of Tonkin	Vietnam
N. moskalevi Chernyshev & Chernova, 2002	Zoological Museum of Far East State University, No H 2666	Japan Sea, Sukhoputnaya Bay	Far East Russia

major clades; however, they were not based on shell height (Nakano et al. 2009a). Similarly, in the phylogeny of 15 *Nacella* species, shell height is not correlated with phylogeny (González-Wevar et al. 2011). Thus, shell height in general is not controlled by phylogeny in patellogastropod limpets (Nakano and Sasaki 2011).

(4) Animal pigmentation: we confirmed that the pigmentation of the snout, cephalic tentacle, and side of the foot is different among species (Fig. 5). The side of the foot of three species included in Clade B and *N. schrenckii* of Clade A tends to be pigmented in black. Ecologically, the dark pigmentation on the foot wall might be effective to avoid visible detection by predators. However, actual ecological significance is uncertain regarding the species-specific animal pigmentation patterns in *Nipponacmea*.

Nipponacmea gloriosa, which inhabits the subtidal zone, lacks pigmentation, and the pale coloration of this animal is possibly a consequence of its habitat. The limpets inhabiting the subtidal zone are unexceptionally pale (e.g., *Niveotectura pallida*, *Tectura emydia*, and *Erginus sybariticus*; Lindberg 2008). For species that inhabit the range from the middle to upper intertidal zone, animal pigmentation is unrelated to tidal level preference in *Nipponacmea*. For example, both *N. concinna* and *N. fuscoviridis* prefer higher tidal levels, but the former species is darkly pigmented, while the latter

lacks pigmentation. Thus, it is not straightforward to correlate animal pigmentation patterns and habitats.

(5) Radular sac: the configuration of the radular sac has been regarded as a useful character for identification of *Nipponacmea* species (Sasaki and Okutani 1993; Sasaki 1999a, b). The looping of this pouch is categorized into four types: (i) a short single loop (*N. gloriosa*), (ii) an intermediate length loop (*N. schrenckii*, *N. boninensis*, *N. nigrans*, and *N. teramachii*), (iii) a long radular sac with two loops (*N. concinna*, *N. fuscoviridis*, and *N. radula*), and finally (iv) a variable type ranging from long to short loops (*N. habei*) (Sasaki and Okutani 1993). In addition to differences among species, vertical distribution in the intertidal zone appears to correlate with radular sac length in *Nipponacmea*, whereby the lengths are longer in species inhabiting the higher intertidal zone and shorter in those in the lower intertidal zone.

(6) Radula: the radula morphology is useful for classifying patellogastropod species (Habe 1944; Macpherson 1955; Moskalev 1970; Ponder and Creese 1980; Lindberg 1981; Lindberg and McLean 1981; Sasaki and Okutani 1993). Clarifying the relationship between food and the radula is important for understanding radula morphology (Lindberg 1988). Among *Nipponacmea* species, *N. concinna* is known to graze on green algae (*Ulva* spp.) (Kawakami and Habe 1986), and *N. gloriosa* is a specialist grazer on coralline algae. The limpets gazing on coralline algae tend to have blunt radula (e.g., *Niveotectura pallida* and *Patelloida signatoides*), whereas the other *Nipponacmea* species are more likely to reveal acute radulae; however, the teeth of *N. boninensis* and *N. habei* are slightly blunt for an unknown reason. At present, the relationship between radular teeth morphology and feeding habits is unclear for non-coralline algae grazers, since there is a lack of detailed data concerning their feeding preferences.

(7) Ovary: the ovaries of *Nipponacmea* species were categorized into three types: (i) green (*N. fuscoviridis* and *N. schrenckii*); (ii) red (*N. boninensis* and *N. gloriosa*); or (iii) brown (*N. concinna*, *N. radula*, *N. teramachii*, *N. nigrans*, and *N. habei*). In relation to the phylogeny, the ovaries of all species in Clade B are pigmented brown, whereas those of Clade A are variable.

In gastropods, the color of the ovary might be constrained according to taxonomic group (e.g., green in vetigastropods such as *Haliotis* and *Turbo*). However, the ovaries of patellogastropods have diversified into various colors. For example, the ovary is brown in *Patelloida lanx* and green in its congener *P. conulus* (Sasaki pers. obs.). The cause for ovary diversification and the ecological significance of color differences in the Patellogastropoda is unknown.

Future studies

In this study, we confirmed that current species identified of the Japanese *Nipponacmea* are corroborated by the results from molecular phylogenetic analyses including topotype sequence data, comparative anatomy, and the reinvestigation of type specimens. This study represents an important step towards the revision of the entire group of Asian *Nipponacmea*. Currently, studying Japanese species is important for

two reasons: (1) 9 of 12 nominal species in the genus have been described from Japan, and (2) all Japanese species have older species names and nomenclatural priority over more recently described non-Japanese species. *Nipponacmea formosa* in Taiwan, *N. vietnamensis* in Vietnam, and *N. moskalevi* in Russia must be verified according to morphology, molecular phylogeny, and ecological traits in future studies. In conclusion, a more comprehensive reinvestigation of the genus *Nipponacmea* must be undertaken using taxonomic, phylogenetic, and phylogeographic analyses over a wide geographic range covering Japan, Korea, Russian Far East, China, Taiwan, and Vietnam.

Acknowledgements

We would like to thank Hirofumi Kubo, Jun Nawa, Kazuyoshi Endo, Kei Sato, Keisuke Shimizu, Kozue Nishida, Masanori Okanishi, Masashi Yamaguchi, Naoki Hashimoto, Rei Ueshima, Rie Nakano, Shigeaki Kojima, Takanobu Tsuihiji, Takashi Okutani, Takuma Haga, Tomoyasu Yamazaki, Yoshihisa Kurita, You Usami, Yusuke Takeda for assistance in sampling and useful suggeston. Also we thank Nobuyuki Suzuki, Hiroaki Fukumori, Rie Sakai, Ryo Nakayama, Saki Kamiyama, Takashi Muranaka, Tatsuki Tsuhako, Toshiaki Shitamitu, Youhei Otaki, Youichi Maeda who helped us to collect samples. This work was supported by Grants-in-Aid for Scientific Research (KAKENHI) no. 14J09937 to S. Teruya and 26291077, 19K21646 and 20H01381 to T. Sasaki from the Japan Society for Promotion of Science.

References

Akaike H (1974) A new look at the statistical model identification. IEEE Transactions Automatic Control 19: 716–723. https://doi.org/10.1109/TAC.1974.1100705

Asakura A, Nishihama S (1987) Studies on the biology and ecology of the intertidal animals of Chichijima Island in the Ogasawara Islands – II. Description, distribution, size structure in the population and allometric growth of the limpet, *Notoacmea schrenckii boninensis* n. subsp. Venus 46: 182–193.

Bird CE, Holland BS, Bowen BW, Toonen RJ (2007) Contrasting phylogeography in three endemic Hawaiian limpets (*Cellana* spp.) with similar life histories. Molecular Ecology 16: 3173–3186. https://doi.org/10.1111/j.1365-294X.2007.03385.x

Boore JL, Brown WM (2000) Mitochondrial genomes of *Galathealinum*, *Helobdella*, and *Platynereis*: sequence and gene arrangement comparisons indicate that Pogonophora is not a phylum and Annelida and Arthropoda are not sister taxa. Molecular Biology and Evolution 17: 87–106. https://doi.org/10.1093/oxfordjournals.molbev.a026241

Bouchet P (2015) *Nipponacmea* Sasaki, Okutani 1993. World Register of Marine Species. http://www.marinespecies.org/aphia.php?p=taxdetails&id=391295 [accessed 10 March 2016]

Branch GM (1975) Ecology of *Patella* species from the Cape Peninsula, South Africa, IV. Desiccation. Marine Biology 32: 179–188. https://doi.org/10.1007/BF00388510

Branch GM (1985a) Limpets: evolution and adaptation. In: Trueman ER, Clarke MR (Eds) The Mollusca, Vol. 10: Evolution. Academic Press, New York, 187–220. https://doi.org/10.1016/B978-0-12-751410-9.50012-5

Branch GM (1985b) Limpets: their role in littoral and sublittoral community dynamics. In: Moore PG, Seed R (Eds) The Ecology of Rocky Coasts. Hodder and Stoughton, London, 97–116.

Chernyshev AV, Chernova TV (2002) *Nipponacmea moskalevi* sp. nov. (Gastropoda, Lottiidae), a new species of limpets from the Japan Sea. Ruthenica 12: 19–22.

Chernyshev AV (2008) *Nipponacmea vietnamensis* sp. nov. (Gastropoda: Lottiidae), a new species of limpets from the Gulf of Tonkin (South China Sea). The Bulletin of the Russian Far East Malacological Society 12: 116–121.

Christlaens J (1980) The limpets of Hong Kong with descriptions of seven new species and subspecies. In: Morton (Ed.) Malacofauna of Hong Kong and Southern China, vol. 1. Hong Kong University Press, Hong Kong, 61–84.

de Aranzamendi MC, Gardenal NC, Martin JP (2009) Limpets of the genus *Nacella* (Patellogastropoda) from the southwestern Atlantic: species identification based on molecular data. Journal of Molluscan Studies 75: 241–251. https://doi.org/10.1093/mollus/eyp025

Doyle JJ, Doyle JL (1990) Isolation of plant DNA from fresh tissue. Focus 12: 13–15. https://doi.org/10.2307/2419362

Folmer O, Black M, Hoen W, Lutz RA, Vrijenhoek CR (1994) DNA primers for amplification of mitochondrial cytochrome c oxidase subunit I from diverse metazoan invertebrates. Molecular Marine Biology and Biotechnology 3: 294–299.

Fukuda H (1993) Marine Gastropoda (Mollusca) of the Ogasawara (Bonin) Islands. Part 1. Archaeogastropoda and Neotaenioglossa. Ogasawaran Research 19: 1–85.

Fukuda H (1994) Marine Gastropoda (Mollusca) of the Ogasawara Islands (Bonin) Islands. Part 2: Neogastropoda, Heterobranchia and fossil species, with faunal accounts. Ogasawara Research 20: 1–126.

Fukuda H (1995a) Marine Gastropoda (Mollusca) of the Ogasawara Islands (Bonin) Islands. Part 3: Additional records. Ogasawara Research 21: 1–142.

Fukuda H (1995b) Marine Gastropoda and phylogeography of the Ogasawara Islands. In: Asakura A (Ed.) Voyage of Northern Mariana Islands. Bunichisogo Shuppan, Tokyo, 264–278.

Goldstien SJ, Gemmell NJ, Schiel DR (2009) Colonisation and connectivity by intertidal limpets among New Zealand, Chatham and sub-Antarctic Islands. I. Genetic connections. Marine Ecology Progress Series 388: 111–119. https://doi.org/10.3354/meps08046

González-Wevar CA, Nakano T, Cañete JI, Poulin E (2011) Concerted genetic, morphological and ecological diversification in *Nacella* limpets in the Magellanic Province. Molecular Ecology 20: 1936–1951. https://doi.org/10.1111/j.1365-294X.2011.05065.x

Habe T, Kosuge S (1967) Common Shells of Japan in Color. Hoikushya, Osaka, 223 pp. [+ 64 pls] [In Japanese]

Habe T (1944) On the family Lottiidae (= Acmaeidae) from Japan. Venus 13: 171–187. [In Japanese; original title translated]

Hebert PDN, Ratnasingham S, Dewaard JR (2003) Barcoding animal life: cytochrome c oxidase subunit 1 divergences among closely related species. Proceedings of the Royal Society of London – Series B: Biological Sciences 270: S96–S99. https://doi.org/10.1098/rsbl.2003.0025

Huang ZG (2008) Marine species and their distribution in China. China Ocean Press, Beijing.
Ino T (1935) Shell variation of *Cellana toreuma* (Reeve) in relation to the environment. Bulletin of the Japanese Society of Scientific Fisheries 4: 31–36. https://doi.org/10.2331/suisan.4.31
Katoh K, Toh H (2008) Recent developments in the MAFFT multiple sequence alignment program. *Briefings in Bioinformatics* 9: 286–298. https://doi.org/10.1093/bib/bbn013
Kawakami H, Habe T (1986) Browsing Scar of *Notoacmaea concinna* (Lischke). Chiribotan 17: 32.
Kimura M (1980) A simple method for estimating evolutionary rate of base substitutions through comparative studies of nucleotide sequences. Journal of Molecular Evolution 16: 111–120. https://doi.org/10.1007/BF01731581
Kira T (1959) Colored Illustrations of the Shells of Japan (Vol. I). Hoikusha Publishing, Osaka, 239 pp. [In Japanese]
Kira T (1961) On three new species of *Notoacmea*. Venus 21: 292–295. https://doi.org/10.2307/1439803
Koufopanou V, Reid DG, Ridgway SA, Thomas RH (1999) A molecular phylogeny of patellid limpets (Gastropoda: Patellidae) and its implications for the origins of their antitropical distribution. Molecular Phylogenetics and Evolution 11: 138–156. https://doi.org/10.1006/mpev.1998.0557
Kuroda T, Habe T, Oyama K (1971) The Sea Shells of Sagami Bay. Maruzen, Tokyo, 1281 pp. [121 pls]
Lindberg DR, Mclean JH (1981) Tropical Eastern Pacific limpets of the family Acmaeidae (Mollusca, Archaeogastropoda): generic criteria and descriptions of six new species from the mainland and the Galápagos Islands. Proceedings of the California Academy of Sciences, fourth series 42: 323–339.
Lindberg DR (1979) *Problacmea moskalevi* Golikov and Kussakin, a new addition to the eastern Pacific limpet fauna. The Veliger 22: 57–61.
Lindberg DR (1981) Invertebrates of the San Francisco Bay Estuary System: Mollusca, Family Acmaeidae. The Boxwood Press, Pacific Grove, California, 120 pp.
Lindberg DR (1988) The Patellogastropoda. Malacological Review Supplement 4: 35–63.
Lindberg DR (2008) Patellogastropoda, Neritimorpha, and Cocculinoidea. In: Ponder WF, Lindberg DR (Eds) Phylogeny and evolution of the Mollusca. University of California Press, California, 271–296. https://doi.org/10.1525/california/9780520250925.003.0011
Lischke CE (1868) Diagnosen neuer meeres Conchylien von Japan. Malakozoologisches Blatter 15: 218–222.
Lischke CE (1869) Japanische Meeres-Conchylien 1. Theodor Fischer, Cassel, 192 pp. [14 pls]
Lischke CE (1871) Japanische Meeres-Conchylien 2. Theodor Fischer, Cassel, 184 pp. [14 pls]
Liu RY (2008) Checklist of marine biota of China seas. Science Press, Beijing, 1267 pp.
Mauro A, Arculeo M, Parrinello N (2003) Morphological and molecular tools in identifying the Mediterranean limpets *Patella caerulea*, *Patella aspera* and *Patella rustica*. Journal of Experimental Marine Biology and Ecology 295: 131–143. https://doi.org/10.1016/S0022-0981(03)00291-0
Min DK (2001) Korean Mollusks with Color Illustration. Shell House, Seoul, 333 pp. [In Korean]
Miura O, Nishi S, Chiba S (2007) Temperature-related diversity of shell colour in the intertidal gastropoda *Batillaria*. Journal of Molluscan Studies 73: 235–240. https://doi.org/10.1093/mollus/eym019

Nakamura H (1986) Family Acmaeidae. In: Okutani T (Ed.) Molluscs (Color illustrated encyclopedia). Sekaibunka-sha, Tokyo, 38–40. [In Japanese]

Nakano T, Ozawa T (2004) Phylogeny and historical biogeography of limpets of the order Patellogastropoda based on mitochondrial DNA sequences. Journal of Molluscan Studies 70: 31–41. https://doi.org/10.1093/mollus/70.1.31

Nakano T, Ozawa T (2005) Systematic revision of *Patelloida pygmaea* (Dunker, 1860) (Gastropoda: Lottiidae), with a description of a new species. Journal of Molluscan Studies 71: 357–370. https://doi.org/10.1093/mollus/eyi039

Nakano T, Ozawa T (2007) Worldwide phylogeography of limpets of the order Patellogastropoda: molecular, morphological and paleontological evidence. Journal of Molluscan Studies 73: 79–99. https://doi.org/10.1093/mollus/eym001

Nakano T, Sasaki T (2011) Recent advances in molecular phylogeny, systematics and evolution of patellogastropod limpets. Journal of Molluscan Studies 77: 203–217. https://doi.org/10.1093/mollus/eyr016

Nakano T, Spencer HG (2007) Simultaneous polyphenism and cryptic species in an intertidal limpet from New Zealand. Molecular Phylogenetics and Evolution 45: 470–479. https://doi.org/10.1016/j.ympev.2007.07.020

Nakano T (2007) Distribution of patellogastropod limpets in the Ogasawara Islands, Japan. Chiribotan 37: 174–179. [In Japanese]

Nakano T, Marshall BA, Kennedy M, Spencer HG (2009a) The phylogeny and taxonomy of New Zealand *Notoacmea* and *Patelloida* species (Mollusca: Patellogastropoda: Lottiidae) inferred from DNA sequences. Molluscan Research 29: 33–59.

Nakano T, Sasaki T, Kase T (2010) Color polymorphism and historical biogeography of the Japanese patellogastropod limpet *Cellana nigrolineata* (Reeve) (Gastropoda: Nacellidae). Zoological Science 27: 811–820. https://doi.org/10.2108/zsj.27.811

Nakano T, Yamazaki T, Kurokawa M, Yamaguchi K, Kuwasawa K (2009b) The origin of the endemic patellogastropod limpets of the Ogasawara Islands in the northwestern Pacific. Journal of Molluscan Studies 75: 87–90. https://doi.org/10.1093/mollus/eyn036

Noseworthy RG, Lim N-R, Choi K-S (2007) A Catalogue of the Mollusks of Jeju Island, South Korea. Korean Journal of Malacology 23: 65–104.

Nylander JAA (2004) MrModeltest, version 2.3. Program distributed by the author. Evolutionary Biology Centre, Uppsala University, Uppsala.

Okutani T, Habe T (1975) Mollusca I, Chiefly from Japan. Gakken, Tokyo, 301 pp. [In Japanese]

Oliver WRB (1926) Australasian Patelloididae. Transactions of the New Zealand Institute 56: 547–582.

Pilsbry HA (1891) Manual of Conchology, Structural and Systematic, with Illustrations of the Species. Vol. 13. Acmaeidae, Lepetidae, Patellidae, Titiscaniidae. Academy of Natural Sciences, Philadelphia, 195 pp.

Ponder WF, Creese RG (1980) A revision of the Australian species of *Notoacmea*, *Collisella* and *Patelloida* (Mollusca: Gastropoda: Acmaeidae). Journal of Malacological Society of Australia 4: 167–208. https://doi.org/10.1080/00852988.1980.10673927

Powell AWB (1973) The Patellid Limpets of the World (Patellidae). Indo-Pacific Mollusca 3: 75–206.

R Core Team (2014) R: a language and environment for statistical computing. R Foundation for Statistical Computing, Vienna.

Reisser CMO, Marchall BA, Gardner JPA (2012) A morphometric approach supporting genetic results in the taxonomy of the New Zealand limpets of the *Cellana strigilis* complex (Mollusca: Patellogastropoda: Nacellidae). Invertebrate Systematics 26: 193–203. https://doi.org/10.1071/IS11042

Reisser CMO, Wood AR, Bell JJ, Gardner JPA (2011) Connectivity, small islands and large distances: the *Cellana strigilis* limpet complex in the Southern Ocean. Molecular Ecology 20: 3399–3413. https://doi.org/10.1111/j.1365-294X.2011.05185.x

Ridgway SA, Reid DG, Taylor JD, Branch GM, Hodgson AN (1998) A cladistic phylogeny of the family Patellidae (Mollusca: Gastropoda). Philosophical Transactions of the Royal Society London, Series B 353: 1645–1671. https://doi.org/10.1098/rstb.1998.0316

Ronquist F, Huelsenbeck JP (2003) MrBayes 3: Bayesian phylogenetic inference under mixed models. Bioinformatics 19: 1572–1574. https://doi.org/10.1093/bioinformatics/btg180

Sasaki T, Nakano T (2007) The Southernmost Record of *Nipponacmea fuscoviridis* (Patellogastropoda: Lottiidae) from Iriomote Island, Okinawa. Venus 66: 99–102.

Sasaki T, Okutani T (1993) New genus *Nipponacmea* (Gastropoda, Lottiidae): a revision of Japanese limpets hitherto allocated in *Notoacmea*. Venus 52: 1–40.

Sasaki T, Okutani T (1994a) Description of a new lottiid limpet, *Nipponacmea habei*, with special reference to morphology and distribution of two intraspecific populations. Venus 53: 1–20.

Sasaki T, Okutani T (1994b) Type specimens of four lottiid limpets described by J. Christiaens (1980) from Hong Kong. Venus 53: 129–132.

Sasaki T, Okutani T (1994c) An analysis on '*Collisella heroldi*' complex (Gastropoda: Lottiidae), with description of three new species. Venus 53: 251–285.

Sasaki T (1998) Comparative anatomy and phylogeny of the recent Archaeogastropoda (Mollusca: Gastropoda). University Museum University of Tokyo Bulletin 38: 1–223.

Sasaki T (1999a) A review on systematics of patellogastropoda limpets (Mollusca: Gastropoda) in Japan. In: Okutani T, Ota S, Ueshima R (Eds) Recent Advances in Marine Invertebrate Zoology. Tokai University Press, Tokyo, 101–119. [In Japanese]

Sasaki T (1999b) The present state and problems of the taxonomy of Japanese Patellogastropoda limpets. Part 2. Lottiidae. Chiribotan 29: 37–46. [In Japanese]

Sasaki T (2000) Patellogastropoda. In: Okutani T (Ed.) Marine Mollusks in Japan. Tokai University Press, Tokyo, 24–33.

Sasaki T (2017) Patellogastropoda. In: Okutani T (Ed.) Marine Mollusks in Japan. 2nd edn. Tokai University Press, Kanagawa, 738–744. [pls 12–16]

Sasaki T (2006) The protoconch and early teleoconch of *Nipponacmea gloriosa* (Patellogastropoda: Lottiidae). Chiribotan 37: 72–73.

Sasaki T, Ishida S, Nakano T, Teruya S (2014) Patellogastropoda in the Kira Collection deposited in the Osaka Museum of Natural History. Chiribotan 45: 62–71. [In Japanese]

Simison WB, Lindberg DR (1999) Morphological and molecular resolution of a putative cryptic species complex: a case study of *Notoacmea fascicularis* (Menke, 1851) (Gastropoda: Patellogastropoda). Journal of Molluscan Studies 65: 99–109. https://doi.org/10.1093/mollus/65.1.99

Simison WB, Lindberg DR (2003) On the identity of *Lottia strigatella* (Carpenter, 1864) (Patellogastropoda: Lottiidae). The Veliger 46: 1–19.

Suter H (1904) Mollusca. In: Hutton FW (Ed.) Index faunae Novae Zealandiae. Dulau, London, 57–95.

Takada T (1992) Multivariate analysis of shell morphology of *Notoacmea* spp. in Amakusa. Venus 51: 175–185.

Takahashi G, Okamoto M (1969) Catalogue of Molluscan Shells of Fukuoka Prefecture. Published by the authors, Fukuoka, 154 pp. [In Japanese]

Talavera G, Castresana J (2007) Improvement of phylogenies after removing divergent and ambiguously aligned blocks from protein sequence alignments. Systematic Biology 56: 564–577. https://doi.org/10.1080/10635150701472164

Tamura K, Stecher G, Peterson D, Filipski A, Kumar S (2013) MEGA6: Molecular Evolutionary Genetics Analysis Version 6.0. Molecular Biology and Evolution 30: 2725–2729. https://doi.org/10.1093/molbev/mst197

Teramachi A (1949) An attempt to find a new collection field of shells in Prov. Satsuma, with a description of a new limpet, *Notoacmea fuscoviridis*. Venus 15: 90–93. [In Japanese]

Thiele J (1929) Handbuch der systematischen Weichtierkunde. 1. Gustav Fischer, Jena, 376 pp.

Vermeij GJ (1973) Mophological patterns in high-intertidal gastropods: adaptive strategies and their limitations. Marine Biology 20: 319–346. https://doi.org/10.1007/BF00354275

Yu SS, Wang J, Wang QL, Huang XW, Dong YW (2014) DNA barcoding and phylogeographic analysis of *Nipponacmea* limpets (Gastropoda: Lottiidae) in China. Journal of Molluscan Studies 80: 420–429. https://doi.org/10.1093/mollus/eyu034

Zwickl DJ (2006) Genetic algorithm approaches for the phylogenetic analysis of large biological sequence datasets under the maximum likelihood criterion. PhD Thesis. University of Texas at Austin, 115 pp.

Supplementary material 1

Figure S1

Authors: Shinnosuke Teruya, Davin H. E. Setiamarga, Tomoyuki Nakano, Takenori Sasaki

Data type: Phylogenetic tree

Explanation note: Fig. S1. Maximum likelihood phylogenetic tree of COI. Numbers above or below the branches are ML bootstrap and Bayesian posterior probabilities, respectively.

Link: https://doi.org/10.3897/zookeys.1087.78193.suppl1

Supplementary material 2

Figure S2

Authors: Shinnosuke Teruya, Davin H. E. Setiamarga, Tomoyuki Nakano, Takenori Sasaki

Data type: Phylogenetic tree

Explanation note: Fig. S2. Maximum likelihood phylogenetic tree of Cytb. Numbers above or below the branches are ML bootstrap and Bayesian posterior probabilities, respectively.

Link: https://doi.org/10.3897/zookeys.1087.78193.suppl2

Supplementary material 3

Figure S3

Authors: Shinnosuke Teruya, Davin H. E. Setiamarga, Tomoyuki Nakano, Takenori Sasaki

Data type: Phylogenetic tree

Explanation note: Fig. S3. Maximum likelihood phylogenetic tree of 12S rRNA. Numbers above or below the branches are ML bootstrap and Bayesian posterior probabilities, respectively.

Link: https://doi.org/10.3897/zookeys.1087.78193.suppl3

Supplementary material 4

Figure S4

Authors: Shinnosuke Teruya, Davin H. E. Setiamarga, Tomoyuki Nakano, Takenori Sasaki

Data type: Phylogenetic tree

Explanation note: Fig. S4. Maximum likelihood phylogenetic tree of 16S rRNA. Numbers above or below the branches are ML bootstrap and Bayesian posterior probabilities, respectively.

Link: https://doi.org/10.3897/zookeys.1087.78193.suppl4

ZooKeys 1087: 199–220 (2022)
doi: 10.3897/zookeys.1087.76720
https://zookeys.pensoft.net

FORUM PAPER

A peer-reviewed open-access journal
ZooKeys
Launched to accelerate biodiversity research

Turbo taxonomy approaches: lessons from the past and recommendations for the future based on the experience with Braconidae (Hymenoptera) parasitoid wasps

Jose L. Fernandez-Triana[1]

1 *Canadian National Collection of Insects, Ottawa, Canada*

Corresponding author: Jose L. Fernandez-Triana (cnc.braconidae@gmail.com)

Academic editor: Lyubomir Penev | Received 18 October 2021 | Accepted 2 February 2022 | Published 25 February 2022

http://zoobank.org/D2DCD7C2-45C1-4C6B-B14C-D87AD2A5514A

Citation: Fernandez-Triana JL (2022) Turbo taxonomy approaches: lessons from the past and recommendations for the future based on the experience with Braconidae (Hymenoptera) parasitoid wasps. ZooKeys 1087: 199–220. https://doi.org/10.3897/zookeys.1087.76720

Introduction

A recent paper (Sharkey et al. 2021a) describing 416 new species of Braconidae parasitoid wasps (Hymenoptera) from Area de Conservación Guanacaste in Costa Rica has reignited the debate about taxonomic best practices when describing species. The new species were treated in a minimalist way, as stated in the very title of the paper and this quote from their abstract: "Most descriptions consist of a lateral or dorsal image of the holotype, a diagnostic COI consensus barcode, the Barcode Index Number (BIN) code with a link to the Barcode of Life Database (BOLD), and the holotype specimen information required by the International Code of Zoological Nomenclature" (Sharkey et al. 2021a: 2).

Sharkey et al. (2021a) is but the latest example of a growing list of papers that aim to accelerate the description of species on a planet facing a biodiversity crisis in which species may become extinct before they are even described. "Turbo taxonomy" is a catchy name proposed by Butcher et al. (2012) to qualify such papers, and it has been rather enthusiastically applied since then – a Google Scholar search for "turbo taxonomy" retrieved 135 results since 2012 through January 2022. A similar concept "fast-track taxonomy" was proposed around the same time by Riedel et al. (2013a); I consider them as equivalent and for the sake of simplicity I will use "turbo taxonomy" henceforth.

Although somewhat subjective, turbo taxonomy can be characterized as the rapid description of many species in "fast" papers (as compared to the "slower" pace of traditionally produced taxonomic papers). This is usually accomplished using a combination of tools and approaches to automate and expedite dealing with the material examined, e.g., morphological traits quickly assessed and scored, often with brief descriptions and/or descriptions generated using software packages, high-quality illustrations, a heavy reliance on molecular and other data (e.g., biological, distributional) to differentiate and diagnose species. The combination of techniques for species recognition and description at least partially intersects with another concept, that of "integrative taxonomy", sensu Dayrat (2005), and perhaps sometimes both terms have been used interchangeably, although integrative taxonomic papers are not necessarily "rapidly produced" as is claimed for the turbo-taxonomy ones.

The main difference between Sharkey et al. (2021a) relative to previous turbo-taxonomy papers, and the reason for the present discussions within the scientific community is that they chose to describe the new species based almost exclusively on DNA barcodes.

Describing new species based only or mostly on molecular data is not new. Hibbett et al. (2011) discussed prospects for sequence-based taxon discovery and description in fungi (see also Taylor 2011; Kõljalg et al. 2013); and Renner (2016) compiled a list of at least 98 names of species of acoels, lichens, angiosperms, annelids, alveolates, arachnids, centipedes, turtles, fishes, butterflies, mollusks, nematodes, and pathogenic fungi that have been published based on diagnostic mitochondrial, plastid, or nuclear DNA substitutions, indels, or rarely genetic distances, with or without the addition of morphological features. Even within Braconidae, some of the coauthors of Sharkey et al. (2021a) had recently published a similar, albeit much smaller paper (Meierotto et al. 2019).

Thus, the novelty of the Sharkey et al. paper is hardly the approach itself but rather the scaling up of the work to a mammoth monograph in which more than 400 new species were described. That is indeed a first. And, as quoted from the very first sentence of their introduction, the authors presented their article as a way to "further refine methods to overcome the taxonomic impediment of ichneumonoid biodiversity" (Sharkey et al. 2021a: 6).

In the months following that paper, the scientific community has engaged in lively discussions about "how useful" such descriptions are, whether they in fact impede the cataloguing of biodiversity, "how valid" (from the ICZN perspective) those species are, and general issues about the future of taxonomy, and the shortcomings of BINs and even BOLD (e.g., Ahrens et al. 2021; Engel et al. 2021; Meier et al. 2021).

In this Forum Paper I discuss some of the above issues, present alternative/complementary ideas from my perspective, and include a detailed proposal on how to approach turbo taxonomy in a hyperdiverse group such as braconid parasitoid wasps balancing rapid descriptions of species while also keeping a higher use value of the final product(s). I do not claim to have better or newer insights than others, and I certainly do not pretend to have any definitive answers, but perhaps my comments could be useful

because a) I am a braconid researcher, like the main authors of the Sharkey et al. (2021a) paper, b) I have published several papers that could be considered as turbo taxonomy and have long been interested in ways to speed up species descriptions, c) I was actually one of the reviewers of Sharkey et al. (2021a) (and for full disclosure, I recommended its acceptance, although I also added many opinions on its taxonomic approach and how it could have been improved, with many of my suggestions being ignored by the authors in the final version), and d) perhaps more importantly, because I think that Sharkey et al. (2021a), even if arguably flawed, demonstrate opportunities that can and should be used by the taxonomic community to improve and speed up work in the future. In that sense, what follows below is less of another critical view of that paper and more of a complementary proposal to improve turbo taxonomic methods.

"Talking the talk and walking the walk" of turbo taxonomy

There are many published papers that discuss the need to and possibilities of speeding up taxonomy by using newer technologies such as DNA barcoding. Unfortunately, most of those papers present somewhat general discussions or are intended just as a proof of concept, without actually applying it to describing new species. In many cases, DNA barcoding is presented as a useful and comparatively rapid tool to rapidly distinguish species, often revealing a much higher species diversity than previously thought based on morphological study and/or revealing complexes of cryptic species. However, usually things stop there, and the next step is not made, i.e., the new taxa are not described in those papers praising how much DNA barcoding brings to the taxonomist's table. I would consider those papers examples of "talking the talk" but not necessarily "walking the walk" (in the sense presented here: https://knowyourphrase.com/talk-the-talk). It is important to stress that this statement does not apply to the four braconid experts and coauthors of the Sharkey et al. (2021a) paper (Michael Sharkey, Scott Shaw, Donald Quicke, and Kees van Achterberg) all of whom are world-renowned taxonomists. Altogether they have described more than three thousand new species in hundreds of published papers (e.g., see Yu et al. 2016), and their contributions to our knowledge of Braconidae and other Hymenoptera groups has been outstanding. They have certainly walked the walk!

But the truth is that comparatively few works could have the turbo taxonomy label applied to them. Examples include lichens (Lücking et al. 2017), annelids (Summers et al. 2014), dragonflies (Dijkstra et al. 2015), frogs (Rakotoariso et al. 2017), phorid flies (Hartop and Brown 2014; Hartop et al. 2015, 2016), histers beetles (Caterino and Tishechkin 2013), weevils (Riedel et al. 2013b, 2014; Riedel and Tänzler 2016; Riedel and Narakusumo 2019), and several papers on braconids (Table 1). There is no doubt that other papers than the ones I list can be found in the literature, but they still constitute a minority of published taxonomic revisions. [Srivathsan et al. (2019) could also be considered here, albeit only partially, because they discuss and present novel methodologies for rapid description of species (= turbo taxonomy) but only describe one new species as an example].

Table 1. Selection of published Braconidae papers (2005–2021) that could be considered as examples of turbo taxonomy. For the sets of data in columns 5–9, the use of "-" means such data was not present in the paper, "+" means that it was used but only in a very basic and limited way, and "++" means that it was fairly used. ACG = Area de Conservación de Guanacaste, Costa Rica.

Paper	Subfamily/ genus covered	Main geographical area	Total species /new species described	Use of dichotomous keys	Use of morphological data	Use of illustrations	Use of molecular data	Use of other data
Sharkey et al. (2021a)	11 Subfamilies of Braconidae	ACG	416/403	–	–	+	++	+
Marsh et al. (2013)	Doryctinae/ *Heterospilus*	Costa Rica	286/280	++	++	++	–	–
Fernandez-Triana et al. (2014)	Microgastrinae/ *Apanteles*	ACG	205/186	++	++	++	++	++
Butcher et a. (2012)	Rogadinae/ *Aleiodes*	Thailand	186/179	++	++	++	++	–
Arias-Penna et al. (2019)	Microgastrinae/ *Glyptapanteles*	ACG/ Ecuador	136/136	++	++	++	++	++
Liu et al. (2020)	Microgastrinae/ *Apanteles*	China	97/48	++	++	++	–	+
Sharkey et al. (2018)	Agathidinae/ *Alabagrus*	ACG	87/66	++	++	++	++	++
Liu et al. (2019)	Microgastrinae/ *Dolichogenidea*	China	67/39	++	++	++	–	+
Ahlstrom (2005)	Macrocentrinae/ *Macrocentrus*	Nearctic	54/13	++	++	++	–	+
Valerio and Whitfield (2015)	Microgastrinae/ *Hypomicrogaster*	ACG	45/40	++	++	++	–	++
Fernandez-Triana et al. (2014)	Microgastrinae/ *Pseudapanteles*	ACG	36/25	++	++	++	++	++
Liu et al. (2018)	Microgastrinae/ *Dolichogenidea*	China	34/26	++	++	++	–	+
Fernandez-Triana et al. (2015)	Microgastrinae/ *Microplitis*, *Snellenius*	ACG	33/28	++	++	++	++	++
Meierotto et al. (2019)	Agathidinae/ *Zelomorpha*	ACG	19/18	–	–	+	++	++

What is somewhat surprising (or worrisome?) is the realization that few of the researchers who have published a paper that could be considered as turbo taxonomy have continued to do afterwards, i.e., they have not produced additional monographs in the same turbo taxonomy style. Based on my, admittedly non-exhaustive, online searches, I can only mention Riedel and colleagues for weevils (Riedel et al. 2013b, 2014; Riedel and Tänzler 2016; Riedel and Narakusumo 2019) and a series of papers on Braconidae (see Table 1 and discussion below) as two examples of researchers doing turbo taxonomy on a more sustained basis.

One may then ask, if turbo taxonomy is touted as "the way to move forward" in taxonomy, why are there so few adopters of the approach, and even fewer who repeat their efforts in subsequent papers? In my opinion the answer is simple: because turbo taxonomy still requires a significant amount of invested work and time, and it is not as

easy and rapid as one might think or as it is purported to be in papers advocating for those revolutionary taxonomic approaches. A simple search of author names reveals that most of the published turbo taxonomy papers have been done primarily by graduate students (M.Sc. and Ph.D.) or postdoctoral fellows. They represent some of the more enthusiastic, hard-working, and "overperformer" researchers in the taxasphere, a great combination of youth, energy, and a desire/need to advance their careers. They certainly put in the effort needed to accomplish their turbo taxonomy feats, and they deserve all the praise for that. But could those papers become the "new normal" for taxonomy? I would argue that it is unrealistic to expect that turbo taxonomy papers can be produced effortlessly and quickly, much less in a sustained way, at least those closer to "traditional taxonomy" in the sense of providing keys and morphological descriptions.

I believe that Meierotto et al. (2019), Sharkey et al. (2021a), and others before them (see Introduction for non-Braconidae examples) are probably correct in their claim that a shift of paradigms is possible and needed to increase the speed of taxonomic results. I also agree that DNA-based species recognition should be one of the major driving forces to speed up the cataloguing of biodiversity. Where I disagree with such authors is in the way to implement turbo taxonomy because I believe that this can and should include components other than DNA that increase the "use value" of the paper while not taking much extra time or resources.

Comparing the works of Meierotto and Sharkey with other Braconidae papers of similar size

First let us look at what has been accomplished with turbo taxonomy relative to Braconidae during the past 15 years or so (2005–present). Table 1 presents basic data on some papers, divided in two somewhat arbitrary categories. The first five rows include papers with the largest numbers of treated species (approximately 100–400 species each), to serve as a direct comparison with Sharkey et al. (2021a) which is, by far, the largest paper discussed here. Included are all the large monographs in Braconidae I am aware of that could be considered as examples of turbo taxonomy. The remaining rows contain a sample of papers with fewer treated species overall (approximately 30–80 each), which are comparable in size species-wise with Meierotto et al. (2019). There are certainly more examples of revisions of Braconidae in this second category than those I have listed.

Four of the large papers provide identification keys, "traditional" (i.e., morphology-based) species descriptions (as opposed to only DNA-based ones), and multiple illustrations of all or most species. The only exception to this is the paper of Sharkey et al. (2021a), which does not provide keys or traditional descriptions and includes only a single image per species (usually a lateral habitus). Molecular data to recognize, differentiate, and/or describe species was used in all papers except Marsh et al. (2013) and Liu et al. (2020). Other data, mostly biological information, usually host data but also number and shape of wasp cocoons, host plant, microhabitat, etc., were less

prevalent, and mostly restricted to those papers treating the Area de Conservación de Guanacaste, Costa Rica (ACG) fauna because of the wealth of biological and ecological information available for Braconidae and other taxa obtained in that area (e.g., Janzen and Hallwachs 2011, 2016, 2020; see also http://janzen.sas.upenn.edu/caterpillars/database.lasso).

The pattern among the shorter papers is mostly similar, with Meierotto et al. (2019) being the only one not to include differential keys or morphological descriptions. All the other papers are more complete from the perspective of morphology, and many also included molecular, biological, and ecological data although, again, the ACG papers were more comprehensive because the authors had access to more information.

An interesting comparison can be drawn between the Meierotto et al. (2019) and Sharkey et al. (2018) papers: both treat a single genus of Agathidinae (Braconidae) but the latter is much more comprehensive in its use of features/traits to recognize, identify, and describe the species.

The examples in Table 1 are comprehensive taxonomic revisions that treated dozens and sometimes even hundreds of species each; they included at least some basic morphological data, usually more. Indeed, if a taxon could claim the crown of turbo taxonomy, Braconidae would be a strong candidate. In just one subfamily, Microgastrinae, a total of 720 new species was described between 2014 and 2019 (Fernandez-Triana et al. 2020), the vast majority in papers that would qualify as turbo taxonomy.

There is no question that these papers could have been produced faster and easier if a minimalistic approach, such as those of Meierotto et al. (2019) and Sharkey et al. (2021a), had been adopted. How fast and how easy are, however, complicated questions to answer. And how "useful" those papers would be for potential users is an even more difficult one.

Speed, practicality, affordability, democratization of taxonomy, and Star Trek

Sharkey et al. (2021a), and for that matter many other papers, my own included, that have treated the ACG fauna benefited immensely from the work previously done by Daniel Janzen, Winnie Halwachs, and their team (e.g., Janzen et al. 2009; Janzen and Hallwachs 2011, 2016, 2020). Thanks to herculean efforts (including their amazing parataxonomists and technicians, mostly in Costa Rica but also in USA and Canada), thousands of specimens have been collected, reared, labelled, and databased with recorded host data, and DNA has been extracted, with the available sequences and additional information readily accessible in the Barcode of Life Data System (BOLD). Some of that work is highly technical, and all of it took a lot of time and significant resources, including financial. All or most of that was done before the actual work of the taxonomists started, and in fact was of critical importance or else it would have taken much more time and considerably more resources to produce those taxonomic papers, whether traditional or turbo taxonomy.

Thus, when considering papers that claim to be "fast" because they only rely on DNA-based descriptions, one must also consider hidden but significant amounts of work done prior to the taxonomy study. If time, expertise, and resources needed to obtain all the previous information on which the taxonomy is based were accounted for, then those papers would suddenly appear less quick and easy to produce than as advertised, at least relative to ACG studies.

Beyond time and resources not being properly assessed in a paper employing only DNA-based descriptions, there is a bigger issue. And that is the fact that any user of such a paper must, by default, obtain DNA data for their own specimens before any meaningful comparison can be made with the species dealt with in that paper. Otherwise, it is not possible to conclude if a specimen at hand belongs to a previously "DNA-described" species or is new. Thus, "DNA-only description" papers force users to do "DNA-only identifications".

There is no problem with that, say some enthusiastic supporters of turbo taxonomy and DNA barcoding. It will actually democratize taxonomy because technical knowledge of a taxon, including the associated morphological jargon used to described it (e.g., number of setae on propodeum or sculpture on mesoscutum), would no longer be required. What used to be the domain of a relatively few taxonomists would become mostly unnecessary, because "soon" everyone would be able to use a device, à la Star Trek tricorder (https://en.wikipedia.org/wiki/Tricorder), to identify species. It would allow even school children to rapidly identify the caterpillar they found in their backyard or farmers in Central America to recognize which pest or parasitoid wasps are found in their crops. It all looks so nice and promising!

I fully agree that DNA barcoding democratizes taxonomy because indeed it reduces somehow the need for trained taxonomists to do routine identifications (e.g., Janzen et al. 2009; Janzen and Hallwachs 2001, 2016). But, while I have no doubts that technology ultimately will be developed to allow fast, easy, and cheap devices to obtain and analyse DNA, and access the comprehensive DNA databases that are necessary to determine whether a specimen at hand represents a described species, that scenario is not yet here (but see Srivathsan et al. 2021 for some new developments that could become viable alternatives in the near future). We are still far from being able to download a "Taxonomy for Dummies" app.

Meanwhile, what we have is the fact that DNA-based taxonomy is not accessible or affordable to everyone (see further analyses and/or other perspectives in Pinheiro et al. 2019; Dupérré 2020; Ahrens et al. 2021; Meier et al. 2021; Srivathsan et al. 2021). At present, it is not possible to obtain a DNA barcode from a single specimen unless the individual has access to a molecular lab, whether this is their own or "one for hire". As an example of the latter, one of the most commonly used such labs is the Canadian Center for DNA Barcoding (formerly the Biodiversity Institute of Ontario), which charges $1,250 Canadian dollars for a single plate of 95 specimens (http://ccdb.ca/pricing/). However, in addition to that cost, single images of every submitted specimen and an Excel file with some basic information are also required when samples are submitted, which will take additional time and money; factors also to consider are the

shipping costs and dealing with national/international laws regulating access, sharing, and exportation of genetic resources.

Never mind the school children or farmers, arguably most world researchers cannot afford the current costs and associated logistic challenges mentioned above to obtain DNA-based identifications for every specimen they may need or want to identify (e.g., Srivathsan et al. 2021). If the route of having to obtain DNA barcodes (or any other molecular marker) to identify species becomes the only route to a scientific name, then this could make taxonomy even less accessible and democratic than using "traditional" techniques such as microscopes and dichotomous keys. At present is certainly valid to argue that the cost of traditional, morphology-based taxonomy is largely a "front end" cost mainly borne by the taxonomist, whereas DNA-only taxonomy necessitates high and significant "back end" user costs.

In addition to cost and who pays this, there is also the problem of the almost two million species described in the pre-molecular era, many with no DNA associated. Those species cannot simply be ignored, as it has been claimed to be the case in the Meierotto et al. (2019) paper. Zamani et al. (2020) thoroughly discussed that problem, although Sharkey et al. (2021a, b) gave some counter replies.

In the end, it comes down to the practicality and benefits/damages that minimalistic (extreme?) taxonomic approaches, such as those relying only on DNA barcodes for species description and recognition, bring. Do future revisions to be produced really need to ignore morphology and previously described species to instead rely entirely or almost exclusively on DNA barcodes, with the "justification" of describing species faster because of the biodiversity crisis? Or is it possible to build upon the works of Meierotto et al. (2019), Sharkey et al. (2021a), and others to try finding a middle-of-the-road approach, where speed and practicality are attained while significantly minimizing efforts and cost?

A "cookbook recipe" for turbo taxonomy, including estimated times needed for each task

What I propose below is a workflow and guidelines for preparing turbo taxonomy papers, including estimated times for each task. The main motivation is to provide an alternative to Meierotto et al. (2019) and Sharkey et al. (2021a) but with the addition of some features that I hope would increase the applicability of the work (from a user perspective) while still maintaining a relatively fast pace. I have based this proposal on my personal experience preparing Braconidae turbo taxonomy papers, but it could be adapted for other taxa, i.e., used like a "cookbook recipe" that can be modified and changed as needed or desired.

I do not pretend to reinvent the wheel, e.g., see Reidel et al. (2013), Hartop and Brown (2014), Srivathsan et al. (2019) for earlier turbo taxonomy proposals and even nicer workflow diagrams (although my proposal includes more detailed analyses

of time involved with each task and consideration of other factors). I also strongly recommend checking the new guidelines for species descriptions posted by ZooKeys: https://zookeys.pensoft.net/about#TaxonomicTreatments), which in some ways intersects what I write below. And it may also be fruitful to check the many exchanged messages in the email list for biological systematics Taxacom (http://mailman.nhm.ku.edu/cgi-bin/mailman/listinfo/taxacom), where the Meierotto and Sharkey papers were vigorously discussed in 2019 and 2021 (while I have refrained from commenting on Taxacom about Sharkey et al. (2021a), in 2019 I did share my opinion about Meierotto et al. (2019), and some of the ideas presented here are based on what I wrote to that list at that time).

a) When is it most efficient to use turbo taxonomy approaches?

– The taxon being studied is hyperdiverse, i.e., species-rich, and mostly poorly known, i.e., most species are still undescribed so there are relatively few names not previously associated with DNA data and type material to be considered.

– DNA barcodes are already available for many/most of the species, unless the research project has sufficient resources (time and money) to accomplish this step.

– Databasing of many/most specimens is already available, unless the research project has sufficient resource (time and money) to accomplish this step.

– Imaging equipment is available capable of generating many images in a short period of time and with automated or semi-automated capabilities of stacking images to produce publication-quality images.

– Other sources of data (biological, ecological, etc.) are available for many/most specimens that provide evidence of species status supplemental to DNA/morphology evidence.

– A 'minimum' set of morphological traits to assess specimens is already available, i.e., features have been discussed or proposed in previous studies of the taxon or related taxa by specialist(s) in the taxon in order to provide supplementary evidence of species status and which is necessary for more "traditional" taxonomic approaches. Alternatively, the paper to be produced presents such a set of minimum morphological traits.

b) Species treatment

– New species will be treated, diagnosed, and described using a combination of basic morphology (basic key and brief diagnostic description), molecular data when available (e.g., DNA barcodes), ecological/ethological data when available, distribution data, and complete details of the primary type(s) and basic details of all other specimens.

– Previously described species will be incorporated into the paper even if in an incomplete manner due to lack of molecular or other data.

c) Use of morphological data

Simplified key(s) and diagnostic descriptions, with a minimum set of morphological traits, will be prepared. The morphological traits, ideally chosen by a specialist in the taxon, need not be numerous but ideally should be easily and quickly assessed and scored (i.e., not requiring dissections, slide preparation, or other labour-intensive techniques). It is understood that DNA evidence likely is being used in most turbo taxonomy studies because of a perceived lack of differential morphological features for the group, and that morphology will not necessarily suffice to tell every species apart. However, morphology should at least be able to place most (ideally all) species within some sort of smaller group of species. A "species group", as here considered, is based on some simple, diagnosable trait(s), e.g., "all species with legs brown or black versus all species with legs yellow" and does not necessarily have to be monophyletic.

The morphology component of the taxonomic revision should serve as the minimum piece of information to allow someone with a basic knowledge of the taxonomic group and simple equipment such as a microscope to recognize a species or species group if no other source of information, such as DNA, is available. [This statement may not be applicable in some groups, such as nematodes, fungi, etc. The present paper was mostly written thinking of insects, and it is mainly directed to groups where morphology has some role in recognizing species or groups.]

Although diagnostic descriptions should be as short as possible based on easily observable features, each species should be illustrated as fully as possible with images showing body areas from different angles in order to document the features important for differentiating species in the group (e.g., coloration, sculpture, etc.) and those features that are otherwise not described. Ideally, illustrations should be based on the holotype or specimens compared with the holotype; if a species is thought to be variable morphologically, then specimens showing the perceived range in variation should also be photographed.

In species complexes with very similar or cryptic morphology, additional effort does not necessarily need to be spent trying to separate them based on detailed study of morphology or morphometrics, but instead other non-morphological criteria (see below), if known, could be used to help distinguish the species.

The estimated time needed for the morphological work is 5 hours per species. This includes scoring and writing the species description based on minimum morphological traits, and also includes studying intraspecific variation and making a few measurements of relevant structures. All of these steps should take, on average, less than one hour per species, the exception being species with many available specimens and/or significant morphological variation. To account for extremes, an estimate of two hours of work per species is considered here. Photographing a species (4–8 shots of a specimen, to capture different angles) can be done in one hour depending on the number of specimens per species imaged, and the photographic equipment and montaging software used. Preparing a plate of images can be done in less than one hour. Estimating the time to prepare a simplified key is very difficult, and here a conservative estimate of one hour per species in the key is proposed. [Obviously, the calculations for this point do not include

the years of taxonomic experience that are required to be able to describe a species in 5 hours. This is indeed another "hidden prior work" and time to factor in. However, it would not only apply similarly to both turbo taxonomy and any other taxonomic approaches but also it would be very difficult, if not impossible, to calculate; thus, that factor is not included here. One simple observation from that problem would be that we still need to have more trained taxonomists to do the work of describing new species!].

d) Use of molecular data

DNA barcoding and/or any other molecular marker will be a very important criterion to recognize and diagnose species, and for morphologically cryptic or very similar species, it may be the primary criterion. Species will be characterized as much as possible by their corresponding Barcode Index Number (BIN) (for a definition of BIN see Ratnasingham and Hebert 2013). If a unique BIN does not "work", i.e., in cases where there is more than one BIN per species or several species share the same BIN, a discussion explaining the rationale to characterize the species molecularly will be necessary.

Where a species is primarily defined and identified by DNA barcodes because, e.g., basic morphology is insufficient or inconclusive, such "DNA-only species" must include sequences from at least two different specimens (to exclude potential definition of a species based on a single sequence, which could be a lab contamination, a chimera, or any other error). Where a species is defined by a combination of traits (morphological, biological, etc.), a less stringent molecular criterion is acceptable, and a single DNA barcode can be sufficient.

The estimated time needed for the molecular tasks is 5 hours per species. Sampling tissue for DNA barcoding from dry, pinned specimens is straightforward and takes less than 10 minutes per specimen. However, the associate requirements for preparing a 96-well plate and submitting it to the lab for processing may require many other tasks, e.g., taking one image per specimen and providing some details of the specimen for the BOLD database (in the case where specimen tissue is sequenced by the Canadian Center for DNA barcoding). A conservative estimate of 30 minutes per specimen is proposed. Because, as discussed above, it is usually necessary to have DNA barcodes of more than one specimen per species, the estimated here includes 3 hours per species. This estimate will vary significantly if specimens are prepared in batches smaller or larger than one 96-wells plate (which accommodates 95 specimens). Basic analysis of DNA barcodes (Neighbour-Joining trees as generated in BOLD) can be done quickly, but more complex and comprehensive analyses will take longer; a conservative estimate of 2 hours per species is proposed here.

e) Use of ecological/ethological data

Any extra information that contributes to recognizing or identifying a species based on ecological or ethological traits should be used as additional evidence supporting species delimitation, but not as the single source to describe a species. Examples in Braconidae include host data, parasitoid ecology, wasp seasonality, etc.

The estimated time needed for the ecological/ethological tasks is 1 hour per species, though this greatly depends on the available information for each taxon; it could be significantly less or even zero. This and the following are probably the least accurate time estimates of the list.

f) Use of distribution data

The minimum standard should be broad geographical distribution, i.e., biogeographical region, country, although detailed locality data is preferable. Information on habitat, e.g., collected in a rainforest or finer details, e.g., collected on understory of forest, on leaves of plant X, should also be provided when available. Distribution data can be used as supplementary evidence supporting a species delimitation and/or recognition, but not as the single source to describe a species.

The estimated time needed for the distribution data task is 1 hour per species, depending on the number of specimens to be data-mined and their geographic breadth, i.e., the amount of data available, and how much of that information is already databased.

g) Dealing with primary type(s) and other specimens

Details of the name-bearing specimens (primary types) should be provided that minimally meet International Code of Zoological Nomenclature (ICZN) publication requirements, such as type depository, but also including the specimen's unique identifier, specimen sex, country and other information on type specimen label(s) (photographs of such labels can be included), and any other detail (e.g., "specimen in good condition" or "missing a leg") that facilitates the unambiguous recognition of the name-bearing type(s). The ZooKeys guidelines mentioned above are a great standard to follow.

For paratypes and other non-type specimens, considerably abbreviated data can be included. For example, just mentioning the unique identifiers for each specimen instead of detailing all the data for every specimen data is sufficient, as long as the unique identifiers are linked to a publicly available database or dataset where more detailed information is available.

The estimated time needed for dealing with specimen details is 1 hour per species, depending on the number of specimens and prior databasing. If most specimens are already databased, as is becoming more the norm in many collections, then the time may be less than 10 minutes for every primary type and another 10 minutes to record the unique identifiers of all other specimens.

h) Treating previously described species

Previously described species should not be ignored, i.e., all species treated in a new paper should not, by default, be considered as new species if there are prior available names. Instead, effort should be made to incorporate the previously described species including a reasonable effort to locate and study their types and/or authenticated mate-

rial. Admittedly, there will be instances when this is not possible and the only data available is just a prior, possibly uninformative, and very short description. However, even if only incomplete information is available for previously described species this should be discussed in the paper as far as possible. Two hypothetical examples are discussed below.

The most extreme example would be that of a previously described species known only from the missing holotype, already lost, and a useless original description a few words long. Such a species should still be dealt with in a manner like this: "Species A cannot be run though our key because it is impossible to assess morphological traits X, Y, and Z used in the key and the only known specimen is lost. Thus, it is not possible to determine whether the name applies to one of the new species described here, but for practical purposes we assume that is not the case." Statements like that would make clear to the user/reader that such names cannot be presently assigned, and may never be, while still allowing progress in describing any new species.

Most cases will be less extreme than the above, with most previously described species being able to be placed within some context of the taxonomic revision, i.e., compared with the new species being described. Included should be at least some sort of basic statement such as: "Species B can only be run to couplet 3 of our key, as characters X and Y (from our key) cannot be assessed for that species, and therefore the name could potentially apply to species C, D, or E (new species being described in our paper), but for practical purposes we assume it is none of them". Again, this method reduces the potential number of names that could (eventually) be found to be synonyms (as at least the species keyed out through the first two couplets would not), while still enabling the new, better characterized species to be recognized.

In these two hypothetical cases, the previously described species are not ignored, even if their status can never be properly assessed. Thus, the new taxonomic revision would bring together all available information, including presenting the shortcomings and gaps in our current knowledge of some species.

The estimated time needed for dealing with previously described species is, conservatively, 2 hours per species, though it will depend on all factors discussed above.

i) Overall estimate time to deal with one species

The sum of all the time estimates above renders a total of 15 hours per species. That is roughly two days of work per species, or 2.5 species per week. Rounding down to 2 species per week and 50 weeks per year, one arrives at an estimate of 100 new species described in one full-time year of work by a turbo taxonomy practitioner.

However, how accurate is this estimate? Are there examples of this in the real world, or is the above just a theoretical, futile exercise?

It is difficult to get actual data from previous turbo taxonomy papers as to the time it took to complete the work because this is rarely (or never) stated by the author(s). But some information is available and other can be guessed.

I have no exact knowledge of how much time it took Sharkey et al. (2021a) to prepare their paper, but from correspondence with some of the coauthors I know that

it took at least two years. Assuming that was the case (and not longer), it would mean a rate of 200 new species per year, an impressive number. But one needs to factor in how much time was spent by the other three coauthors of that paper who are braconid taxonomists, in addition to the primary author. As such, I suspect that the actual number is below 200 species described per year.

Many of the other larger papers listed in Table 1 represent the work of a Ph.D. thesis or postdoctoral research, each of which probably included at least 3 years of work with the specimens. Based on the total number of species for those revisions, that would give values between 40 and 100 species per year per paper.

Fortunately, I can provide a more accurate estimate for my own work revising *Apanteles* (Braconidae) in Mesoamerica (Fernandez-Triana et al. 2014), which took two years to complete. The revision treated 205 species and at the time I was working full time on the project. Consequently, the pace was approximately 100 species per year. But, very importantly, I benefited greatly from previous work accomplished by Dan Janzen and Winnie Hallwachs in ACG, and some preliminary sorting of species by James Whitfield (University of Illinois at Urbana-Champaign) and his students before I started – all those contributors were rightfully included as coauthors. Thus, the pace to produce that paper is not as fast as it would first appear, and it underscores the difficulties in calculating the actual amount of time it takes to produce comprehensive taxonomic revisions. If anything, I cannot take much credit for the results of that paper (more criticism of my own work below).

Another factor to consider is that a rate of 100 species/year can only be accomplished if treating species "in bulk", i.e., if the purported review would include many new species. But not all taxonomic groups to be studied have hundreds of undescribed species and a taxonomic revision of "just" a dozen species would not be as time efficient. Furthermore, most people cannot spend 100% of their time doing taxonomic revisions. Even Ph.D. students have other things to do than just taxonomic revisions! Thus, a rate of 100 species/year is, in my opinion, a very high and somewhat unfair standard to expect, much less to meet on a consistent, year to year, basis; at least with current technology.

However, regardless of the actual time used for any taxonomic revision, efficiencies can be realized, such as including brief descriptions instead of traditional, longer, and more comprehensive ones, as proposed above. Going back to the real-world example of my own *Apanteles* paper, for that work I measured and scored 49 morphological characters (altogether more than 15,000 measurements). Many of those characters ultimately proved to be uninformative to distinguish species, being repetitive, too variable, or too subjective or complex to assess. In retrospect, the keys were also unnecessarily long, and some species almost impossible to tell apart based on the keys only (Eduardo Shimbori, pers. comm.). Looking back, eight years after I completed that paper in 2013, I see many inefficiencies in my work, and much superfluous data that could have been eliminated. Had I chosen a lower number of morphological characters and simplified the keys, it could have been completed quicker, without diminishing the final quality of the work. Had I assumed an approach similar to my proposed "cookbook recipe" above, the species would have been mostly recognized by

DNA and host data, and the keys would have been constructed to serve a more basic and limited function than what I had intended, while still retaining some utility to recognize basic species-groups. Of course, one could argue that the potential value of any character cannot be comprehended until it has been analyzed. One cannot know that there are "x" number of useful characters, and what they are, prior to studying them. This is what research is all about. Perhaps the "useless" time spent on some measurements is actually an example of what is necessary and a part of all taxonomic revisions, unless morphological features are completely ignored.

One example of how work can be reduced and made faster but still retain value is the case of the *Apanteles leucostigmus* species group, which comprises 39 species and is, by far, the largest and most difficult group of *Apanteles* to recognize and separate species in Mesoamerica. The key from Fernandez-Triana et al. (2014) for that group (reproduced here in Fig. 1) starts by dealing with a species that cannot be keyed out due to lack of data, with only one specimen known, and is an actual example on how to deal with historical species where information is not available. The remaining 38 species are keyed out using some characters difficult to assess and at some points the differences between halves of the same couplet are very subtle (the paper also included 4–8 images each of the adult wasps for every species). This key may look good on paper, but in practice it is very difficult and prone to error. Indeed, morphology does not work well for this group, which is suspected to include several morphologically cryptic species. Instead, I could have prepared a much simpler key that only used a few characters that are relatively easy to assess. Obviously, some species would end in the same point of the key, and thus could only be reliably identified by molecular and biological data. Such a "new" key

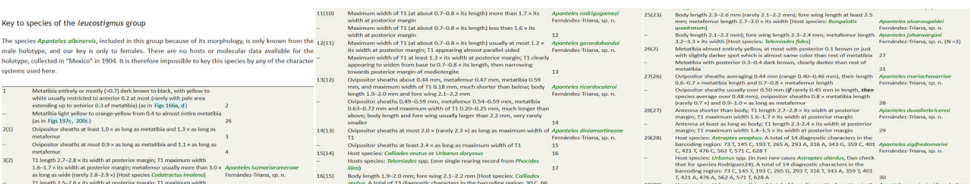
Key to species of the *leucostigmus* group

The species *Apanteles albinervis*, included in this group because of its morphology, is only known from the male holotype, and our key is only to females. There are no hosts or molecular data available for the holotype, collected in "Mexico" in 1904. It is therefore impossible to key this species by any of the character systems used here.

Figure 1. Details of the key to the *Apanteles leucostigmus* species group as it appeared in Fernandez-Triana et al. (2014). The plate shows a composite image of the key in the same format it appeared in the online version of that key (https://zookeys.pensoft.net/articles.php?id=3394).

1 Metatibia entirely or mostly (>0.7) dark brown to black, with yellow to white usually restricted to anterior 0.2 at most (rarely with pale area extending up to anterior 0.3 of metatibia) (as in Figs 166a, d) 2
– Metatibia light yellow to orange-yellow from 0.4 to almost entire metatibia 4

2(1) Ovipositor sheaths at least 1.0 × as long as metatibia and 1.3 × as long as metafemur ..... ***Apanteles luzmeriaromeroae*** [Host: *Codatractus imalena*] [DNA barcode]
Apanteles marcovenicioi [Host *Astraptus talus*] [DNA barcode]
– Ovipositor sheaths at most 0.9 × as long as metatibia and 1.1 × as long as metafemur 3

3(2) Fore wing with veins C+Sc+R and R1 mostly brown; usually veins r, 2RS, 2M, (RS+M)b, 1CU, 2Cua, and 1m-cu partially brown; interior area of other veins, and at least part of pterostigma, usually light brown or yellowish-white .....
Apanteles josecortesi [Host: *Nascus* spp.] [DNA barcode]
Apanteles eugeniaphilipsae [*Narcosius samson*] [DNA barcode]
Apanteles rodrigogamezi [Host: *Bungalotis diophorus*][DNA barcode]
Apanteles gerardobandoi [Host: *Telemiades fides*] [DNA barcode]
Apanteles ricardocalero [Hosts: *Aguna asander*, *A. panama*, *A. arunce hypozonitus*] [DNA barcode]
Apanteles dinamartinezae [Hosts: *Astraptes augeas*, *A. obstupefactus*, *A. gyneodoche*, *A. inflatio*, *A. fruticibus*] [DNA barcode]
Apanteles pabloumanai [Host: *Calliades zeuxi*] [DNA barcode]
Apanteles josemonteroi [Host: *Urbanus doryssus*] [DNA barcode]
Apanteles carloviquezi [Host: *Telemiades oicles*] [DNA barcode]
Apanteles inesolisae [Hosts: *Telemiades antiope*, *T. fides*] [DNA barcode]
Apanteles manuelzumbadoi [Host: *Telemiades fides*] [DNA barcode]
– Fore wing with veins C+Sc+R and R1 with brown coloration restricted narrowly to borders, interior area of those veins and pterostigma (and sometimes veins r, 2RS and 2M) transparent or white; other veins mostly transparent .....
Apanteles cirilloumanai [Host: *Bungalotis erythus*] [DNA barcode]
Apanteles cynthiacorderoae [Host: *Oxyba calathana*] [DNA barcode]
Apanteles hazelcambroneroae [Host: *Cephise aelius*] [DNA barcode]
Apanteles randellgarcesi [Hosts: *Phocides* spp.] [DNA barcode]
Apanteles raulsolorsanoi [Host: *Narcosius helen*] [DNA barcode]
Apanteles juanmatai [Host: *Phocides lilea*] [DNA barcode]
Apanteles minorcarmonai [Host: *Aguna* sp. Burm01] [DNA barcode]
Apanteles jesusgaldezi [Host: *Aguna* sp. Burm02] [DNA barcode]
Apanteles eliethcantillanoae [Host: *Urbanus* spp.] [DNA barcode]
Apanteles federicomatarritai [Hosts: *Chioides zilpa*, *Polygonus leo*] [DNA barcode]
Apanteles alvarosaldezi [Host: *Bungalotis quadratum*] [DNA barcode]
Apanteles johanvargasi [Host: *Telemiades fides*] [DNA barcode]

4(1) Metatibia almost entirely yellow, at most with posterior 0.1 brown or just with slightly darker spot which is almost same color than rest of metatibia .....
Apanteles mariechavarriae [Host: *Urbanus teleus*] [DNA barcode]
Apanteles duvalierbricenoi [Host: *Urbanus dorantes*] [DNA barcode]
Apanteles sigifredomarini [Host: *Astraptes anaphus*] [DNA barcode]
Apanteles sergiorioi [Host: *Urbanus simplicius*] [DNA barcode]
Apanteles ronaldzunigai [Hosts: *Urbanus dorantes* and 2 *Astraptes* records] [DNA barcode]
– Metatibia with posterior 0.3–0.4 dark brown, clearly darker than rest of metatibia .....
Apanteles lilliammenae [Host: *Urbanus doryssus*] [DNA barcode]
Apanteles wadyobandoi [Host: *Urbanus dorantes*, *Urbanus teleus*] [DNA barcode]
Apanteles leucostigmus [Host: *Urbanus proteus*] [DNA barcode]
Apanteles jorgehernandezi [Hosts: mostly *Astraptes* spp., four known records of *Urbanus* spp. (all different han *Urbanus proteus*)] [DNA barcode]
Apanteles rostermoragai [Host: Mostly *Urbanus albimargo* and *U. doryssus* (rarely *Autochton* sp.] [DNA barcode]
Apanteles angelsolisi [Host: *Urbanus albimargo*, rarely *Achalarus toxeus*, *Cogia calchas* and *Thecla jalapus*] [DNA barcode]
Apanteles gladysrojasae [Host: *Urbanus belli* (one record of *Urbanus viterboana*) [DNA barcode]
Apanteles bernardoespinozai [Host: *Astraptes alardus*, *A. brevicauda*, *A. talus*, *A. tucuti*, *Narcosius samson*, *Urbanus belli*, *U. dorantes*, *U. doryssus*] [DNA barcode]

Figure 2. Details of the key to the *Apanteles leucostigmus* species group as it would look based on modifications detailed in the present paper (see section "h) Overall estimated time to deal with one species" in the current manuscript).

(Fig. 2) would be much shorter and thus faster to prepare. As for the user of such key, there would still be the need of obtaining DNA barcodes and/or host data to obtain species identifications, but even if the user does not have such data, specimens could still be placed at least in some sub-group.

The above example, which I chose because it was the most difficult and problematic group of the *Apanteles* revision, illustrates how a mostly-but-not-only DNA based paper could be constructed in a more time-effective way. Other *Apanteles* groups from that Fernandez-Triana et al. (2014) revision (and indeed many groups in other taxa) might work even better. The proposed methods could shorten the time to produce a taxonomic revision while still providing some basic elements of more traditional papers.

Concluding remarks

I do not pretend that my suggestions above will "solve" the problem of describing millions of additional species in a short period of time. Even a "fast" pace of 100 species/year per taxonomist would still take a few hundred years to finish the task, a luxury we cannot afford, or would require a significant increase in the number of professional taxonomists (an unlikely scenario). There is no easy or simple answer to the necessity (and urgency!) of accelerating taxonomic inventories. My opinion is that it will require a wide embracement of current and additional technology advances,

but also some consensus-building among the taxonomic community on how to move forward, and perhaps even a broader involvement of citizen science. The present paper must be seen only as a modest attempt to provide some alternatives, even if insufficient. For some different perspectives and opinions on these topics, I recommend the reading of what the reviewers of the present paper had to say (Suppl. material 1).

It is very telling to see how many strong reactions a single paper has awakened in just a few months after its publication (or two papers, if we account for Meierotto et al. 2019), and the reasoning and pleas of other colleagues to avoid a future à la Sharkey et al. (2021a). I strongly recommend the reading of papers such as Pinheiro et al. (2019), Dupérré (2020), Zamani et al. (2020), Ahrens et al. (2021), Engel et al. (2021), Meier et al. (2021), Srivathsan et al. (2021), and references cited therein (other papers providing slightly different alternatives or approaches are also recommended reading, e.g., Brower (2010), Blaxter (2016), Goulding and Dayrat (2016), Renner (2016), Brown and Wong (2020), Vences (2020); this list is not exhaustive). And to present a more complete and fairer picture, the reader should also consider a second paper by Sharkey et al. (2021b) which tried to provide counterarguments to some of the received criticism, although that paper has also been met with additional counterarguments on its own, e.g., Ahrens et al. (2021), Engel et al. (2021), and Meier et al. (2021).

The authors cited in the previous paragraph have discussed in a more coherent, compelling, and convincing way that I probably could about the dangers and shortcomings of approaches such as those of Meierotto et al. (2019) and Sharkey et al. (2021a). While I agree with most of those arguments, I also think that the Meierotto and Sharkey papers provide an opportunity to critically look at and improve our own work. In that sense I prefer to be optimistic and focus on examples and the potential of what could be done (or has already been done by other authors) so that future turbo taxonomy papers can accomplish the (very much needed) dual goal of being fast and useful for the scientific community and the general public.

Acknowledgements

I want to acknowledge the reviewers Marko Mutanen (University of Oulu, Oulu, Finland), Stefan Schmidt (Bavarian State Collection, Munich, Germany), Brian V. Brown (Natural History Museum of Los Angeles County, Los Angeles, USA), and Istvan Miko (University of New Hampshire, Durham, USA), as well as the subject editor Lyubo Penev (Pensoft) for providing additional ideas and suggestions that not only improved the final version of this paper, but also significantly contributed to the wider dialogue about taxonomy and biodiversity crisis. I am also very grateful to John Huber and Gary Gibson (Canadian National Collection of insects, Ottawa, Canada) for their excellent reviews of earlier versions of the manuscript. This work was supported by Project J-002276 "Systematics of beneficial arthropods in support of resilient agroecosystems", from Agriculture and Agri-Food Canada.

References

Ahlstrom KR (2005) Revision of the subfamily Macrocentrinae (Hymenoptera: Braconidae) in America north of Mexico. Thomas Say Publications in Entomology: Monographs. Entomological Society of America, 274 pp.

Ahrens D, Ahyong ST, Ballerio A, Barclay MV, Eberle J, Espeland M, Huber BA, Mengual X, Pacheco TL, Peters RS, Rulik B, Vaz-deMello F, Wesener T, Krell FT (2021) Is it time to describe new species without diagnoses?–A comment on Sharkey et al. (2021). Zootaxa 5027(2): 151–159. https://doi.org/10.11646/zootaxa.5027.2.1

Arias-Penna DC, Whitfield JB, Janzen DH, Hallwachs W, Dyer LA, Smith MA, Hebert PDN, Fernández-Triana JL (2019) A species-level taxonomic review and host associations of *Glyptapanteles* (Hymenoptera, Braconidae, Microgastrinae) with an emphasis on 136 new reared species from Costa Rica and Ecuador. ZooKeys 890: 1–685. https://doi.org/10.3897/zookeys.890.35786

Blaxter M (2016) Imagining Sisyphus happy: DNA barcoding and the unnamed majority. Philosophical Transactions of the Royal Society B: Biological Sciences 371: e20150329. https://doi.org/10.1098/rstb.2015.0329

Brower AVZ (2010) Alleviating the taxonomic impediment of DNA barcoding and setting a bad precedent: names for ten species of '*Astraptes fulgerator*' (Lepidoptera: Hesperiidae: Eudaminae) with DNA-based diagnoses, Systematics and Biodiversity 8(4): 485–491. https://doi.org/10.1080/14772000.2010.534512

Brown BV, Wong MA (2020) Identification of *Megaselia* (Diptera: Phoridae) species using wing vein landmarking, Journal of Natural History 54: 37–38, 2513–2527. https://doi.org/10.1080/00222933.2020.1856431

Butcher BA, Smith MA, Sharkey MJ, Quicke DL (2012) A turbo-taxonomic study of Thai *Aleiodes* (Aleiodes) and *Aleiodes* (*Arcaleiodes*) (Hymenoptera: Braconidae: Rogadinae) based largely on COI barcoded specimens, with rapid descriptions of 179 new species. Zootaxa 3457(1): 1–232. https://doi.org/10.11646/zootaxa.3457.1.1

Caterino M, Tishechkin A (2013) A systematic revision of *Operclipygus* Marseul (Coleoptera, Histeridae, Exosternini). ZooKeys 271: 1–401. https://doi.org/10.3897/zookeys.271.4062

Dayrat B (2005) Towards integrative taxonomy. Biological Journal of the Linnean Society 85(3): 407–417. https://doi.org/10.1111/j.1095-8312.2005.00503.x

Dijkstra KDB, Kipping J, Mézière N (2015) Sixty new dragonfly and damselfly species from Africa (Odonata). Odonatologica 44(4): 447–678.

Dupérré N (2020) Old and new challenges in taxonomy: what are taxonomists up against? Megataxa 1(1): 59–62. https://doi.org/10.11646/megataxa.1.1.12

Engel MS Ceríaco LMP, Daniel GM, Dellapé PM, Löbl I, Marinov M, Reis RE, Young MT, Dubois A, Agarwal I, Lehmann P, Alvarado M, Alvarez N, Andreone F, Araujo-Vieira K, Ascher JS, Baêta D, Baldo D, Bandeira SA, Barden P, Barrasso DA, Bendifallah L, Bockmann FA, Böhme W, Borkent A, Brandão CRF, Busack SD, Bybee SM, Channing A, Chatzimanolis S, Christenhusz MJM, Crisci JV, D'elía G, Da Costa LM, Davis SR, De Lucena CAS, Deuve T, Fernandes SE, Faivovich J, Farooq H, Ferguson AW, Gippoliti S, Gonçalves FMP, Gonzalez VH, Greenbaum E, Hinojosa-Díaz IA, Ineich I, Jiang J, Kahono S, Kury AB, Lucinda PHF, Lynch JD, Malécot V, Marques MP, Marris

JWM, Mckellar RC, Mendes LF, Nihei SS, Nishikawa K, Ohler A, Orrico VGD, Ota H, Paiva J, Parrinha D, Pauwels OSG, Pereyra MO, Pestana LB, Pinheiro PDP, Prendini L, Prokop J, Rasmussen C, Rödel MO, Rodrigues MT, Rodríguez SM, Salatnaya H, Sampaio I, Sánchez-García A, Shebl MA, Santos BS, Solórzano-Kraemer MM, Sousa ACA, Stoev P, Teta P, Trape JF, Van-Dúnem Dos Santos C, Vasudevan K, Vink CJ, Vogel G, Wagner P, Wappler T, Ware JL, Wedmann S, Zacharie CK (2021) The taxonomic impediment: a shortage of taxonomists, not the lack of technical approaches. Zoological Journal of the Linnean Society 193(2): 381–387. https://doi.org/10.1093/zoolinnean/zlab072

Fernandez-Triana J, Whitfield J, Rodriguez J, Smith M, Janzen D, Hajibabaei M, Burns J, Solis A, Brown J, Cardinal S, Goulet H, Hebert P (2014) Review of *Apanteles* sensu stricto (Hymenoptera, Braconidae, Microgastrinae) from Area de Conservación Guanacaste, northwestern Costa Rica, with keys to all described species from Mesoamerica. ZooKeys 383: 1–565. https://doi.org/10.3897/zookeys.383.6418

Fernandez-Triana J, Janzen D, Hallwachs W, Whitfield J, Smith M, Kula R (2014) Revision of the genus *Pseudapanteles* (Hymenoptera, Braconidae, Microgastrinae), with emphasis on the species in Area de Conservación Guanacaste, northwestern Costa Rica. ZooKeys 446: 1–82. https://doi.org/10.3897/zookeys.446.8195

Fernandez-Triana JL, Whitfield JB, Smith MA, Kula RR, Hallwachs W, Janzen DH (2015) Revision of the genera *Microplitis* and *Snellenius* (Hymenoptera, Braconidae, Microgastrinae) from Area de Conservación Guanacaste, Costa Rica, with a key to all species previously described from Mesoamerica. Deutsche Entomologische Zeitschrift 62(2): 137–201. https://doi.org/10.3897/dez.62.5276

Fernandez-Triana J, Shaw MR, Boudreault C, Beaudin M, Broad GR (2020) Annotated and illustrated world checklist of Microgastrinae parasitoid wasps (Hymenoptera, Braconidae). ZooKeys 920: 1–1089. https://doi.org/10.3897/zookeys.920.39128

Goulding TC, Dayrat B (2016) Integrative taxonomy: ten years of practice and looking into the future. In: Аспекты биоразнообразия (Biodiversity Aspects). Archives of Zoological Museum of Lomonosov Moscow State University, 116–133.

Hartop E, Brown B (2014) The tip of the iceberg: a distinctive new spotted-wing *Megaselia* species (Diptera: Phoridae) from a tropical cloud forest survey and a new, streamlined method for *Megaselia* descriptions. Biodiversity Data Journal 2: e4093. https://doi.org/10.3897/BDJ.2.e4093

Hartop EA, Brown BV, Disney RHL (2015) Opportunity in our ignorance: urban biodiversity study reveals 30 new species and one new Nearctic record for *Megaselia* (Diptera: Phoridae) in Los Angeles (California, USA). Zootaxa 3941(4): 451–484. https://doi.org/10.11646/zootaxa.3941.4.1

Hartop E, Brown B, Disney R (2016) Flies from L.A., The Sequel: A further twelve new species of *Megaselia* (Diptera: Phoridae) from the BioSCAN Project in Los Angeles (California, USA). Biodiversity Data Journal 4: e7756. https://doi.org/10.3897/BDJ.4.e7756

Hibbett DS, Ohman A, Glotzer D, Nuhn M, Kirk P, Nilsson RH (2011) Progress in molecular and morphological taxon discovery in Fungi and options for formal classification of environmental sequences. Fungal Biology Reviews 25(1): 38–47. https://doi.org/10.1016/j.fbr.2011.01.001

Janzen DH, Hallwachs W (2011) Joining inventory by parataxonomists with DNA barcoding of a large complex tropical conserved wildland in northwestern Costa Rica. PLoS ONE 6(8): e18123. https://doi.org/10.1371/journal.pone.0018123

Janzen DH, Hallwachs W (2016) DNA barcoding the Lepidoptera inventory of a large complex tropical conserved wildland, Area de Conservacion Guanacaste, northwestern Costa Rica. Genome 59(9): 641–660. https://doi.org/10.1139/gen-2016-0005

Janzen DH, Hallwachs W (2020) Área de Conservación Guanacaste, northwestern Costa Rica: Converting a tropical national park to conservation via biodevelopment. Biotropica 00: 1–20. https://doi.org/10.1111/btp.12755

Janzen DH, Hallwachs W, Blandin P, Burns JM, Cadiou J, Chacon IS, Dapkey T, Deans AR, Epstein ME, Espinoza B, Franclemont JG, Haber WA, Ibabaei MH, Hall JP, Hebert PDN, Gauld ID, Harvey DJ, Hausmann A, Kitching IJ, Lafontaine D, Landry J-F, Lemaire C, Miller JE, Miller JS, Miller L, Miller SE, Montero J, Munroe E, Green SR, Ratnasingham S, Rawlins JE, Robbins RK, Rodriguez JJ, Rougerie R, Sharkey MJ, Smith MA, Solis MA, Sullivan JB, Thiaucourt P, Wahl DB, Weller SJ, Whitfield JB, Willmott KR, Wood DM, Woodley NE, Wilson JJ (2009) Integration of DNA barcoding into an ongoing inventory of complex tropical biodiversity. Molecular Ecology Resources 9(Suppl. 1): 1–26. https://doi.org/10.1111/j.1755-0998.2009.02628.x

Kõljalg U, Nilsson RH, Abarenkov K, Tedersoo L, Taylor AFS, Bahram M, Bates ST, Bruns TD, Bengtsson-Palme J, Callaghan TM, Douglas B, Drenkhan T, Eberhardt U, Dueñas M, Grebenc T, Griffith GW, Hartmann M, Kirk PM, Kohout P, Larsson E, Lindahl BD, Lücking R, Martín MP, Matheny PB, Nguyen NH, Niskanen T, Oja J, Peay KG, Peintner U, Peterson M, Põldmaa K, Saag L, Saar I, Schüßler A, Scott JA, Senés C, Smith ME, Suija A, Taylor DL, Telleria MT, Weiss M, Larsson K-H (2013) Towards a unified paradigm for sequence-based identification of fungi. Molecular Ecology 22(21): 5271–5277. https://doi.org/10.1111/mec.12481

Liu Z, He JH, Chen XX (2018) The *laevigata*-group of the genus *Dolichogenidea* Mason, 1981 from China, with descriptions of 26 new species. Zootaxa 4436(1): 1–74. https://doi.org/10.11646/zootaxa.4436.1.1

Liu Z, He JH, Chen XX, Gupta A, Moghaddam MG (2019) The *ultor*-group of the genus *Dolichogenidea* Viereck (Hymenoptera, Braconidae, Microgastrinae) from China with the descriptions of thirty-nine new species. Zootaxa 4710(1): 1–134. https://doi.org/10.11646/zootaxa.4710.1.1

Liu Z, He JH, Chen XX, Gupta A (2020) The *ater*-group of the genus *Apanteles* Foerster (Hymenoptera, Braconidae, Microgastrinae) from China with the descriptions of forty-eight new species. Zootaxa 4807(1): 1–205. https://doi.org/10.11646/zootaxa.4807.1.1

Lücking R, Dal Forno M, Moncada B, Coca LF, Vargas-Mendoza LY, Aptroot A, Lawrey JD (2017) Turbo-taxonomy to assemble a megadiverse lichen genus: seventy new species of *Cora* (Basidiomycota: Agaricales: Hygrophoraceae), honouring David Leslie Hawksworth's seventieth birthday. Fungal Diversity 84(1): 139–207. https://doi.org/10.1007/s13225-016-0374-9

Lücking R, Aime MC, Robbertse B, Miller AN, Ariyawansa HA, Aoki T, Cardinali G, Crous PW, Druzhinina IS, Gieser GM, Hawksworth DL, Hyde KD, Irinyi L, Jeewon R, Johnston PR, Kirk PM, Malosso E, May TW, Meyer W, Öpik M, Robert V, Stadler M, Thines

M, Vu D, Yurkov AM, Zhang N, Schoch CL (2020) Unambiguous identification of fungi: where do we stand and how accurate and precise is fungal DNA barcoding? IMA Fungus 11(1): 1–32. https://doi.org/10.1186/s43008-020-00033-z

Marsh P, Wild A, Whitfield J (2013) The Doryctinae (Braconidae) of Costa Rica: genera and species of the tribe Heterospilini. ZooKeys 347: 1–474. https://doi.org/10.3897/zookeys.347.6002

Meier R, Blaimer BB, Buenaventura E, Hartop E, von Rintelen T, Srivathsan A, Yeo D (2021) A re-analysis of the data in Sharkey et al.'s (2021) minimalist revision reveals that BINs do not deserve names, but BOLD Systems needs a stronger commitment to open science. Cladistics: 1–12. https://doi.org/10.1111/cla.12489

Meierotto S, Sharkey MJ, Janzen DH, Hallwachs W, Hebert PDN, Chapman EG, Smith MA (2019) A revolutionary protocol to describe understudied hyperdiverse taxa and overcome the taxonomic impediment. Deutsche Entomologische Zeitschrift 66(2): 119–145. https://doi.org/10.3897/dez.66.34683

Pinheiro HT, Moreau CS, Daly M, Rocha LA (2019) Will DNA barcoding meet taxonomic needs? Science 365(6456): 873–874. https://doi.org/10.1126/science.aay7174

Rakotoarison A, Scherz MD, Glaw F, Koehler J, Andreone F, Franzen M, Glos J, Hawlitschek O, Jono T, Mori A, Ndriantsoa SH, Raminosoa NRP, Riemann JC, Rödel MO, Rosa GM, Vieites DR, Crottini A, Vences M (2017) Describing the smaller majority: integrative taxonomy reveals twenty-six new species of tiny microhylid frogs (genus *Stumpffia*) from Madagascar. Vertebrate Zoology 67(3): 271–398.

Ratnasingham S, Hebert PD (2013) A DNA-based registry for all animal species: the Barcode Index Number (BIN) system. PLoS ONE 8(7): e66213. https://doi.org/10.1371/journal.pone.0066213

Renner SS (2016) A return to Linnaeus's focus on diagnosis, not description: the use of DNA characters in the formal naming of species. Systematic Biology 65(6): 1085–1095. https://doi.org/10.1093/sysbio/syw032

Riedel A, Sagata K, Suhardjono YR, Tänzler R, Balke M (2013a) Integrative taxonomy on the fast track – towards more sustainability in biodiversity research. Frontiers in Zoology 10: e15. https://doi.org/10.1186/1742-9994-10-15

Riedel A, Sagata K, Surbakti S, Tänzler R, Balke M (2013b) One hundred and one new species of *Trigonopterus* weevils from New Guinea. ZooKeys 280: 1–150. https://doi.org/10.3897/zookeys.280.3906

Riedel A, Tänzler R, Balke M, Rahmadi C, Suhardjono YR (2014) Ninety-eight new species of *Trigonopterus* weevils from Sundaland and the Lesser Sunda Islands. ZooKeys 467: 1–162. https://doi.org/10.3897/zookeys.467.8206

Riedel A, Tänzler R (2016) Revision of the Australian species of the weevil genus *Trigonopterus* Fauvel. ZooKeys 556: 97–162. https://doi.org/10.3897/zookeys.556.6126

Riedel A, Narakusumo RP (2019) One hundred and three new species of *Trigonopterus* weevils from Sulawesi. ZooKeys 828: 1–153. https://doi.org/10.3897/zookeys.828.32200

Sharkey MJ, Meierotto S, Chapman E, Janzen DH, Hallwachs W, Dapkey T, Solis MA (2018) *Alabagrus* Enderlein (Hymenoptera, Braconidae, Agathidinae) species of Costa Rica, with an emphasis on specimens reared from caterpillars in Area de Conservación Guanacaste. Contributions in Science (Los Angeles County Museum of Natural History) 526: 31–180. https://doi.org/10.5962/p.320146

Sharkey MJ, Janzen DH, Hallwachs W, Chapman EG, Smith MA, Dapkey T, Brown A, Ratnasingham S, Naik S, Manjunath R, Perez K, Milton M, Hebert P, Shaw SR, Kittel RN, Solis MA, Metz MA, Goldstein PZ, Brown JW, Quicke DLJ, van Achterberg C, Brown BV, Burns JM (2021a) Minimalist revision and description of 403 new species in 11 subfamilies of Costa Rican braconid parasitoid wasps, including host records for 219 species. ZooKeys 1013: 1–665. https://doi.org/10.3897/zookeys.1013.55600

Sharkey M, Brown B, Baker A, Mutanen M (2021b) Response to Zamani et al. (2020): The omission of critical data in the pursuit of "revolutionary" methods to accelerate the description of species. ZooKeys 1033: 191–201. https://doi.org/10.3897/zookeys.1033.66186

Srivathsan A, Hartop E, Puniamoorthy J, Lee WT, Kutty SN, Kurina O, Meier R (2019) Rapid, large-scale species discovery in hyperdiverse taxa using 1D MinION sequencing. BMC Biology 17(1): 1–20. https://doi.org/10.1186/s12915-019-0706-9

Summers MM, Al-Hakim II, Rouse GW (2014) Turbo-taxonomy: 21 new species of Myzostomida (Annelida). Zootaxa 3873(4): 301–344. https://doi.org/10.11646/zootaxa.3873.4.1

Taylor JW, Jacobson DJ, Kroken S, Kasuga T, Geiser DM, Hibbett DS, Fisher MC (2000) Phylogenetic species recognition and species concepts in fungi. Fungal Genetics and Biology 31(1): 21–32. https://doi.org/10.1006/fgbi.2000.1228

Valerio AA, Whitfield JB (2015) Taxonomic review of the genus *Hypomicrogaster* Ashmead (Hymenoptera: Braconidae: Microgastrinae), with descriptions of 40 new species. Zootaxa 3979(1): 1–98. https://doi.org/10.11646/zootaxa.3979.1.1

Vences M (2020) The promise of next-generation taxonomy. Megataxa 1(1): 35–38. https://doi.org/10.11646/megataxa.1.1.6

Yu DSK, Van Achterberg C, Horstmann K (2016) Taxapad 2016, Ichneumonoidea 2015. Database, Ottawa.

Zamani A, Vahtera V, Sääksjärvi IE, Scherz MD (2020) The omission of critical data in the pursuit of 'revolutionary' methods to accelerate the description of species. Systematic Entomology 46: 1–4. https://doi.org/10.1111/syen.12444

Supplementary material 1

Comments from the reviewers

Authors: Jose L. Fernandez-Triana

Data type: docx file

Explanation note: Comments from the reviewers of the manuscript, ordered as they were submitted. All reviewers agreed to be named in this supplementary file.

Link: https://doi.org/10.3897/zookeys.1087.76720.suppl1